COCKAYNE SYNDROME MOUSE MODELS:

LINKING IMPAIRED DNA REPAIR AND PREMATURE AGING

Muismodellen voor Cockayne Syndroom:
verband tussen defect DNA herstel en
vroegtijdige veroudering

Proefschrift

ter verkrijging van de graad van doctor aan de
Erasmus Universiteit Rotterdam
op gezag van de rector magnificus
Prof.dr. S.W.J. Lamberts

en volgens het besluit van het College voor Promoties.

De openbare verdediging zal plaatsvinden op
woensdag 15 november 2006 om 15:45 uur

door

Ingrid van der Pluijm
geboren te Rotterdam

Promotiecommissie

Promotor:	**Prof.dr. J.H.J. Hoeijmakers**
Overige leden:	**Prof.dr. H. van Steeg** **Prof.dr. P. van der Spek** **Dr. W. Vermeulen**
Copromotor:	**Dr. G.T.J. van der Horst**

Dit proefschrift kwam tot stand binnen de vakgroep Genetica van de faculteit der Geneeskunde en Gezondheidswetenschappen van de Erasmus Universiteit Rotterdam. De vakgroep maakt deel uit van het Medisch Genetisch Centrum Zuid-West Nederland. Het onderzoek is financieel ondersteund door NIH, Senter (Biopartner) en DNage.

Look, if you had one shot, one opportunity
To seize everything you ever wanted
One moment
Would you capture it or just let it slip?
..
You better lose yourself in the music,
the moment.
You own it; you better never let it go
You only get one shot,
do not miss your chance to blow
This opportunity comes once in a lifetime

(Eminem, Lose yourself)

Contents

Chapter 1 .... **9**
Introduction..9
Chapter 2 .... **43**
Impaired Genome Maintenance Suppresses the GH/IGF1 Axis in Cockayne Syndrome Mice 43
Chapter 3 .... **73**
Retinal degeneration and ionizing radiation hypersensitivity in a mouse model for Cockayne syndrome.. 73
Chapter 4 .... **89**
Conditional *Csb/Xpa* mice reveal cerebral atrophy, characteristic of the progeroid DNA repair disorder Cockayne Syndrome 89
Appendix Chapter 4.. **113**
Tamoxifen administration causes lethality in $Csb^{m/m}Xpa^{c/-}$ mice........................... 113
Chapter 5 .... **123**
Mouse models for Cockayne Syndrome: towards an intervention strategy.......... 123
Chapter 6 .... **143**
Concluding remarks and perspectives 145
Samenvatting 151
References 155
Dankwoord 171
Curriculum Vitae 175

Chapter 1

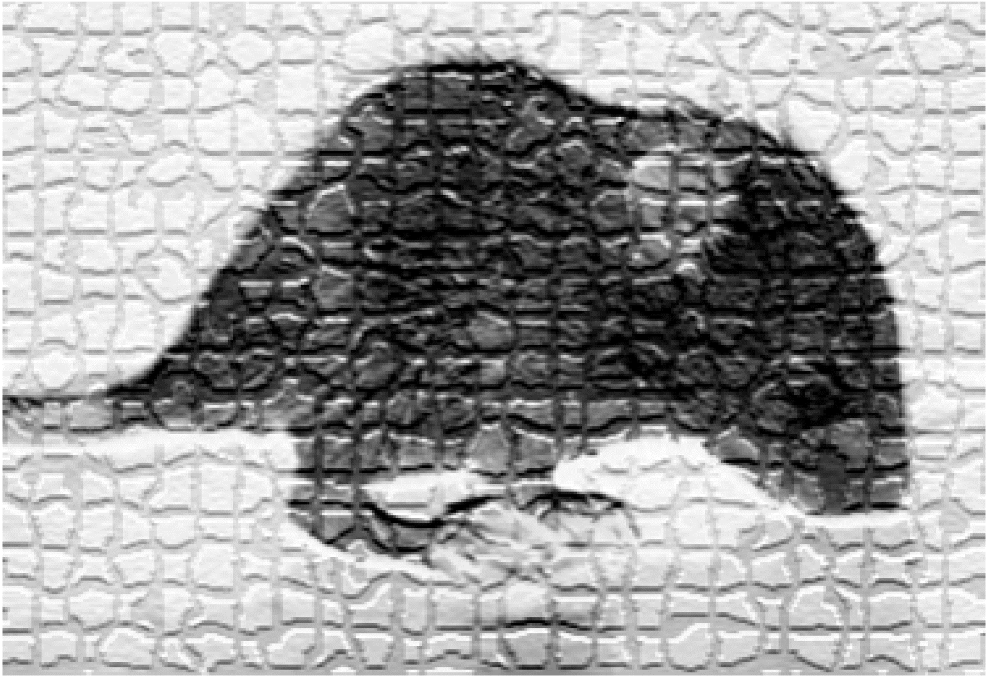

CHAPTER 1

Introduction

1.1 DNA lesions and their consequences

DNA is considered the blueprint of life that carries the genetic information, necessary to sustain life at both the cellular and organismal level. Although random changes that drive evolution occur frequently in the genome, its overall stability is an essential prerequisite for all species. Yet, genomic information is constantly attacked by a variety of genotoxic agents, present in the environment or otherwise generated as byproducts of natural metabolism. For instance, ultraviolet radiation (UV) represents a physical DNA damaging agent that mainly produces helix-distorting lesions (i.e. cyclobutane pyrimidine dimers, CPDs and pyrimidine-(6,4)-pyrimidone products, 6-4PPs) (Buschta-Hedayat et al., 1999; Wood, 1999). Similarly, ionizing radiation (IR), induces the formation of double strand breaks (DSBs), as well as single strand breaks (SSBs) (van Gent et al., 2001). However, IR can also generate reactive oxygen species (ROS) that in turn may induce other oxidative DNA lesions (Cadet et al., 2003). Chemical agents (e.g. in cigarette smoke, solvents, dyes) can induce a variety of base modifications in the DNA. In addition, superoxide anions, hydroxyl radicals and hydrogen peroxide (referred to as ROS) and byproducts of lipid peroxidation can all be produced endogenously inducing a broad spectrum of oxidative DNA lesions ranging from simple base modifications (8-oxo-G, thymin glycols and cyclopurines) to single and DSBs (Cadet et al., 2003; Hasty et al., 2003). Last but not least, the genome is threatened by its intrinsic chemical instability (e.g. spontaneous deamination and depurination) (Lindahl, 1993).

The presence of damage in our genome can interrupt vital cellular processes with severe consequences for the overall organismal survival. For example, lesions present in the transcribed strand of an active gene, can block RNA polymerases, thereby resulting in transcriptional arrest. The presence of stalled polymerases can trigger programmed cell death, known as apoptosis (Bernstein et al., 2002). Similarly, lesions can interfere with the replication machinery, thereby inducing replicative arrest, preventing cell division. Overall, the presence of damage in the genome could trigger a temporary cell cycle arrest to allow time for repair of the damaged DNA. However, in case of unrepairable, persistent DNA lesions, this could lead to permanent cell cycle arrest, senescence (cytostatic effect) (Campisi, 2001), or else cell death (cytotoxic effect). Examples of cytotoxic or cytostatic lesions are DSBs, bulky adducts (e.g. the UV-induced CPD photoproduct), intrastrand crosslinks (ICLs) and certain oxidized bases (thymine glycols and cyclopurines). To ensure that replication can continue, cells are equipped with a series of translesion synthesis (TLS) polymerases that can bypass replication-blocking lesions. However, depending on the fidelity of the TLS polymerase, error-free or error-prone bypass of lesions may occur, which in the latter case results in fixation of mutations (mutagenic effect). Whereas programmed cell death or permanent growth arrest, induced by cytotoxic and cytostatic lesions, is believed to ultimately contribute to aging (Hasty et al., 2003; Mitchell et al., 2003) (Figure 1), mutagenic lesions (e.g. spontaneous deaminations, depurination, oxidized bases and UV-induced lesions) contribute to inborn errors (when occurring in germ cells) and carcinogenesis. Although both cancer and aging are consequences of unrepaired DNA damage, the focus of this thesis will mainly be on the process of aging.

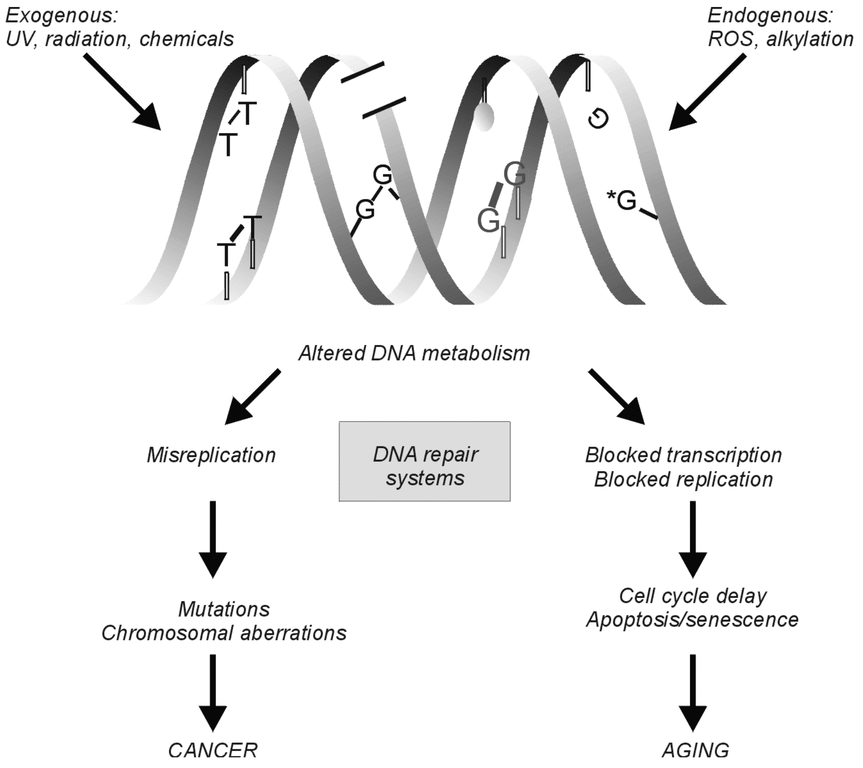
Exogenous:
UV, radiation, chemicals
Endogenous:
ROS, alkylation
T
T
T
T
G
G
G
G
*G
Altered DNA metabolism
Misreplication
DNA repair systems
Blocked transcription
Blocked replication
Mutations
Chromosomal aberrations
Cell cycle delay
Apoptosis/senescence
CANCER
AGING

Figure 1. Types of DNA damages and their consequences. *DNA damage, inflicted by DNA-damaging agents like UV, IR and ROS, can affect cellular processes and have severe consequences for human health. DNA lesions can cause misreplication, resulting in mutations, ultimately leading to cancer. DNA lesions can also exert cytotoxic and cytostatic effects when they block transcription or replication. Continuous blockage leads to apoptosis or senescence, which contributes to aging (adapted from (de Boer and Hoeijmakers 2000)).*

1.2 Excision repair pathways

To counteract the deleterious effects of DNA lesions and guard the vital genetic information, cells are equipped with an intricate network of genome-caretaking mechanisms that have overlapping as well as distinct functions in lesion recognition (and thus specificity) and timing of repair. The main repair pathways in mammals are Nucleotide Excision Repair (NER), Base Excison Repair (BER), Transcription-Coupled Repair (TCR), which all have in common that they deal with lesions that only affect one strand, allowing the use of the complementary strand as a template for repair, Homologous Recombination (HR) and Non-Homologous End-Joining (NHEJ) which deal with DNA strand breaks, and Mismatch Repair (MMR) (Friedberg, 2003; Hanawalt, 2002; Hanawalt et al., 1994; Hoeijmakers, 2001; van Gent et al., 2001). The importance of these repair systems is well illustrated by their evolutionary conservation in eukaryotes and the presence of similar mechanisms in prokaryotes, as well as by the occurrence of DNA repair disorders in man. This thesis focuses on the excision repair pathways NER, TCR and BER and the NER disorder Cockayne Syndrome.

1.2.1 Nucleotide Excision Repair

Nucleotide excision repair (NER) is a multistep process that deals mainly with helix-distorting lesions, like the UV-induced 6-4PPs and CPDs. Other substrates for NER include bulky chemical adducts, intrastrand crosslinks and the oxygen free-radical-induced helix-distorting 5’,8-purine cyclodeoxynucleotides (Brooks et al., 2000; Kuraoka et al., 2000). NER is an evolutionary conserved damage removal mechanism throughout eukaryotes whereas its importance is also underscored by the fact that it bears similarities with prokaryotes as well.

This ‘cut and patch’ process involves at least 30 proteins and consists of four successive steps: (i) lesion recognition, (ii) local opening of the double helix, (iii) excision of the damaged strand and (iv) gap-filling DNA synthesis (Aboussekhra et al., 1995; de Laat et al., 1999; Gillet and Scharer, 2006; Hoeijmakers, 2001; Wood, 1999). NER consists of two subpathways: global genome NER (GG-NER) and transcription-coupled NER (TC-NER). GG-NER recognizes and removes lesions in the entire genome. GG-NER has to scan the whole genome for lesions and is often regarded as a relatively slow and inefficient process. Furthermore, the efficiency of GG-NER is lesion-dependent. For instance, in UV-induced lesions, repair of 6-4PPs, which distort the DNA double helix severely, is fast throughout the genome and is predominantly done by GG-NER. In contrast, GG-NER of CPDs, which mildly distort the double helix, is relatively slow (Mitchell and Nairn, 1989). To avoid that slowly repaired lesions block transcription for long, mammalian cells have evolved the TC-NER pathway, which selectively removes lesions from the transcribed strand of active genes. As it is directly coupled to the transcription machinery, TC-NER is considered a fast and efficient process (Bohr et al., 1985; Hanawalt, 2002; Mellon et al., 1986; Mellon et al., 1987). In agreement, TC-NER was previously shown to remove CPD and 6-4PP lesions with similar rates (van Hoffen et al., 1995). Interestingly, repair of CPDs in humans is much faster than in rodents. However, this “human-rodent paradox” may likely reflect the absence of GG-NER for this particular lesion (see below).

GG-NER and TC-NER are mechanistically the same, except for the initial damage-recognition step. In GG-NER, the XPC/hHR23B complex and the UV-damaged DNA binding protein (UV-DDB; composed of the DDB1 and DDB2/XPE subunits) are involved in lesion recognition. In TC-NER, the CSB, CSA, RNApolII and XAB2 proteins are thought to be responsible for damage detection. After DNA damage recognition by either GG- or TC-NER specific components, TFIIH binds the DNA, followed by XPA and RPA. Together these factors allow subsequent helix unwinding by the TFIIH complex, verification and demarcation of the damaged site and excision of the damaged strand by the XPG and ERCC1/XPF endonucleases. Finally, the repair reaction is completed by the regular replication machinery consisting of Pol δ/ε and Pol κ (Ogi and Lehmann, 2006) and Lig I/III, that fills the resulting 25-30 base long single strand DNA gap (see Figure 2 for a schematic representation of the NER reaction). The function of the various NER proteins will be discussed in more detail below.

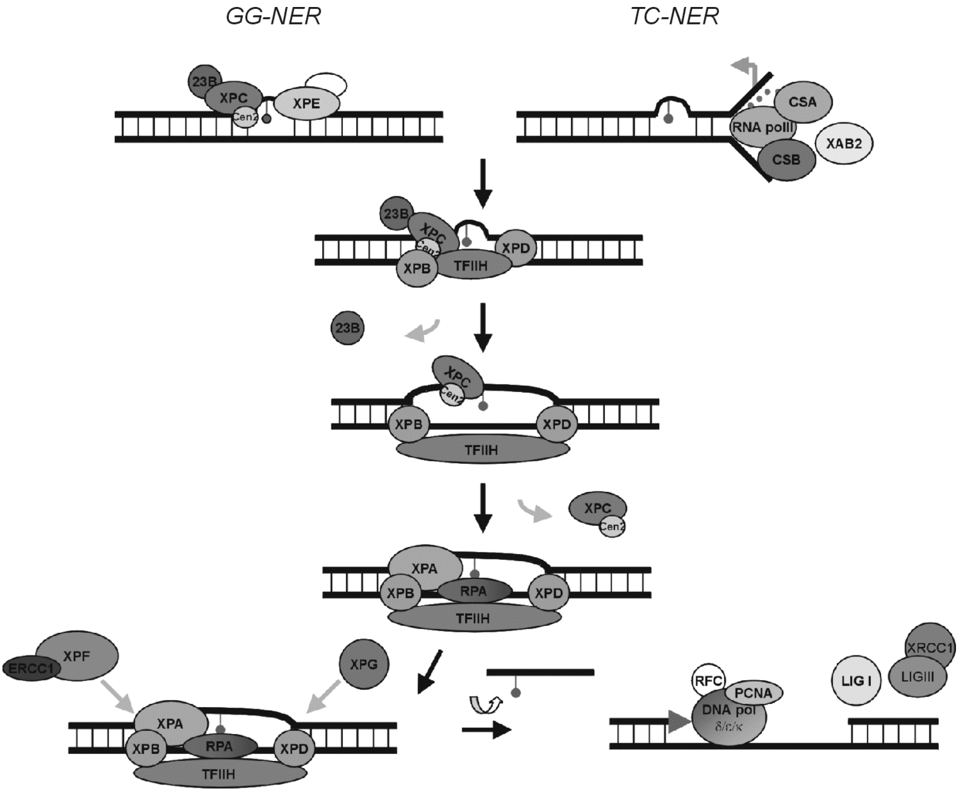

Figure 2. Repair of damaged DNA by nucleotide excision repair (NER). *The mechanism consists of two subpathways, global genome (GG-) (left) and transcription coupled (TC-) NER (right). DNA damage recognition requires XPC/hHRad23B for recognition of helical distortion anywhere in the genome (GG-NER). TC-NER is initiated when RNA polymerase II progression is blocked by damage in the transcribed strand of DNA. XPC/hHRad23B or stalled RNA polymerase II complex induce the recruitment of basal transcription factor TFIIH followed by XPG to the damaged site. The XPB and XPD helicases, which are part of the TFIIH complex, unwind the DNA around the lesion. The XPA/RPA complex is recruited to the damaged lesion: XPA verifies the DNA damage and RPA serves to stabilize the open intermediate by binding the undamaged strand. Next XPF/ERCC1 is recruited: XPG and ERCC1/XPF respectively cleave at the 3'and 5' site of the damaged strand, thereby removing a 24-32-base oligonucleotide containing the damage. The resulting gap is filled in by DNA polymerase δ, ε and κ together with Ligase I and III.*

As mentioned above, a stalled RNA polymerase (RNAP) is considered to trigger TC-NER (Tornaletti et al., 1999). Currently, however, there are two models for how TC-NER might actually work: 1) When the RNA polymerase is blocked at a particular lesion, it is temporarily displaced from the damaged site, without actual removal from the DNA. After repair has succeeded, transcription elongation resumes and finishes the incomplete mRNA (Tornaletti et al., 1999). 2) Blockage of RNA polymerase can result in polyubiquitination of the largest subunit of RNAPII (Rpb1) and its subsequent proteolysis. In this scenario, the unfinished mRNA is discarded and the RNA polymerase sacrificed. After repair, reinitiation of transcription will produce a new mRNA transcript (Ratner et al., 1998).

Transcription-coupled repair (TCR) also applies to repair of transcription-blocking oxidative DNA lesions, e.g. minor base damage induced by oxidizing agents that are generally not helix-distorting, but still arrest transcription (Dianov et al., 1999; Satoh et al., 1993; Satoh and Lindahl, 1994). Normally, these types of lesions are removed by Base Excision Repair (BER). It is important to note that it is currently unknown whether in the TCR reaction BER is responsible for the actual removal of these oxidative lesions or whether the core of NER takes care for this. Therefore this thesis refers to TC-NER when only the transcription-coupled repair pathway of NER is employed involving helix-distorting damage. TCR is referred to in those cases where all transcription-blocking lesions are included, involving either NER and/or BER.

Proteins involved in NER

Important clues as to which proteins might actually have a crucial role in the mammalian NER mechanism originate from three genetic disorders, Xeroderma Pigmentosum (XP), Cockayne Syndrome (CS) and Trichothiodystrophy (TTD) (described in more detail below), all with defects in repairing UV-induced DNA damage. In addition to patient cells, proteins involved in the NER process have been also identified in NER-deficient yeast mutants and Chinese hamster ovary cell lines (CHO) by employing methods such as complementation analysis and *in vitro* reconstitution assays involving purified proteins and DNA substrates containing site-specific or random damage (Aboussekhra et al., 1995), for reviews see (de Laat et al., 1999; Gillet and Scharer, 2006; Hoeijmakers, 2001; Wood, 1999) and references therein. Since NER-deficient cells are sensitive to UV, cellular survival after UV exposure is an excellent read-out to test sensitivity. However, there are distinct ways to assay UV-sensitivity. Since the final step in the NER reaction is filling of the single-stranded gap (Aboussekhra et al., 1995; Shivji et al., 1995), unscheduled DNA synthesis (UDS), in which repair-mediated ^{3}H-thymidine incorporation is measured after exposure of cells to UV irradiation, is often used as a read-out for the overall DNA repair capacity, which is mainly GG-NER. Thus, this method represents a reliable measure for functional GG-NER. RNA synthesis recovery (RRS) measures the time it takes for cells to repair and have normal levels of RNA synthesis, e.g. after UV exposure. In wild type cells, although dependent on which dose is used, transcription resumes after several hours, but in TC-NER-deficient cells, the damage in the transcribed strands of active genes cannot be repaired and removal is very slow or absent. Therefore transcription, measured by RNA synthesis recovery, will remain low, making RRS a good measure for functional TC-NER (Mayne and Lehmann, 1982).

The XPC/HR23B and UV-DDB complexes

Both helical distortion and alteration of DNA chemistry are necessary for lesions to be recognized by NER (Hess et al., 1997). XPC is the one of the first essential NER factors that takes action in the NER cascade (Sugasawa et al., 1998; Volker et al., 2001). It specifically acts in the initial damage recognition step of GG-NER as a complex together with hHR23B and centrin2 (designated the XPC-hHR23B complex). Although *in vitro* studies show that NER is functional when XPC alone is present, addition of centrin2 and hHR23B stimulates the NER reaction (Ng et al., 2003; Nishi et al., 2005; Sugasawa et al., 1996). The XPC-hHR23B complex is essential for recruitment of other NER components (TFIIH, XPA and RPA) to the site of damage to initiate the repair process (Batty et al., 2000; Sugasawa et al., 1996; Sugasawa et al., 1997). Although the heterotrimer can bind both single- and double-stranded undamaged DNA, it has a much higher affinity for damaged DNA (Masutani et al., 1994; Shivji et al., 1994). After binding to the lesion, the XPC-hHR23B complex recruits the subsequent factors of the repair machinery to the sites of damage (Volker et al., 2001). It was found that hHR23B stabilizes the heterotrimer most probably by inhibiting polyubiquitination of XPC (by DDB2, see below), which prevents degradation by the 26S proteasome (Ng et al., 2003; Ortolan et al., 2000). *In vitro* studies have previously shown that hHR23A, a protein with high homology to the hHR23B protein, can similarly form a complex with XPC. However, although both hHR23 proteins are functionally interchangeable, the main complex found *in vivo* is XPC-hHR23B.

Another protein, specifically involved in GG-NER, is the UV-damaged DNA binding protein (UV-DDB). UV-DDB consists of two subunits; p125 (DDB1) and p48 (XPE/DDB2) (Hwang et al., 1999; Tang et al., 2000). Although the precise function of this protein is currently unknown, it appears to facilitate recognition of lesions that are less well-recognized by the XPC-hHR23B complex (i.e. CPDs (Hwang et al., 1999; Keeney et al., 1993) via (poly)ubiquitiylation of XPC (Sugasawa et al., 2005; Wang et al., 2005). Following UV exposure, transcription of the gene encoding the p48 subunit of UV-DDB is up-regulated in a p53-dependent manner. As a consequence, the UV-DDB protein plays an important role in facilitating more efficient repair of CPDs. Rodent cells, however, lack the p53 responsive element in the promoter of the p48 subunit (Tan and Chu, 2002). This might well explain the absence of GG-NER of CPDs in mice (Hwang et al., 1999). DDB1 and DDB2 are also part of a larger complex including cullin4a, Roc1 and the COP9 signalosome (CSN) (Groisman et al., 2003). Cullin4a displays ubiquitin ligase activity and was shown to ubiquitylate DDB2 both *in vitro* and *in vivo* (Chen et al., 2001; Matsuda et al., 2005; Nag et al., 2001), which led to degradation of DDB2 by the 26S proteasome (Fitch et al., 2003; Rapic-Otrin et al., 2002). The CSN, on the other hand, displays deubiquitilation activity. These observations have led to a model where UV-induced DNA damage triggers the (poly)ubiquitylation of both XPC and DDB2. Hence, DDB2 is degraded by the 26S proteasome, whereas (as mentioned above) XPC is not. This degradation of DDB2 most probably prevents further ubiquitylation of XPC, which can also enhance its unspecific binding to DNA (Sugasawa et al., 2005), a process that might impede the subsequent steps in the NER pathway.

The CSB and CSA proteins

CSA and CSB proteins are both indispensable for proper functioning of the TC-NER subpathway, and are not involved in GG-NER (Henning et al., 1995; Troelstra et al., 1992). In agreement, CSA and CSB-deficient cells demonstrate low RRS levels, whereas UDS levels are found to be within the normal range. CSB belongs to a family of SWI/SNF-like DNA-dependent ATPases. This family of proteins is involved in a wide array of nuclear processes, including transcription, chromatin remodeling and various repair and translesion synthesis processes. The CSA protein contains five WD repeats, a regulatory rather than catalytic domain that is often found in multiprotein complexes involved in processes such as cell cycle regulation and RNA processing (Henning et al., 1995). CSA mainly interacts with CSB, XAB2 (XPA binding protein 2) and the p44 subunit of TFIIH. Recently, exposure of cells to UV irradiation was shown to induce CSA translocation to the nuclear matrix in a CSB-dependent manner (Kamiuchi et al., 2002). Although the precise function of CSA in TC-NER remains to be identified, this protein was previously shown to colocalize with the phosphorylated form of RNApolI and it is, therefore, most likely to be required for TCR during elongation of the transcription process (Groisman et al., 2003; Kamiuchi et al., 2002). Both CSB and CSA are also components of RNApolII associated complexes (CSA not via direct interaction), dealing with transcriptional blocks and resumption of transcription, which is most probably linked to their function in TC-(NE)R. Interestingly, similar to DDB2, CSA was found to reside in a complex with cullin4a, Roc1 and the COP9 signalosome. This finding establishes a link between TC-NER, GG-NER and ubiquitin-dependent protein degradation (Groisman et al., 2003). Whereas the DDB2 associated ubiquitin ligase activity acts early in the GG-NER process and is inhibited by association with CSN at later time, the CSA associated ligase activity is silenced by CSN at the beginning of the repair process and becomes active at later stages (Groisman et al., 2003). Recently, it was found that CSB becomes ubiquitylated by this CSA ligase complex and is subsequently degraded by the 26S proteasome in a UV-dependent manner, an important step necessary for the recovery of RNA synthesis after TCR (Groisman et al., 2006).

The CSB protein is considered to have a plethora of additional functions outside NER. For instance, it can act as an elongation factor for RNApolII, particularly when damaged DNA is encountered, thereby, promoting RNApolII transcription past natural pausing sites. Also, it is reported to promote transcription of genes with highly structured RNA like U1, U2, snRNA and 5SrRNA or else it may stimulate rRNA synthesis both *in vitro* and *in vivo*. This implicates CSB in PolI, PolII and PolIII (ssRNA) transcription, reviewed by (Licht et al., 2003). This is in agreement with the previously documented overall reduced level of transcription in CSB-deficient cells (Balajee et al., 1997). Additionally, CSB is also a SNF2-like factor, related to hBrg1, hBrm and Dros/SWI involved in chromatin remodeling, reviewed by (Licht et al., 2003). Also, Rad26, the yeast homologue of CSB, has been implicated in chromatin remodeling (Gregory and Sweder, 2001). In agreement, CSB can act as a chromatin remodeling factor and can interact with core histones, inducing negative supercoiling (Citterio et al., 2000). As it is known that chromatin structure changes during transcription regulation and repair, CSB may also likely participate in this process. Although under debate, CSB has been implicated in the removal of oxidative DNA damage. In CSB-deficient CHO cells (UV61) and CS-B patient fibroblasts (CS1AN), the incision by FPG (Formamidopyrimidine DNA glycosylase), a glycosylase involved in BER, turned out to be dependent on CSB (Sunesen et al., 2002). This was shown both with an *in vitro* approach involving cellular extracts, as well as an *in vivo* approach which allows assaying repair of intragenomic sequences. Moreover, the same results were confirmed in human CS1AN cells (Stevnsner et al., 2002). Also, CSB cells not only have reduced incision activity of 8oxoA(:T) and 8oxoA(:C) containing oliginucleotides (Tuo et al., 2002b), they have reduced OGG1 (8-hydroxyguanine DNA glycosylase) mRNA levels as well (Dianov et al., 1999; Tuo et al., 2002a). Recently, by use of a host cell reactivation assay that determines the ability to transcribe an in vitro damaged plasmid, it was shown that both CS-A and CS-B human cells are defective in TCR of 8-oxo-G and TG (Spivak and Hanawalt, 2006). Finally, CSB cells have been shown to be sensitive to genotoxic agents that give rise to oxidative DNA damage, like IR and paraquat (de Waard et al., 2003; Deschavanne et al., 1984). Taken together, CSB represents a versatile protein with many different functions involved in a diversity of distinct and overlapping processes.

The TFIIH complex

After lesions are detected by the XPC-hHR23B complex, the TFIIH complex is recruited to the site of the damage in an ATP-independent step. In a second, ATP-dependent step, TFIIH unwinds the DNA, allowing other DNA repair factors to enter the site of the lesion. TFIIH was first identified as a factor involved in basal transcription. Subsequently, however, it was found that two of its subunits were XPB (p89) and XPD (p80), which were known before to participate in NER revealing a dual function of TFIIH in both transcription and repair (Bootsma and Hoeijmakers, 1993; Drapkin et al., 1994; Evans et al., 1997; Schaeffer et al., 1994; Schaeffer et al., 1993; Vermeulen et al., 1994; Winkler et al., 2000). XPB and XPD are two DNA helicase proteins with opposite ATP-dependent DNA unwinding activity. In transcription, DNA unwinding activity is essential for promoter opening and promoter escape, whereas in repair, this activity is an obligatory step to permit lesion demarcation and dual incisions (Evans et al., 1997). The helicase activity of XPB is essential for transcription initiation. On the contrary, XPD seems to have a more structural role in promoter opening and escape, since its helicase activity is dispensable for *in vitro* transcription (Bradsher et al., 2000; Tirode et al., 1999; Winkler et al., 2000). In yeast, the TFIIH core complex was found to possess ubiquitin ligase activity, which seemed to be involved in the transcriptional response to DNA damage (Takagi et al., 2005). It is not yet known whether this is the same for TFIIH in mammalian cells.

TFIIH is a multifunctional protein complex, consisting of ten subunits (Giglia-Mari et al., 2004), harboring both helicase and protein kinase activities. Seven of these subunits (XPB, XPD, p62, p52, p44, p34 and p8) form a tight ‘core complex’ together. Other subunits are the cyclin-dependent kinase Cdk7, cyclin H and MAT1, which together form the cdk-activating kinase (CAK) complex, associated with TFIIH. The CAK complex can phosphorylate cyclin-dependent kinases involved in cell cycle regulation and is essential for the C-terminal phosphorylation of RNAPolII during transcription initiation (Nigg, 1995; Svejstrup et al., 1995). Furthermore, TFIIH has been found to interact directly with the tumor suppressor p53 (Leveillard et al., 1996; Wang et al., 1996), pointing to a potential role of TFIIH in cell cycle regulation as well. Considering its essential function in these vital processes (e.g. transcription and repair), it is hardly surprising that TFIIH is indispensable for life.

The XPA protein

After initial opening of the DNA around lesions by TFIIH, a ‘preincision’ complex consisting of RPA, XPA and XPG is assembled to the site of the damage. XPA is involved in the lesion verification step of NER and in the proper organization of the repair machinery around the damage, together with the single-strand DNA binding complex RPA (Sugasawa et al., 1998; Volker et al., 2001). As such, XPA is involved in both subpathways of NER (Volker et al., 2001). Since XPA has to verify the presence of a particular lesion in the DNA, it is able to bind many different types of damages in DNA. XPA is also involved in open complex formation around the damage resulting in lesion demarcation (de Laat et al., 1998; Li et al., 1995). Furthermore, XPA interacts with XAB2, TFIIH, XPF/ERCC1, XPC-hHR23B and RPA. XAB2 is a tetratricopeptide that is involved in both TCR and transcription, thereby thought to function as a bridge between transcription, NER and TCR (Nakatsu et al., 2000). Together, these functions demonstrate the central and essential role XPA has in NER.

The XPG protein and the ERCC1/XPF complex

Following local unwinding and demarcation of the lesion, the damaged DNA has to be excised. Both XPG and the ERCC1/XPF complex are involved in this part of the repair process (Mu et al., 1996; O'Donovan et al., 1994b; Sijbers et al., 1996). XPG is a structure-specific 3’ endonuclease believed to be involved in both stabilization of the preincision complex (Araujo et al., 2000) and incision at the 3’ end of the damaged nucleotide (O'Donovan et al., 1994a). The incision at the 5’ end of the damaged DNA is made by the ERCC1/XPF complex (Sijbers et al., 1996). *In vitro*, the 3’ incision by XPG can be detected in the absence of ERCC1/XPF (Mu et al., 1996). In contrast, the excision by ERCC1/XPF requires the presence, but not the catalytic activity of XPG (Wakasugi et al., 1997). However, in the presence of both proteins, 5’ and 3’ uncoupled incisions have been detected, suggesting that both incisions can happen almost simultaneously (Matsunaga et al., 1996; Moggs et al., 1996; Mu et al., 1996). The combined action of XPG and the ERCC1/XPF complex results in excision of a 24-32 nucleotides long ssDNA fragment (containing the lesion) from the locally opened DNA. As mentioned above, XPG (like XPA) is also implicated in stabilizing the open complex formation in the NER process (Evans et al., 1997; Mu et al., 1996). The role of XPG in this process is likely structural, since its nuclease activity is not needed for stabilization of the open complex. Furthermore, XPG has been found to interact with XPB, XPD, p62 and p44, subunits of the TFIIH complex. This interaction could help stabilizing the open complex that is formed during the NER mechanism. Although XPG recruitment does not require the XPA protein, there is no detectable incision activity in XPA-deficient cells (Volker et al., 2001). Apart from its function in NER, XPG seems to have a function in the removal of oxidative DNA damage. It can stimulate hNTH1 activity on thymine glycol, but this stimulation does not depend on the endonuclease function of XPG (Bessho, 1999). This suggests that different domains in the XPG protein are responsible for its different functions. In addition, XPG has been reported to be involved in TCR of oxidative damage as well as in RNApolI and RNApolII transcription (Klungland et al., 1999; Lee et al., 2002). Similar to CSB, XPG is a multipurpose protein with many different occupations.

ERCC1 was the first mammalian NER gene to be cloned (Westerveld et al., 1984) and is essential for proper functioning of the NER process. The ERCC1 protein acts in a complex with XPF as a structure-specific endonuclease to make the incision at the 5’ end of the damaged DNA strand. In contrast to XPG, recruitment of ERCC1/XPF to the damaged site requires XPA. Both XPF and ERCC1, like XPG, have functions outside the context of NER. For instance, ERCC1/XPF is also involved in interstrand crosslink repair (Niedernhofer et al., 2001), HR and potentially immunoglobulin class-switch recombination (CSR). Consequently, both XPF and ERCC1 deficient cells are not only sensitive to UV, but also to cross-linking agents like mitomycin C

(MMC). Whether the ERCC1/XPF protein complex makes an incision next to a crosslink (similar to its function in NER), or whether it is involved in a later step of the crosslink repair reaction, is not yet understood. Analysis of different XPF point mutants revealed that the DNA binding activity of the ERCC1/XPF complex can be separated from its catalytic activity on the DNA (Enzlin and Scharer, 2002). This finding might help to elucidate the role of this protein complex in the various DNA repair processes that it is involved in.

1.2.2 BER pathway/proteins

Base Excision Repair (BER) eliminates chemically altered deoxyribonucleotides, like oxidative modifications and deaminations, which are mostly, but not exclusively, caused by DNA damaging agents of endogenous origin, such as ROS or methylating agents. 8-oxo-guanine (8-oxo-G), O6-methyl-guanine (O6-me-G) and thymine glycol (TG) represent typical BER lesions (Beckman and Ames, 1997; Fortini et al., 2003; Krokan et al., 2000; Krokan et al., 1997; Wilson and Thompson, 1997). Occasionally, BER substrates (e.g. TG) can block transcription, but most often they give rise to miscodings in the DNA, that if left unrepaired, may result in mutation fixation. To this end, BER is considered a crucial mechanism to prevent mutagenesis.

In the mammalian genome, over a hundred different oxidative lesions have been identified (Cadet et al., 1997), thereby demanding a high level of versatility from the BER process. To cope with this complexity, BER lesions are recognized by a wide range of DNA glycosylases, with specific, although overlapping lesion recognition abilities. These glycosylases catalyze the release of damaged base residues in free form, leaving behind an abasic site in the DNA backbone, for review see (Dodson and Lloyd, 2002) and references therein. Abasic sites are very toxic to cells and have to be removed quickly. Thus, subsequent to base removal, a more general mechanism, involving APE1/HAP1, XRCC1, LIG1 and Polβ proteins, can deal with the abasic site by endonucleolytic cleavage and subsequent gap/filling/ligation activity (Demple et al., 1991). The reaction proceeds either via short patch repair, in which the single nucleotide gap is filled, or via long patch repair, in which a short stretch of DNA (including the abasic site) is removed and replaced, involving in part other proteins (Matsumoto and Kim, 1995; Sobol et al., 1996). Although some epidemiological studies claim correlations between certain types of cancers (lung, colorectal) and mutations in BER genes, these results are not conclusive and mutations in BER genes have not been found to be associated with inherited human disorders (Frosina, 2004).

1.3 NER syndromes

In humans, NER represents the major defense mechanism against the carcinogenic effects of UV light. Therefore, it is not surprising that a defect in NER can lead to extreme sun sensitivity and an elevated risk of developing skin cancer. Deficiencies in NER genes have been associated with three rare autosomal recessive UV-sensitive disorders: Xeroderma Pigmentosum (XP), Cockayne Syndrome (CS) and a photosensitive form of the brittle hair disorder Trichothiodystrophy (TTD) (Bootsma, 2001; Lehmann, 2003; Nance and Berry, 1992). All three disorders share photosensitivity of the skin, but differ markedly in UV-induced skin cancer proneness as well as in the occurrence of additional pathology.

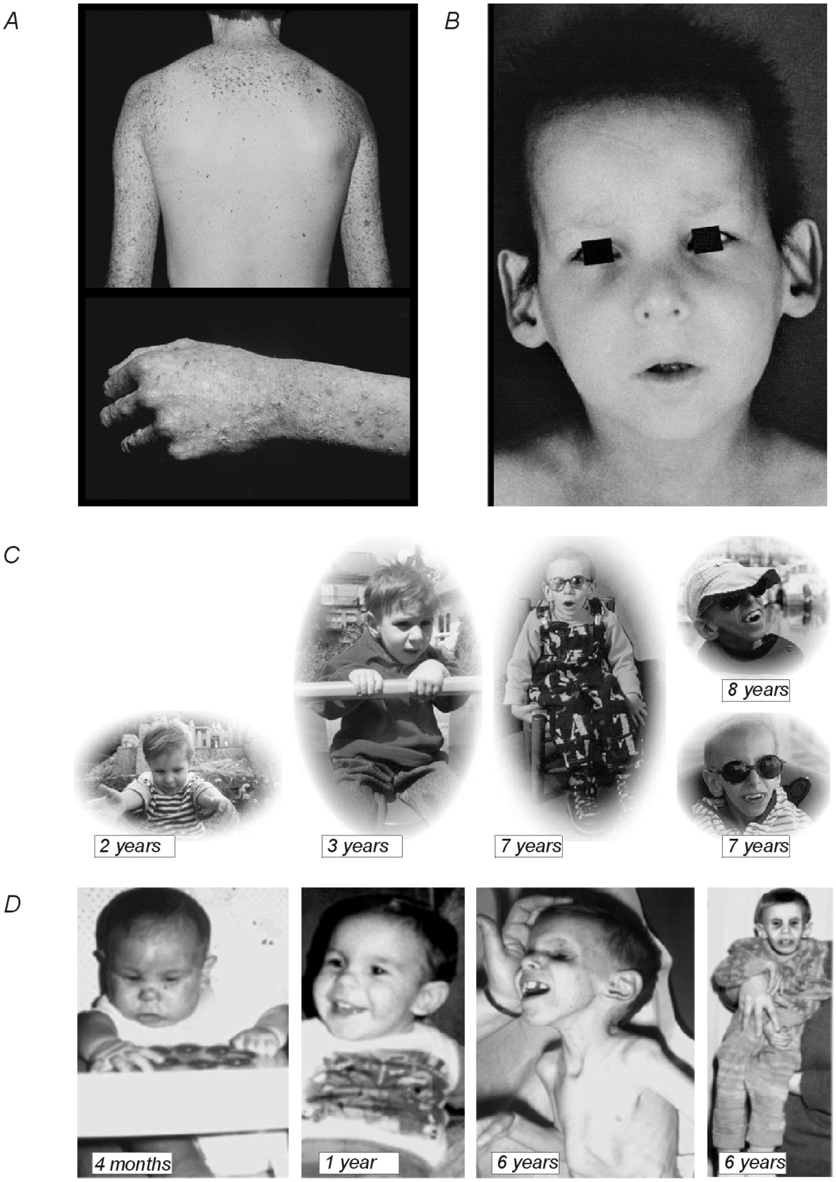

Figure 3. Human NER-deficient syndromes: XP, TTD, CS and XP/CS. *A) Picture of the back of an XP patient. Note the increased freckling on the UV-exposed skin. B) Picture of a TTD patient. (adapted from (McCuaig, Marcoux et al. 1993)) C) Pictures of a patient with CS at different ages. Note the progressive nature of the disease with close to normal appearance at the age of 2 years and the typical CS appearance at the age of 7 years with deep set eyes, prominent ears and profound cachexia (adapted from Share and Care Cockayne Syndrome Network, http://www.cockayne-syndrome.org) D) Pictures of patient XP20BE with XP/CS at different ages. Note the progressive nature of the disease with normal appearance at the age of 4 months and 1.5 years and the typical CS appearance at the age of 6 years with deep set eyes, prominent ears and profound cachexia (adapted from Lindenbaum et al., 2001).*

1.3.1 Xeroderma Pigmentosum

Xeroderma Pigmentosum is characterized by extreme sun sensitivity, photophobia, and high UV-induced cancer susceptibility with early development of malignancies in sun-exposed parts of the skin, eyes and tip of the tongue (Bootsma, 2001) (Figure 3A). Benign lesions like freckles or hyperpigmented spots are frequently found. The disease is mostly symptomatic in childhood, except for the adult variant form (XP-V, see text below).

Initial lab diagnosis of XP cells usually involves testing of cultured fibroblasts (obtained from skin biopsies) for hypersensitivity towards UV-C exposure. When positive, further molecular diagnosis includes determination of the level of UDS. In addition, complementation assays or mutation screening can be performed, which revealed that excision-deficient XP is due to a mutation in one of seven genes; *XPA-XPG*. Cells from XP patients are characterized by low UDS (in other words deficient GG-NER) and low RRS (defective TC-NER). XP-C and XP-E however, are an exception to the latter; patient cells display low UDS, but normal RRS, as a consequence of deficient GG-NER but proficient TC-NER (Hwang et al., 1999; Hwang et al., 1998; Tang et al., 2000; Venema et al., 1991; Venema et al., 1990). The most common forms of XP are XP-A and XP-C (Bootsma, 2001).

Over 1000 cases of XP have been described. Due to their NER defect, sun exposure of XP patients causes degenerative alterations in both skin and eyes (Bootsma, 2001), which can start as early as at the age of two (Kraemer, 1997). XP patients have a more than 1000-fold elevated risk of getting sun-induced skin cancers strikingly restricted to sun-exposed areas like face, neck and head. Most frequently, basal cell or squamous cell carcinomas (45% of XP patients) develop, and less frequently melanomas are found. Furthermore, UV can induce eye anomalies such as atrophy of the skin around the eye, loss of lashes or even the whole eyelid and corneal clouding (Kraemer et al., 1987). The mean age at onset of these neoplasms is 8 years, which is extremely early (50 years earlier than in the general population). Apart from the sun-induced skin cancers, XP patients have a 10-20 fold increased risk to develop internal cancers before the age of 20 years (Kraemer et al., 1984).

Neurological degeneration is found in 20% of XP cases, (complementation groups XP-A, G and D) and is referred to as XP neurological disease. These neurological abnormalities result from the degeneration of neurons that initially develop normally (Rapin et al., 2000). Neurological symptoms include microcephaly, peripheral neuropathy, sensorineuronal deafness and loss of reflexes, followed by ataxia and mental retardation or dementia. The age at onset and rate of progression vary greatly between patients. A possible explanation for the onset of neurologic abnormalities in XP patients is that unrepaired endogenous NER lesions in neurons trigger apoptosis (Kuraoka et al., 2000). The most severe early-onset neurologic subtype of XP (mostly caused by mutations in XPA) is De Sanctis-Cacchione Syndrome (XP-DSC). In addition to the neurological symptoms mentioned above, this disease involves dwarfing, hypogonadism and a 10-20 fold increase in frequency of several types of internal cancers (DeSanctis, 1932; Kraemer et al., 1987).

In addition, complementation analysis has revealed another class of XP patients, XP-variant. Interestingly, a mutation in the responsible gene (*XPV)* does not cause NER impairment, as measured by UDS and RRS, but instead leads to a defect in postreplication repair. The responsible *XPV* gene has been cloned and was previously shown to encode hRad30A, the damage-specific DNA polymerase η that is involved in translesion synthesis (Masutani et al., 1999). As under normal conditions, this polymerase can bypass UV-induced CPDs in a relatively error free manner, a defect in this protein can also lead to an XP-like disease, including UV-sensitivity and skin cancer predisposition.

1.3.2 Cockayne Syndrome

Similar to XP, Cockayne Syndrome (CS) is a pleiotropic disorder that is characterized by cutaneous photosensitivity. However, CS differs from XP by the occurrence of severe progressive postnatal growth failure (cachexia) and progressive neurological dysfunction, as well as the absence of UV-induced skin cancer predisposition in all cases reported so far (Nance and Berry, 1992) (Figure 3C).

CS is specifically associated with defective TC-NER, while GG-NER functions normally, and consequently lab diagnostics for CS cells reveal normal UV-induced UDS and low RRS even after 24 hours, when exposed to a UV dose from which normal cells recover in 6-8 hours (Lehmann et al., 1979). Two complementation groups have been identified in CS, designated CS-A and CS-B, of which the majority of studied cases belong to the latter (Lehmann, 1982; Tanaka et al., 1981). As seen for XP, CS patients are highly UV-sensitive, and show atrophy of sun-exposed skin. Despite the DNA repair defect, CS is not associated with an increased risk of skin cancer. This might be explained by the fact that the disease is often noted early in the life of patients, because of both growth and neurological defects, which allows adequate protection from sun exposure. Another explanation could be that CS patients simply do not get old enough to get skin cancer. Finally, the type of repair defect, TC-NER/TCR, may protect from cancer as this repair system, when defective, will cause cell death, rather than mutations causing cancer.

Patients with CS are divided in different clinical groups according to severity and onset of the disease. Type I refers to the ‘classical’ or less severe form of the disorder, with onset in the postnatal period and survival into adolescence or young adult life. Type II is a more severe infantile form with onset before birth and death by the age of 6 or 7 years (Lowry, 1982), reviewed by (Rapin et al., 2000). Both forms of CS are characterized by progressive growth failure and multiorgan degeneration.

The clinical features are severe and diverse. In CS patients, growth (both height and weight) is retarded, but this is more pronounced for weight. This phenomenon, together with the severe and progressive nature of the growth retardation, is described by the term cachectic dwarfism. A very prominent feature of CS is a ‘birdlike face’, characterized by enophthalmia (sunken eyes), a beaked nose and a narrow mouth that results from reduced amounts of subcutaneous fat. Furthermore, patients present with dental caries and skeletal abnormalities such as kyphosis. The mean age at death of CS patients, ranging from neonatal to 55 years (1 reported patient), is 12.5 years. The most common cause of death is pneumonia as a result of general atrophy and cachexia.

CS patients display several neurological symptoms. Delayed psychomotor development, mental retardation, microcephaly and ataxia are most commonly associated with this syndrome (Rapin et al., 2000). The extremely small size of the brain, together with the fact that head circumference is relatively normal at birth, indicates that the failure of brain growth is mainly of postnatal origin. Neuropathological examination revealed multifocal patchy demyelination in cerebral and cerebellar cortex, dilated ventricles, calcium deposits in basal ganglia and cerebral cortex, and loss of neurons (moderately near calcium deposits), which is most pronounced in the cerebellum (Itoh et al., 1999). Nerve defects, such as reduced velocity of nerve conduction and changes in muscle innervation are also often observed. Additionally, most patients have sensorineuronal hearing loss and structural eye abnormalities, including cataracts, ciliary body defects and pigmentary degeneration of the retina (60-100% of the reported cases). Furthermore, patients have a ‘salt and pepper’ like fundus that progresses throughout life. If cataracts are detected within the first three years of life, this usually points to a poor prognosis. (Dollfus et al., 2003).

In 10% of reported CS cases, the disease is caused by mutations in the *XPD*, *XPB* or *XPG* gene, resulting in a combined form of XP and CS (Lindenbaum et al., 2001). XP/CS patients differ from classical CS patients in that GG-NER is also affected. So far, nine XP/CS cases have been reported with skin features of XP combined with the systemic and neurological features of CS. Although the few known XP/CS patients all have XP skin disease (dry skin and abnormally pigmented sun-exposed areas), only two of them actually have developed skin cancer (Dupuy et al., 1974; Lindenbaum et al., 2001). XP/CS, like CS, has a variable phenotype with respect to age at onset, symptoms displayed and severity of the defect (Figure 3D).

A syndrome that shares similarity with CS (type II) is Cerebro-Oculo-Facio-Skeletal Syndrome (COFS). This is a recessive, progressive brain and eye disorder with symptoms including dramatic growth failure, severe mental retardation, facial dysmorphisms (deep-set eyes, large ears, prominent nose), cataracts, progressive joint contractures, microcephaly and cerebral atrophy. Most patients die before the age of 3 years (Longman et al., 2004; Meira et al., 2000). The eye abnormalities in COFS are usually more severe than in CS, but no cutaneous photosensitivity has been described. Since this disease shares many overlaps with CS, they are often difficult to distinguish from one another. COFS can actually be regarded as an early infantile form of CS and in some of these patients, mutations have been found in the CSB, XPG and XPD gene, arguing that they constitute part of one continuing clinical spectrum (Graham et al., 2001; Meira et al., 2000).

The severe developmental and neurological features observed in CS patients can not be attributed to a NER defect alone (Bootsma and Hoeijmakers, 1993). In agreement with the previously suggested role of CSA and CSB in transcription, transcriptional deficiency, presumably induced by DNA damage, may also contribute to the clinical picture. Cells from CS patients are not only sensitive to UV, but also to IR (Deschavanne et al., 1984) suggesting that CSB is also involved in repair of other types of damages (e.g. oxidative damage). Therefore, an inability to repair both UV- and endogenous DNA lesions combined with transcriptional deficiency likely underlies the CS phenotype as well as the observed heterogeneity.

Since many of the features observed in CS (e.g. neurologic degeneration, kyphosis, cataracts) are also found in the naturally aging population, this disease has been classified as a segmental premature aging syndrome (Martin, 2005). The term segmental is often used to point out that some, but not all, of the features associated with normal aging are found to be accelerated.

1.3.3 Trichothiodystrophy

The hallmarks of Trichothiodystrophy (TTD) are Photosensitivity, Ichthyosis, Brittle hair and nails, Intellectual impairment, Decreased fertility and Short stature (referred to by the acronym PIBIDS) (Itin et al., 2001; Lehmann, 2001) (Figure 3B). Other prominent features are an aged appearance and shortened lifespan. Also, skeletal abnormalities like osteopenia, axial osteosclerosis, peripheral osteoporosis (McCuaig et al., 1993), kyphosis (Norwood, 1964) and retardation of skeletal age are often observed. Whereas the brittle hair and nails are unique to TTD patients, other features are strikingly similar to CS, including the absence of cancer predisposition. The abnormalities typical for this disease are generally noted around birth. The brittle hair is caused by a reduction of cystein-rich matrix proteins that normally provide strength to the hair shaft by crosslinking the keratin filament (Itin and Pittelkow, 1990; Stefanini et al., 1993). Furthermore, lab diagnosis of UV-sensitive TTD cells shows UDS levels at about 50% of WT. Hence, by measuring UDS in cells and isolated hair follicles, a positive diagnosis for UV-sensitive TTD can be made. Up to now, mutations in three genes have been found to cause TTD, namely *XPD*, *XPB* and *TTDA*. Since most of the symptoms are quite similar to that of CS, TTD has likewise been classified as a segmental premature aging syndrome (Martin, 2005).

Fascinatingly, non-UV-sensitive forms of TTD also exist. As the name suggests, patients display all TTD features except for cutaneous photosensitivity. Recently, the first gene that causes this form of TTD was identified: *C7orf11*. Although no UV-sensitivity could be detected, this gene was found to localize to the nucleus and is therefore thought be involved in transcription rather than DNA repair (Nakabayashi et al., 2005).

Interestingly, mutations in either the *XPD* or *XPB* gene can give rise to three disorders, namely XP, XP/CS or TTD (de Boer and Hoeijmakers, 2000; Lehmann, 2001). This, together with the fact that the XPB and XPD proteins are not only involved in NER, but (as part of the TFIIH complex) are also involved in transcription, and the fact that mutations causing TTD are all found in components of the TFIIH complex, caused Bootsma and Hoeijmakers to speculate that the TTD phenotype is a combination of a repair deficiency together with a transcription deficiency (Bootsma and Hoeijmakers, 1993). The transcriptional defect in TTD is likely responsible for the brittle hair and ichthyosis phenotype of (Bootsma et al., 1995; Stefanini et al., 1993) as TTD mutations in XPD are found to cause instability of the TFIIH complex, which results in depletion of this transcription initiation factor prior to completion of terminal differentiation of hair and skin, which are consequently unfinished. The occurrence of non-UV sensitive forms of TTD in which repair is not affected, strengthens this hypothesis. In addition, the TCR hypothesis suggests that proteins involved in CS are not only needed for TC-NER, but also for a more general TCR pathway that deals with the removal of any lesion that would block transcription, which includes oxidative lesions that are normally repaired by BER (Citterio et al., 2000; Cooper et al., 1997). The fact that CS cells are sensitive to oxidative DNA damaging agents supports this notion (de Waard et al., 2003; Deschavanne et al., 1984; Spivak and Hanawalt, 2006).

The complex involvement of NER genes in these different inherited human disorders that display cancer and/or segmental aging features, underscores the importance of this repair pathway for both processes. Whereas the UV sensitivity and cancer predisposition of these patients can be well explained by the gene defect, it poorly explains many of the non-UV related features, which have been, so far, puzzling. To this end, the generation of mouse models mimicking these disorders has shed some light on the underlying pathogenic mechanism as well as the cause of the non-UV related phenotype.

1.4 Mouse models for NER disorders

To study the consequences of mutations in NER genes, as well as the etiology of NER disorders at the level of the intact organism, mouse models were generated mimicking existing human NER mutations or else deletion of a few exons. Since NER is involved in the repair of several, potentially mutagenic and/or carcinogenic DNA lesions, these models represent powerful tools to screen for sensitivity to a variety of genotoxic substances. However, certain factors need to be taken into account when studying mouse models for human diseases. For instance, there are documented differences between the repair characteristics of mouse and man, one of them being that CPDs are less efficiently removed from the non-transcribed strands of active genes and the remainder of the genome in rodents as compared to humans (Bohr et al., 1985). Next, there is a substantial difference between the lifespan of mice and men, and many of the observed clinical features of human NER syndromes are age-dependent evolving in a time period considerably longer than the mouse lifespan. Also, distinct genetic backgrounds of mouse strains demonstrate a high phenotypic diversity. This can influence both embryonic lethality as well as the lifespan of a given NER mutation in a specific background. The latter represents an important factor that should be taken into account at all times, especially when comparing phenotypes of the same mouse model between different labs. Finally, considerable differences have been documented between human and mouse fibroblasts cultured under 20% oxygen in respect to onset of their replicative senescence and/or spontaneous transformation (Parrinello et al., 2003). This suggests that it is challenging (or even impossible) to make parallels between the growth characteristics of human and mouse cells.

Nevertheless, the substantial contribution of existing NER mouse models in elucidating the underlying causes of human NER diseases is widely acknowledged.

1.4.1 XPA

Two independent XPA knock-out mouse models have been generated, both of which are viable and develop normally (de Vries et al., 1995; Nakane et al., 1995) (Figure 4A). *Xpa*$^{-/-}$ MEFs are impaired in the expected NER characteristics UDS and RRS. In addition survival of *Xpa*$^{-/-}$ fibroblasts is extremely low after exposure to UV or dimethyl-benz[*a*]anthracene (DMBA). *Xpa*$^{-/-}$ animals do not show enhanced spontaneous mortality up to 1.5 years of age, yet a slightly enhanced level of spontaneous liver carcinomas and lymphomas has been reported (de Vries et al., 1997). Importantly, *Xpa*$^{-/-}$ mice are an excellent model to study UV-induced carcinogenesis in the skin as observed in XP patients. UV exposure of *Xpa*$^{-/-}$ mice first leads to hyperkeratosis and erythema (sunburn) together with massive epidermal hyperplasia. Long-term UV exposure of *Xpa*$^{-/-}$ mice leads to a high incidence of skin tumours, especially squamous cell carcinomas.

In agreement with these findings, an enhanced mutation frequency is observed in DNA from spleen, lung and liver of *Xpa*$^{-/-}$ mice, not only after treatment with the DNA-damaging agent benzo[a]pyrene (B[a]P) (de Vries et al., 1997), but also spontaneously with age in DNA of the liver (Giese et al., 1999). Additionally, XPA-deficient animals are sensitive to a broad class of DNA damaging agents such as the carcinogen DMBA, benzo[*a*]pyrene B[a]P, N-OH-AAF (2AAF) and 2-amino-1-methyl-phenylimidazo[4.5-*b*]-pyridine (PhIP). For example, treatment with DMBA by topical administration leads to acute skin defects like acanthosis, epidermal hyperplasia and an increase in papillomas, and oral B[a]P treatment results in increased levels of lymphomas (de Vries et al., 1995; Nakane et al., 1995). This suggests that a wide variety of DNA lesions is repaired by NER, thereby making *Xpa*$^{-/-}$ mice a very important mouse model in the identification of new carcinogens and their effects on different tissues (van Steeg et al., 1998). Taken together, *Xpa*$^{-/-}$ mice show a strong cancer predisposition, but lack prominent features of accelerated aging.

1.4.2 XPC

Similar to the *Xpa*$^{-/-}$ mice, two independent *XPC* knockout mice were generated that are both viable and develop normally. In contrast to *Xpa*$^{-/-}$ mice, however, *Xpc*$^{-/-}$ animals have not been noted to display an increase in spontaneous tumor frequency (Cheo et al., 1997; Sands et al., 1995). Consistent with the role of XPC in GG-NER, *Xpc*$^{-/-}$ MEFs demonstrate impaired UDS, and normal RRS. Similar to *Xpa*$^{-/-}$ mice, *Xpc*$^{-/-}$ animals develop skin tumors upon UV exposure. (Berg et al., 1998; Cheo et al., 2000). Although the GG-NER defect leads to skin cancer susceptibility, the acute effects of sun sensitivity as seen for the *Csb*$^{m/m}$ mouse are not influenced (see below), which means that this must be due to a TC-NER defect. Additionally, *Xpc*$^{-/-}$ mice are sensitive to various chemical genotoxic agents like 2AAF (or N-OH-AAF), DMBA and PhIP (Cheo et al., 1999). Furthermore, an age-related elevation in spontaneous mutation frequency has been found in *Xpc*$^{-/-}$ mice, as opposed to both *Xpa*$^{-/-}$ and *Csb*$^{m/m}$ mice (Wijnhoven et al., 2000). Although previous reports fail to demonstrate increased spontaneous tumorigenesis in *Xpc*$^{-/-}$ animals, it was recently found that these GG-NER deficient animals do develop multiple spontaneous long tumors (Hollander et al., 2005), (van Steeg et al., personal communication). Surprisingly, *Xpc*$^{+/-}$ animals also demonstrate a higher spontaneous mutation frequency and increased skin cancer predisposition as a result of UV exposure. The latter suggests that haplo-insufficiency of the *XPC* gene is present, at least in the mouse (Cheo et al., 2000). This could also imply an important risk factor for UV-induced skin cancer in humans. In support of this notion, inactivation of one XPC allele in *Csa*$^{-/-}$ mice results in enhanced UV-mediated skin cancer sensitivity (van der Horst et al., 2002). This observation might point to the fact that XPC is a rate-limiting factor for GG-NER, consistent with findings reported at the cellular level.

1.4.3 CSB and CSA

An animal model for CS-B was generated by mimicking a mutation found in a CSB patient (CS1AN mutation: Lys337→stop), resulting in a N-terminal truncation of the CSB protein at amino acid 343 in the mouse, rendering the TC-NER pathway inactive (van der Horst et al., 1997) (figure 4B). *Csb*$^{m/m}$ MEFs and mice exhibit all CS repair characteristics: both are sensitive to UV, have defective TC-NER yet they are normal in GG-NER. *Csb*$^{m/m}$ mice show a mild UV- and DMBA-induced cancer predisposition (van der Horst et al., 1997). This seems to be in contrast to CS-B patients, which do not show elevated UV-induced skin cancer predisposition. This discrepancy could be attributed to the man-mouse differences in the efficiency of GG-NER of some types of lesions. Alternatively, it could also be explained by the fact that the diagnosis for CS is made early in the life of a patient so that there has not been sufficient exposure to UV to induce cancer whereas after the diagnosis has been made, measures are taken to avoid further exposure, together with the fact that the doses to which *Csb*$^{m/m}$ mice were exposed are much higher than those that humans are normally exposed to.

In addition to UV sensitivity, *Csb*$^{m/m}$ mice also display mild CS symptoms such as reduced body weight, photoreceptor loss and slightly abnormal behavior in various tests, pointing to mild neurological impairment (van der Horst et al., 1997). Furthermore, a cohort study of *Csb*$^{m/m}$ animals revealed karyomegaly and/or polyploidy in the kidney of aging mutant animals, all hallmarks of natural aging in wild type mice (van Steeg et al., unpublished). Importantly, cells from *Csb*$^{m/m}$ mice are sensitive towards IR and other types of oxidative stress producing chemicals, like paraquat (de Waard et al., 2003). *Csb*$^{m/m}$ animals show slightly increased sensitivity upon exposure to X-rays and the peroxisome proliferator di (2-ethylhexyl) phthalate (DEHP) (de Waard et al., 2004). In agreement, the presence of (UV-induced) DNA lesions in actively transcribed genes is very toxic to the cell (Berg et al., 2000; Wijnhoven et al., 2001). This suggests that the accumulation of endogenous (oxidative) damage could contribute to the (mild) aging phenotype observed in *Csb*$^{m/m}$ mice (and CS patients). Yet, the levels of unrepaired endogenous DNA damage in *Csb*$^{m/m}$ mice may be too low to have an effect on their life span or otherwise to induce a severe phenotype. Other (redundant) pathways might take over minimizing the repair defect.

The CS-A mouse model was made by disrupting exon 2 of the *Csa* gene, giving rise to a complete null mutant, thereby (like in the *Csb*$^{m/m}$ mouse) inactivating the TC-NER pathway (van der Horst et al., 2002). As seen for the *Csb*$^{m/m}$ mouse, *Csa*$^{-/-}$ mice appear not only sensitive to UV and DMBA, but similarly demonstrate mild growth failure and neurological abnormalities. An important difference between both models, however, is that *Csa*$^{-/-}$ mice are not sensitive to DEHP as *Csb*$^{m/m}$ mice and that *Csa*$^{-/-}$ cells are less sensitive to IR and paraquat than *Csb*$^{m/m}$ cells (de Waard et al., 2003). *Csa*$^{-/-}$ cells, however, appear more sensitive to mitomycin C (de Waard et al., 2004). Therefore, it could be that both CSA and CSB are involved in TC-(NE)R of UV-lesions and endogenous lesions, but exhibit variation in lesion specificity.

Taken together, both mouse models demonstrate mild progeria with rather mild cancer predisposition, only observed after exposure.

1.4.4 TTD

So far, attempts to make viable knock-out mouse models (or even cells) for XP-B or XP-D by complete inactivation of the XPB or XPD gene have failed, thereby supporting the crucial role of TFIIH in transcription (de Boer et al., 1998b). A viable TTD mouse model was generated by mimicking a causative TTD point mutation in man within the *Xpd* gene (TTD1BEL; Arg722→Trp) (de Boer et al., 1998a) (Figure 4C). These animals faithfully recapitulate many symptoms present in the patient; *Xpd*^{TTD} mice have a reduction of hair-specific cysteine-rich matrix proteins resulting in brittle hairs, which is a hallmark feature of the disorder. Additionally, *Xpd*^{TTD} animals develop progeroid symptoms like growth delay, osteoporosis (trabecular bone loss in the femur), osteosclerosis, kyphosis, gray hair, cachexia and a reduced fertility and lifespan (de Boer et al., 1998a), (Diderich et al., submitted). It was hypothesized that the observed aging features were caused by unrepaired DNA damage that compromises transcription, leading to functional inactivation of critical genes and enhanced apoptosis (de Boer et al., 2002). Apart from the observed aging phenotype, *Xpd*^{TTD} animals are mildly UV and DMBA sensitive, although recent findings suggest that this feature is not noted when the animals are maintained in a hairless background (Rebel et al., unpublished results). In accordance with their NER defect, *Xpd*^{TTD} cells have reduced NER capacity and are mildly sensitive to UV and DMBA. *Xpd*^{TTD} animals have also been observed to have induced skin carcinogenesis (in contrast to human TTD patients), but much less than *Xpa*$^{-/-}$ mice. Similar to *Csb*$^{m/m}$ mice, this may be attributed to the inability of rodents to repair certain types of UV-induced DNA lesions by GG-NER (Bohr et al., 1985). Wijnhoven et al. extensively studied the pathology of a cohort of 45 *Xpd*^{TTD} females, which revealed that the *Xpd*^{TTD} phenotype consists of 1) aging-related, 2) TTD-specific and (paradoxically) 3) caloric restriction (CR) features. The aging-related phenotype consisted of a reduced body weight (noticed from 13 weeks onwards) and a reduced lifespan, confirming the previously observed phenotype. Furthermore, aging-related pathology, including reduced amounts of subcutaneous fat in the skin and abdominal cavity, cachexia, anemia and ovarian dysfunction were found. The premature aging phenotype of *Xpd*^{TTD} mice is further underlined by the enhanced accumulation of lipofuscine (a known marker for aging) in liver Kupffer cells (Wijnhoven et al., 2005). They hypothesized that the aging-related features are caused by a defect in DNA repair, whereas the TTD specific characteristics are most probably due to a transcription defect. Interestingly, *Xpd*^{TTD} mice also showed signs suggestive of caloric restriction (CR), like diminished incidence of cataract and pituitary adenomas. CR is a condition in which mice are limited in their caloric intake of food, and this type of intervention has been associated with retardation of age-related pathology and life extension. Since the CR related phenotype is not caused by a decreased food intake, the authors speculate that this might represent an attempt to lower ROS (Wijnhoven et al., 2005). From the above studies, it has become evident that many of the TTD features are reminiscent of premature aging (de Boer et al., 2002; Hasty et al., 2003), again pointing to the involvement of unrepaired DNA damage in inducing an aging phenotype.

A knock-in mouse model for the rare combined cancer and progeroid disorder XPCS was recently generated (*Xpd*^{XPCS} mice) by mimicking a patient-derived point mutation in XPD (XPD^{G602D}). Strikingly, *Xpd*^{XPCS} mice are more skin cancer prone than *Xpa*$^{-/-}$ animals. Moreover, *Xpd*^{XPCS} mice also displayed symptoms of segmental progeria including cachexia and progressive loss of germinal epithelium. These data indicate that cancer and segmental progeria can be experimentally modulated by different point mutations in a single DNA repair-associated gene as was previously discussed for the human XPD gene (Andressoo et al., 2006).

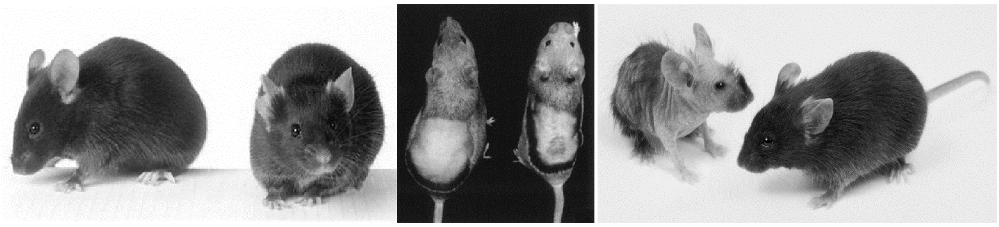

Figure 4. Mouse models for human NER-deficient syndromes: XPA, CSB, and TTD. *Picture of an adult Xpa*$^{-/-}$ *mouse together with its wt littermate (left). The Xpa*$^{-/-}$ *mouse has no obvious aberrant phenotype (courtesy of Harry van Steeg). Picture of an adult Csb*$^{m/m}$ *mouse together with its wt littermate (middle). Note the erythema on the skin of UV-irradiated Csb*$^{m/m}$ *mice (adapted from (van der Horst, van Steeg et al. 1997)). Picture of an adult Xpd*^{TTD} *mouse together with its wt littermate (right). Note the brittle hair, which is a hallmark feature of TTD in humans. Progeroid symptoms (cachexia and kyphosis) start to develop in TTD mice at age 3 to 4 months onward and become increasingly severe (adapted from (de Boer and Hoeijmakers 1999)).*

1.4.5 XPG

Xpg$^{-/-}$ animals were made by knocking out exon 3 of the XPG gene resulting in a null mutant (Harada et al., 1999). The animals suffered from postnatal growth failure and premature death varying from day 3 to 24 postpartum. Additionally, the intestine and spleen were found to be relatively small and the liver displayed remarkably small hepatocytes. Also, primary MEFs experienced premature senescence, early onset of immortalization and accumulation of p53. Since, apart from its role in NER, XPG is required for TCR of thymine glycol by BER and is thought to be involved in TCR of oxidative DNA damage, it is surprising to find that *Xpg*$^{-/-}$ MEFs are not sensitive to H_2O_2 or γ-irradiation (Harada et al., 1999). A similarly severe phenotype was found in the *Xpg*$^{D811STOP/D811STOP}$ mouse, in which the last 360 amino acids of the XPG protein were deleted (Shiomi et al., 2004). In yet another XPG mutant mouse, a point mutation was introduced into exon 11, rendering the nuclease catalytic site inactive (*Xpg*$^{D811A/D811A}$) (Shiomi et al., 2004). This mutation did not result in the severe phenotype as observed for the *Xpg*$^{-/-}$ mouse. However, it did result in hypersensitivity of these *Xpg*$^{D811A/D811A}$ mice to UV. Similarly, deletion of exon 15 of the *XPG* gene (*Xpg* $^{\Delta ex15/\Delta ex15}$) resulted in UV-sensitivity without any severe phenotype observed in the mouse (Wang et al., 2006). Since both the D811A and Δex15 mutation only affected the NER function of XPG, these results suggest that the severe phenotype observed in the *Xpg*$^{-/-}$ mouse is due to a function of XPG outside the context of NER.

1.4.6 Ercc1

So far, mutations in the human *ERCC1* gene have not been reported to be associated with human disease. Yet, a defect in the mouse *Ercc1* gene (giving rise to a complete null mutant) results in viable mice with a severe phenotype (McWhir et al., 1993; Weeda et al., 1997) (Figure 5C). *Ercc1*$^{-/-}$ mice are born at Mendelian frequency (in a hybrid Fvb|C57Bl6/J F1 background) and, apart from a 10% reduction in size and body weight, are indistinguishable from wild-type littermates at birth and through the first week of life. However, soon after that they develop an accelerated, segmental aging phenotype. Besides cachexia and sarcopenia, *Ercc1*$^{-/-}$ mice display characteristics of dystonia and progressive ataxia. In addition, ferritin deposition in spleen, progressive renal and liver dysfunction as well as hepatocellular polyploidization and intra-nuclear inclusions in the liver were observed, which are considered symptoms associated with age-related pathology in mammals (McWhir et al., 1993; Weeda et al., 1997). Additionally, *Ercc1*$^{-/-}$ mice demonstrate multilineage cytopenia and fatty replacement of bone marrow, similar to old wild-type mice, together with reduced hematopoietic progenitors and stress erythropoiesis (Prasher et al., 2005). *Ercc1*$^{-/-}$ mutant cells are not only compromised in NER and crosslink repair, but also undergo rapid, premature replicative senescence. In line with this observation, p53 accumulation has been detected in liver, kidney and brain and p21 accumulation was observed in *Ercc1*$^{-/-}$ MEFs (Chipchase et al., 2003; Melton et al., 1998), (Niedernhofer et al., unpublished observations).

Another ERCC1 mouse model, *Ercc1*$^{\Delta7/\Delta7}$, expresses the ERCC1 protein with a 7 amino-acid carboxy terminal truncation (Weeda et al., 1997), resulting in a milder phenotype, when compared to the *Ercc1*$^{-/-}$ mouse (Niedernhofer et al., unpublished results). Interestingly, this mutation partially inactivates the repair function of ERCC1 but does not cause dramatic protein instability. Initial experiments with a limited number of *Ercc1*$^{\Delta7/-}$ mice revealed *Ercc1*$^{-/-}$ features like kyphosis, infertility, progressive cachexia, sarcopenia and liver polyploidy, but with onset at an older age. Although these animals also exhibit retarded growth and premature death (about 6 months of age), this is not considered as pronounced as that observed in the *Ercc1*$^{-/-}$ mouse. Moreover, the *Ercc1*$^{\Delta7/-}$ mouse show signs of progressive neurodegeneration, e.g. dystonia, ataxia and priapism (Niedernhofer, unpublished results).

Since *Xpa*$^{-/-}$ mice -that are totally NER-deficient-, do not show signs of aging, the progeria observed in the *Ercc1*$^{-/-}$ or *Ercc1*$^{\Delta7/-}$ mouse can not be due solely to their NER defect. Instead, the involvement of ERCC1 in crosslink repair could give rise to the accumulation of interstrand crosslinks in these *Ercc1*$^{-/-}$ or *Ercc1*$^{\Delta7/-}$ animals, that are extremely toxic DNA lesions for cells and organisms.

1.4.7 XPF

XP-F patients have only mild symptoms of photosensitivity. However, in these patients the causative XPF mutations usually do not give rise to complete loss of functions, resulting in residual repair activity. Most probably, complete null mutants are incompatible with life. Therefore, an XPF knockout mouse was created by mimicking a point mutation (XP23OS) reported to be found in XP-F patients, which resulted in an early STOP (with the other allele being a null), and which was presumed to be compatible with human life. Although initial development seemed normal, *Xpf*$^{m/m}$ pups lagged behind in growth. At about 3 weeks of age the animals died of unknown cause. As was observed for the *Ercc1*$^{-/-}$ mouse, the liver showed cells with enlarged nuclei. MEFs showed no obvious growth defects, but were sensitive to UV and also MMC (Tian et al., 2004).

1.4.8 NER double mutant mouse models and the link with aging

It is interesting to note that *Csb*$^{m/m}$, *Csa*$^{-/-}$ (TC-NER deficient), *Ercc1*$^{-/-}$, *Ercc1*$^{\Delta7/-}$ and *Xpd*^{TTD} mice (partial NER defect), display aging symptoms, whereas both *Xpc*$^{-/-}$ and *Xpa*$^{-/-}$ mice, defective in

GG-NER and the entire NER process respectively, do not have any overt aging phenotype. This would suggest that CSA, CSB and XPD proteins have additional functions outside the context of NER, which, when defective, result in an aging phenotype. Interestingly, when Xpd^{TTD} mice were crossed to $Xpa^{-/-}$ animals in order to generate double mutant mice and study the effect of a total NER deficiency in the Xpd^{TTD} mouse model, this resulted in an accelerated premature aging phenotype (de Boer et al., 2002) (Figure 5A), which included retarded growth, cachexia, disturbed gait, excessive hypodermal keratosis, spinal kyphosis and severely shortened lifespan. Likewise, when $Csb^{m/m}$ or $Csa^{-/-}$ mice were crossed to either $Xpa^{-/-}$ or $Xpc^{-/-}$ mice, this resulted in a very severe phenotype, including growth retardation, neurological abnormalities and an extremely short life span. (Murai et al., 2001) (Figure 5B). In contrast, $Xpc^{-/-}/Xpa^{-/-}$, $Csb^{m/m}/Csa^{-/-}$ and $Xpc^{-/-}/Xpd^{TTD}$ animals were viable and quite normal.

Taken together, these findings suggest that a complete NER deficiency in combination with a CSA, CSB or XPD is necessary to induce this premature aging phenotype. Similar, but not always identical, phenotypes have been observed for the previously mentioned $Ercc1^{-/-}$, $Xpf^{m/m}$ and $Xpg^{-/-}$ mice, and this could indicate that these animals too display aging features. Moreover, when the previously mentioned $Xpg^{\Delta ex15/\Delta ex15}$ mouse was crossed to $Xpa^{-/-}$ mice to generate double mutant mice, this also resulted in a similarly severe phenotype (Shiomi et al., 2005).

The above-mentioned mouse models have in common that DNA repair is impaired and some of them have been shown to display signs of a premature aging phenotype (de Boer et al., 2002; Weeda et al., 1997). Because these animals have not been subjected to exogenous DNA-damaging agents, this could point toward the contribution of unrepaired endogenous DNA damage to the observed aging phenotypes.

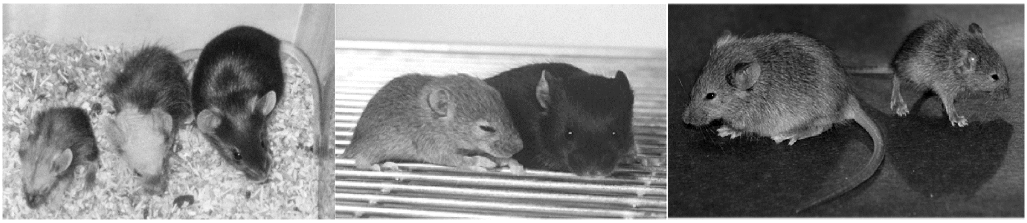

Figure 5. Mouse models with accelerated progeroid symptoms: $Xpd^{TTD}Xpa^{-/-}$, $Csb^{m/m}Xpa^{-/-}$ and $Ercc1^{-/-}$. *Photograph of a 3-week-old* $Xpd^{TTD}Xpa^{-/-}$ *double-mutant,* Xpd^{TTD}*, and* $Xpa^{-/-}$ *mouse (left). These* $Xpd^{TTD}Xpa^{-/-}$ *double mutants develop severe growth retardation, neurologic abnormalities, kyphosis (indicative of osteoporosis), and extreme cachectic appearance. (adapted from de (de Boer, Andressoo et al. 2002)) Photograph of a 3-week-old* $Csb^{m/m}Xpa^{-/-}$ *double-mutant and an age-matched* $Xpa^{-/-}$ *mouse (middle). These* $Csb^{m/m}Xpa^{-/-}$ *double mutants develop growth retardation, neurological abnormalities and an extremely short life span. Photograph of a 3-week-old* $Ercc1^{-/-}$ *mouse and wt control (right).* $Ercc1^{-/-}$ *mice develop an accelerated, segmental aging phenotype, including cachexia, sarcopenia and progressive ataxia (courtesy of Laura Niedernhofer).*

1.5 Other genome instability syndromes and mouse models with progeria

1.5.1 Human syndromes with progeria

Progeroid features are not an exclusive hallmark of the NER disorders CS, COFS, XP/CS and TTD. Other well-known examples of progeroid syndromes are Werner Syndrome, Bloom Syndrome and Hutchinson-Gilford progeria.

About 1300 cases of Werner Syndrome (WS) have been described, making it the most commonly known progeroid syndrome (Shimamoto et al., 2004). Patients with WS suffer from cancer predisposition and segmental progeria, including short stature, alopecia, atrophic skin, thin gray hair, type II diabetes, osteoporosis, cataracts, arteriosclerosis and atherosclerosis. WS patients die usually in their fifth decade of life from cardiovascular disease or cancer (Kipling et al., 2004). The mutated gene responsible for this severe disease is *WRN*, which encodes a RecQ-like helicase with 3’-5’ exonuclease activity and 3’-5’ helicase activity, involved in resolving secondary DNA structures (Gray et al., 1997). One of the major functions of WRN is thought to be the reinitiation of stalled replication forks. When WRN is absent, these structures are resolved by a complex mechanism involving illegitimate recombination causing deletions, resulting in cell cycle arrest in the S phase (Rodriguez-Lopez et al., 2002). Therefore, a defect in this gene disrupts primarily DNA synthesis, resulting in genomic instability. Accordingly, WS cells cultured *in vitro* have a limited capacity to replicate, having on average only 20 population doublings (PD), whereas WT cells can reach 40-100 PDs, a process that is called replicative senescence. In addition, WRN has been implicated in telomere metabolism. A comparative cDNA microarray study performed on cells of WS patients and those of ‘normal’ young and old individuals revealed a high similarity between WS and natural aging. A large percentage of genes that showed similarity have a function in the processing of either RNA or DNA (Kyng et al., 2003), reviewed in (Puzianowska-Kuznicka and Kuznicki, 2005). Although it is still unclear what exactly causes the premature aging phenotype in WS patients, one possibility could be that the combination of defective genome maintenance with the mutator phenotype and replicative senescence of WS cells give rise to the observed WS phenotype.

Bloom Syndrome (BS) is characterized by growth deficiency with prenatal onset, resulting in short stature. Other important features are a birdlike face, sensitivity to sunlight, skin lesions, disproportionally long extremities, hyper- and hypopigmentation, immunodeficiency at a variable degree, diabetes mellitus, fertility problems and an unusually high incidence (150-300 fold) of many types of cancer at an early age (Risinger and Groden, 2004). BS is believed to be the most malignancy prone chromosomal disorder (Kaneko and Kondo, 2004). The affected gene is *BLM*, which belongs to the same RecQ-like helicase family as WRN and encodes a 3’ to 5’ DNA helicase (Karow et al., 1997). BLM is necessary for normal double strand break (DSB) repair and is particularly involved in the unwinding of DNA structures like Holiday junctions and D-loops (Karow et al., 2000; Sun et al., 1998). Its function is to maintain genome stability by suppressing illegitimate recombination between imperfect homologous sequences (Kaneko and Kondo, 2004) and in the resolution of DNA intermediates that arise during homologous recombination reactions (Wu et al., 2005). The majority of mutated BLM proteins fails to translocate to the nucleus, resulting in increased sister chromatid exchange (SCE) and an abnormal profile of DNA replication intermediates (Risinger and Groden, 2004), which results in defective replication and repair. Furthermore, defective p53 dependent apoptosis and absence of p53 were detected in BS cells. Most probably this abnormal regulation of p53 together with the observed genome instability is involved in the cancer-prone phenotype of BLM patients (from (Puzianowska-Kuznicka and Kuznicki, 2005)).

Most people recognize progeria from having seen children with Hutchinson-Gilford progeria (HGPS) (Figure 6), of which about 100 cases have been described in medical journals. Although HGPS patients have a normal appearance at birth, the typical manifestations of the disease develop gradually in the next 6-12 months. These features are: short stature, prominent eyes, alopecia, atrophic skin, reduced subcutaneous fat, osteoporosis with pathologic fractures and cardiovascular disease (Sarkar and Shinton, 2001). Signs of brain aging are not apparent, as both the intelligent and emotional development are normal. Importantly, like CS, no increased risk of malignancies has been found. The median age at death is about 13.4 years (for review see (Baker et al., 1981; Pollex and Hegele, 2004)). Recently, the gene mutated in this disease was found to be *LMNA*, which encodes both the lamin A and C protein (Cao and Hegele, 2003; De Sandre-Giovannoli et al., 2003; Eriksson et al., 2003; Novelli et al., 2002). Both proteins are components of the nuclear lamina, a structure near the inner nuclear membrane that is involved in many genome maintenance processes, like chromatin organization, cell cycle and apoptosis regulation and the processing of DNA and RNA. Considering the many functions of the nuclear lamina, it is not difficult to envision that disruption of this structure leads to genomic instability, reviewed in (Lans and Hoeijmakers, 2006; Puzianowska-Kuznicka and Kuznicki, 2005; Vijg and Calder, 2004).

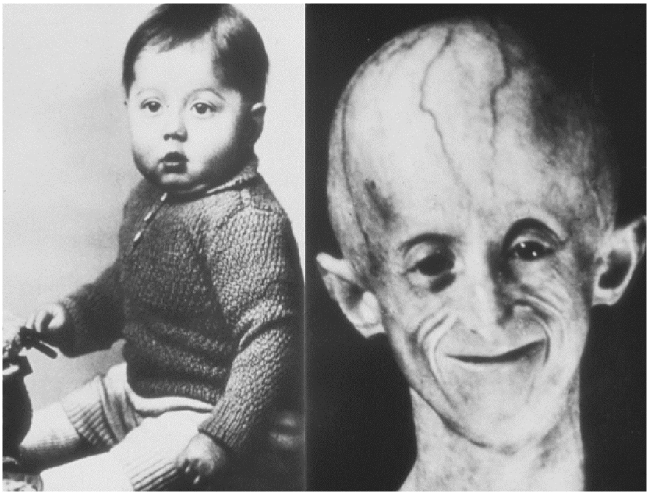

Figure 6. Patient with Hutchinson-Gilford progeria. *Picture of a patient with HGPS. These patients have a normal appearance at birth; the typical manifestations of the disease develop gradually in the next 6-12 months. These features include short stature, prominent eyes, alopecia, atrophic skin and reduced subcutaneous fat.*

Although it is not generally believed that the above-mentioned progeroid syndromes represent true physiological aging, they all do show many hallmarks of accelerated aging. Therefore, taking a closer look at the mutated genes that are responsible for these segmental aging syndromes might learn us more about the actual aging process. It is striking that in most progeroid syndromes, protein defects affect one or more functions in the maintenance or caretaking of the genome. This suggests that failure to maintain genome integrity underlies at least some aging phenotypes or aging-related pathologies.

1.5.2 Mouse models with progeria

Besides the previously mentioned mouse models for NER genes, other mouse models for genes involved in genome stability also display progeroid features.

P53 plays a very important role in different cellular functions like cell cycle control, apoptosis, and transcription. It has been known for a long time as a tumour suppressor gene and inactivation of this gene both in cells as well as in the mouse (*p53*$^{-/-}$ animals) logically gives rise to cancer (Jacks et al., 1994). P53 can also promote repair and has recently been connected to aging. A *p53*$^{m/+}$ mouse that expressed a mutant p53 protein which enhanced wildtype p53 activity (Tyner et al., 2002) displayed dwarfism, osteopenia, generalized organ atrophy, lymphoid atrophy, osteoporosis, atrophic skin, diminished stress tolerance, decreased cancer incidence and a decreased longevity. Thus, modulated forms of p53 can either give rise to cancer or a decreased lifespan, which is reminiscent of NER-deficient disorders.

Ku80$^{-/-}$ mice, defective in NHEJ, have several aging symptoms including osteoporosis, premature growth failure, incomplete plate closure, atrophic skin, liver pathology, sepsis, cancer and a shortened life-span. Furthermore, their sensitivity to ROS is also increased (Gu et al., 2000; Nussenzweig et al., 1996; Zhu et al., 1996).

mTR knockout mice are defective in the catalytic subunit of telomerase. Normally, when telomeres become too short, cell division stops and replicative senescence follows (Blasco et al., 1997). Hence, *mTR*$^{-/-}$ present with alopecia, skin ulcerations, impaired wound healing, cancer and a shortened lifespan in their fifth generation, when telomeres are sufficiently shortened (Herrera et al., 1999; Rudolph et al., 1999). Interestingly, a WRN knock-out mouse was generated to model WS, and although it mimicked the cellular phenotypes observed in WS (mutator phenotype and sensitivity to DNA-damaging agents), it did not at all show a premature aging phenotype (Lombard et al., 2000). However, when this mouse model was ‘humanized’ by crossing it to *mTR*$^{-/-}$ animals (thereby shortening their telomeres considerably) they did show an aging phenotype similar to that observed in WS patients (Du et al., 2004). This observation might signify a role for telomere shortening in the premature aging phenotype of WS patients.

The above mentioned mouse models together with the previously described NER deficient mouse models all have in common that they are defective in a process involved in genome maintenance and as a result suffer from age-related pathologies. It is striking that defects in genes involved in the maintenance of DNA give rise to progeroid features. This again, points to the fact that DNA integrity plays an important role in the aging process.

1.6 The DNA damage-aging connection

1.6.1 Current aging theories

Helfand and Rogina defined aging as the inevitable consequence of being a multicellular organism, associated with a random, passive decline in function, leading to global loss of homeostasis and increased mortality with advancing age (Helfand and Rogina, 2003). This notion suggests that aging is a complex multifactorial process, responsible for the deterioration of an organism over time and inevitably leading to organismal death. However, an accurate description of aging is currently lacking. For example, aging, senescence and age-related diseases are often interchangeably used, though they do not always represent the same thing. Interestingly, the maximum organismal lifespan is directly linked to aging, whereas lifespan extension is often perceived as an anti-aging strategy (Liang et al., 2003; Longo and Finch, 2003). However, defeating a disease that would otherwise severely limit organismal life span, (*e.g.* cancer) does not necessarily imply an anti-aging strategy itself. Even more, secondary effects may often obscure the primary source of aging, which might not be consistent in its nature or unique in its origin. For example, when trying to find the cause of aging, one should bear in mind that different organisms, tissues or even types of cells might actually age differently underlying the possibility that one unifying aging theory might not exist. Many distinct and overlapping theories attempt to explain the complicated mechanism of aging (For a comprehensive review see (Kirkwood and Austad, 2000)). The genetic imprinting theory (first postulated by (Weismann, 1889)) and the mutation accumulation theory of aging (first postulated by (Medawar, 1952)) appear as two representative, entirely different, examples.

Developmental geneticists believe that aging is genetically imprinted, as are development and maturation (Weismann, 1889). This implies that aging is an active process, initiated by the organism itself. Nevertheless, it seems unlikely that genes contributing to aging were positively selected for in evolution and evidence for this theory is scarce. In the mutation accumulation theory (Medawar, 1952), it is hypothesized that aging results from random accumulation of mutations in genes ultimately leading to pathology and senescence. Since these mutations would be expected to act late in the life of an organism, they might have escaped selective pressure. Although this theory seems unquestionable for cancer, it is unlikely that age-related disease such as neurodegeneration is also caused by accumulation of mutations, since the brain is a post-mitotic tissue. Also, the fact that XPC mice have a high spontaneous mutation frequency, but do not experience aging features (Cheo et al., 2000), argues against this theory. Other more generally accepted theories of aging are discussed in further detail below.

The disposable soma theory argues that the “soma” is maintained to ensure reproductive success (Kirkwood and Rose, 1991). It is hypothesized that aging results from the gradual accumulation of damage in cells and tissues during this process. Organisms are not programmed to age, but rather to survive long enough to ensure successful reproduction by using their intricate network of cell-maintenance and stress-response systems. One could simplify this theory by saying that the mere reason for the soma to exist is to ensure reproduction. Once reproductive capacity has ceased, there is no further reason to maintain the ‘disposable soma’. This theory is paralleled by the Antagonistic Pleiotropy Theory (Kirkwood and Rose, 1991), which states that some genes that may be selected for their beneficial effects early in life, have unselected deleterious defects later in life, thereby contributing directly to the aging process. In this regard the process of replicative senescence could be considered as an antagonistic pleiotropic process that avoids malignant transformation, but by doing so, contributes to aging.

The ‘rate of living’ theory (Pearl, 1928; Sohal, 1976) states that the lifespan of an organism is dependent on its energy utilization or metabolic rate and the amount of energy consumed during adult life or metabolic potential, which ultimately determines its life expectancy (Finkel and Holbrook, 2000; Sohal and Weindruch, 1996). In line with this, Harman’s ‘free-radical theory of aging’ implies that endogenous ROS, generated by cellular metabolism, continually damage macromolecules, like proteins, lipids and DNA, ultimately contributing to the physical decline of an organism (Harman, 1956). A faster rate of respiration leads to higher energy consumption by which more radicals are formed and therefore results in faster aging, which would imply that organisms with a higher metabolic rate experience a shorter lifespan. Evidence for this theory comes from the fact that increased resistance to oxidative stress can extend the lifespan of *C. elegans*, *Drosophila*, and rodents (Melov et al., 2001; Melov et al., 2000; Orr and Sohal, 1994; Schriner et al., 2005). Hypersensitivity to oxygen, on the other hand, significantly reduces the lifespan of nematodes. Furthermore, caloric restriction (CR) (or limited food intake) has been proven a potent lifespan enhancer in worms, flies and rodents (Lakowski and Hekimi, 1998; Longo and Finch, 2003; Mair et al., 2003). This positive effect of CR on lifespan is most probably due to the attenuation of the oxidative stress by lowering metabolism and increasing antioxidant defense.

Eventually, although not every theory is supported by the same amount of convincing evidence, most of them are not necessarily mutually exclusive. In fact, it is equally convincing to assume that combinations of certain currently existing theories are the best way to explain aging.

1.6.2 Oxidative DNA damage and antioxidant defense

Although it is apparent that many different theories exist to explain the causes of aging, many of them seem to involve the damaging of macromolecules, in particular the damaging of DNA. Moreover, in the previously mentioned double knock out mouse models, which display many premature aging features, unrepaired endogenous DNA damage could be a major contributing factor to the observed phenotype. IR, UVA, ROS, and endogenously produced metabolic products can lead to oxidative DNA damage, which can disrupt transcription and DNA replication and give rise to mutations (Bernstein et al., 2002; Campisi, 2001; Hasty et al., 2003). H_2O_2 and IR can induce oxidative base damage or single stranded (SS) breaks, which are thought to be removed by BER. Other examples of oxidative DNA lesions are 8-oxo-guanine (8-oxo-G) and thymin glycol (TG), which are thought to be transcription-blocking lesions (Hatahet et al., 1994; Htun and Johnston, 1992). Under normal conditions 1 base modification per 130.000 bases is induced in nuclear DNA. For mitochondrial DNA this number is even higher: approximately 1 damage per 8000 bases is found (Ames, 1989; Beckman and Ames, 1997).

Inevitable byproducts of cellular metabolism are reactive oxygen species (ROS), e.g. superoxide anion ($O_2^{-}\bullet$), singlet oxygen ($^1O_2$), hydrogen peroxide (H_2O_2) and hydroxyl radical

(•OH) (Davies, 1995; Fridovich, 1995). Endogenous oxygen radical generation occurs *in vivo* as a by-product of enzymatic redox chemistry and, accordingly, mitochondria are the principal source of endogenous oxidants (Beckman and Ames, 1998; Halliwell, 1989). Other sources of ROS are the cytochrome P450 detoxification system, phagocytic oxidative bursts and peroxisomal leakage (Balaban et al., 2005; Finkel and Holbrook, 2000). The location of DNA close to sites of ROS generation increases its susceptibility, which explains why mitochondrial DNA suffers more oxidative DNA damages than nuclear DNA. Superoxide is a precursor to various other ROS, whereas hydroxyl free radicals are the primary DNA-damaging species. ROS can cause adducts to bases (all four can be oxidatively modified) and sugar groups, as well as single and double strand breaks in the DNA backbone, DNA-DNA or DNA-protein crosslinks (Hoeijmakers, 2001). Given the amount of repair processes, present in the cell, to remove oxidative DNA lesions, it seems likely that they pose a significant threat to the genome. Additionally, ROS can damage other macromolecules like RNA, lipids and proteins. However, these can always be replaced by *de novo* synthesis, a non-applicable option for DNA. Since ROS form a necessary constituent of cellular processes (for example signal transduction) (Finkel, 2001), and are inherent to life, they are an unavoidable hazard.

Fortunately, organisms have different defense mechanisms against radicals. To the first category of defense systems against radicals belong molecules that directly quench radicals before they can confer damage to cellular components. Examples are vitamin E or C and ß-carotene (Ames et al., 1995; Yu, 1994). The second category of defense mechanisms encompasses enzymes that catalyze the decomposition of radicals/oxidants. Examples are catalases, gluthatione peroxidases and superoxide dismutases (Beckman and Ames, 1998). Furthermore, enzymes involved in the reduction of antioxidant enzymes (for example GSH reductase) and the cellular machinery that maintains a reductive environment, provide a strong barricade against radicals. Radical scavenging (either by small molecules or enzymes) can be represented as follows: X• + IH → XH + I• (antioxidant derived radical). A potent radical scavenger/antioxidant involves a quick reaction and the resulting antioxidant-derived radical is not stable enough to form a chain reaction, reviewed by (Beckman and Ames, 1998; Niki, 2000). The more reactive a radical is the less scavenging of that radical is dependent on the chemical reactivity of the antioxidant. Instead concentration becomes far more important. An antioxidant can only scavenge free aqueous radicals if the antioxidant itself is water-soluble, so it cannot suppress lipophilic oxidation, which will also induce a chain reaction. Examples of water-soluble radical scavenging molecules are vitamin C, uric acid and bilirubin (Niki et al., 1988). Vitamin C, which by itself is not a very good antioxidant, can act synergistic with vitamin E (fat-soluble) (Burton et al., 1985; Sato et al., 1990). Other lipid-soluble radical scavengers are ubiquinol and probucol. Their activity depends both on the local concentration and their mobility at a specific site. The most common radical scavenging enzymes are superoxide dismutase (SOD, very highly conserved between species), GSH peroxidase and catalase. (Beckman and Ames, 1998) SOD converts O_2^- to H_2O_2, which is converted to H_2O by catalase. SOD levels increase as a result of oxidative stress, but the enzyme can be irreversibly inactivated by its product H_2O_2 (Niki, 2000).

Unfortunately, the defense mechanisms mentioned above are not foolproof, because over time all organisms accumulate damaged lipids, proteins, carbohydrates and nucleic acids. To remove these oxidized products different oxidant repair systems exist; 1) enzymes that restore biomolecules to their native conformation (e.g. DNA repair) 2) catabolic enzymes that specifically degrade non-functional proteins, lipids and nucleic acids 3) the degradation of oxidatively damaged cell components (indirectly). Production of ROS, without proper defense, is a major rate-limiting factor of lifespan, which is illustrated by *Sod2*$^{-/-}$ mice. These mice lack the mitochondrial SOD2 enzyme, which is a major player in the protection against radicals in mitochondria, and as a result they die within the first week of life. *Sod2*$^{-/-}$ mice have dilated cardiomyopathy, liver dysfunction, metabolic acidosis, mitochondrial enzyme abnormalities and a mean lifespan of 8 days (Melov et al., 1998). The cause of this phenotype is most probably toxicity of mitochondrial oxidants derived from normal cellular metabolism. Consequently, modulation of metabolic ROS can have a profound effect on the lifespan of *Sod2*$^{-/-}$ mice: synthetic SOD mimetics increase their lifespan dramatically and rescue part of the phenotype (Melov et al., 2001).

As mentioned before, defective TCR of oxidative lesions may contribute to CS features. Moreover, defective DNA repair seems to be a hallmark of many progeroid syndromes and oxidative stress has been implicated in neurodegenerative diseases (e.g. Alzheimer's disease), atherosclerosis and retinal degeneration (Betarbet et al., 2002). Finally, the amount of oxidative DNA damage increases by as much as two-fold with age in a number of species and tissues (Hamilton et al., 2001; Hirano et al., 1995; Kaneko et al., 1996). This may point to the fact that a 50-100% increase in the steady state levels of oxidative DNA damage are physiologically relevant, but such an elevation is difficult to quantify due to artifacts in background levels introduced during the process of DNA extraction (Beckman and Ames., 2000; Poulsen., 2005). Taken together, it is reasonable to assume that endogenously generated oxidative DNA damage contributes to aging.

1.6.3 Mouse models to study aging

Currently, the most frequently used mouse models to study aging are the ones that, either due to mutations or due to caloric restriction (CR), have an extended lifespan. The best known examples are the Snell and Ames dwarf mice, which have a mutation in the pit-1 or prop-1 gene, respectively (Andersen et al., 1995; Li et al., 1990; Liang et al., 2003). As a result of these mutations, pituitary cells that produce growth, thyroid stimulating and prolactin hormones (GH, TSH and Prl) are not developed properly, causing these animals to have reduced serum levels of GH, TSH and Prl. As a consequence, they have alterations in IGF1 signaling with reduced levels of plasma insulin, IGF1 and glucose. Hence, Ames and Snell dwarf mice have severe growth retardation (size is only 1/3 of their wt littermates), reduced metabolism and a life span extension of 25-65%, reviewed by (Liang et al., 2003; Longo and Finch, 2003). In addition, less oxidative damage to proteins and DNA together with upregulated antioxidant defense was observed in these animals when compared to wt mice (Brown-Borg et al., 1999; Brown-Borg, 2001; Hauck, 2001). Ames and Snell dwarf mice even seem to have a delayed occurrence of presumably fatal neoplastic disease and lung adenocarcinomas, although these data are controversial, reviewed by (Liang et al., 2003). Additionally, behavioral aspects, like learning, memory and locomotor activities are improved. On the contrary, mice with elevated GH levels (throughout life) have low expression of catalase mRNA and low activity of the corresponding protein, high levels of ROS, increased oxidative damage to tissues and a shortened lifespan (Sonntag et al., 1980). The GH/IGF1 axis is conserved from nematodes to mammals and it has been shown that mutations in *C. elegans* and *Drosophila* similar to pit-1 and prop-1 extend the lifespan of these organisms (Longo and Finch, 2003). Therefore, the GH/IGF1 axis is an important determinant of organismal lifespan. However, the exact mechanism by which it acts is not yet known.

Another well-known mechanism to extend lifespan is caloric restriction (CR), which means under-nutrition, not malnutrition. CR prolongs both mean and maximal lifespan of laboratory rats and also retards and reduces most of the age-related diseases and physiological changes that occur with age, reviewed by (Koubova and Guarente, 2003). Rodents subjected to CR have lower serum glucose and IGF1 levels (Mobbs et al., 2001). CR also reduces production of metabolic toxins, increases the free-radical scavenging function and induces protein synthesis both in liver and skeletal muscle so that the number of oxidized proteins is reduced which all together leads to reduction of the amount of endogenous damage (Longo and Finch, 2003).

Although CR mice display significant overlap with Snell and Ames dwarf mice, they are not identical, since CR of these animals further extends their lifespan (Bartke et al., 2001; Liang et al., 2003). As mentioned before, the exact mechanism by which the GH/IGF1 axis and CR have an effect on lifespan and aging is not yet clear. Since both mouse models have a lowered metabolism and an up-regulated antioxidant defense, it is tempting to speculate that the underlying cause of the lifespan extension is the lowering of damage to macromolecules. In this respect, it is not surprising that animals with a defect in DNA repair would suffer from premature aging features and a shortened lifespan. Therefore, a more detailed study of these prematurely aging animals with a shortened lifespan could provide a powerful tool in studying the complex mechanism of aging, equivalent to the long-lived animal models that are now used to study aging.

1.7 Scope of this thesis

It is known that deficiencies in NER lead to a repair deficiency that result in UV sensitivity. However, in addition to this, human syndromes and mouse models with a NER or TC-NER defect display features reminiscent of aging, of which the cause is largely unknown. In this thesis, we set out to study the etiology of CS aging features further by use of both $Csb^{m/m}$ and $Csb^{m/m}Xpa^{-/-}$ mouse models. First, we describe the aging phenotype of NER mice, in particular that of the $Csb^{m/m}$ and $Csb^{m/m}Xpa^{-/-}$ mouse models in more detail (Chapter 3 and 2). Furthermore, we investigated the mechanism behind the aging phenotype of the $Csb^{m/m}Xpa^{-/-}$ mouse by means of transcriptome profiling (Chapter 2). In addition, we developed a conditional *Xpa* mouse, in order to study the phenotype of $Csb^{m/m}Xpa^{-/-}$ mice in a (Cre-recombinase-mediated) tissue-specific and time-dependent manner (Chapter 4), with special emphasis on the brain. Finally, we address the question whether it is possible to interfere with aging by means of radical scavenger intervention (Chapter 5).

Chapter 2

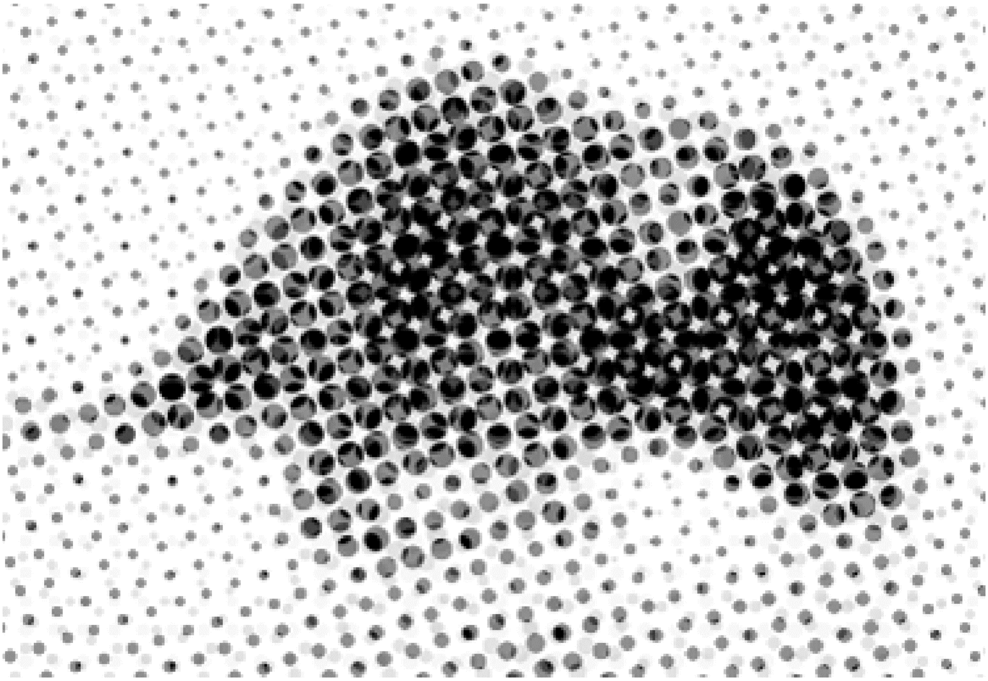

..

CHAPTER 2

Impaired Genome Maintenance Suppresses the GH/IGF1 Axis in Cockayne Syndrome Mice

Ingrid van der Pluijm, George A. Garinis, Renata M.C. Brandt, Theo G.M.F. Gorgels, Susan W. Wijnhoven, Karin E.M. Diderich, Jan de Wit, James R. Mitchell, Conny van Oostrom, Rudolf Beems, Laura J. Niedernhofer, Susana Velasco, Errol C. Friedberg, Kiyoji Tanaka, Harry van Steeg, Jan H.J. Hoeijmakers, and Gijsbertus T.J. van der Horst

Abstract

Cockayne syndrome (CS) is a photosensitive, DNA repair disorder associated with progeria caused by a defect in the transcription-coupled repair (TCR) subpathway of nucleotide excision repair (NER). Here, complete inactivation of NER in $Csb^{m/m}/Xpa^{-/-}$ *mutants causes a phenotype that reliably mimics the human progeroid CS syndrome. Newborn* $Csb^{m/m}/Xpa^{-/-}$ *mice display attenuated growth, progressive neurological dysfunction, retinal degeneration, cachexia, kyphosis and die before weaning. Mouse liver transcriptome analysis and several physiological endpoints revealed systemic suppression of the GH/IGF1 somatotroph axis and oxidative metabolism, increased antioxidant responses, hypoglycemia together with hepatic glycogen and fat accumulation. Broad genome-wide parallels between* $Csb^{m/m}/Xpa^{-/-}$ *and naturally aged mouse liver transcriptomes suggested that these changes are intrinsic to natural aging and to DNA repair-deficient mice. Importantly, wild type mice exposed to a low dose of chronic genotoxic stress recapitulated this response, thereby pointing to a novel link between genome instability and the age-related decline of the somatotroph axis.*

..

Introduction

A prevailing hypothesis to explain the molecular basis of aging is Harman's "free-radical theory of aging", which states that endogenous reactive oxygen species (ROS), resulting from cellular metabolism, continually damage biomolecules (Harman, 1956). In line with this hypothesis, it has been shown that increased resistance to oxidative stress (*e.g.* by improved antioxidant defense) extends the life span of *C. elegans*, *Drosophila*, and rodents (Melov et al., 2000; Orr and Sohal, 1994; Schriner et al., 2005), whereas oppositely, hypersensitivity to oxygen considerably reduces the life span of nematodes (Ishii et al., 1998). A key macromolecule at risk for ROS-mediated damage is nuclear DNA (Harman, 1956), as evident from the wide range of oxidative DNA lesions that accumulate gradually in rodents and humans with advancing age (Hamilton et al., 2001; Lu et al., 2004).

In humans, the causative role of DNA damage in aging is supported by a variety of progeroid disorders with defects in DNA repair pathways (de Boer et al., 2002; Martin, 2005). One such condition is Cockayne Syndrome (CS; affected genes: *CSA* or *CSB*), a photosensitive disorder, originating from a defect in transcription-coupled repair (TCR) that specifically removes DNA lesions, which obstruct RNA polymerases, to allow resumption of transcription and promote cellular survival from DNA damage. TCR of helix-distorting DNA damage is a dedicated subpathway of the multi-step 'cut-and-patch' nucleotide excision repair (NER) system, and is designated TC-NER (Hanawalt, 2002) to distinguish it from the so-called global genome NER (GG-NER) subpathway that operates genome-wide to eliminate distorting damage. Available evidence suggests that CS cells are also defective in TCR of non-helix distorting DNA lesions that block transcription such as transcription-blocking oxidative DNA lesions (de Waard et al., 2003; Spivak and Hanawalt, 2005), which are normally removed genome-wide by base excision repair. We will use TCR, when referring to transcription-coupled repair in general. CS patients present with growth failure (cachectic dwarfism), progressive neurological abnormalities (including delayed psychomotor development, mental retardation, microcephaly, gait ataxia, sensorineural hearing loss, retinal degeneration), along with impaired sexual development, kyphosis, osteoporosis and severely reduced life span (mean age of death: 12.5 years) (Bootsma et al., 2002; Nance and Berry, 1992). A related yet distinct disorder is Trichothiodystrophy (TTD; affected genes: *XPB*, *XPD* or *TTDA*). TTD patients are partially defective in TCR, as well as in the global genome repair subpathway of NER, and share the symptoms associated with CS. In addition, these patients have a partial defect in transcription itself, causing additional symptoms such as ichthyosis and brittle hair and nails (Vermeulen et al., 2001). Many of the CS and TTD features are progressive and resemble premature aging. As patients develop some but not all aspects of normal aging in an accelerated manner, CS and TTD are considered "segmental progeroid syndromes" (Martin, 2005)

Mouse mutants for CS-A and CS-B reliably mimic the UV-sensitivity of CS patients and show accelerated photoreceptor loss, reduced body weight, and mild neurologic abnormalities (van der Horst et al., 2002; van der Horst et al., 1997). Similarly, mice homozygous for a causative TTD point mutation in the *Xpd* gene faithfully mirror the symptoms in TTD patients (de Boer et al., 2002) whereas complete inactivation of NER (by concurrent inactivation of the *Xpa* gene) dramatically aggravates the CS features of partially NER-defective TTD mice (de Boer et al., 2002). These observations, together with the notion that DNA lesions can provoke a permanent cell cycle arrest or apoptosis, led us to propose that aging can result from (oxidative) DNA lesions that interfere with transcription and/or replication causing cell death or cellular senescence, ultimately leading to loss of tissue homeostasis and onset of age-related diseases (de Boer and Hoeijmakers, 2000; Hasty et al., 2003; Mitchell et al., 2003).

Here, we report that mice with engineered mutations in both *Csb* and *Xpa* genes display many CS features in a dramatic form, including postnatal growth attenuation, progressive kyphosis, ataxia, retinal degeneration, motor dysfunction and premature death. Importantly, full genome transcriptome analysis of the $Csb^{m/m}/Xpa^{-/-}$ mouse liver at the age of 15 days uncovered a systemic response seen also in wt mice exposed to chronic oxidative stress. These findings disclose a novel link between DNA damage, compromised genome maintenance and the somatotrophic axis that determines life span and shed new light on the etiology of Cockayne Syndrome and natural aging.

Results

Attenuated growth and perinatal death in $Csb^{m/m}/Xpa^{-/-}$ and $Csb^{m/m}/Xpc^{-/-}$ mice

TCR-defective $Csb^{m/m}$ mutant mice (van der Horst et al., 1997) were intercrossed with GG-NER-defective $Xpc^{-/-}$ (Cheo et al., 1997) and GG/TC-NER-defective $Xpa^{-/-}$ (de Vries et al., 1995) animals to investigate whether an increase in the endogenous burden of unrepaired DNA damage, as provoked by inactivation of GG-NER, enhances the phenotype, including progeroid features. Analysis of UV-induced repair synthesis and RNA synthesis recovery (indicative for GG-NER and TC-NER capacity, respectively) confirmed complete inactivation of NER in $Csb^{m/m}/Xpa^{-/-}$ and $Csb^{m/m}/Xpc^{-/-}$ animals (Fig. 1A). As expected on the basis of previous work, $Xpa^{-/-}$ cells display highest UV-sensitivity, whereas $Xpc^{-/-}$ and $Csb^{m/m}$ cells show intermediate sensitivities ($Xpa^{-/-} > Csb^{m/m} > Xpc^{-/-} >$ wt; see Fig. 1B). Interestingly, inactivation of GG-NER in $Csb^{m/m}$ MEFs (resulting in $Csb^{m/m}/Xpa^{-/-}$ and $Csb^{m/m}/Xpc^{-/-}$ cells) renders cells more UV-sensitive than already completely NER-deficient $Xpa^{-/-}$ MEFs. We attribute this enhanced sensitivity to the absence of CSB-mediated TCR of UV-induced lesions that do not form a substrate for NER. Thus the repair defect in the double mutant appears to be more severe than that of the single mutants. We could not detect a similar increased sensitivity to ionizing radiation in double mutant cells above that of $Csb^{m/m}$ cells ((de Waard et al., 2003), data not shown), supporting the notion that MEFs in culture are already under high oxygen stress.

As evident from their overall appearance and weight (Fig. 1C to E), $Csb^{m/m}/Xpa^{-/-}$ and $Csb^{m/m}/Xpc^{-/-}$ pups (hybrid C57BL/6Jx129ola genetic background) displayed a strikingly attenuated growth, resulting in pronounced dwarfism. Whereas the number of double mutant pups was ~3-fold below that expected for Mendelian inheritance (data not shown), E18.5 $Csb^{m/m}/Xpa^{-/-}$ and $Csb^{m/m}/Xpc^{-/-}$ embryos were present at Mendelian frequency, pointing to considerable lethality during or shortly after birth. Importantly, double mutant embryos were morpho- and histologically indistinguishable from wt and single mutant embryos (Fig. 1F, data not shown), indicating that the growth defect was postnatal and did not reflect impaired embryonic development *per se*. Approximately around the third week of life, however, *Csb*$^{m/m}$/*Xpa*$^{-/-}$ and *Csb*$^{m/m}$/*Xpc*$^{-/-}$ pups developed progressive cachexia (evident from the weight loss after day 15; see Fig. 1E), ultimately resulting in death before postnatal day 22.

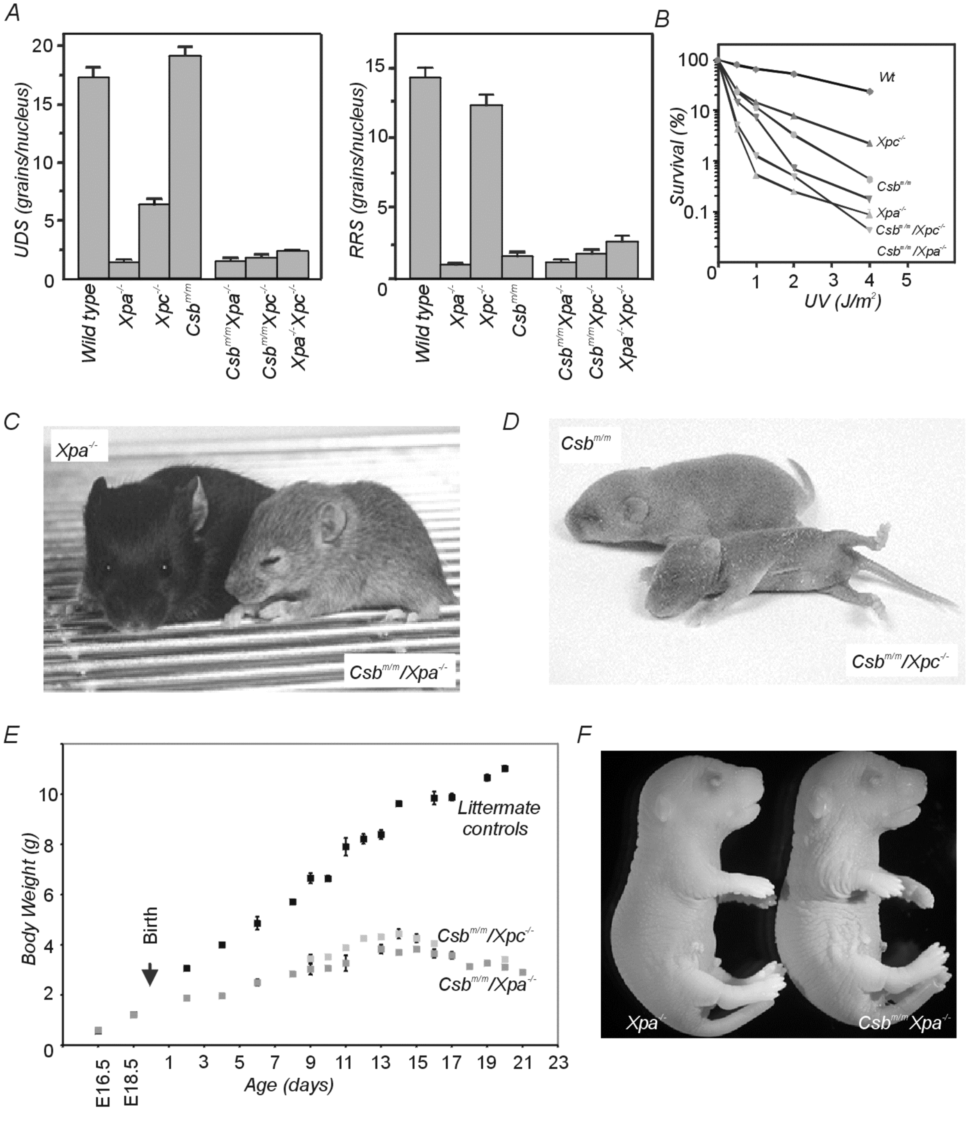

Figure 1. Growth retardation, cachexia, and premature death in *Csb*$^{m/m}$/*Xpa*$^{-/-}$ and *Csb*$^{m/m}$/*Xpc*$^{-/-}$ mice. *A) UV repair characteristics of wild type, single mutant, and double mutant primary mouse embryonic fibroblasts (MEFs). UV-induced Unscheduled DNA Synthesis (UDS; left panel) and Recovery of RNA Synthesis (RRS, right panel) are indicative for GG-NER and TC-NER capacity, respectively. Error bars indicate s.e.m. B) Survival of primary MEFs exposed to increasing doses of UV-C light (254 nm). Error bars (in most cases smaller than symbols used) indicate s.e.m. C) Photograph of a 14-day old Csb*$^{m/m}$*/Xpa*$^{-/-}$ *mouse with an Xpa*$^{-/-}$ *littermate (hybrid 129Ola/C57BL/6J background). D) Photograph of an 8-day old Csb*$^{m/m}$*/Xpa*$^{-/-}$ *mouse with a Csb*$^{m/m}$ *littermate (hybrid 129Ola/C57BL/6J background). E) Body weight curve of Csb*$^{m/m}$*/Xpa*$^{-/-}$ *and Csb*$^{m/m}$*/Xpc*$^{-/-}$ *mice (n=7) compared to those defective in a single NER gene (n=7) all in a hybrid 129Ola/C57BL/6J background. The arrow indicates birth. Error bars (in most cases smaller than symbols used) indicate s.e.m. F) Photographs of day 18.5 Csb*$^{m/m}$*/Xpa*$^{-/-}$ *and Xpa*$^{-/-}$ *embryos (C57BL/6J).*

Neither removal of wt or single mutant pups from the litter (to reduce competition for breast milk), nor moistened food pellets (to facilitate intake of solids), improved the physical condition or the lifespan of $Csb^{m/m}/Xpa^{-/-}$ and $Csb^{m/m}/Xpc^{-/-}$ pups. Necropsy revealed milk or solid food in the stomach, indicating that insufficient access to supplied nutrition was not the underlying cause of growth retardation, weight loss, and early death. Importantly, progressive growth retardation, cachexia and short life expectation (~12.5 years) are also observed in CS patients (Nance and Berry, 1992). Combined inactivation of *Xpa* and *Xpc* rendered mice without any overt phenotype (data not shown), leading us to conclude that the dramatic phenotype of $Csb^{m/m}/Xpa^{-/-}$ and $Csb^{m/m}/Xpc^{-/-}$ pups results from a combined GG-NER/TC-NER/TCR defect.

Growth and neurological abnormalities in $Csb^{m/m}/Xpa^{-/-}$ mice

Further analysis of the $Csb^{m/m}/Xpa^{-/-}$ phenotype, performed in an isogenic C57BL/6J background, revealed a near to normal size of the skull at day 11 and 21 (autoradiographs shown in Fig. 2A), implying that the (postnatal) growth defect is restricted to the trunk, and to a lesser extent, the extremities. All 21-day old double mutant animals showed kyphosis (abnormal curvature of the spinal column, Fig. 2A, middle left and bottom right), which was also observed in $Csb^{m/m}/Xpa^{-/-}$ pups younger than 21 days, indicating that it is not determined by terminal illness. The normal appearance of the spine in 11-day old double mutant pups excluded a prenatal developmental defect and further pointed to an extremely accelerated onset of kyphosis, a feature observed in naturally aged (2-year old) C57BL/6J mice (see Fig. 2A, bottom left panel). Two-dimensional images of proximal end-to-mid-diaphysis micro-computed tomography (micro-CT) scans of fixed tibiae from 10-, 15- and 20-day old wt and $Csb^{m/m}/Xpa^{-/-}$ mice revealed retarded, yet steady longitudinal as well as radial (perimeter) growth, along with a thinner bone cortex and a less developed growth plate (Fig. 2B). In line with this observation, we observed a reduction in tibia length (Fig. 2C). Notably, while $Csb^{m/m}/Xpa^{-/-}$ pups lose weight in the third week of life, bone growth proceeds, resulting in relatively large extremities, a representative feature of CS and TTD (Nance and Berry, 1992).

Motor coordination problems, manifesting as tremors and abnormal posture of the hind limbs (flexion rather than extension in tail suspension test), became evident around day 10 in $Csb^{m/m}/Xpa^{-/-}$ mice (data not shown). Foot print analysis revealed a disturbed gait from day 15 onwards. While wt and single mutant animals maintained a straight path with regular alternating strides, $Csb^{m/m}/Xpa^{-/-}$ mice demonstrated a non-uniform alternating left-right step pattern and unevenly spaced shorter strides (Fig. 2D). Despite their runted size, the front base width of $Csb^{m/m}/Xpa^{-/-}$ animals was significantly greater than that of wt and single mutant littermates, which likely illustrates an attempt to maintain balance (Fig. 2D). These data are consistent with the profound early postnatal ataxia, abnormal cerebellar development in $Csb^{m/m}/Xpa^{-/-}$ mice (Murai et al., 2001), and the progressive neurodegeneration observed in CS patients (Itoh et al., 1999).

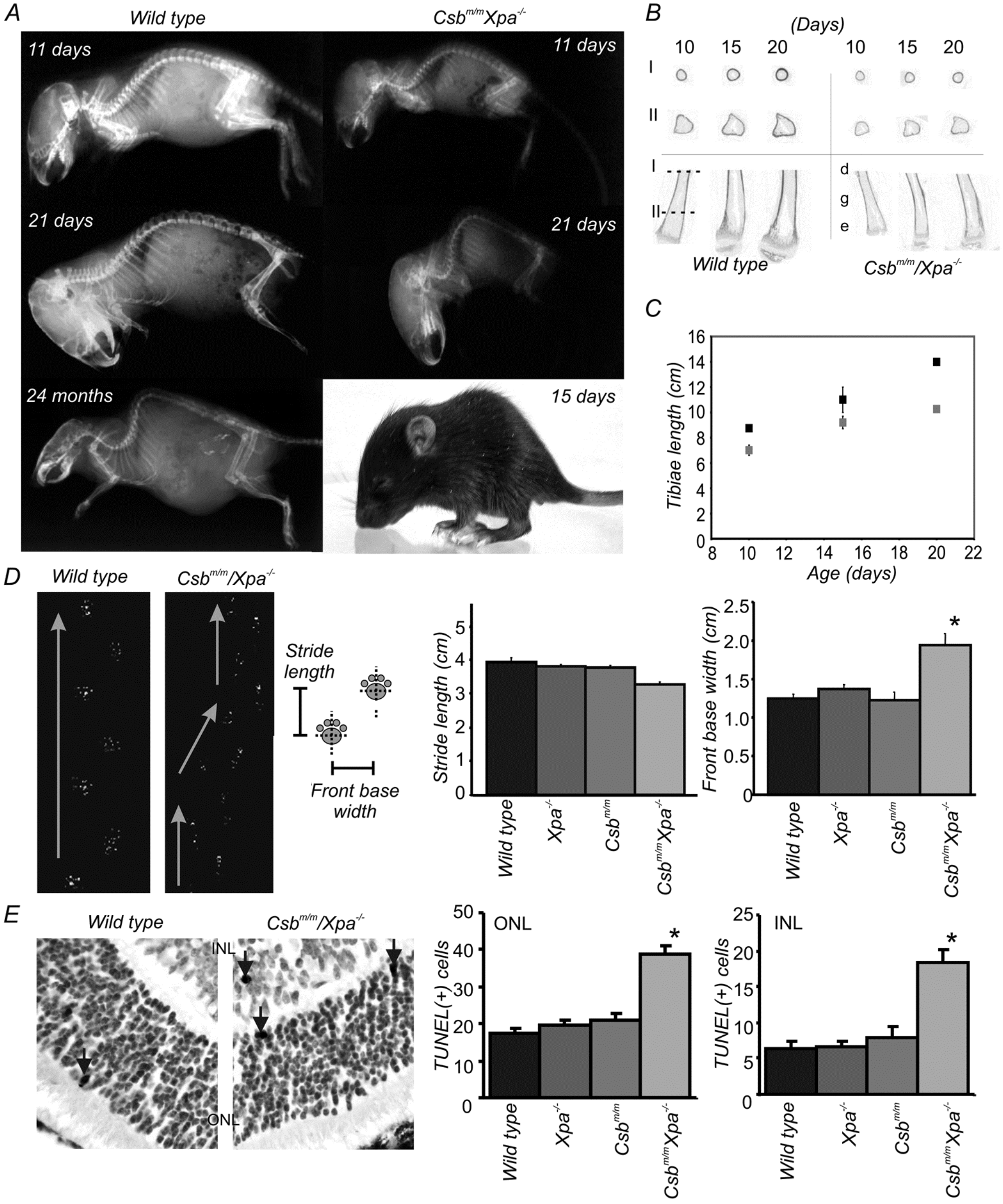

Figure 2. Skeletal and neurological abnormalities in Csb$^{m/m}$/Xpa$^{-/-}$ mice. *A) Radiographs of wt and Csb$^{m/m}$/Xpa$^{-/-}$ mice and photograph of a 15-day old Csb$^{m/m}$/Xpa$^{-/-}$ mouse. B) 2D micro-CT scans of tibiae taken from Csb$^{m/m}$/Xpa$^{-/-}$ animals and wt littermates. I = section through smaller part, II = section through broader part of the diaphysis; e = epiphysis, g = growth plate and d = diaphysis. C) Growth of tibiae in time of Csb$^{m/m}$/Xpa$^{-/-}$ animals (light squares) and wt littermates (dark squares). D) Representative footprint patterns of 19-day old wt and Csb$^{m/m}$/Xpa$^{-/-}$ mice. Arrows indicate the trajectory of each mouse. Stride length and front base width measurements on 15-day old wt, Xpa$^{-/-}$, Csb$^{m/m}$ and Csb$^{m/m}$/Xpa$^{-/-}$ mice. The significantly (*; $p<0.001$) greater base width in the double mutant mouse indicates ataxia. E) Representative pictures of a TUNEL staining in the retina of wt and Csb$^{m/m}$/Xpa$^{-/-}$ mice and quantification of the number of TUNEL positive cells. Arrows indicate TUNEL positive cells in the outer nuclear layer (ONL) and inner nuclear layer (INL). Note the significantly higher number of TUNEL-positive cells in both the ONL and the INL in the retina of Csb$^{m/m}$/Xpa$^{-/-}$ compared to wt mice (*; $p<0.05$).*

We next examined the retina of 15-day old *Csb*$^{m/m}$/*Xpa*$^{-/-}$ pups for the presence of apoptotic cells as retinal degeneration is a prominent neurological feature of CS patients (Traboulsi et al., 1992) and adult CS mice (Chapter 3). At this age, cell loss occurs as part of the normal development of the retina. Yet, as shown by TUNEL (Fig. 2E) and caspase-3 staining (data not shown), the number of apoptotic cells in the outer (ONL) and inner nuclear (INL) layers of the retina of *Csb*$^{m/m}$/*Xpa*$^{-/-}$ pups was significantly increased (ANOVA, S-N-K posthoc test, $p<0.05$), as compared to wt and single mutant littermates (Fig. 2E). Thus, the *Xpa* defect enhanced the apoptotic sensitivity of photoreceptor cells in *Csb*$^{m/m}$ mice, thereby pointing to DNA damage as a trigger for age-related retinal degeneration. As 15-day old *Csb*$^{m/m}$ mice still have wt levels of apoptotic cells, spontaneous photoreceptor loss in the *Csb*$^{m/m}$ mouse initiates in the second/third month of life.

With the exception of substantial loss of abdominal fat, visual inspection and histological analysis of most internal organs of 15-day old *Csb*$^{m/m}$/*Xpa*$^{-/-}$ mice did not reveal any obvious pathological abnormalities (data not shown). As we did not find any sign of infections, necrosis, or abnormal cellular proliferation (as determined by BrdU staining) in the gastrointestinal tract of 15- and 21-day old *Csb*$^{m/m}$/*Xpa*$^{-/-}$ animals, intestinal malfunction is an unlikely cause of the growth defect (Fig. 3A). In addition, the liver has a normal histological appearance (Fig. 3B), and neither BrdU (Fig. 3C), PCNA (Fig. 3D), and Ki67 staining (data not shown), nor TUNEL (Fig. 3E) and caspase 3 staining (data not shown) revealed any significant difference between *Csb*$^{m/m}$/*Xpa*$^{-/-}$ and wt livers. This finding indicates that aberrant cell proliferation or apoptosis in the liver does not likely contribute to the *Csb*$^{m/m}$/*Xpa*$^{-/-}$ phenotype. Moreover, inactivation of the *p53* tumor suppressor gene failed to rescue the mutant phenotype, as *Csb*$^{m/m}$/*Xpa*$^{-/-}$/*p53*$^{-/-}$ triple mutant pups appeared indistinguishable from *Csb*$^{m/m}$/*Xpa*$^{-/-}$ pups (data not shown). Thus, the precise etiology of the overall physical deterioration and the cause of death of *Csb*$^{m/m}$/*Xpa*$^{-/-}$ mice remain unknown.

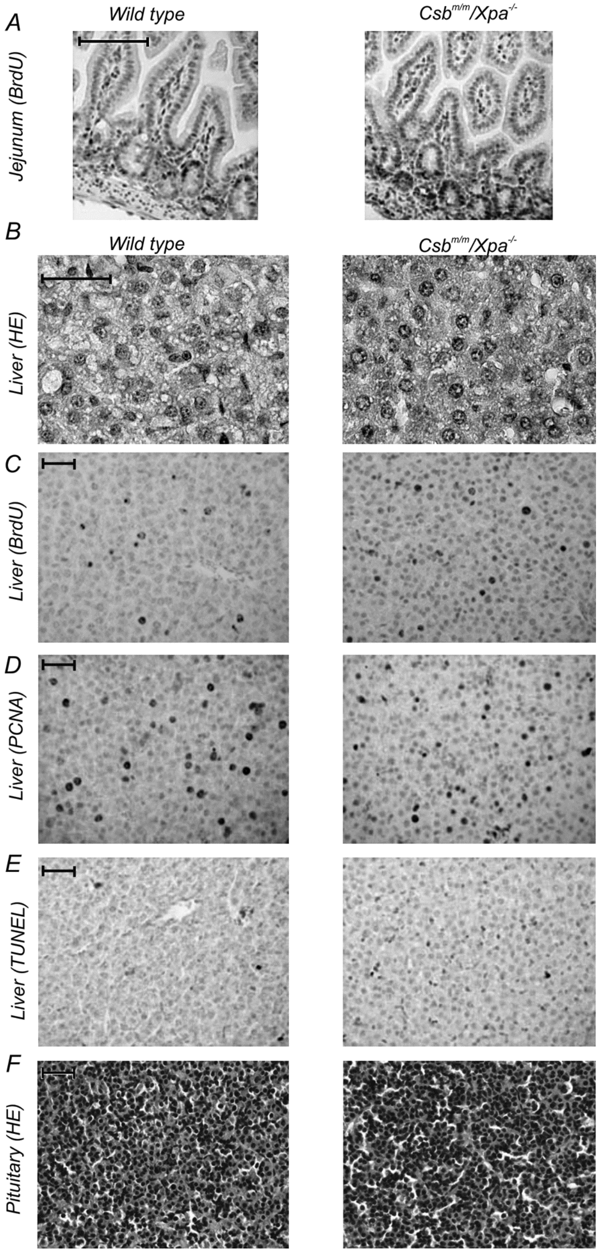
A
Wild type
$Csb^{m/m}/Xpa^{-/-}$
Jejunum (BrdU)
B
Wild type
$Csb^{m/m}/Xpa^{-/-}$
Liver (HE)
C
Liver (BrdU)
D
Liver (PCNA)
E
Liver (TUNEL)
F
Pituitary (HE)

Figure 3. Histological examination of $Csb^{m/m}/Xpa^{-/-}$ tissues. *A) BrdU staining of the jejunum of* $Csb^{m/m}/Xpa^{-/-}$ *and littermate control mice, showing normal proliferative capacity of the intestine in the double mutant mouse. B-E) Histological examination of liver sections of 15-day old* $Csb^{m/m}/Xpa^{-/-}$ *and littermate control mice, stained with HE (B), immunostained for the proliferation markers (incorporated) BrdU (C) and PCNA protein (D), or TUNEL-stained for the presence of apoptotic cells (E) Quantification of the number of proliferative or apoptotic cells did not reveal significant differences between* $Csb^{m/m}/Xpa^{-/-}$ *and wild type littermate mice. F) HE staining of the pituitary pars distalis of* $Csb^{m/m}/Xpa^{-/-}$ *and littermate control mice.*

Enhanced ionizing radiation sensitivity of the *Csb$^{m/m}$/Xpa$^{-/-}$* mouse retina

The spontaneous age-related and ionizing radiation (IR)-induced loss of post-mitotic photoreceptor cells in *Csb$^{m/m}$* mice underscores the relevance of DNA repair in the removal of (oxidative) DNA damage for the long-term survival of terminally differentiated cells in the retina (Chapter 3).

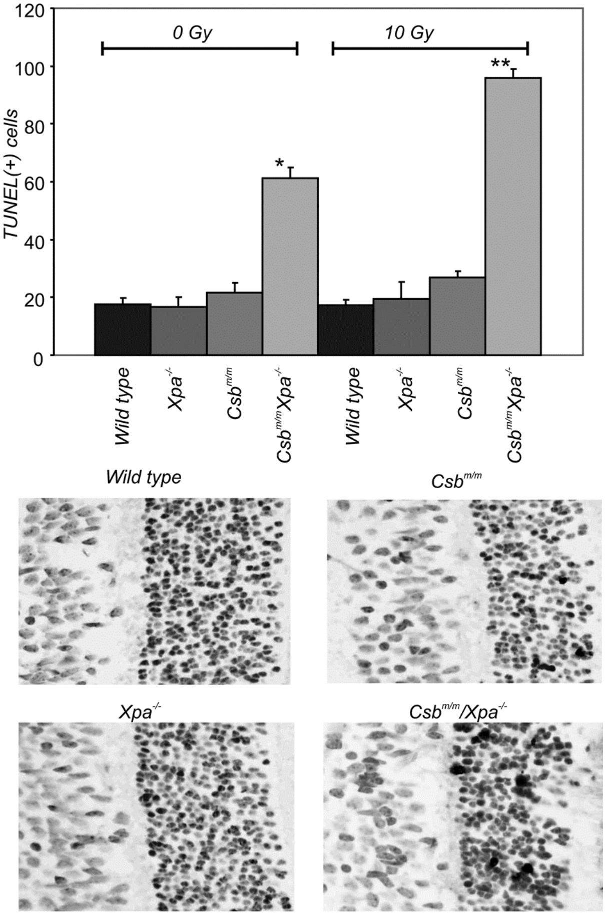

Figure 4. Enhanced sensitivity of *Csb$^{m/m}$/Xpa$^{-/-}$* retinal photoreceptor cells to genotoxic insults. *Representative pictures of TUNEL stained retinas of 19-day old wt, Csb$^{m/m}$, Xpa$^{-/-}$ and Csb$^{m/m}$/Xpa$^{-/-}$ mice (lower panel), 20 hours after exposure of animals to 10 Gy of ionizing radiation, together with quantification of the number of TUNEL positive cells in the ONL (upper panel). Note the significantly higher number of TUNEL-positive cells in the retina of Csb$^{m/m}$/Xpa$^{-/-}$ mice, as compared to wt and single mutant littermate controls (* indicates statistically significant differences between unirradiated Csb$^{m/m}$/Xpa$^{-/-}$ mice and littermate controls, ** indicates statistically significant differences between unirradiated and irradiated Csb$^{m/m}$/Xpa$^{-/-}$ mice; $p<0.05$).*

To test whether *Csb*$^{m/m}$/*Xpa*$^{-/-}$ animals are more sensitive to genotoxic insults than single mutant *Csb*$^{m/m}$ and Xpa-/- animals, we next examined if the additional Xpa defect further enhances the IR sensitivity of the *Csb*$^{m/m}$ retina. To this end, we exposed 19-day old *Csb*$^{m/m}$/*Xpa*$^{-/-}$ pups and wild type and single mutant littermates to γ-rays to a dose of 10 Gy and quantified the number of apoptotic cells in the by TUNEL staining 20 hours after exposure. As shown in Fig. 4, the number of apoptotic cells in the ONL of untreated (20-day old) *Csb*$^{m/m}$/*Xpa*$^{-/-}$ pups further increased, as compared to 15-day old double mutant animals (see Fig. 2E). While IR exposure did not increase the frequency of apoptotic photoreceptors in the ONL of wt and *Xpa*$^{-/-}$ animals, *Csb*$^{m/m}$ mice already show a tendency to increased photoreceptor loss, as characteristic for mature *Csb*$^{m/m}$ animals (Chapter 3). In contrast, the retina of IR-exposed *Csb*$^{m/m}$/*Xpa*$^{-/-}$ animals showed an almost two-fold increase in the level of TUNEL-positive photoreceptor cells (Student's t-test $p=0.021$). Taken together, these findings not only further point to unrepaired DNA damage (likely originating from oxidative stress) as the underlying trigger for photoreceptor loss, but importantly, also show that inactivation of Xpa further enhances the sensitivity of *Csb*$^{m/m}$ mice to genotoxic stress.

Analysis of the *Csb*$^{m/m}$/*Xpa*$^{-/-}$ mouse liver transcriptome

To investigate whether a disturbance in growth and metabolism could explain the pronounced accelerated organismal deterioration seen in *Csb*$^{m/m}$/*Xpa*$^{-/-}$ mice, we evaluated the liver transcriptome of 15-day old wt, single and double mutant mice (n=4). At this age, the *Csb*$^{m/m}$/*Xpa*$^{-/-}$ pups have not yet become cachectic. Two-tail, pair wise analysis of variance of Affymetrix full mouse genome arrays revealed 1865 genes with significantly changed expression patterns between wt and *Csb*$^{m/m}$/*Xpa*$^{-/-}$ livers ($p \leq 0.01$, 1.2 fold change up- or down regulated, for summary see table 1), a number that significantly exceeds the 80 genes that are expected to occur by chance under these selection criteria. Among the set of 1865 genes, we identified those GO-classified biological processes with a significantly disproportionate number of responsive genes relative to those printed on microarrays (False detection rate ≤ 0.10). This unbiased approach revealed processes implicated in the derivation of energy from oxidation of organic compounds, homeostasis of energy reserves, cell growth and maintenance and the redox status of the cell.

Subsequent analysis of these processes led us to identify:

1. a profound attenuation of the somatotroph axis as evidenced by the consistent down-regulation of genes encoding main components of the GH/IGF1 axis (e.g. *IGF1*, *Igfbp3*, *Igfbp4*, *Igfals*, *Ghr*), as well as lactotroph (e.g. *Prlr*) and thyrotroph functions (e.g. *Dio1*) in *Csb*$^{m/m}$/*Xpa*$^{-/-}$ livers, in addition to a decrease in the expression of several genes associated with a variety of mitogenic signals (e.g. *Esr1*, *Fgf1*, *Fgfr3*, *Fgfr4*).

2. an extensive suppression of catabolic metabolism in the *Csb*$^{m/m}$/*Xpa*$^{-/-}$ liver, as evident from the significant down-regulation of key genes involved in glycolysis, tricarboxylic acid cycle and oxidative phosphorylation pathways (summarized in Table 1), coupled with a significant up-regulation of genes associated with glycogen synthesis (e.g. *Gyg1* and *Gys2* and down-regulation of glycogen phosphorylase, *Pygl*) suggesting that the *Csb*$^{m/m}$/*Xpa*$^{-/-}$ liver stores glucose into glycogen, rather than burn it for energy derivation. These changes were further accompanied by the broad down-regulation of genes associated with electron transport and oxidative phosphorylation (e.g. several cytochrome P450 monooxygenases, the NADH dehydrogenase complex and the NADPH-dependent oxidative metabolism; Table 1) and the significant down-regulation of several genes associated with peroxisomal biosynthesis (Table 1). Apparently, the complete catabolic metabolism is restrained in the *Csb*$^{m/m}$/*Xpa*$^{-/-}$ liver.

3. a broad upregulation of genes associated with fatty acid synthesis and transport (several genes listed in Table 1), the up-regulation of the receptor for the adipocyte hormone leptin (*Lepr*) and the central fat regulator peroxisome proliferator-activated receptor-gamma (*Pparγ*). Thus, similar to reserved glucose utilization and enhanced glycogen synthesis, *Csb*$^{m/m}$/*Xpa*$^{-/-}$ mice attempt to store rather than burn fat.

4. an up-regulation of genes encoding key enzymatic and non-enzymatic low molecular mass scavengers and antioxidant defense enzymes (e.g. Sod1, Prdx2 and 3, Txnip, Ephx1, Hmox1 and 5 components of the glutathione system; Table 1), suggesting that *Csb*$^{m/m}$/*Xpa*$^{-/-}$ mice try to minimize the induction of (DNA) damage by counteracting ROS.

Importantly, none of these genes were identified as significantly differentially expressed in the livers of *Csb*$^{m/m}$ or *Xpa*$^{-/-}$ littermate controls (Table 1). Quantitative real-time PCR (Q-PCR) evaluation of the expression levels of key genes involved in the somatotroph axis, energy metabolism and antioxidant defense in the liver of *Csb*$^{m/m}$/*Xpa*$^{-/-}$ mice, and wt, *Csb*$^{m/m}$ and *Xpa*$^{-/-}$ littermates, as well as further biochemical analysis (see below), confirmed the validity of the microarray data (Fig. 5A, upper left panel).

Postnatal systemic changes in somatotroph axis, energy metabolism, and antioxidant defense in *Csb*$^{m/m}$/*Xpa*$^{-/-}$ mice

Next, we analyzed whether the onset of aforementioned transcriptional changes paralleled the progressive postnatal growth attenuation, as well as the weight loss observed later. Consistent with the normal embryonic development, the expression levels of genes involved in the somatotroph axis (*Ghr*, *Igf1*, *Prlr*), antioxidant defense (*Gstt2*, *Hmox1*, *Ephx1*) and oxidative metabolism (*Gck, Gyg1, Cs, Ndufs8*) did not differ significantly between wt and *Csb*$^{m/m}$/*Xpa*$^{-/-}$ livers at postnatal day 1 (Fig. 5B). In contrast, during the first two weeks of life, wt mice exhibited a robust up-regulation in *Igf1*, *Ghr*, *Prlr* gene expression, a response that was virtually absent in *Csb*$^{m/m}$/*Xpa*$^{-/-}$ animals (Fig. 5B, left panels) and well explains the severe growth retardation of double mutant pups after birth. Analysis of *Gstt2*, *Hmox1*, and *Ephx1* mRNA levels revealed that the up-regulation of the antioxidant defense system in the *Csb*$^{m/m}$/*Xpa*$^{-/-}$ liver already initiated before postnatal day 10, and thus well ahead of the initiation of the physiological decline (i.e. weight loss) (Fig. 5B, middle panels). When comparing mRNA levels of key genes in glycolysis (Gck), TCA cycle (Cs), and mitochondrial oxidative phosphorylation (Ndufs8), we noticed that beginning postnatal day 10, *Csb*$^{m/m}$/*Xpa*$^{-/-}$ livers do not show the prominent up-regulation of these catabolic genes seen in the wt liver (instead expression levels continued to decline), while they up-regulate glycogen synthesis (Gyg1, Fig. 2B, right panels). In agreement, the enzymatic activity of citrate synthase was significantly lower ($p \leq 0.01$) in the liver of 15-day old *Csb*$^{m/m}$/*Xpa*$^{-/-}$ mice (119 ± 15 mU/mg protein), as compared to wt littermate controls (70 ± 13 mU/mg protein).

Code	**Title**	**Symbol**	$Csb^{m/m}$ $Xpa^{-/-}$		$Xpa^{-/-}$		$Csb^{m/m}$	
The IGF-1/GH growth axis			**FC**	**P-value**	**FC**	**P-value**	**FC**	**P-value**
1448556_at	prolactin receptor	Prlr	-2.03	0.0000	-1.3	0.1	-1.1	0.66
1419519_at	insulin-like growth factor 1	Igf1	-2.13	0.0000	-1.1	0.16	-1.13	0.19
1421991_a_at	IGF-binding protein 4	Igfbp4	-1.74	0.0000	-1.1	0.82	-1.16	0.39
1458268_s_at	IGF-binding protein 3	Igfbp3	-1.44	0.0010	-1.1	0.25	1.06	0.59
1422826_at	IGF-binding protein, acid labile subunit	Igfals	-2.36	0.0000	1.06	0.53	1.13	0.26
1417962_s_at	growth hormone receptor	Ghr	-1.53	0.0000	1.03	0.15	1.1	0.05
1425458_a_at	growth factor receptor bound protein 10	Grb10	1.84	0.0000	1.11	0.59	1.24	0.19
1427777_x_at	fibroblast growth factor receptor 4	Fgfr4	-1.32	0.0090	-1.1	0.71	-1.19	0.11
1421841_at	fibroblast growth factor receptor 3	Fgfr3	-1.43	0.0010	-1.3	0.03	-1.12	0.87
1450869_at	fibroblast growth factor 1	Fgf1	-1.38	0.0030	-1.2	0.09	-1.01	0.84
1435663_at	estrogen receptor 1 (alpha)	Esr1	-1.91	0.0010	-1.1	0.32	-1.31	0.12
1417991_at	deiodinase, iodothyronine, type I	Dio1	-2.12	0.0000	1	0.28	-1.04	0.28
Carbohydrate metabolism								
1423644_at	aconitase 1	Aco1	-1.26	0.0020	1.05	0.5	-1	0.96
1422577_at	citrate synthase	Cs	-1.28	0.0060	1.16	0.2	-1.03	0.2
1419146_a_at	glucokinase	Gck	-6.59	0.0040	1.16	0.28	-1.01	0.66
1424815_at	glycogen synthase 2	Gys2	1.78	0.0000	-1	0.22	-1.01	0.3
1459522_s_at	glycogenin 1	Gyg1	1.26	0.0140	1.05	0.153	1.03	0.364
1417741_at	liver glycogen phosphorylase	Pygl	-1.42	0.0000	1.02	0.5	1.06	0.03
Steroid metabolism and biosynthesis								
1417871_at	hydroxysteroid (17-beta) dehydrogenase 7	Hsd17b7	-1.5	0.0000	-1.3	0.14	-1.32	0.13
1449038_at	hydroxysteroid 11-beta dehydrogenase 1	Hsd11b1	-1.32	0.0010	1.1	0.34	1.01	0.71
1460192_at	oxysterol binding protein-like 1A	Osbpl1a	-1.38	0.0000	-1.1	0.5	-1.08	0.52
1427345_a_at	sulfotransferase family 1A, member 1	Sult1a1	-1.29	0.0020	-1.1	0.69	-1.05	0.59
1419528_at	sulfotransferase, hydroxysteroid preferring 2	Sth2	-1.61	0.0000	-1.1	0.92	-1.2	0.26
Cytochrome (Cyt) P450, NADH-and NADPH-dependent Oxidative metabolism								
1418821_at	Cyt. P450, family 2, subfam. a, polyp. 12	Cyp2a12	-1.51	0.0000	1.06	0.21	-1.06	0.33
1422257_s_at	Cyt. P450, family 2, subfam. b, polyp. 10	Cyp2b10	-2.81	0.0010	-1.4	0.75	-1.39	0.75
1449479_at	Cyt. P450, family 2, subfam. b, polyp. 13	Cyp2b13	-2.24	0.0020	-1.2	0.77	-1.27	0.98
1425645_s_at	Cyt. P450, family 2, subfam. b, polyp. 20	Cyp2b20	-2.94	0.0010	-1.3	0.95	-1.42	0.36
1419590_at	Cyt. P450, family 2, subfam. b, polyp. 9	Cyp2b9	-1.55	0.0000	-1.1	0.78	-1.04	0.49
1417651_at	Cyt. P450, family 2, subfam. c, polyp. 29	Cyp2c29	-1.59	0.0040	-1.4	0.09	-1.41	0.09
1440327_at	Cyt. P450, family 2, subfam. c, polyp. 70	Cyp2c70	-2.58	0.0010	-1.2	0.15	-1.23	0.58
1448792_a_at	Cyt. P450, family 2, subfam. f, polyp. 2	Cyp2f2	-2.36	0.0010	1.76	0.05	1.3	0.43
1417532_at	Cyt. P450, family 2, subfam. j, polyp. 5	Cyp2j5	-3.08	0.0000	-1.5	0.1	-1.31	0.36
1418767_at	Cyt. P450, family 4, subfam. f, polyp. 13	Cyp4f13	-1.67	0.0080	-1.1	0.46	-1.4	0.36
1419559_at	Cyt. P450, family 4, subfam. f, polyp. 14	Cyp4f14	-3.58	0.0000	1.57	0.06	-1	0.92
1417070_at	Cyt. P450, family 4, subfam. v, polyp. 3	Cyp4v3	-1.41	0.0010	1.04	0.4	-1.09	0.81
1422100_at	Cyt. P450, family 7, subfam. a, polyp. 1	Cyp7a1	-2.36	0.0060	1.14	0.86	-1.39	0.24
1417429_at	flavin containing monooxygenase 1	Fmo1	-1.38	0.0000	1.04	0.23	1	0.57
1422904_at	flavin containing monooxygenase 2	Fmo2	-4.51	0.0080	-2.2	0.4	-2.05	0.49
1449525_at	flavin containing monooxygenase 3	Fmo3	-14.19	0.0040	-2	0.84	-2.34	0.59
1423908_at	NADH dehydrogenase (ubiquinone) Fe-S protein 8	Ndufs8	-1.23	0.0020	1.02	0.87	-1.04	0.13
Antioxidant and detoxification response								
1422438_at	epoxide hydrolase 1, microsomal	Ephx1	2.1	0.0000	1.14	0.3	-1.12	0.02
1421816_at	glutathione reductase 1	Gsr	1.2	0.0090	1.19	0.18	-1.01	0.95
1421041_s_at	glutathione S-transferase, alpha 2 (Yc2)	Gsta2	1.9	0.0030	-1.2	0.09	-1.59	0.51
1416842_at	glutathione S-transferase, mu 5	Gstm5	1.29	0.0000	1.02	0.82	-1.02	0.34
1449575_a_at	glutathione S-transferase, pi 2	Gstp2	1.4	0.0000	1.07	0.64	1.07	0.69
1417883_at	glutathione S-transferase, theta 2	Gstt2	2.76	0.0000	1.18	0.13	-1.3	0.05
1448239_at	heme oxygenase (decycling) 1	Hmox1	2.43	0.0000	-1.5	0.04	-1.17	0.12
1452592_at	microsomal glutathione S-transferase 2	Mgst2	2.89	0.0000	1.02	0.29	1.1	0.29
1448300_at	microsomal glutathione S-transferase 3	Mgst3	1.49	0.0010	1.29	0.04	1.02	0.1
1430979_a_at	peroxiredoxin 2	Prdx2	1.61	0.0010	1.75	0.01	1.34	0.26
1416292_at	peroxiredoxin 3	Prdx3	1.27	0.0100	1.24	0.19	1.09	0.18
1451124_at	superoxide dismutase 1, soluble	Sod1	1.22	0.0030	1.26	0.03	1.16	0.1
1415996_at	thioredoxin interacting protein	Txnip	2.11	0.0080	1.05	0.49	1.05	0.42
1440221_at	thioredoxin-like	Txnl	1.5	0.0020	1.26	0.58	1.17	0.83
Peroxisomal biogenesis								
1416679_at	ATP-binding cassette, sub-family D member 3	Abcd3	-1.29	0.0000	1.03	0.63	1.03	0.6
1449442_at	peroxisomal biogenesis factor 11a	Pex11a	-1.78	0.0100	-1.97	0.04	-1.6	0.37
1451213_at	peroxisomal biogenesis factor 11b	Pex11b	-1.24	0.0100	-1.03	0.82	-1.05	0.69
Fatty acid biosynthesis and elongation								
1455994_x_at	ELOVL1 long chain fatty acid elongatiion	Elovl1	1.28	0.0010	1.24	0.03	1.22	0.08
1417403_at	ELOVL6, long chain fatty acid elongatiion	Elovl6	1.37	0.0010	1.18	0.23	1.09	0.38
1415823_at	stearoyl-Coenzyme A desaturase 2	Scd2	1.39	0.0010	1.29	0.15	1.23	0.45
1424119_at	protein kinase beta 1 non-catalytic subunit	Prkab1	1.44	0.0000	1.28	0.15	1.11	0.8
1418438_at	fatty acid binding protein 2, intestinal	Fabp2	1.4	0.0010	1.09	0.21	1.13	0.03
1416021_a_at	fatty acid binding protein 5, epidermal	Fabp5	1.63	0.0000	-1.2	0.17	1.14	0.57
1450779_at	fatty acid binding protein 7, brain	Fabp7	2.16	0.0000	1.52	0.21	1.66	0.05
1425875_a_at	leptin receptor	Lepr	2.78	0.0000	-1.6	0.02	-1.3	0.07
1420715_a_at	peroxisome proliferator activated receptor gamma	Pparg	1.99	0.0000	1.53	0.01	1.11	0.73
1417900_a_at	very low density lipoprotein receptor	Vldlr	1.81	0.0010	1.01	0.86	-1.1	0.4

Table 1. Significant gene expression changes in the livers of $Csb^{m/m}/Xpa^{-/-}$, $Csb^{m/m}$ and $Xpa^{-/-}$ mice compared to wt controls.

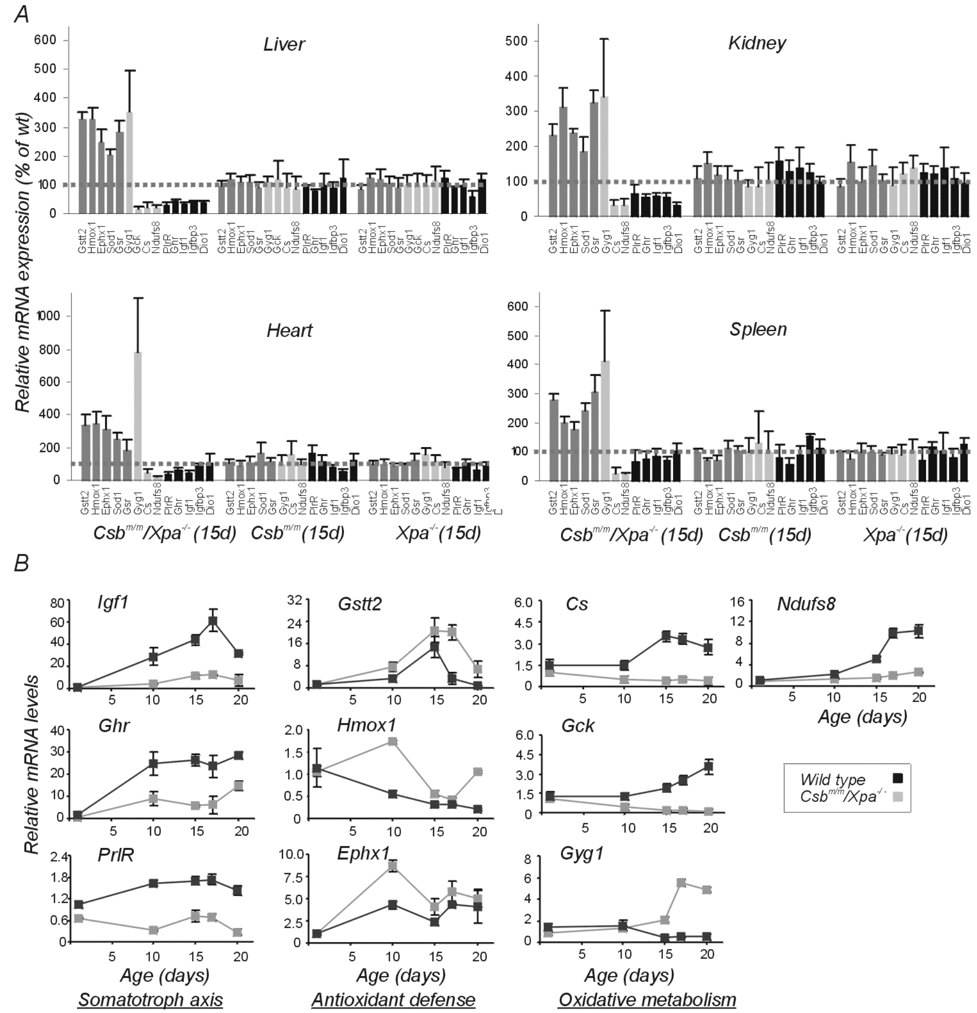

Figure 5. Expression levels of genes associated with the somatotroph axis, antioxidant defense, and metabolism in mutant and wt mouse liver and other organ at various ages. *A) Q-PCR evaluation of mRNA levels of genes associated with antioxidant defense (dark gray bars), oxidative metabolism (light gray bars) and the GH/IGF1 axis (black bars) in the liver, kidney, heart and spleen of 15-day old Csb$^{m/m}$/Xpa$^{-/-}$, Csb$^{m/m}$, and Xpa$^{-/-}$ pups. For each gene, expression levels in the mutant tissue are plotted relative to that of age-matched wt control tissues (dotted line). Error bars indicate S.E.M between replicates (n ≥ 3). B) Relative mRNA expression levels (fold changes, relative to embryonic day 18) of genes involved in the GH/IGF1 growth axis, antioxidant defense, and oxidative metabolism in the liver of wt and Csb$^{m/m}$/Xpa$^{-/-}$ pups, plotted as a function of time. Error bars indicate S.E.M between replicates (n ≥ 3).*

We next determined the expression levels of aforementioned genes in the kidney, heart and spleen of the same set of animals employed in the microarray experiment. Expression levels markedly mirrored the deviant expression patterns observed in the liver, while mRNA levels in *Csb$^{m/m}$* and *Xpa$^{-/-}$* tissues were not significantly different from wt animals (Fig. 5A). Thus, attenuation of the GH/IGF1 axis and down-regulation of metabolism, along with the enhanced antioxidant/detoxification response, represents a systemic, rather than liver-specific response of the $Csb^{m/m}/Xpa^{-/-}$ pups to the DNA repair defect. Interestingly, when 96-week old wild type livers were tested for expression levels of this same set of $Csb^{m/m}/Xpa^{-/-}$ responsive genes, we noticed a remarkable resemblance (data not shown).

Comparison of the $Csb^{m/m}/Xpa^{-/-}$ and naturally aged mouse liver transcriptomes

The previous result prompted us to investigate whether and to which extent the gene expression changes in the $Csb^{m/m}/Xpa^{-/-}$ mouse liver overlap with those observed in a natural aged liver. To this end, we first compared the full mouse liver transcriptome of adult 16-, 96- and 130-week old wt C57Bl/6J mice (n=4) with that of adult 8-week old wt C57Bl/6J mice (n=4). Using the same analytical method as applied to the $Csb^{m/m}/Xpa^{-/-}$ mouse livers, we identified homeostasis of energy reserves, oxidative metabolism along with cell growth and maintenance to be significantly overrepresented in 96- and 130-week old wt mice, but not in 16-week old animals (for summary, see Fig 6C). These findings fit well with previous studies suggesting the repression of oxidative metabolism to represent a conserved response shared by highly diverged species (McCarroll et al., 2004).

Next, we implemented a previously described method (Fraser et al., 2005) to evaluate the extent of genome-wide similarity between the liver transcriptomes of 2-week old $Csb^{m/m}/Xpa^{-/-}$ mice and, wt animals of various ages. We first classified all significantly differentially expressed genes in the $Csb^{m/m}/Xpa^{-/-}$ liver transcriptome as having increased or decreased expression (as compared to wt), and asked how many of these genes respond in a similar direction in the 16/8 wk, 96/8 wk, and 130/8 wk data sets. If the $Csb^{m/m}/Xpa^{-/-}$ liver resembles an aged liver, one expects the Spearman's rank correlation coefficient rho (r +1.0 or -1.0 in case of perfect similarity or dissimilarity, respectively, and 0.0 in case of no correlation) to increase with age. Notably, whereas the liver transcriptome of $Csb^{m/m}/Xpa^{-/-}$ mutant mice was dissimilar to that of 16-week old wt mice (Spearman's r = -0.28), as it was with 15-day old littermates, this turned into a significant positive correlation when the comparison was made between the $Csb^{m/m}/Xpa^{-/-}$ and 96-week old mouse liver transcriptomes (r = +0.15) and even more with the 130-week old wt mouse group (r = +0.44, $p \leq 0.0001$, Fig. 6A). Comparable results were obtained when the same approach was applied over the whole mouse transcriptome (including all Affymetrix probe sets with signals above the detection cut-off value; see Methods), thus avoiding any initial pre-selection or introduction of bias. Using the same approach, we did not find a significant correlation between the liver transcriptomes of 15-day old $Csb^{m/m}$ or $Xpa^{-/-}$mice and aged wt mice.

The genome-wide resemblance between the short-lived $Csb^{m/m}/Xpa^{-/-}$ mice and the 130-week old mice was substantially higher (>90%) when the comparison was restricted to those functional categories that were significantly overrepresented in the double mutant and 130-week old mice, such as the GH/IGF1 axis, oxidative metabolism (i.e. glycolysis, Krebs and oxidative phosphorylation), cytochrome P450 electron transport and peroxisomal biogenesis (Fig. 6B and C). Despite the occurrence of dissimilarities between the liver transcriptome of $Csb^{m/m}/Xpa^{-/-}$ pups and aged wt mice (the latter animals showing over-representation of genes involved in the immune and inflammatory responses, ATP biosynthesis and protein glycosylation, along with a lack of the anti-oxidant response), these findings strongly underline the genome-wide parallels between the *Csb*$^{m/m}$/*Xpa*$^{-/-}$ repair mutants and natural aging, thereby validating the progeria in the double mutant pups.

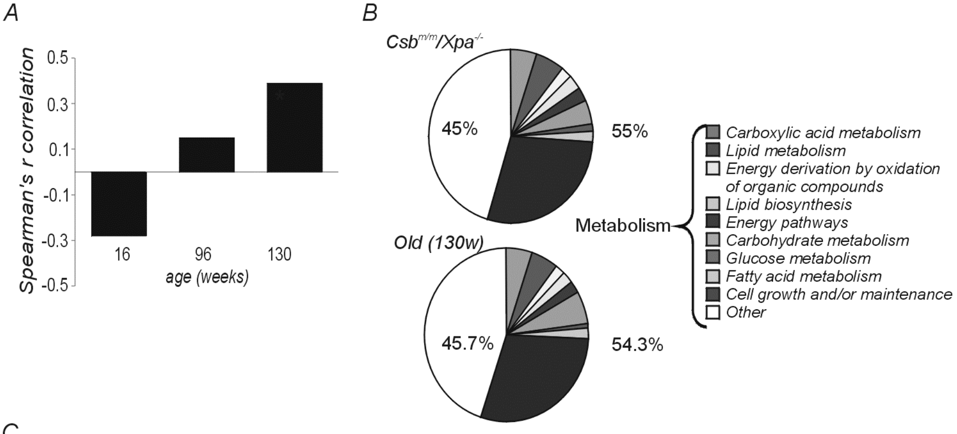

C

Code	**Title**	**Gene Symbol**	***Csb*** $^{m/m}$ ***Xpa*** $^{-/-}$		**130W**		**96W**	
			fc	**p**	**fc**	**p**	**fc**	**p**
The IGF-1/GH growth axis								
1419519_at	insulin-like growth factor 1	Igf1	-2.13	0.000	-1.48	0.005	-1.44	0.006
1451871_a_at	Growth hormone receptor	Ghr	-2.21	0.012	-2.37	0.001	1.06	0.186
1417991_at	deiodinase, iodothyronine, type I	Dio1	-2.12	0.000	-1.69	0.043	-1.28	0.105
1435663_at	estrogen receptor 1 (alpha)	Esr1	-1.91	0.001	-1.36	0.090	1.50	0.016
1421841_at	fibroblast growth factor receptor 3	Fgfr3	-1.43	0.001	-2.66	0.016	1.20	0.237
1427777_x_at	fibroblast growth factor receptor 4	Fgfr4	-1.32	0.009	-1.97	0.044	1.44	0.054
1450869_at	fibroblast growth factor 1	Fgf1	-1.38	0.003	-2.42	0.001	-1.38	0.008
Carbohydrate metabolism								
1425303_at	glucokinase	Gck	-4.80	0.004	-2.24	0.052	-1.18	0.295
1417741_at	liver glycogen phosphorylase	Pygl	-1.42	0.000	-1.83	0.002	-1.41	0.001
1423644_at	aconitase 1	Aco1	-1.26	0.002	-2.08	0.001	-1.26	0.036
1422577_at	citrate synthase	Cs	-1.28	0.006	-1.74	0.000	-1.46	0.001
Cytochrome (Cyt) P450, NADH-and NADPH-dependent Oxidative metabolism								
1417070_at	cytochrome P450, family 4, subfamily v, polypeptide 3	Cyp4v3	-1.41	0.001	-2.51	0.002	-2.56	0.001
1418821_at	cytochrome P450, family 2, subfamily a, polypeptide 12	Cyp2a12	-1.51	0.000	-1.42	0.042	-1.29	0.002
1425365_a_at	cytochrome P450, family 2, subfamily d, polypeptide 13	Cyp2d13	-2.17	0.006	-2.51	0.008	-1.87	0.004
1417532_at	cytochrome P450, family 2, subfamily j, polypeptide 5	Cyp2j5	-3.08	0.000	-2.90	0.019	-5.47	0.006
1418767_at	cytochrome P450, family 4, subfamily f, polypeptide 13	Cyp4f13	-1.67	0.008	-1.98	0.008	-1.64	0.009
1419559_at	cytochrome P450, family 4, subfamily f, polypeptide 14	Cyp4f14	-3.58	0.000	-2.09	0.009	-1.39	0.002
1417429_at	flavin containing monooxygenase 1	Fmo1	-1.38	0.000	-2.46	0.009	-1.64	0.038
1448589_at	NADH dehydrogenase (ubiquinone) 1 beta subcomplex, 5	Ndufb5	-1.17	0.007	-1.79	0.002	-1.65	0.000
1423908_at	NADH dehydrogenase (ubiquinone) Fe-S protein 8	Ndufs8	-1.23	0.002	-1.43	0.008	-1.31	0.015
Peroxisomal biogenesis								
1422471_at	peroxisomal biogenesis factor 13	Pex13	-1.16	0.000	-1.68	0.002	-1.48	0.000
1424078_s_at	peroxisomal biogenesis factor 6	Pex6	-1.43	0.003	-1.92	0.006	-1.12	0.160
1448910_at	peroxisomal trans-2-enoyl-CoA reductase	Pecr	-1.38	0.009	-1.76	0.018	-1.39	0.010
1451213_at	peroxisomal biogenesis factor 11b	Pex11b	-1.24	0.010	-2.16	0.011	-1.13	0.226
1451226_at	peroxisomal biogenesis factor 6	Pex6	-1.40	0.000	-2.01	0.006	-1.11	0.224

Figure 6. Transcriptome similarities between *Csb*$^{m/m}$/*Xpa*$^{-/-}$ and naturally aged mice. *A) Spearman's r correlation of 16-, 96- and 130-week old mice with 15-day old Csb*$^{m/m}$*/Xpa*$^{-/-}$ *mice, where -1.0 is a perfect negative (inverse) correlation, 0.0 is no correlation, and 1.0 is a perfect positive correlation. B) Similarities between significantly overrepresented biological processes of Csb*$^{m/m}$*/Xpa*$^{-/-}$ *and naturally aged mice. Note that in both Csb*$^{m/m}$*/Xpa*$^{-/-}$ *and naturally aged mice transcriptional changes were mostly associated with metabolic processes. C) Correlation in significant expression changes of genes associated with the GH/IGF1 axis and oxidative metabolism in the livers of Csb*$^{m/m}$*/Xpa*$^{-/-}$ *and naturally aged (96- and 130-week old) mice.*

Reduced IGF1 serum levels, glucose and fat utilization in $Csb^{m/m}/Xpa^{-/-}$ mice

In agreement with the down-regulation of *Igf1* gene expression in the liver (the main source of circulating IGF1 (Frystyk, 2004)), we observed a significant reduction ($p<0.004$) in serum IGF1 levels in 7-, 10- and 15-day old $Csb^{m/m}/Xpa^{-/-}$ mice (Fig. 7A) together with significantly lower blood glucose levels ($p<0.04$, Fig. 7B). Following an initial reduction of ~30% ($p<0.04$) in 7-, 10- and 15-day old $Csb^{m/m}/Xpa^{-/-}$ mice, blood glucose levels further dropped at day 16, gradually reaching very low levels in 20-day old $Csb^{m/m}/Xpa^{-/-}$ mice (~3 mM) contrasting the steady blood glucose levels (~ 9 mM) in wt and single mutant pups (data not shown). The presence of milk and food in the stomach of the double mutant pups along with the normal appearance of the intestinal epithelium (Fig. 3A) indicates that the hypoglycemia is not due to impaired food intake. Even more, the suppression of the somatotroph axis and subsequent decreased IGF1 production in 15-day old $Csb^{m/m}/Xpa^{-/-}$ mice appeared not to originate from a pituitary dysfunction as histological examination (Fig 3F) and TUNEL staining of sections from the pituitary pars distalis, intermedia and nervosa did not reveal any abnormalities (data not shown). Moreover, serum GH levels in 15-day old $Csb^{m/m}/Xpa^{-/-}$ mice (15.2 +/- 4.2 ng/ml, n=8) did not differ significantly from wt littermates (12.8 +/- 2.8 ng/ml, n=6). Interestingly, the normal serum GH levels together with the significant systemic down regulation of Gh receptor gene expression, likely points to growth hormone resistance in 15-day old $Csb^{m/m}/Xpa^{-/-}$ mice.

PAS staining of liver sections from 10- to 20-day old pups and naturally aged mice revealed enhanced accumulation of glycogen in unusually large vesicles in $Csb^{m/m}/Xpa^{-/-}$ pups and 96-week old mice when compared to wt littermates and 8-week old wt mice (Fig. 7C). This observation fits our microarray data, suggesting that both the $Csb^{m/m}/Xpa^{-/-}$ and naturally aged mice store, rather than utilize glucose. Overnight fasting of $Csb^{m/m}/Xpa^{-/-}$ pups and littermate controls resulted in a near-to-complete depletion of liver glycogen (Fig. 7D) indicating that the glycogen accumulation is not due to inability to split glycogen into its constitutive glucose monomers.

Consistent with the broad up-regulation of genes associated with fatty acid synthesis (Table 1), oil Red O staining of liver sections from 15-day old pups and naturally aged mice revealed enhanced accumulation of triacylglycerides in both compared to control littermates and 8-week old mice (Fig. 7C), indicating hepatic steatosis. This and the absence of adipose tissue suggest that $Csb^{m/m}/Xpa^{-/-}$ mice display generalized lipodystrophy (loss and abnormal redistribution of body fat) (Ahima and Osei, 2004).

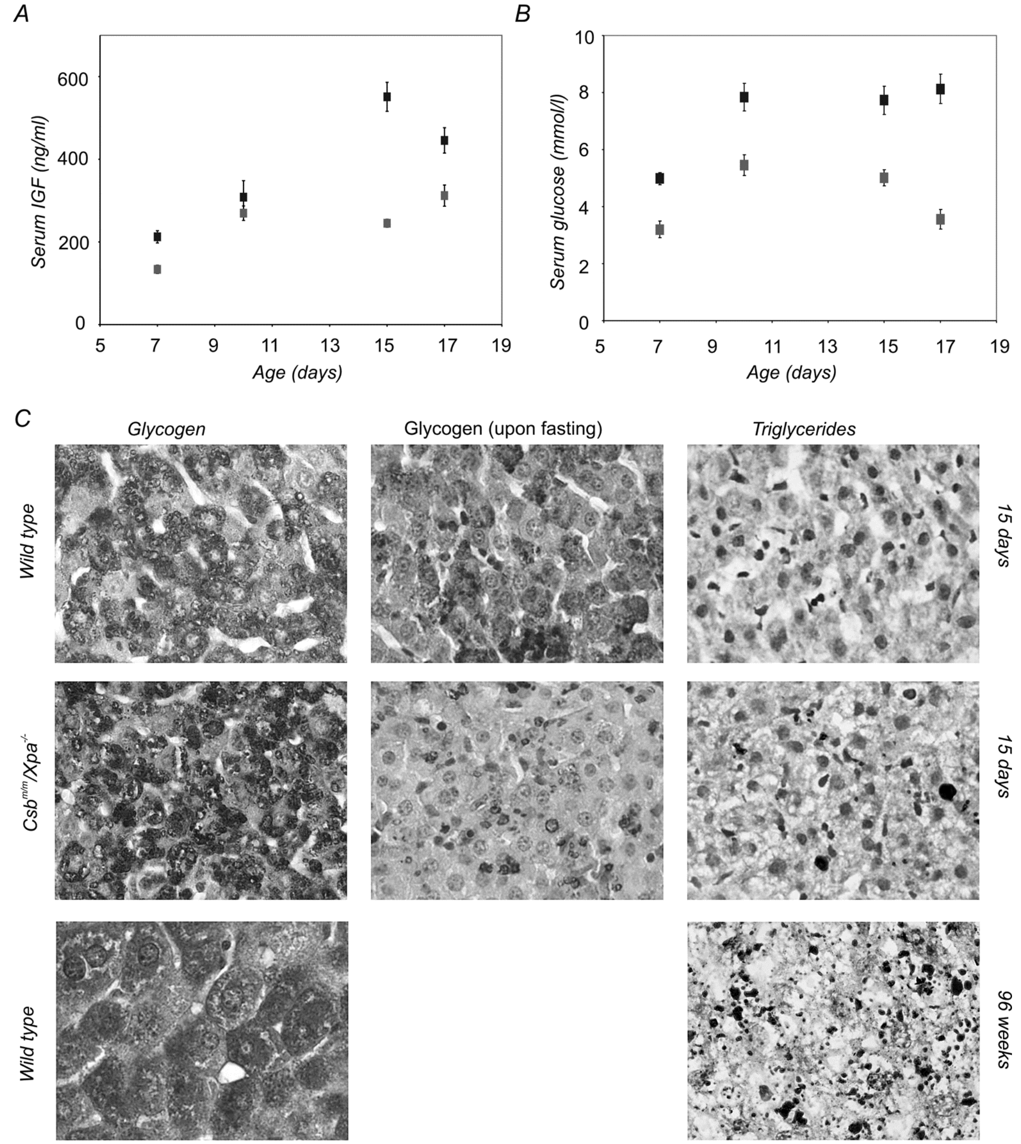

Figure 7. Carbohydrate/fat metabolism and IGF1 serum levels. *A) IGF1 (ng/ml) and B) glucose (mmol/l) levels in the serum of 15-day old* $Csb^{m/m}/Xpa^{-/-}$ *mice and control littermates (n=6). The levels of IGF1 and glucose in the serum of* $Csb^{m/m}/Xpa^{-/-}$ *mice are significantly lower than that of control littermates (p<0.0004 and p< 0.04, respectively). C) PAS staining for glycogen (left) and Oil Red O staining for triglycerides (right) in livers of 15-day old wt and* $Csb^{m/m}/Xpa^{-/-}$ *mice and 96-week old wt mice. Pictures were taken at 100x magnification. Note the large polyploid nuclei in the 96-week old wt mouse liver. PAS staining for glycogen (middle) in livers of 15-day old wt and* $Csb^{m/m}/Xpa^{-/-}$ *mice after overnight starvation. Pictures were taken at 100x magnification.*

Systemic Changes in Somatotroph Axis and Antioxidant Defense in DEHP-Treated wt Mice

To test whether the presence of endogenous (oxidative) DNA damage can provoke the somatotrophic drop and enhanced antioxidant potential, wt C57BL/6J mice (n=6; 4-week old) were fed *ad libitum* for 9 weeks with standard food containing sub-toxic levels of an oxidative DNA damage-inducing agent; di(2-ethylhexyl)phthalate, DEHP, 1500 ppm (Seth, 1982). Neither body weight nor appetite and food intake of DEHP-exposed animals deviated from that of untreated control animals. As shown in Figure 8, subsequent analysis revealed suppression of the expression of genes associated with the somatotroph axis (*Igf1*, *Igfbp3, Ghr*, and *Dio1*) and oxidative metabolism (*Gck*, *Cs* and *Ndufs8*), along with the up-regulation of glycogenin 1 (*Gyg1*, Fig 5A) in DEHP-exposed animals. Consistent with the ability of DEHP to generate ROS-induced DNA damage in the liver, we also noticed a significant up-regulation of genes associated with the antioxidant and detoxification responses (*Hmox1, Ephx1, Gsr*, *Sod1*, *Gstt2*). These findings suggest that accumulation of unrepaired (oxidative) DNA damage likely comprises one of the causes underlying the observed suppression of the GH/IGF1 and oxidative metabolism in *Csb*$^{m/m}$/*Xpa*$^{-/-}$ mice.

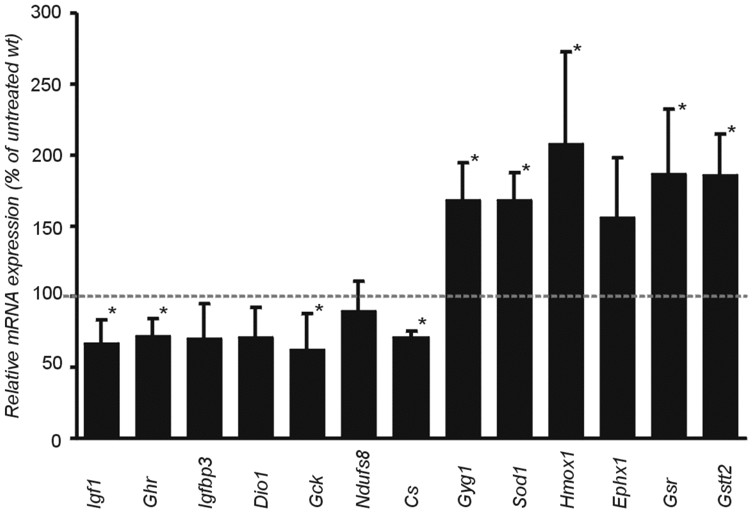

Figure 8. Expression levels of genes associated with the GH/IGF1 axis, oxidative metabolism and antioxidant defense in livers of DEHP-treated wild type mice. *Relative mRNA expression levels of genes involved in the GH/IGF1 growth axis, oxidative metabolism and antioxidant defense in 13-week old wt mice treated with a low dose of the pro-oxidant DEHP. For each gene, expression levels in the treated wt mouse livers are plotted relative to that of untreated wt littermate controls (dotted line) (*; p≤ 0.05).*

Discussion

Csb$^{m/m}$ mice exhibit several CS features (e.g. attenuated growth, blindness, neurological dysfunction), but their phenotype is overall milder than the human syndrome (van der Horst et al., 1997) despite that the truncation in the N-terminal part (mimicking a mutant allele of CS-B patient CS1AN) completely inactivates the protein and TC-NER (van der Horst et al., 1997). Although the severity of clinical features in humans does not seem to correlate with the severity of the molecular defect (Horibata et al., 2004), the absence of the complete spectrum of CS features in the *Csb*$^{m/m}$ mouse model likely originates from man-mouse differences (i.e. adaptation to stress, tolerance to DNA damage/genome instability), rather than from the nature of the *Csb*$^{m/m}$ mutation. This idea is supported by our observations that *Xpd*^{TTD} and *Xpd*^{XPCS} mice (all carrying causative point mutations) also fail to show the severe CS features associated with XPCS and TTD (Andressoo et al., 2006; de Boer et al., 2002).

Yet, the present study reveals that inactivation of GG-NER or complete abrogation of NER (through inactivation of *Xpc* or *Xpa*, respectively) in TCR-deficient *Csb*$^{m/m}$ mice dramatically aggravates the *Csb*$^{m/m}$ mouse phenotype. As animals were not exposed to exogenous genotoxic agents, we attribute this effect to enhanced levels of unrepaired endogenous (oxidative) DNA damage. In further support of this, we have shown that *Csb*$^{m/m}$/*Xpc*$^{-/-}$ and *Csb*$^{m/m}$/*Xpa*$^{-/-}$ MEFs, as well as *Csb*$^{m/m}$/*Xpa*$^{-/-}$ retinal photoreceptor cells, are more sensitive to environmental genotoxic insults (i.e. UV-light, ionizing radiation) than their single mutant counterparts. A comparable phenotypic deterioration has been noticed when *Xpa* was inactivated in *Xpd*^{TTD} (de Boer et al., 2002), *Xpd*^{XPCS} (Andressoo et al., 2006), compound heterozygous *Xpd*$^{TTD/XPCS}$ animals (carrying causative mutations for TTD and combined XP/CS; van de Ven et al., pending revision), and *Xpg*^{deltaEx15} mice (Shiomi et al., 2005).

Importantly, *Csb*$^{m/m}$/*Xpa*$^{-/-}$ mice appeared normal at birth, indicating a normal intra-uterine development and ruling out that this condition is an embryonic developmental disorder. Instead, after birth, the *Csb*$^{m/m}$/*Xpa*$^{-/-}$ pups displayed progressive kyphosis, cachexia, photoreceptor loss, and motor dysfunction, all common postnatal manifestations of CS (Nance and Berry, 1992), as well as of natural mammalian aging (Arking, 1998; Kalu, 1995; Weiss et al., 1991). Also similar to CS patients (average age at death 12.5 years), *Csb*$^{m/m}$/*Xpa*$^{-/-}$ pups fail to grow into adulthood and die before weaning. The relation between (residual) repair capacity, time and severity of a particular phenotype is well illustrated by the retinal photoreceptor loss in the *Csb*$^{m/m}$ mouse models. While aging C57Bl/6J mice lose about 5-10% of their rods and cones in 30 months, TCR-deficient *Csb*$^{m/m}$ mice have already lost about 50% of their photoreceptor cells by the age of 16 months (Chapter 3). This spontaneous retinal degeneration in *Csb*$^{m/m}$ mice originates from enhanced apoptotic sensitivity of photoreceptor cells (Chapter 3), evolving in the first one or two months after weaning (this study). Interestingly, further crippling of NER in *Csb*$^{m/m}$ animals by inactivation of *Xpa* accelerates the onset of photoreceptor loss, now becoming visible as early as postnatal day 15, and progressively increasing thereafter. The strong correlation between the severity of the repair deficiency and the onset of photoreceptor loss, as well as the enhanced ionizing radiation hypersensitivity of photoreceptor cells of *Csb*$^{m/m}$/*Xpa*$^{-/-}$ mice (as compared to age-matched *Csb*$^{m/m}$ animals), well support the hypothesis that (oxidative) DNA damage likely underlies the retinal degeneration.

Full genome transcriptome analysis of the $Csb^{m/m}/Xpa^{-/-}$ mouse liver, aiming at unraveling the etiology of the severe double mutant phenotype, led us to identify significant genome-wide parallels between the 2-week old $Csb^{m/m}/Xpa^{-/-}$ and 130-week (but not 16-week) old wt animals at the fundamental level of gene expression. Importantly, this resemblance was largely attributable to the substantial down regulation of genes associated with processes implicated in oxidative energy and growth metabolism, previously revealed by others to represent a conserved transcriptional response in aging (McCarroll et al., 2004).

The down-regulation of genes associated with the GH/IGF1 growth axis in the liver, the systemic reduction in *GH receptor* mRNA levels and the impaired *Igf1* gene expression in liver and other tissues (resulting in low serum IGF1 levels) likely underlies the postnatal growth defect in $Csb^{m/m}/Xpa^{-/-}$ pups. These changes were not due to reduced GH serum levels or pituitary abnormalities. Importantly, a steady decline in the GH/IGF1 somatotroph axis is also observed in rodents and humans during natural aging (Carter et al., 2002). Furthermore, $Csb^{m/m}/Xpa^{-/-}$ pups failed to up-regulate metabolism; instead they displayed a sharp, systemic reduction in the expression levels of genes involved in glycolysis, tricarboxylic acid cycle (including decreased citrate synthase activity), and oxidative respiration, which coincided with the onset of weight loss (cachexia). In addition, $Csb^{m/m}/Xpa^{-/-}$ pups up-regulated genes associated with glycogen and fatty acid synthesis, leading to increased hepatic glycogen storage and fat accumulation (steatosis) and pronounced hypoglycemia. Simultaneously subcutaneous fat tissue was virtually absent. Given that, in mammals, the GH/IGF1 signaling pathway comprises one of the major regulators of energy homeostasis to integrate metabolism with growth (Frystyk, 2004; Longo and Finch, 2003; Puigserver et al., 2003), it is tempting to speculate that reduced IGF1 signaling is responsible for the postnatal metabolic shift and growth defect seen in $Csb^{m/m}/Xpa^{-/-}$ mice. Interestingly, several CS patients have been previously reported with hypoglycemia and low IGF1 serum levels (Fujimoto et al., 1969; Park et al., 1994), low metabolic rate (Ellaway et al., 2000) and abnormal fat deposition (Laszlo and Simon, 1986).

Paradoxically, however, the systemic suppression of the somatotrophic axis and energy metabolism, along with the up-regulation of antioxidant defenses, low IGF1 serum and blood glucose levels, observed in the $Csb^{m/m}/Xpa^{-/-}$ mouse, are all associated with increased longevity, rather than with the short lifespan of this mouse model. In lower paradigms for life span extension (*C. elegans*, *D. melanogaster*), genetic interference in the insulin-signaling pathway can prolong life multi-fold (Kenyon, 2005; Partridge et al., 2005). In mammals, IGF1-deficient, Ames and Snell dwarf mice (characterized by defects in the development of the anterior pituitary due to mutations in the *Prop-1* and *Pit1* loci and diminished levels of GH, thyroid stimulating and prolactin hormones) combine hypoglycemia, low body temperature, and increased storage of carbohydrates and lipids (Carter et al., 2002; Longo and Finch, 2003) with up-regulation of antioxidant defense capacity and extended lifespan (Brown-Borg et al., 1999; Brown-Borg and Rakoczy, 2000). Conversely, GH-overexpressing transgenic mice display reduced lifespan and antioxidant responses (Bartke et al., 2002). These findings have also been recently confirmed by our identification of genome-wide parallels between the extremely short-lived DNA repair mutants (i.e. $Csb^{m/m}/Xpa^{-/-}$, $Ercc1^{-/-}$) and the extremely long-lived Ames and Snell dwarfs and growth hormone receptor knockout ($Ghr^{-/-}$) mice (Garinis *et al*. manuscript in preparation). Last but not least, IGF1 plasma levels decline with age in humans and rodents (Florini et al., 1981; Johanson and Blizzard, 1981; Rudman et al., 1981). Along with this hormonal shift, aging cells surmount an intricate antioxidant defense response (Camougrand and Rigoulet, 2001; Ji et al., 1998) that is thought to prevent the detrimental consequences of oxidative stress. Interestingly, the progressive, age-related decrease in the somatotroph axis has been suggested to confer a selective advantage by postponing the onset of age-related disease and prolonging life span through the reduction of toxic free radicals (Carter et al., 2002).

How would repair-deficient mice benefit from such a response? During development, the mitogenic action of GH and IGF1 fuels cellular metabolism, thereby promoting tissue growth and function (Bartke, 2003; Carter et al., 2002; Chandrashekar et al., 2004). A high metabolic activity, however, leads to higher oxygen consumption (Carter et al., 2002) and may also increase the ROS burden through the parallel increase of mitochondrial electron transport, peroxisomal fatty acid metabolism and/or microsomal cytochrome *P-450* enzymes (Beckman and Ames, 1998). Despite antioxidant defense and DNA repair, oxidative DNA damage will still accumulate, leading to transcriptional stress, impaired replication, cellular senescence, malfunction or death and eventually to progressive loss of tissue homeostasis and organismal decline (see model, Fig. 9). We hypothesize that complete abrogation of NER (by inactivation of *Xpa*) renders TCR-deficient $Csb^{m/m}$ mice unable to adequately cope with the increased burden of DNA damage in the transcribed strand of active genes. This triggers an adaptive response i.e. reduction of metabolic activity through down-regulation of the GH/IGF1 axis to relieve the pressure on their genome. We interpret this as an attempt to limit the deleterious effects of arrested transcription, such as cellular senescence and death causing accelerated aging. As a consequence, the initially normal growth becomes arrested soon after birth, leading to severe growth retardation. This scenario provides a plausible explanation for the growth defect in CS patients. However, this response is unable to fully compensate for the repair defect, thus damage still accumulates to critical levels and triggers apoptosis and/or senescence, thereby leading to aging-associated pathology such as neurodegeneration (as illustrated by the photoreceptor cells in $Csb^{m/m}/Xpa^{-/-}$ mice).

The conceptual link between DNA damage and the systemic adaptive response is supported by our observation that chronic exposure of wt mice to a sub-toxic dose of DEHP (a pro-oxidant that enhances the DNA damage load; see de Waard et al, 2004) triggers a response similar to that observed in (untreated) $Csb^{m/m}/Xpa^{-/-}$ mice. Although DEHP at much higher concentrations has been previously documented to affect the endocrine function of the pituitary, proteome analysis revealed that synthesis of prolactin and growth hormone appears unaffected in DEHP-treated rats (Hirosawa et al., 2006). This suggests that the observed suppression of genes associated with the somatotroph axis and oxidative metabolism in the liver of DEHP-exposed mice is triggered by DNA damage in the liver, rather than by a pituitary defect or hypothalamic defect.

As one would predict, other short-lived NER mouse models (e.g. Xpg, Xpf mice, (Harada et al., 1999; Tian et al., 2004)) or NER mutant mice with a milder progeroid phenotype could also show accelerated attenuation of the somatotrophic axis in response to their DNA repair defect. Indeed, $Ercc1^{-/-}$ animals, carrying a combined NER/crosslink DNA repair defect and a life span of only a few weeks, demonstrate a remarkable genome-wide similarity in liver gene expression profiles with *Csb*$^{m/m}$/*Xpa*$^{-/-}$ mice (Niedernhofer et al., pending revision), while Xpd^{XPCS}/Xpa$^{-/-}$ and compound heterozygous *Xpd*$^{TTD/XPCS}$/*Xpa*$^{-/-}$ mice contain lower serum IGF1 levels (van de Ven et al., submitted). Furthermore, *Xpd*^{TTD} mice, which manifest accelerated aging in many (but not all) organs and tissues, have recently been shown to display features related to a caloric restricted-like phenotype and suppression of the GH/IGF1 axis in a limited set of organs and tissues, stressing the segmental nature that is characteristic of all progeroid syndromes and the systemic nature of the response (Wijnhoven et al., 2005). Finally, proper glucose homeostasis and normal IGF1 levels were recently shown to require Sirt6 activity, a chromatin deacetylase that may promote DNA repair (Mostoslavsky et al., 2006). As ROS-mediated DNA damage appears to be the underlying cause of the *Csb*$^{m/m}$/*Xpa*$^{-/-}$ progeria, it is tempting to speculate that one can attenuate the premature onset of age-related features by directly counteracting the harmful byproducts of metabolism (i.e. ROS), and consequently DNA damage. Interestingly, an antioxidant-based nutraceutical intervention pilot study with *Csb*$^{m/m}$/*Xpa*$^{-/-}$ mice, aiming at extending life span and delaying onset of pathology, yielded promising results (Chapter 5).

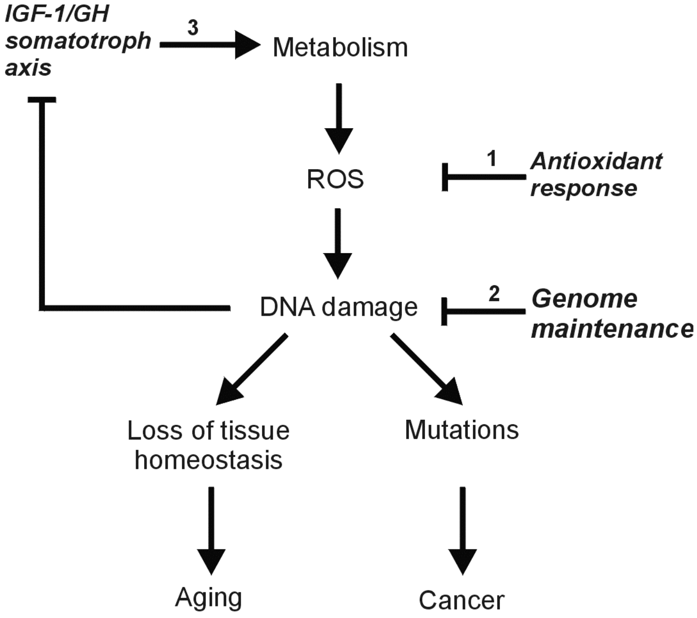

Figure 9. The proposed link between DNA damage and the decline of the GH/IGF1 somatotroph axis. *ROS are natural byproducts of metabolism and can injure several macromolecules including DNA, thus contributing to a slow but steady accumulation of damage, transcriptional stress, impaired replication and eventually the progressive loss of tissue homeostasis and gradual organismal deterioration. Cells and tissues will respond by (1) up regulating their antioxidant defense responses that would moderate the harmful effects of ROS, (2) employing a battery of genome maintenance pathways that would repair or remove damaged macromolecules and help to resist the oxidative stress, and (3) suppressing their GH/IGF1 somatotroph axis along with the oxidative metabolism, thus substantially moderating their metabolic activity that would otherwise lead to high oxygen consumption and increased generation of oxidants. To this end, the physiologic reduction of the somatotroph axis and oxidative metabolism is envisaged to be beneficial in terms of net life span.*

Materials and Methods

Animals

The generation and characterization of NER-deficient *Xpa*$^{-/-}$, *Xpc*$^{-/-}$, and *Csb*$^{m/m}$ mice has been previously described (Cheo et al., 1996; de Vries et al., 1995; Nakane et al., 1995; van der Horst et al., 1997) *p53*$^{-/-}$ mice (Lowe et al., 1993) were kindly provided by Dr. T. Jacks (MIT, Cambridge, MA). Unless stated otherwise, all mice were kept in a C57BL/6J genetic background. In the DEHP exposure study, 4-week old male wt mice (C57BL/6J; n=6) were put on a di(2-ethylhexyl)phthalate (DEHP; 1500 ppm; Sigma) containing diet or on a regular diet for 9 weeks. Animals were daily screened for discomfort and weighed once a week. Food consumption was registered by weighing the food. In the ionizing irradiation exposure study, 18-day old *Csb*$^{m/m}$/*Xpa*$^{-/-}$ and littermate control animals (n=4-6/genotype) were exposed to 10 Gy, sacrificed 20 hours after exposure (age 19 days) and eyes were further processed. As required by Dutch law, all animal studies were approved by an independent Animal Ethical Committee (Dutch equivalent of the IACUC).

Cellular sensitivity studies

UV sensitivity was determined as described (Sijbers et al., 1996). Sparsely seeded petri dish cultures were exposed to different doses of UV (254 nm, Philips TUV lamp). After 4 days, the number of proliferating cells was estimated from the amount of radioactivity incorporated during a 2 hr pulse with [^{3}H] thymidine. Cell survival was expressed as the percentage of radioactivity in exposed cells in relation to the radioactivity in untreated cells. UV-induced global genome repair was assayed using the UDS method described by (Vermeulen et al., 1994). In brief, coverslip-grown cells were exposed to 16 J/m^2 of 254 nm UV light and labeled with [^{3}H] thymidine. Repair capacity was quantified by grain counting after autoradiography. RNA synthesis recovery was measured according to (Ma et al., 1997). In short, coverslip-grown cells were exposed to 10 J/m^2 of 254 nm UV light, allowed to recover for 16 hr, labeled with [^{3}H] uridine, and processed for autoradiography. The relative rate of RNA synthesis was expressed as G_{UV}/G_C (percentage), where G_{UV} and G_C represent the number of grains over UV-exposed and non-exposed nuclei, respectively.

Ionizing radiation sensitivity of immortalized MEFs was determined using a colony assay. Cells were plated in 6-cm-diameter dishes at various densities. After 16 h, cells were exposed to a single dose of ionizing radiation (137Cs source; dose range of 0 to 8 Gy. Cells were grown for another 5 to 14 days, and after fixation and staining, colonies were counted. All experiments were performed in triplicate.

Immunohistological examination and blood parameters

Detailed histopathological examination was performed on all organs and tissues. Internal organs were isolated and either fixed in 10% phosphate-buffered formalin and paraffin-embedded (histopathological analysis) or snap-frozen in liquid N_2 (for transcription profiling by microarray analysis or quantitative PCR). Paraffin-embedded tissues were sectioned at 5 µm and stained with haematoxylin/eosin solution. Liver sections were stained with Periodic Acid Schiff (PAS) or

Oil Red O (cryosections) to detect glycogen and triglycerides respectively. Apoptotic cells were detected using a TdT-mediated dUTP Nick-End Labeling (TUNEL) assay as described by the manufacturer (Apoptag Plus Peroxidase *In Situ* Apoptosis Detection Kit, Chemicon). For immunohistochemical procedures, paraffin sections (5 µm) were dewaxed and rehydrated, followed by an antigen retrieval step, comprising 1 x 7 minute and 2 x 3 minute incubations of tissue sections with a 0.01M sodium citrate buffer in a 800 Watt microwave. Sections were washed in phosphate buffered saline (PBS) for 2 minutes. Endogenous peroxidase activity was blocked by incubating the sections for 30 minutes in PBS, containing 30% H_2O_2 and 12.5% sodiumazide. Sections were washed in PBS (1 x 2 minutes) and PBS, containing 0.5% milk powder, and 0.15% glycine (PBS+ buffer, 2 x 2 minutes). Immunohistochemical staining was performed by incubating sections with primary antibodies against PCNA (PC10, Abcam, dilution 1:1000) or BrdU (Bu20a, DAKO, dilution 1:100) in PBS+ (16 hr; 4 ^{o}C). In case of BrdU, sections were first covered with 0.1M HCl for 60 minutes at 37 ^{o}C and rinsed with PBS, prior to incubation with the primary antibody. Next, sections were washed in PBS+ (3 x 5 minutes) and incubated for 1 hour at room temperature with rat-anti-mouse Immunoglobulins antibody (1:1000) coupled to horseradish peroxidase (DAKO). After sections were washed in PBS+ (3 X 5 minutes) and PBS 1 x 2 minutes), color was developed for 8 minutes in 3,3'-diaminobenzidine solution (DAKO Liquid DAB substrate-chromogen system), all according to the instructions of the manufacturer. Sections were counterstained in haematoxylin before dehydration and mounting. All histology images were acquired at 40x objective magnification on an Olympus BX40 microscope (London, United Kingdom), equipped with a CCD camera.

For retinal evaluation, eyes were marked nasally with Alcian blue (5% Alcian blue in 96% ethanol), enucleated, fixed in 4 % paraformaldehyde in 0.1M phosphate buffer, washed in PBS and embedded in paraffin. Horizontal sections (5 µm thick) of the retina were cut and sections in the middle of the retina were selected by Alcian blue marking and proximity of the optic nerve. Sections were stained for degenerating cells by TdT-mediated dUTP Nick-End Labeling (TUNEL), according to the manufacturer's instructions (Apoptag Plus Peroxidase *In Situ* Apoptosis Detection Kit, Chemicon). For quantification, the number of TUNEL-positive cells in the inner nuclear layer (INL) and outer nuclear layer (ONL) were counted in 6 whole sections per mouse. Differences between the genotypes were tested for statistical significance using multivariate analysis of variance (ANOVA), followed by a posthoc test of Student-Newman-Keuls (S-N-K). Significance was set at $p<0.05$. Serum IGF1 and GH levels were determined with the Active mouse/rat IGF1 ELISA and Active mouse/rat GH ELISA kits respectively, as described by the manufacturer (Diagnostic Systems Laboratories Inc., Texas). Blood glucose was measured using a Freestyle mini blood glucose measurement device (Abbott Diabetes Care).

Radiography and micro-computed tomography

Mice were anaesthetized by intraperitoneal injection of ketalin and rompun (120 and 7.5 µg/g body weight). Lateral films were taken at 2x magnification using a CGR Senograph 500T X ray system operated at 30 kV and 32 mAS (de Boer et al., 2002). Formalin fixed tibiae from wt and mutant mice were scanned from proximal end to mid-diaphysis, using a SkyScan 1072 microtomograph (SkyScan, Antwerp, Belgium) with a foxel size of 8.82 µm. Scans were processed, and 2D images of the bones were obtained.

Citrate synthase enzyme activity

Frozen livers were transferred into ice-cold buffer (SHE) consisting of 250 mM sucrose, 10 mM HEPES, pH 7.4, and minced. Fresh SHE was added and homogenized by 12 passes in a tight-fitting glass/Teflon power-driven Potter-Elvejehem homogenizer. Citrate synthase activity of the homogenate was measured by monitoring the CoA-coupled conversion of Ellman's reagent into TNB at 412 nm at 37ºC in the presence of 0.005% (v/v) Lubrol-WX to solubilize the mitochondrial inner membrane and expressed in mU as nmol 5-thio-2-nitrobenzoate (TNB)/min per mg protein. Protein concentrations were determined by the Bio-Rad DC protein assay (Bio-Rad Laboratories, Inc., Veenendaal, The Netherlands) with BSA as a standard.

Footprint studies

Footprint analysis was performed by painting the hind and fore paws of the mice with different colors of water-soluble non-toxic paints. Animals were allowed to walk along a 30 x 7 cm walled runway, lined with paper, into a darkened, enclosed space. Tests were performed in duplicate at day 15 and 19. Footprint patterns were analyzed for (1) stride length, measured as the average distance between each stride, (2) front base width and (3) hind base width, measured as the average distance between contralateral footprints (Carter et al., 1999).

Microarray Analysis

Standard procedures were used to obtain total RNA (Qiagen) from the liver of wt, *Xpa*$^{-/-}$, *Csb*$^{m/m}$, and *Csb*$^{m/m}$/*Xpa*$^{-/-}$ mice (4 animals per genotype) at postnatal day 15 and from the liver of 8-, 16-, 96- and 130-week old mice (5 animals per genotype). Synthesis of double stranded cDNA and biotin labeled cRNA was performed according to the instructions of the manufacturer (Affymetrix, USA). Fragmented cRNA preparations were hybridized to full mouse genome oligonucleotide arrays (Affymetrix, mouse expression 430 V2.0 arrays), using Affymetrix hybridization Oven 640 (Affymetrix, USA), washed, and subsequently scanned on a GeneChip Scanner 3000 (Affymetrix, USA). Initial data extraction and normalization within each array was performed by means of the GCOS software (Affymetrix). Data intensities were Log transformed and normalized within and between arrays by means of the quantile normalization method as previously described (Peeters et al. 2004). Based on the quality report files generated by the manufacturer (Affymetrix, USA), the threshold background noise was set at 40. For each probe set, signals were considered to be valid when they were marked as "Present" and exhibit a signal higher than 40 in at least one microarray experiment. All probe sets with a signal below 40 were set to be equal to 40. Where appropriate, two-tail, pair wise analysis or two-way analysis of variance was employed by means of the Spotfire Decision Site software package 7.2 v10.0 (Spotfire Inc., MA, USA) to extract the statistically significant data from each of the four individual microarrays obtained for each genotype (wt, *Xpa*$^{-/-}$, *Csb*$^{m/m}$, and *Csb*$^{m/m}$/*Xpa*$^{-/-}$ livers) as well as from the four microarrays in each of four groups of normally aged mice (8-, 16-, 96-

and 130-week old mice, n=4). The criteria for significance were set at $p \leq 0.010$ and a ≥ ±1.2-fold change with the exception of glycogenin 1 where after quantitative real-time PCR the difference in expression (1.26-fold upregulation) was considered to be significant despite the slightly deviant p-value of 0.012 (the cut-off was set at 0.010). All correlations reported here were calculated by Pearson's correlation coefficient and significance was calculated by Fisher's exact test.

Gene Ontology Classification and Overrepresentation of Biological Themes

All significant gene entries were subjected to GO classification (http://www.geneontology.org). Significant over-representation of GO-classified biological processes was assessed by comparing the number of pertinent genes in a given biological process to the total number of the relevant genes printed on the array for that particular biological process (Fisher exact test, $p \leq 0.01$ False discovery rate (FDR) ≤ 0.1) using the publicly accessible software Ease (Hosack et al. 2003).

Quantitative PCR Evaluation

Total RNA was isolated from liver, heart, kidney and spleen of wt, $Xpa^{-/-}$, $Csb^{m/m}$, $Csb^{m/m}/Xpa^{-/-}$ mice at postnatal day 15 using a Total RNA isolation kit (Qiagen) as described by the manufacturer. Quantitative PCR (Q-PCR) was performed with a DNA Engine Opticon device according to the instructions of the manufacturer (MJ Research). Primer pair designed to generate intron-spanning products of 180-210bp were as follows: *Sod1*: 5'-GGG ACA ATA CAC AAG GCT GT-3' and 5'-GCC AAT GAT GGA ATG CTC TC-3'; *Gsr1*: 5'- CCG CCT GAA CAC CAT CTA T -3' and 5'-TTC CCA TTG ACT TCC ACC G-3'; *Ghr*: 5'-ATT CAC CAA GTG TCG TTC CC-3' and 5'-TCC ATT CCT GGG TCC ATT CA-3'; *Igf1*: 5'-TGC TTG CTC ACC TTC ACC A-3' and 5'-CAA CAC TCA TCC ACA ATG CC-3'; *Prlr*: 5'-GCA TCT TTC CAC CAG TTC CG-3' and 5'-GCT CGT CCT CAT TGT CAT CC-3'; *Gstt2*: 5'-GCC CAA GTC CAC GAA TAC CT-3' and 5'-CTC TGT TCC GTT CCA CCT TC-3'; *Ephx1*: 5'-CAG CCA AAG AAG ATG AGA GCA-3' and 5'-AGC CAT AGT GGA AGC GAC T-3'; *Hmox1*: 5'-AAC ACT CTG GAG ATG ACA CCT-3' and 5'-TGT GAG GGA CTC TGG TCT TTG-3'; *ApoA4*: 5'-CAC CGT TTC TTC TGA CTC CG-3' and 5'-AAT CCC ACA CCA CAT TGG C-3'; *Igfbp3*: 5'-GTG ACC GAT TCC AAG TTC CA-3' and 5'-TGT CCT CCA TTT CTC TGC GG-3'; *Dio1*: 5'-CCC TGG TGT TGA ACT TTG GC-3' and 5'-TGA GGA AAT CGG CTG TGG A-3'. The generation of specific PCR products was confirmed by melting curve analysis (which measures product specificity by the decrease in fluorescence signal when the PCR product is denatured) and gel electrophoresis (using Roche Agarose MS for analyzing small PCR products). Each primer pair was tested with a logarithmic dilution of a cDNA mix to generate a linear standard curve (crossing point (CP) plotted versus log of template concentration), which was used to calculate the primer pair efficiency ($E = 10^{(-1/\text{slope})}$). Hypoxanthine guanine phosphoribosyltransferase1 (*Hprt-1*) mRNA was used as an external standard. For data analysis, the second derivative maximum method was applied: $(E_{\text{1gene of interest}}{}^{\Delta\text{CP (cDNA of wt mice - cDNA of } \textit{Xpa-/-} \text{ or } \textit{Csbm/m} \text{ or } \textit{Csbm/m/Xpa-/-}\text{) gene of interest}}) / (E_{\text{hprt-1}}{}^{\Delta\text{CP (cDNA wt mice-cDNA of } \textit{Xpa-/-} \text{ or } \textit{Csbm/m} \text{ or } \textit{Csbm/m/Xpa-/-}\text{) hprt-1}})$.

Acknowledgements

We thank Wiebeke van Leeuwen and Willem Sluiter for assistance with X-ray analysis and citrate synthase activity measurements, respectively. This research was supported by the Netherlands Organization for Scientific Research (NWO) through the foundation of the Research Institute Diseases of the Elderly, as well as grants from SenterNovem IOP-Genomics (IGE03009), NIH (1PO1 AG17242-02), NIEHS (1UO1 ES011044), EC (QRTL-1999-02002; LSHC-CT-2005-512113), and the Dutch Cancer Society (EUR 99-2004). L.J.N. was supported by Postdoctoral Fellowship #PF-99-142 from the American Cancer Society.

Chapter 3

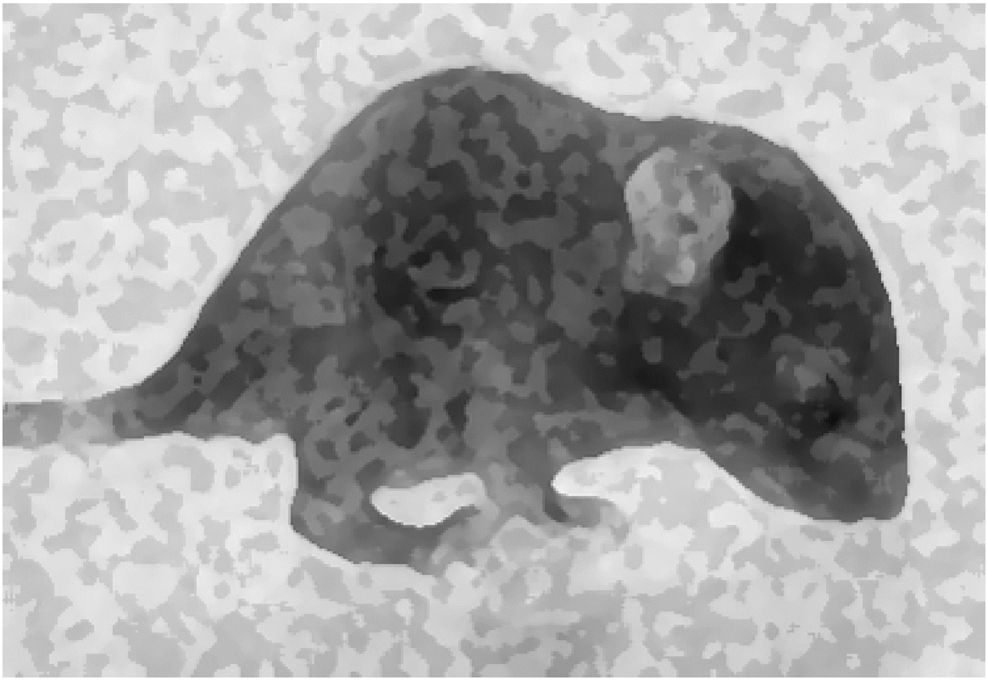

CHAPTER 3

Retinal degeneration and ionizing radiation hypersensitivity in a mouse model for Cockayne syndrome

Theo G.M.F. Gorgels, Ingrid van der Pluijm, Renata M.C. Brandt, Harry van Steeg, Gerard van den Aardweg, Gerard H. Jansen, Jan M. Ruijter, Arthur A.B. Bergen, Dirk van Norren, Jan H.J. Hoeijmakers, Gijsbertus T.J. van der Horst.

Abstract

Mutations in the CSB *gene cause Cockayne Syndrome (CS), a DNA repair disorder characterized by UV-sensitivity and severe physical and neurological impairment. CSB functions in the transcription-coupled repair subpathway of nucleotide excision repair (NER). This function may explain the UV-sensitivity, but hardly clarifies the other CS symptoms. Many of these, among which retinopathy, are associated with premature aging. We studied the eye pathology in a mouse model for CS.* $Csb^{m/m}$ *mice were hypersensitive to ultraviolet light and developed epithelial hyperplasia and squamous cell carcinomas in the cornea, which underscores the importance of transcription-coupled repair of photolesions in the mouse. In addition, we observed a spontaneous loss of retinal photoreceptor cells with age in the* $Csb^{m/m}$ *retina, resulting in a 60% decrease in the number of rods by the age of 18 months. Importantly, when* $Csb^{m/m}$ *mice were exposed to a low dose of ionizing radiation (10 Gy), we noticed an increase in apoptotic photoreceptor cells, which was not observed in wild type animals. The ionizing radiation hypersensitivity of the retina of the* $Csb^{m/m}$ *mouse suggests that (endogenous) oxidative DNA lesions play a role in this CS-specific premature aging feature and supports the oxidative DNA damage theory of aging.*

Introduction

Cockayne Syndrome (CS; complementation group A and B) is a rare, autosomal recessive DNA repair disorder, characterized by a photosensitive skin and severely impaired physical and intellectual development (Nance and Berry, 1992). Patients generally show a postnatal growth defect (leading to cachectic dwarfism) and develop skeletal abnormalities such as a bird-like face (sunken eyes and a beaked nose), kyphosis and, in older patients, osteoporosis. Characteristic neurological features are delayed psychomotor development, microcephaly, disturbed gait, ataxia, sensorineuronal hearing loss, and pigmentary retinopathy. Other CS features include dental caries, impaired sexual development, and cataract. The mean age of death in reported cases is 12.5 years (although patients as old as 55 years have been described), with the most common cause of death being pneumonia resulting from general atrophy and cachexia. Many of the CS features are progressive and resemble premature aging, for which reason CS is regarded a progeroid syndrome (Martin, 2005). In contrast to other photosensitive DNA repair disorders (i.e. Xeroderma Pigmentosum), CS is not associated with increased UV-induced skin cancer proneness.

CS originates from mutations in the CSA or CSB gene, which encode components of the Nucleotide Excision Repair (NER) pathway. This DNA repair mechanism removes a wide variety of helix-distorting DNA lesions from the genome, including UV-induced cross-links between adjacent pyrimidines (Hoeijmakers, 2001). The repair process involves the concerted action of more than 25 proteins that sequentially recognize the damaged nucleotide, locally unwind the helix, excise a 22-31-mer oligonucleotide containing the damage, and fill in the gap by DNA synthesis and ligation (de Laat et al., 1999; Lindahl and Wood, 1999). Two sub-pathways of NER are recognized: (i) global genome NER (GG-NER), which scans and repairs damage throughout the entire genome which is thought to serve mainly to prevent mutations, and (ii) transcription-coupled NER (TC-NER), which selectively repairs lesions in the transcribed strand of active genes and thus may enable the cell to quickly resume transcription and prevent cell death (Hanawalt, 2002). Cells from CS-A and CS-B patients are specifically defective in TC-NER, while GG-NER remains functional (van Hoffen et al., 1993; Venema et al., 1990). This may well provide an explanation for the cutaneous UV sensitivity and absence of skin cancer predisposition. However, the partial NER defect hardly clarifies the etiology of the other CS symptoms, since these features are absent in the related syndrome Xeroderma Pigmentosum (XP), even in those XP patients that completely lack both NER subpathways (XP-A patients). The CS-specific features may be attributed to other roles of CSA and CSB proteins outside the context of NER. There are indications that these proteins are involved in transcription elongation (Balajee et al., 1997; Dianov et al., 1997; Licht et al., 2003; Selby and Sancar, 1997) and in repair of other, non-NER types of DNA damage, e.g. oxidative DNA lesions (de Waard et al., 2004; de Waard et al., 2003; Dianov et al., 1999; Osterod et al., 2002; Spivak and Hanawalt, 2006; Tuo et al., 2003).

To facilitate experimental research on the etiology of CS, we have previously generated animal models for CS-A and CS-B by complete inactivation of the mouse Csa gene ($Csa^{-/-}$ mice) (van der Horst et al., 2002) and by mimicking a specific truncation (as found in CS-B patient CS1AN) in the mouse Csb gene ($Csb^{m/m}$ mice) (van der Horst et al., 1997). Both mouse models display a specific TC-NER defect and show increased photosensitivity of the skin (van der Horst et al., 2002; van der Horst et al., 1997). In contrast to human CS patients, *Csa*$^{-/-}$ and *Csb*$^{m/m}$ mice display modest skin cancer susceptibility, which becomes apparent after chronic exposure of animals to daily dose of ultraviolet light (Berg et al., 2000; van der Horst et al., 1997). This paradox is well explained by the fact that UV-induced cyclobutane pyrimidine dimers are the major causative lesion for UV-skin cancer (Jans et al., 2005) and that rodents lack efficient GG-NER for removal of this lesion from the DNA and thus primarily rely on TC-NER (Bohr et al., 1985). Other CS features, like growth failure and neurological abnormalities, are only present in a mild form (van der Horst et al., 2002; van der Horst et al., 1997). Interestingly, complete inactivation of NER (by concurrent inactivation of the Xpa gene) in the *Csb*$^{m/m}$ mouse dramatically aggravates the CS features (including premature aging). *Csb*$^{m/m}$/*Xpa*$^{-/-}$ double mutant animals display dramatic postnatal growth retardation, kyphosis, ataxia, abnormal locomotor activity, as well as progressive weight loss, and die before weaning (Murai et al., 2001). In view of the premature aging features in DNA repair disorders and elaborating on Harman's "free-radical theory of aging" (Harman, 1956), we recently postulated that aging can result from (oxidative) DNA lesions that interfere with transcription and/or replication and cause cell death and/or cellular senescence, ultimately leading to loss of tissue homeostasis and onset of age-related disease (Hasty et al., 2003; Mitchell et al., 2003). According to this theory, oxidation of DNA by endogenous free radicals, generated as by-product of cellular metabolism, plays an important role in the etiology of the CS-specific features, notably premature aging. In line with this, *Csb*$^{m/m}$ animals and cells are susceptible to oxidative damage producing agents like ionizing radiation and paraquat, which points to a defect in repair of oxidative DNA lesions, in addition to a TC-NER deficiency (de Waard et al., 2003).

The present study addresses the eye pathology of CS, which includes photosensitivity and pigmentary retinopathy. The latter feature was first described by Cockayne in 1936 (Cockayne, 1936) and has since been considered a hallmark of the disease. Moreover, it is reported in at least 55% of the published cases (Nance and Berry, 1992). The CS retinopathy is one of the yet unexplained CS-specific features, which suggests that accelerated aging occurs in CS. Here, we show that the defect in the *Csb*$^{m/m}$ mouse not only causes corneal UV sensitivity and cancer susceptibility, but also predisposes to age-related retinopathy, as evident from the spontaneous photoreceptor loss. Importantly, we show that the *Csb*$^{m/m}$ mouse retina is hypersensitive to low doses of ionizing radiation, which suggests that oxidative lesions are at the basis of this premature aging phenotype.

Results

Csb deficiency predisposes to UV-induced cornea pathology

Chronically UV-B exposed *Csb*$^{m/m}$ mice have been shown to develop skin cancer, notably squamous cell carcinomas (Berg et al., 2000; van der Horst et al., 1997). To establish the effect of chronic UV exposure on the eyes of wild type (*Csb*$^{+/+}$), heterozygous (*Csb*$^{+/m}$) and homozygous mutant (*Csb*$^{m/m}$) mice, animals (n=7-9 mice per genotype) were exposed to low daily doses of UV-B light for up to 38 weeks. After five weeks, *Csb*$^{m/m}$ mice started to develop photophobia, while eyes appeared irritated with red eyelids. Ten weeks after the first exposure (cumulative UV dose ± 9 kJ/m^2), the cornea of *Csb*$^{m/m}$ mice started to become opaque (Fig. 1A), while some eyes became enlarged and bulging.

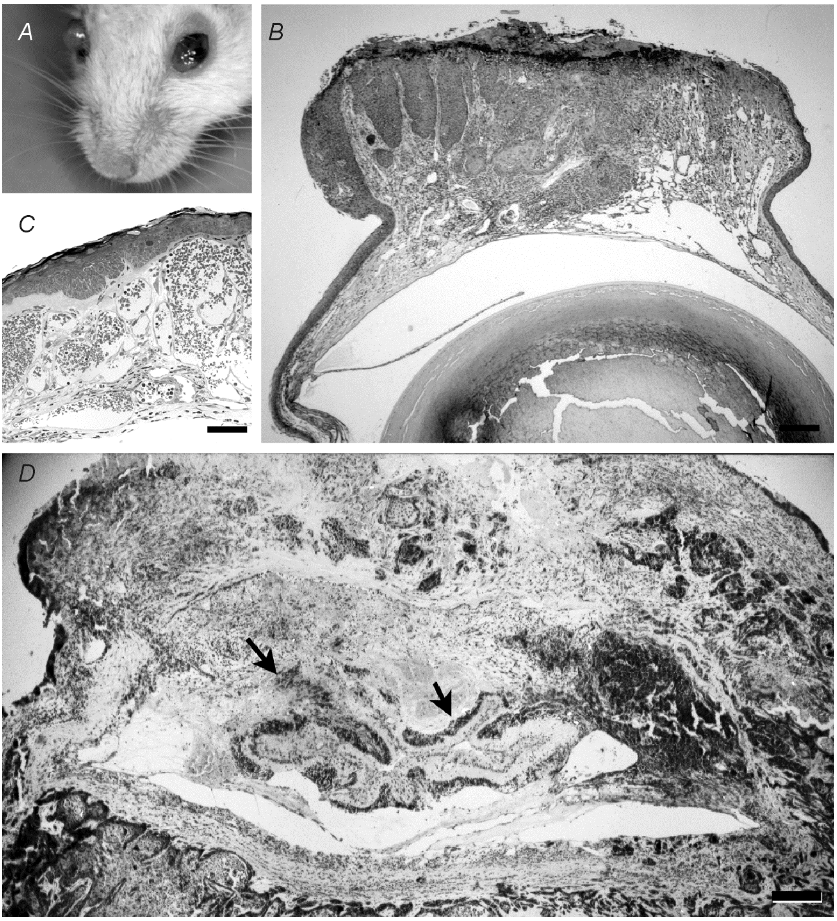

Figure 1. Increased UV-sensitivity of the eyes of *Csb*$^{m/m}$ mice. *A) Representative example of a UV-B exposed Csb*$^{m/m}$ *mouse with macroscopic ocular abnormalities. The photograph was taken 29 weeks after the start of the experiment (cumulative dose: ± 35 kJ/m2). The right eye is enlarged and opaque; the left eye is red with an irregular corneal surface. B-D) Micrographs of toluidine blue stained plastic sections of eyes of UV-exposed Csb*$^{m/m}$ *mice. B) Histopathology of an eye with an opaque macroscopic appearance, revealing epithelial hyperplasia in the central part of the cornea. C) One of the enlarged, bulging eyes showed extensive vascularization of the corneal stroma. D) Example of a corneal squamous cell carcinoma, infiltrating into other parts of the eye (arrows point at remnants of the retina).*

After 29 weeks (cumulative UV dose ± 35 kJ/m^2), the corneal surface of 3 *Csb*$^{m/m}$ mice became distorted and bleedings occurred (Fig. 1A). These animals were euthanized, and their eyes were processed for histology. After 38 weeks of UV exposure (cumulative dose ± 50 kJ/m^2), the experiment was terminated and all animals remaining were euthanized. By that time, all irradiated *Csb*$^{m/m}$ mice had developed macroscopic eye abnormalities (Table 1). In marked contrast, UV-exposed $Csb^{+/+}$ and $Csb^{+/m}$ animals, as well as non-UV-treated $Csb^{m/m}$ mice did not show any eye abnormalities visible to the naked eye.

Subsequent histopathological analysis of eyes collected from UV-exposed $Csb^{+/+}$ and $Csb^{+/m}$ animals did not show any abnormalities, except for the presence of a few capillaries in the corneal stroma in one out of 7 $Csb^{+/+}$ eyes investigated (Table 1).

Genotype	*UV Exposure (weeks)*	*Macroscopic appearance*	*Histopathology*
$Csb^{+/+}$ *n = 7*	*38*	*Normal (14/14)*	*No pathology (6/7)* *Neovascularization (1/ 7)*
$Csb^{+/m}$ n = 7	*38*	*Normal (14/14)*	*No pathology (7/7)*
$Csb^{m/m}$ *n = 9*	*28-38*	*Opaque (8/18)*	*Stroma vascularization and epithelial hyperplasia (7/8)* *Bulla (1/8)*
		Enlarged, bulging eye, often with bleedings (10/18)	*Severe hyperplasia of epithelium (5/10)* *Squamous cell carcinoma (4/10)* *Severe neovascularization in the stroma (1/10)*
$Csb^{m/m}$ *n = 5*	*no*	*Normal (10/10)*	*No pathology (4/4)*

Table 1. UV-induced pathology of the cornea of wt and $Csb^{m/m}$ mice.

Similarly, the cornea of untreated $Csb^{m/m}$ mice appeared normal. In marked contrast, UV-exposed $Csb^{m/m}$ eyes disclosed many abnormalities. Opaque $Csb^{m/m}$ eyes revealed epithelial hyperplasia in the central part of the cornea, along with a reactive stroma and neovascularization. In addition, Bowman's membrane was increased in thickness. Enlarged, bulging eyes generally displayed severe hyperplasia of the corneal epithelium (Fig. 1B), accompanied by local disruptions and hemorrhages at the corneal surface. At least 4 of the bulging eyes carried a corneal squamous cell carcinoma with infiltrations into other regions of the eye, including the retina (Fig. 1D). One of the enlarged bulging eyes showed a different pathology. In this eye, there was only a modest hyperplasia of the epithelium. Most striking in this eye was the extensive vascularization of the corneal stroma (Fig. 1C).

These findings demonstrate that the TC-NER defect renders the eyes of $Csb^{m/m}$ mice sensitive to semi-acute (hyperplasia) and long-term (carcinogenesis) effects of UV exposure.

Csb deficiency predisposes to age-related retinal degeneration

While analyzing the UV-induced eye pathology in the CS mouse model, we noticed a severe reduction in the number of photoreceptor cells (hereafter referred to as photoreceptors) in the eyes of UV-exposed as well as in non-exposed (58-week old) $Csb^{m/m}$ mice (data not shown).

This finding, together with the notion that retinal degeneration is a characteristic clinical feature of Cockayne patients (Nance and Berry, 1992), prompted us to study the spontaneous changes in the morphology of the retina of *Csb*$^{m/m}$ mice. To this end, we isolated the eyes of wild type (wt) and *Csb*$^{m/m}$ mutant mice of defined age (all in a C57Bl/6J genetic background and housed under identical light-conditions) and quantified the number of photoreceptors and other cell types in defined regions of stained sections of the eye. At 3 months of age, we could not detect any difference between the wt and *Csb*$^{m/m}$ retina, which excludes developmental abnormalities as primary cause of the reduced number of photoreceptors in the retina of old *Csb*$^{m/m}$ animals. However, in 18-month old *Csb*$^{m/m}$ mice, the outer nuclear layer (ONL; containing the nuclei of the photoreceptor cells) and the outer segment layer (containing the rod and cone moiety of the photoreceptor cells) was clearly reduced in thickness, when compared to wt mice (Fig. 2A**)**.

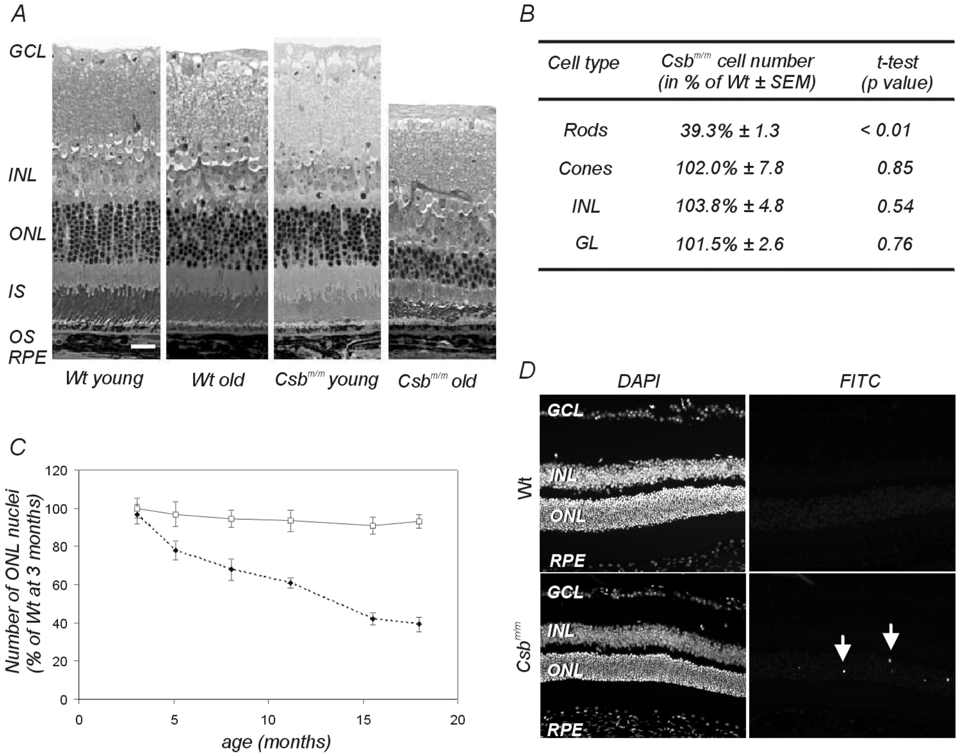

Cell type	*Csb$^{m/m}$ cell number (in % of Wt ± SEM)*	*t-test (p value)*
Rods	*39.3% ± 1.3*	*< 0.01*
Cones	*102.0% ± 7.8*	*0.85*
INL	*103.8% ± 4.8*	*0.54*
GL	*101.5% ± 2.6*	*0.76*

Figure 2. Progressive loss of photoreceptors with age in the *Csb*$^{m/m}$ mouse. *A) Representative micrographs of the central region of the retina of young (3 months) and old (18 months) wt and Csb*$^{m/m}$ *mice. Note the specific loss of ONL nuclei and distortion of the outer segment layer in the 18-month-old Csb*$^{m/m}$ *mouse. Bar 25 µm. B) Quantification of the number of nuclei in the various layers of the retina of 18-month old wt and Csb*$^{m/m}$ *mice, demonstrating specific loss of rods in the aged Csb*$^{m/m}$ *retina (ANOVA, followed by t-test). C) Kinetics of photoreceptor cell loss in Csb*$^{m/m}$ *mice. The relative number of rod nuclei in wt and Csb*$^{m/m}$ *mice is plotted as the percentage of nuclei, relative to that observed in 3-month old wt mice. Open squares: wt; closed diamonds: Csb*$^{m/m}$*. Error bars indicate standard deviation D) Micrographs of the retina of 3-month old wt and Csb*$^{m/m}$ *mice, stained for apoptosis using the TUNEL method. Arrows indicate FITC staining for TUNEL positive cells in the ONL (right panels). Nuclei are visualized using the DAPI staining method (left panels).*

Quantification of the number of nuclei in the various layers of the retina did not yield significant differences between wt and $Csb^{m/m}$ mice with respect to cell number in the ganglion cell layer and the inner nuclear layer (INL, containing the cell bodies of bipolar, horizontal, amacrine and Müller cells) (Fig. 2B). In marked contrast, the number of rod nuclei in the ONL of $Csb^{m/m}$ mice was significantly reduced ($p<0.01$) to less than 40 % of the wt level. The number of cones, identified on the basis of their characteristic distribution of heterochromatin in the nucleus, appeared unchanged. We next determined the kinetics of photoreceptor loss in the retina of $Csb^{m/m}$ animals. Quantification of the ONL nuclei showed that the number of photoreceptors gradually decreased with age in $Csb^{m/m}$ mice (Fig. 2C). We did not observe an obvious photoreceptor loss in wt mice, although there may be a tendency (yet not statistically significant) of an aging-related decline in the number of ONL nuclei (Fig. 2C). Other retinal layers appeared unaffected (data not shown). Thus, $Csb^{m/m}$ mice specifically lose rods during aging.

To investigate whether the process of spontaneous photoreceptor loss involves cell death via apoptosis, we next performed a TUNEL staining on horizontal sections of the retina of 3 and 11.5 months old wt and $Csb^{m/m}$ mice. In line with the near constant number of nuclei in the ONL and other layers of the retina of aging wt animals, we could hardly detect any TUNEL positive cells (0.3 ± 0.2 and 0.6 ± 0.1 stained nuclei per section at 3 and 11.5 month respectively; mean ± s.e.m.). In marked contrast, the retina of 3-month old $Csb^{m/m}$ mice contains 14.1 ± 1.6 TUNEL-positive cells per section, which localized almost exclusively to the ONL (Fig. 2D) without overt regional specificity for the central or peripheral retina. In the retina of 11.5-month old $Csb^{m/m}$ mice we observed 10.7 ± 2.3 positive cells, which translates into approximately 17 positive cells when corrected for the loss of photoreceptors at this age (≈40 %, see Fig. 2C), and does not significantly differ from the number of apoptotic photoreceptor cells in 3 month old mutant animals (t-test, $p=0.48$). Similar results were obtained when cells were stained for caspase 3 (data not shown).

Taken together, these findings indicate that a CSB deficiency makes retinal photoreceptors (notably the rods) more sensitive to apoptosis, resulting in age-related photoreceptor loss.

The $Csb^{m/m}$ retina is hypersensitive to ionizing radiation

Since oxidative DNA damage may play a role in CS as well as in aging, we next explored the ionizing radiation (IR) sensitivity of the retina of wt and $Csb^{m/m}$ mice. In addition to DNA strand breaks (which are repaired normally in CS cells (Spivak and Hanawalt, 2006)), IR is known to induce oxidative DNA damage via reactive free radicals that originate from the radiolysis of water (Cooke et al., 2003; Ward, 1975). Animals were locally exposed to various doses of X-rays and sacrificed 7 days after treatment. Next, eye pathology was examined in horizontal sections of the retina. For wt mice, no overt pathology was noticed in the retina at any time point after irradiation at 10 or 15 Gy. In marked contrast, damage to photoreceptors became apparent 7 days after exposure to 18.5 Gy, culminating in extensive photoreceptor loss at doses of 22 and 25 Gy (Fig. 3A). The cell loss was most prominent in the periphery, where hardly any photoreceptor cells were left. This observation is well explained by the fact that the periphery has been the closest to the irradiation source, and accordingly has received the highest dose of X-rays. In addition to photoreceptor damage, we noticed the appearance of swollen RPE cells, containing large vacuoles, in the retina of animals exposed to 22.5 and 25 Gy of X-rays (Fig. 3A). These findings fit well with a previous study on the acute effects of ionizing radiation on the rat retina, which identified photoreceptors as the most sensitive cell type, followed by the RPE cell (Amoaku et al., 1989). Surprisingly, *Csb*$^{m/m}$ mice essentially showed the same pathology at each given dose. Quantification of the cell loss (by counting the surviving cells in the periphery), did not reveal a statistically significant difference in photoreceptor loss between *Csb*$^{m/m}$ mice and wild type mice (Fig 3B).

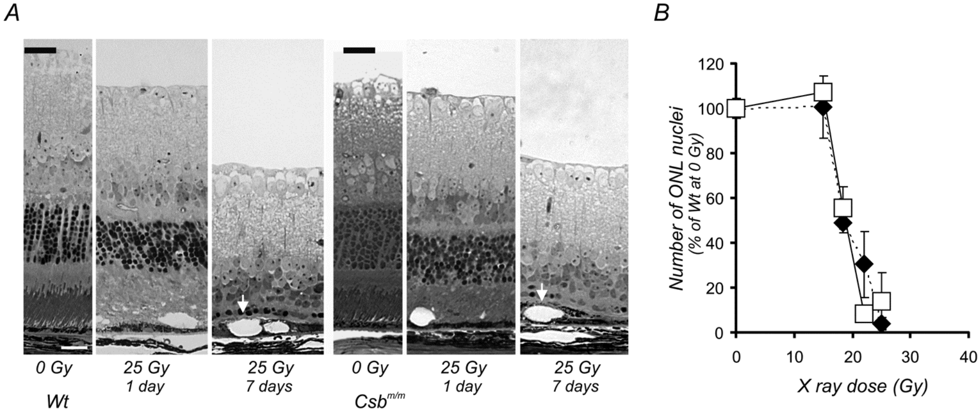

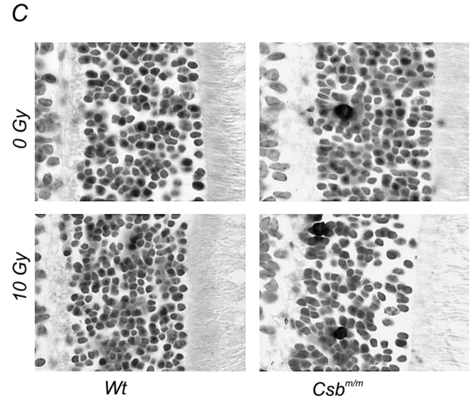

D

		Dose 0 Gy	Dose 10 Gy	t-test p	Two-way ANOVA $p_{interaction}$
ONL	Wt	0.6 ± 0.3	0.8 ± 0.4	0.53	
	Csb$^{m/m}$	9.5 ± 2.5	20.3 ± 4.2	0.002	
	t-test p	0.0003	0.0004		<0.001
INL	Wt	0.11 ± 0.12	0.11 ± 0.12	1	
	Csb$^{m/m}$	0.4 ± 0.3	1.5 ± 0.7	0.024	
	t-test p	0.12	0.01		0.003
GCL	Wt	0.04 ± 0.10	0.04 ± 0.10	1	
	Csb$^{m/m}$	0.0 ± 0.0	0.46 ± 0.57	0.15	
	t-test p	0.36	0.18		0.058

Figure 3. Hypersensitivity of the *Csb*$^{m/m}$ retina to low doses of ionizing radiation. *A) Micrographs of the retina of wt and Csb*$^{m/m}$ *mice before, and seven days after focused exposure of the eye to a high dose of ionizing radiation (25 Gy; X-rays). Note the near complete loss of photoreceptors in the exposed wt and Csb*$^{m/m}$ *retina. Arrows indicate swollen RPE cells with large vacuoles. (B) Quantification of photoreceptor cell loss in wt and Csb*$^{m/m}$ *mice, exposed to various doses (15-25 Gy) of X-rays. ONL nuclei were counted in the peripheral retina and expressed as percentage of the number of ONL nuclei present in the unexposed wt retina. Open squares: wt; closed diamonds: Csb*$^{m/m}$. *C-D) Effect of low dose (10 Gy; γ-rays) whole body ionizing radiation exposure on the retina of wt and Csb*$^{m/m}$ *mice (6 animals/genotype; 8-10 weeks of age). C) Example of apoptotic cells (recognized by a dark nucleus), as visualized by TUNEL staining. D) Quantification of apoptotic (TUNEL-positive) cells in the retinal layers. Two-way ANOVA was used to test the independent effects of γ-rays and genotype on the number of TUNEL positive cells, as well as the interaction between these variables.*

We reasoned that the failure to detect a difference in ionizing radiation sensitivity between the wt and $Csb^{m/m}$ retina might have been caused by the design of the experiment: at a high IR dose, the heavy damage load could have masked a possible subtle effect of the *Csb* deficiency, whereas at a lower IR dose the method of counting surviving cells may not be sensitive enough. To overcome this problem, we performed a whole body γ-ray exposure experiment (10 Gy) with wt and $Csb^{m/m}$ animals, and quantified the number of apoptotic cells in sections stained with the TUNEL assay. As shown in Fig. 3C and D, the frequency of apoptotic cells in the ONL (photoreceptor cells), INL and GCL of the wt retina did not significantly increase after exposure ($p > 0.5$ for each layer), indicating that the wt mouse eye is not sensitive to a single dose of ionizing radiation at doses ≤ 10 Gy. In marked contrast, the already higher frequency of apoptotic photoreceptors in the ONL of the $Csb^{m/m}$ retina (as compared to the wt retina; two-way ANOVA, followed by t-test, $p = 0.0003$) increased over two-fold ($p = 0.002$) after exposure. Similarly, IR exposure of the $Csb^{m/m}$ retina resulted in a higher frequency of apoptotic INL cells ($p = 0.024$). These findings clearly indicate that retinal cells in $Csb^{m/m}$ mice are hypersensitive to ionizing radiation (two-way ANOVA, followed by t-test $p<0.05$) and point to unrepaired DNA damage (originating from oxidative stress) as the underlying trigger.

Discussion

The present study shows that the absence of a functional CSB protein in the $Csb^{m/m}$ mouse model for the progeroid DNA repair disorder Cockayne syndrome increases the UV-sensitivity of the cornea. Effects are noticed both in the stroma and epithelium, with epithelial hyperplasia and carcinoma formation as the most prominent pathologic consequence. This finding fits well with our previous observation that $Csb^{m/m}$ (and $Csa^{-/-}$) mice are photosensitive and predisposed to develop skin cancer upon UV irradiation (Berg et al., 2000; van der Horst et al., 1997), and underscores the potential carcinogenicity of photolesions in sun/UV-exposed areas of the body.

Yet, neither skin nor corneal neoplasms have been reported to occur in human CS patients. This human-rodent paradox is believed to originate at least in part from the inability of rodent cells to upregulate the p48 subunit of the XP-E p48-p125 UV-DDB (DNA Damage Binding) heterodimer, required to enhance CPD recognition by the GG-NER machinery (Hwang et al., 1999; Tang et al., 2000). TC-NER deficient rodents, like $Csb^{m/m}$ mice, thus lack the slower GG-NER back-up mechanism to remove CPDs from transcribed strands of active genes, allowing this lesion to contribute to mutagenesis and carcinogenesis at doses that do not yet give apoptosis.

Retinal degeneration is regarded a hallmark of CS. Based on the fundus appearance, the retinopathy of CS patients is generally referred to as a pigmentary retinopathy. Yet, case reports with detailed morphological data on CS eye pathology are scarce (Nance and Berry, 1992). To our knowledge, literature contains only one report on a 44-month-old boy documenting loss of photoreceptors, in addition to other pathological changes such as ganglion cells and nerve fiber loss, and irregular RPE pigmentation (Levin et al., 1983). We have shown here that, similar to this patient, $Csb^{m/m}$ mice undergo spontaneous retinal degeneration, which consists of a gradual loss of rods with age. Other cell types, like cones and ganglion cells are spared, at least up to an age of 18 months. As such, the $Csb^{m/m}$ mouse model does not exactly mimic the retinopathy of the human syndrome, although it currently can not be excluded that additional aging-related pathology (e.g. in the RPE) will develop at a later age.

CS is considered a progeroid syndrome, since many of the CS symptoms resemble premature aging. In this respect, it is interesting to note that a gradual and selective loss of photoreceptors with age (with rods degenerating earlier than cones) is also observed in the aging human central retina and in patients with age-related macular degeneration (AMD) (Curcio et al., 1993; Jackson et al., 2002). In a primate study, involving 6-34 year old rhesus monkeys, the thickness of the ONL was shown to decrease with age as a result of apoptosis of photoreceptors, which distributed equally over all ages except for an increase in the number of TUNEL-positive cells in the oldest animals (Lambooij et al., 2000). This, together with the notion that wild type mice may also lose photoreceptors at high age, indicates that the selective loss of rods in the $Csb^{m/m}$ mouse and in CS patients reflect accelerated aging.

What is the trigger for the photoreceptor loss in the $Csb^{m/m}$ mouse? Preliminary data from a cohort study with the GG-NER/TC-NER deficient *Xpa* mouse model (de Vries et al., 1995) revealed that 7-month old $Xpa^{-/-}$ mice contain a normal number of photoreceptors, while the thickness of the ONL in $Csb^{m/m}$ animals of the same age was already reduced by 30% (Gorgels, van Steeg, van der Horst, unpublished data). This finding suggests that a NER defect is not the major driving force behind the CS mouse retinopathy. Rather, it appears that the severe photoreceptor loss in $Csb^{m/m}$ animals represents a CS-specific trait, related to a function of CSB protein outside the context of NER. The nature of this non-NER function is not yet clear, but there are indications that the CSB protein has an auxiliary function in transcription elongation, notably the bypass of pause-sites and RNA secondary structures (Balajee et al., 1997; Dianov et al., 1997; Licht et al., 2003; Selby and Sancar, 1997), as well as in repair of other (non-NER type) oxidative DNA lesions (de Waard et al., 2003; Dianov et al., 1999; Osterod et al., 2002; Spivak and Hanawalt, 2006). $Csb^{m/m}$ mouse embryonic fibroblasts, embryonic stem cells and keratinocytes are ionizing radiation-sensitive (de Waard et al., 2003). While IR induces a variety of DNA lesions, it is likely that oxidative DNA modifications determine the observed hypersensitivity. Indeed, γ-irradiated human fibroblasts of CS-B patients accumulate more 8-oxoG damage than control cells (Tuo et al., 2003). Furthermore, $Csb^{m/m}$ mice are sensitive to the pro-oxidant di-(2-ethylhexyl) phthalate (DEHP) and exposed animals contain higher levels of 8-oxoG in the liver than wt mice (de Waard et al., 2004; de Waard et al., 2003). Importantly, Spivak and Hanawalt (Spivak and Hanawalt, 2006) recently showed that plasmids containing 8-oxoG are less well repaired by CS patient cells, whereas strand breaks (also produced by ionizing radiation) are repaired at normal rate. In view of this, and noting that the photoreceptor layer is oxygen rich and has a high metabolic activity, it is tempting to speculate that endogenous, oxidative DNA modifications contribute to the CS retinopathy. Indeed, we found that exposure of animals to a dose of 10 Gy caused increased cell death in the $Csb^{m/m}$ retina, while leaving the wt retina unaffected. At higher doses the $Csb^{m/m}$ and wt retina show equal sensitivity, which may be attributed to high levels of DNA strand breaks, masking the effects of oxidative damage. Together these findings support the hypothesis that oxidative DNA damage is at the basis of photoreceptor cell loss in the aging $Csb^{m/m}$ retina. Moreover, as shown for CSB cells in vitro, these data for the first time provide in vivo evidence for ionizing radiation sensitivity in CS.

How would oxidative DNA lesions contribute to cell death in the $Csb^{m/m}$ retina? As shown for UV lesions, stalled RNA polymerase II forms a major trigger for apoptosis (Ljungman et al., 1999), and it has been hypothesized that transcription might serve as a DNA-damage dosimeter where the severity of blockage acts as a go/no go decision point for the induction of cell death (Ljungman and Lane, 2004). One can envisage a scenario in which some oxidative lesions may remain unrepaired in the absence of the CSB protein, and accordingly will accumulate in time until the damage load reaches a threshold that sets off apoptosis. Such a mechanism would imply that the probability of cell death (and thus the frequency of apoptotic photoreceptors) would increase with age. Our observation that the frequency of apoptotic photoreceptors does not significantly increase between the age of 3 and 11.5 months suggests that such a scenario is not the major driving force. Alternatively, it could be that back-up mechanisms such as GG-NER and GG-BER still enable the CSB-deficient cell to repair oxidative DNA lesions, albeit at a slower pace. In this case, the CSB-deficient mouse would have higher steady state levels of oxidative DNA damage, which would result in slower transcription rates with a higher (stochastic) risk of stalling RNA polymerase II, and subsequent induction of apoptosis. Since retinal photoreceptors are post-mitotic cells and are not replaced by dormant stem/progenitor cells (Moshiri et al., 2004), analysis of the kinetics of cell loss might discriminate between the two models. Curve fitting on the dataset provided in Fig. 2C showed that the relation between the number of photoreceptors and age is well described by a mathematical model in which the chance of cell death is constant in time ($R^2 = 0.945$). In contrast, fitting to a model in which the risk of cell death increases with age did not yield a significant regression result, as the parameter reflecting the increasing risk did not significantly differ from zero ($p=0.505$). This analysis suggests that, at least within the age range investigated, the retinal photoreceptor loss in the $Csb^{m/m}$ mouse is related to higher steady state levels of oxidative DNA damage, rather than to the age-related accumulation of this type of lesions.

In conclusion, we found spontaneous age-related retinal degeneration in the *Csb* mouse model for Cockayne syndrome, along with an increased sensitivity of photoreceptor cells for ionizing radiation. This finding underscores the importance of DNA repair and control of oxidative stress levels for long-term survival of photoreceptor cells in the retina and supports Harman's "free-radical theory of aging" (Harman, 1956). In addition, it warrants further investigation of these mechanisms in the etiology of (age-related) retinal disease and other brain disorders. The recent finding that a polymorphism in the promoter region of *CSB* is associated with AMD susceptibility, strongly supports this view (Tuo et al., 2006). Finally, the spontaneous and induced loss of terminally differentiated, post-mitotic photoreceptor cells in the $Csb^{m/m}$ retina may serve as a sensitive readout for the screening of compounds that may retard or prevent onset of pathology in the (aging) retina and brain.

Materials and Methods

Mice

The generation and PCR-mediated genotyping of $Csb^{m/m}$ mice has been described previously (Berg et al., 2000; van der Horst et al., 1997). Except for the chronic UV exposure study (performed with animals in a FVB and 129ola hybrid genetic background) experiments were performed with animals in a C57BL/6J background. Animals are housed in a controlled environment (food and water ad libitum, 12h light:12 hr dark cycle, light intensity 70-90 lux) at the Animal Resource Center (Erasmus University Medical Center), which operates in compliance with the “Animal Welfare Act” of the Dutch government, using the “Guide for the Care and Use of Laboratory Animals” as its standard. All animal studies were approved by an independent Animal Ethical Committee (Dutch equivalent of the IACUC).

Chronic exposure to UV-B light

Whole body UV exposures studies were performed according to an incremental-dose protocol as described previously (van der Horst et al., 1997). In brief, 9 $Csb^{m/m}$, 7 $Csb^{+/m}$, and 7 $Csb^{+/+}$ mice (age 20 weeks) received an initial daily dose of 100 J/m^2 UV-B (250-400 nm; American Philips F40 sunlamps; dose rate 8.3 J/m^2/min), gradually increasing up to 250 J/m^2. Animals were thoroughly screened twice a week for the occurrence of skin and eye abnormalities. Mice that developed tumors were sacrificed by CO_2 inhalation and subsequent cervical dislocation. Eyes were isolated and processed for histopathological examination as described below. After 38 weeks (cumulative dose received: ≈ 50 kJ/m^2) remaining animals were sacrificed and eyes were processed for histopathological analysis.

Exposure to ionizing radiation

Animals (5-8 weeks old; n=4-6/genotype) were anaesthetized by intraperitoneal injection of pentobarbital (50 mg/kg), positioned with the left eye in focus of a 50 kV X-ray source (diameter 1.5 cm, 1 mm aluminum filter, 40 mm final optics assembly, dose rate 830 R/min, 7.47 Gy/min), and exposed at doses as indicated in the text. Animals were sacrificed 7 days after exposure and the exposed eye was further processed for histopathological analysis. In a second experiment, mice (8-10 week old; n = 6/genotype) received a brief (13 min) total body irradiation of 10 Gy using a ^{137}Cs source. After 20 hrs, animals were sacrificed and eyes were processed for further analysis.

Isolation of the eyes

Animals were anaesthetized by CO_2 inhalation, followed by cervical dislocation. Eyes were marked on the nasal side with Alcian blue (5% Alcian blue in 96% ethanol) and subsequently enucleated and fixed in 2.5% glutaraldehyde in 0.1 M cacodylate buffer. After rinsing in buffer, the anterior segment was removed and the eye cup was postfixed in 1% OsO_4 and embedded in epon. Horizontal sections of 1 µm thickness were cut, stained with toluidine blue and examined with a light microscope. Alternatively, for the chronic UV exposure study, enucleated eyes were fixed in 2% glutaraldehyde and 2% paraformaldehyde in 0.1 M cacodylate buffer, and either embedded in paraffin, or postfixed in 1% OsO4 in Na-cacodylate buffer, and embedded in epon. For TUNEL staining (see below) eyes were fixed in 4 % paraformaldehyde in 0.1 M phosphate buffer and embedded in paraffin.

Quantification of retinal cell loss and visualization of apoptosis

Digital images of the retina (horizontal, central sections, passing through the optic nerve head) were taken at 200 µm nasally and temporally of the optic nerve head, using a microscope equipped with a high resolution camera (Prog/Res/3012, Kontron, Germany). The number of nuclei in the outer and inner nuclear layer (ONL and INL, respectively) within a rectangular field of 500 µm^2 was counted. For each mouse two sections (separated by 15 µm) were analysed and counts were averaged. In addition, an estimate of the number of cones was obtained by specifically counting ONL profiles with the characteristic heterochromatin distribution (Carter-Dawson and LaVail, 1979). For an estimate of the number of ganglion cells we counted the nuclei in the ganglion cell layer in the whole horizontal section.

Apoptotic cells were visualized in horizontal paraffin sections (5 µm thick) of paraformaldehyde fixed eyes using the TdT-mediated dUTP Nick-End Labeling (TUNEL) method, according to the specifications of the manufacturer of the kit (Fluorescein Apoptosis Detection System, Promega; Apoptag Plus Peroxidase In Situ Apoptosis Detection Kit, Chemicon).

The observed differences in cell densities and the number of apoptotic cells were tested for significance using a Student t-test and one-way analysis of variance (ANOVA). In case of statistical significance the ANOVA was followed by the post hoc test of Student-Newman-Keuls (S-N-K). Two-way ANOVA was used to determine the independent effects of ionizing radiation and genotype on apoptosis in the various retinal layers, as well as the interaction between these two variables. Significance was accepted at $p < 0.05$.

The decrease in photoreceptor number in *Csb*$^{m/m}$ mice with increasing age (Fig. 2C, dotted line) was fitted to a mathematical model with constant risk of cell death

$$(ONL(t) = ONL(0).e^{-\mu 0.t})$$

as well as to a model with age-related increasing risk of cell death

$$(ONL(t) = ONL(0).e^{-\frac{(e^{R.t}-1)\mu 0}{R}})$$

using non-linear regression (SPSS, version 11.5.1). A model was considered appropriate when all parameter estimates differed significantly from zero (Clarke et al., 2000).

Acknowledgements

We thank Dr. Rob Berg for technical assistance with the UV experiment. This research was supported by the Rotterdamse Vereniging Blindenbelangen and the Algemene Nederlandse Vereniging ter Voorkoming van Blindheid, the Netherlands Organization for Scientific Research (NWO) through the foundation of the Research Institute Diseases of the Elderly, as well as the National Institute of Health (NIH 1PO1 AG17242-02).

Chapter 4

CHAPTER 4

Conditional *Csb/Xpa* mice reveal cerebral atrophy, characteristic of the progeroid DNA repair disorder Cockayne Syndrome

Ingrid van der Pluijm, Renata Brandt, Marcel Vermeij, Carel Meijers, Ype Elgersma, Alex Maas, Harry van Steeg, Jan H.J. Hoeijmakers, and Gijsbertus T.J. van der Horst

Abstract

Cockyane Syndrome (CS) is a severe inherited progeroid disorder, resulting from a defect in genes involved in transcription-coupled nucleotide excision repair. Hallmark features of CS are a sun-sensitive skin, early cessation of growth, progressive neurodegeneration and premature death. Recently, we have shown that whereas $Csb^{m/m}$ *animals display only mild CS features,* $Csb^{m/m}/Xpa^{-/-}$ *mice, which are further compromised in repair, recapitulate many symptoms of this disease. As the extremely short lifespan of* $Csb^{m/m}/Xpa^{-/-}$ *mice precludes studies on brain and other CS-associated pathology, we now generated a Cre-lox-based conditional Xpa knock-out mouse in which the Xpa gene can be inactivated in a time- and/or tissue-specific manner. Importantly, specific inactivation of the conditional Xpa allele in the cerebrum of* $Csb^{m/m}$ *animals triggers dramatic CS-like neurological features, including dilated ventricles and cerebral atrophy. This mouse model shows that the CS neuropathology is a direct consequence of the DNA repair defect, ruling out indirect systemic causes, points to spontaneous, endogenous DNA damage as the underlying culprit and supports the idea that DNA damage contributes to aging. Furthermore, it provides an important new tool to selectively study the etiology of CS (neuro)pathology, including progeroid features in a setting in which accelerated aging in other organs and tissues is absent.*

Introduction

Preservation of the genetic information encrypted in the DNA is of utmost importance as DNA contains the blueprint of life. Yet, the genome of every living organism is continuously challenged by environmental physical and chemical genotoxins (e.g. ultraviolet light (UV), ionizing radiation, industrial pollutants, solvents, cigarette smoke) that damage the DNA. Even more, as a direct consequence of normal metabolism, the genome is daily assaulted by superoxide anions, hydroxyl radicals, hydrogen peroxide (commonly referred to as reactive oxygen species or ROS), reactive nitrogen species, malondialdehyde and other (side) products of cellular metabolism (Beckman and Ames, 1998; Davies, 1995; Fridovich, 1995). Replication of damaged DNA can cause mutations, which ultimately can result in the onset of carcinogenesis (Hoeijmakers, 2001). DNA lesions can also obstruct progressing DNA and RNA polymerases during the essential process of replication and transcription respectively, which can lead to cellular senescence or apoptosis, and this is believed to contribute to aging (Mitchell et al., 2003). DNA, in contrast to other biomolecules (e.g. RNA, proteins), can not be replaced once damaged. Therefore, cells have acquired a variety of complex repair systems with overlapping substrate specificities to counteract the harmful events of DNA injuries (for review (Friedberg, 2006; Hoeijmakers, 2001)). The importance of genome maintenance as anti-cancer and anti-aging strategy is highlighted by a series of inherited disorders, associated with cancer predisposition and/or early onset of aging-associated symptoms (Hoeijmakers, 2001; Kipling et al., 2004; Martin, 2005; Puzianowska-Kuznicka and Kuznicki, 2005).

Cockayne Syndrome (CS; complementation group A and B) is an autosomal recessive photosensitive disorder, arising from a partial defect in nucleotide excision repair (NER), responsible for the elimination of UV-induced photoproducts, as well as a wide variety of other structurally unrelated, distorting DNA lesions, like chemically-induced bulky adducts and intrastrand crosslinks (for review see (Friedberg, 2006; Hoeijmakers, 2001)). CS patients are specifically defective in transcription-coupled NER (TC-NER), a sub-pathway preferentially focusing on transcription-blocking lesions in the template strand of active genes (Hanawalt et al., 1994), while global genome NER (GG-NER), covering lesions in the entire genome, is intact (van Hoffen et al., 1993; Venema et al., 1990). As a consequence, CS patients display a photosensitive skin, likely because stalled RNA polymerase II is an efficient inducer of apoptosis (Hamdi et al., 2005). Unlike Xeroderma Pigmentosum (XP; complementation group A through G; reviewed by (Bootsma, 2001)), another photosensitive disorder caused by a GG-NER or combined GG-NER/TC-NER defect (as in XP-C and XP-A, respectively), CS is not associated with UV-mediated skin cancer predisposition (Nance and Berry, 1992), which may be attributed to the fact that CS cells are still GG-NER proficient (van Hoffen et al., 1993; Venema et al., 1990).

Remarkably, despite the notion that CS carries only a partial NER defect, the clinical symptoms are more severe and different from those observed in XP, in which a combined GG-NER/TC-NER defect occurs. CS is a highly pleiotropic disorder, generally characterized by severe (postnatal) growth failure and wasting (cachectic dwarfism), physical and mental retardation, and progressive neurological abnormalities (i.e. delayed psychomotor development, mental retardation, microcephaly, gait ataxia, sensorineural hearing loss, retinal degeneration), impaired sexual development, kyphosis, osteoporosis and an average life span of 12.5 years, with pneumonia (resulting from cachexia) as the most common cause of death (reviewed by (Bootsma, 2001; Nance and Berry, 1992)). Neuropathological examination revealed multifocal patchy demyelination in cerebral and cerebellar cortex, dilated ventricles, calcium deposits in basal ganglia and cerebral cortex, and loss of neurons near calcium deposits, which is most pronounced in the cerebellum. Peripheral nerve defects, like reduced velocity of nerve conduction, sensorineuronal hearing loss, and changes in muscle innervation are often observed (Itoh et al., 1999; Nance and Berry, 1992; Rapin et al., 2000). In some cases, CS features combine with cancer-prone XP (XP/CS), due to mutations in the *XPB*, *XPD* or *XPG* genes. Since patients have many, but not all characteristics of natural aging, CS (and XP/CS) is considered a segmental progeroid syndrome, suggesting a link between defective DNA repair and aging (Martin, 2005).

Animal models for photosensitive disorders have contributed substantially to our understanding of the function of NER proteins and their involvement in battling cancer and aging. *Xpa*$^{-/-}$ and *Xpc*$^{-/-}$ knock-out mice reliably recapitulate the UV-sensitivity and skin cancer predisposition of XP-A and XP-C patients respectively, and do not show any other overt phenotype (Cheo et al., 1996; de Vries et al., 1995; Nakane et al., 1995; Sands et al., 1995). Mice carrying an inactivated *Csa* gene or a *Csb* gene with a premature stop codon similar as found in patient CS1AN, also have a UV-sensitive skin, but in contrast to human CS, display a mild UV skin cancer susceptibility (van der Horst et al., 2002; van der Horst et al., 1997). This can be attributed to the fact that rodents do not show efficient GG-NER of cyclobutane pyrimidine dimers (the most abundant UV-induced photoproduct and the primary lesion responsible for photocarcinogenesis; (Jans et al., 2005)), and thus entirely depend on TC-NER for removal of this lesion (Bohr et al., 1985). In contrast to the severe growth defect and neurological problems associated with human CS, *Csa*$^{-/-}$ and *Csb*$^{m/m}$ animals only display mild other features of human CS, as evident from the slight reduction in body weight, and minor neurological abnormalities such as reduced motor coordination (van der Horst et al., 2002; van der Horst et al., 1997), and age-related loss of photoreceptor cells (Chapter 3).

Along the lines of Harman's "free radical theory of aging" (Harman, 1956), we recently hypothesized that (oxidative) DNA lesions, originating from reactive oxygen species (ROS) and other by-products of cellular metabolism, are at the basis of the etiology of progeroid DNA repair disorders. Such endogenously produced lesions are hypothesized to hamper transcription and replication, resulting in enhanced apoptosis and/or cellular senescence, eventually followed by loss of tissue homeostasis and onset of (aging-related) pathology (Hasty et al., 2003; Mitchell et al., 2003). In this scenario, the onset of tissue/organ-specific pathology is expected to relate to the level of genotoxic stress, notably endogenous oxidative stress (the net result of metabolic ROS production and anti-oxidant capacity) and (residual) DNA repair capacity in the specific organ or tissue. This well explains the segmental character of the progeroid features and the striking link between genome stability disorders and premature aging syndromes. The involvement of oxidative DNA lesions in the onset of (non-UV-related) CS features is well supported by the observations that (i) *Csb*$^{m/m}$ mouse embryonic fibroblasts, as well as cells from human CS-B patients and *CSB* siRNA-silenced HeLa cells, are susceptible to known sources of oxidative DNA damage such as ionizing radiation, and paraquat (de Waard et al., 2004; de Waard et al., 2003; Deschavanne et al., 1984; Liu et al., 2006), (ii) *Csb*$^{m/m}$ animals show increased apoptosis of retinal cells in response to ionizing radiation exposure (Chapter 3), (iii) *Csb*$^{m/m}$ mice are sensitive to chronic exposure to the pro-oxidant di(2-ethylhexyl)phthalate

(DEHP) (de Waard et al., 2004), and, as discussed in detail below, (iv) further impairment of repair dramatically aggravates the phenotype of *Csb*$^{m/m}$ mice (Chapter 2).

When *Csb*$^{m/m}$ or *Csa*$^{-/-}$ mice were crossed into an *Xpc*$^{-/-}$ or *Xpa*$^{-/-}$ background (resulting in complete inactivation of NER), double mutant mice display a segmental premature aging phenotype similar to that of CS patients, as evident from the dramatic postnatal growth retardation, cachexia, kyphosis, ataxia, photoreceptor loss, abnormal locomotor activity, as well as progressive weight loss, and premature death around weaning (Murai et al., 2001; van der Horst et al., 2002), (Chapter 2). Analysis of the *Csb*$^{m/m}$/*Xpa*$^{-/-}$ mouse liver transcriptome revealed a systemic suppression of the GH/IGF1 somatotroph axis and oxidative metabolism, along with an increased antioxidant response. Importantly, a similar response is observed in old wild type mice and in pro-oxidant treated young wild type mice (Chapter 2). Additionally, down-regulation of the somatotroph axis in *C.elegans* and mice is associated with enhanced longevity (Andersen et al., 1995; Carter et al., 2002; Li et al., 1990; Liang et al., 2003; Longo and Finch, 2003). On this basis, we hypothesized that this response is (i) intrinsic to natural aging, (ii) can be triggered by DNA lesions (iii) may act as a feed back regulatory mechanism to diminish damage levels in the genome by ROS and other reactive metabolites via reduction of metabolism and up-regulation of anti-oxidant response, and (iv) intends to extend life span (Chapter 2). Thus, the increased genotoxic stress initiates the adaptive response shortly after birth, allowing CS patients and *Csb*$^{m/m}$/*Xpa*$^{-/-}$ mice to live longer at the expense of early cessation of growth resulting in the characteristic dwarfism. A similar transcriptional response has been documented in *Ercc1* knockout and *Xpd*^{XPCS} mouse models (Andressoo et al., Niedernhofer et al., pending revision) and likely extends to other NER models (e.g. *Xpd*^{TTD}/*Xpa* and *Xpg* mice; de Boer et al., 2002; Harada et al., 1999).

Evidently, the short life span of *Csb*$^{m/m}$/*Xpa*$^{-/-}$ animals hampers further studies on the etiology of CS. Here, we describe the generation, characterization and use of a loxP/Cre-recombinase conditional *Xpa* mouse model to study in a time- and tissue-specific manner the onset of the *Csb*$^{m/m}$/*Xpa*$^{-/-}$ (aging) phenotype, and the role of apoptosis therein. Particularly, by crossing conditional *Csb*$^{m/m}$/*Xpa*$^{c/-}$ mice with *CamKII*-promoter-driven *Cre* transgenic mice (expressing the Cre-recombinase predominantly in cerebrum, and to a lesser extent in the cerebellum), we focus on the brain, as it is a tissue with one of the highest levels of oxygen consumption (Halliwell, 1985; Halliwell, 1989), and progressive neurological dysfunction is a hallmark feature of CS (Nance and Berry, 1992).

Results

Generation and characterization of a conditional *Xpa* mouse model

To establish a conditional *Xpa* mouse model, we generated a targeting construct in which exon 4 was fused in frame to the mouse *Xpa* cDNA (including a synthetic polyA sequence), followed by a PGK promoter-driven hygromycin (*Hygro*) selectable marker gene (see Fig. 1A). LoxP sites were introduced in intron 3 and downstream the *Hygro* marker to allow Cre-mediated excision of the *Xpa* cDNA part and *Hygro* marker gene and concomitant formation of an *Xpa* null allele lacking exon 4, which is known to act as a functional null allele (de Vries et al., 1995).

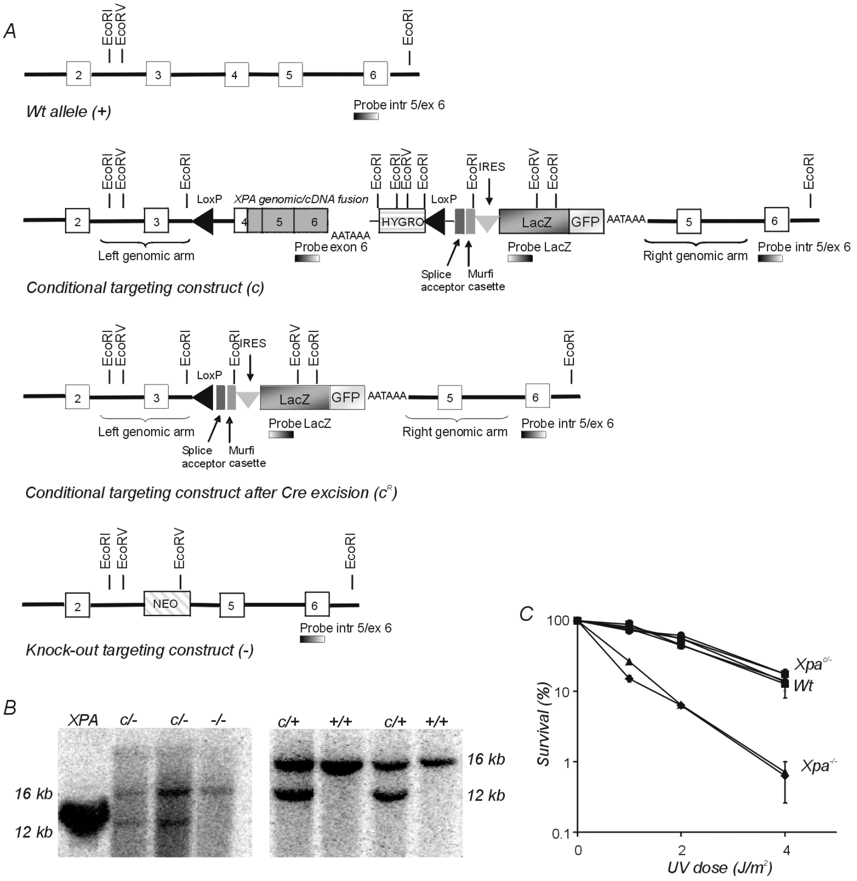
A
EcoRI
EcoRV
EcoRI
2
3
4
5
6
Wt allele (+)
Probe intr 5/ex 6
LoxP
XPA genomic/cDNA fusion
HYGRO
IRES
LacZ
GFP
AATAAA
Left genomic arm
Probe exon 6
Splice acceptor
Murfi casette
Probe LacZ
Right genomic arm
Conditional targeting construct (c)
Conditional targeting construct after Cre excision (c^R)
NEO
Knock-out targeting construct (-)
B
XPA
c/-
c/-
-/-
c/+
+/+
c/+
+/+
16 kb
12 kb
C
100
10
1
0.1
Survival (%)
0
2
4
UV dose (J/m²)
Xpa c/-
Wt
Xpa -/-

Figure 1. Targeting of the mouse Xpa allele with a floxed genomic/cDNA fusion construct. *A) Schematic representation of the wild type mouse Xpa locus (exon 2 to 6), the targeting construct, the conditional Xpa allele, and conditional Xpa allele following Cre-recombinase-mediated inactivation. For completeness, we also have indicated the classical knock out allele, as generated by de Vries et al.,1995. Open and gray boxes represent exon and cDNA sequences, respectively. Hygromycin (HYGRO) and neomycin (NEO) marker cassettes (for selection of targeted ES clones) as well as the LacZ/GFP fusion reporter gene (used to report successful inactivation of the conditional allele) are indicated as gray stripes, gray squares, and dark/light gray shaded boxes respectively. Triangles represent LoxP sites, while the position of splice acceptor, ochre multiple reading frame insertion (Murfi) linker (containing stopcodons in all three reading frames), and Internal Ribosomal Entry Site (IRES) are indicated as light and dark gray colored squares, and a light gray triangle, respectively. Polyadenylation sites are indicated by AATAAA. Probes are indicated by black shaded bars. R and RV represent EcoRI and EcoRV restriction sites. B) Southern blot analysis of* $Xpa^{-/-}$ *(left panel) and wild type (right panel) ES cell DNA after transfection of cells with the conditional Xpa construct. DNA was digested with EcoRI and hybridized with an intron 5/exon 6 probe, external to the targeting construct. Wild type and targeted alleles gave fragments of 12 and 16 kb, respectively. C) Survival curves of wt (circles),* $Xpa^{-/-}$ *(diamonds and triangles) and* $Xpa^{c/-}$ *(squares) ES cells, exposed to increasing doses of UV-C light*

To visualize inactivation of the conditional *Xpa* allele at the cellular level, we inserted a *LacZ-GFP* fusion marker gene, preceded by splice acceptor (SA) and internal ribosomal entry site (IRES) sequences to allow translation of the marker. A multiple reading frame insertion (Murfi) linker with stopcodons in all 3 reading frames was placed between the SA and IRES to prevent translation of potential read-through transcripts from the *Hygro* marker gene, which would cause false positive staining.

To test the functionality of the genomic/cDNA fusion allele, we first transfected *Xpa*$^{-/-}$ ES cells (de Waard et al., 2003) with the conditional *Xpa* construct and obtained targeted ES clones at a frequency of 20%, as detected by Southern blot analysis using an intron 5/exon 6 probe, which hybridizes downstream of the targeting site and is external to the targeting construct (Fig. 1B; left panel). As shown in Fig. 1C, replacement of one knockout allele by the conditional *Xpa* allele (as in *Xpa*$^{c/-}$ ES cells) fully averted the previously described extreme UV sensitivity of *Xpa*$^{-/-}$ ES cells (de Waard et al., 2003), while subsequent transient transfection of the corrected cells with a *Cre-recombinase* expression construct reinstated UV-hypersensitivity (data not shown), thus proving functionality of the conditional *Xpa* allele.

We next transfected ES line IB10 with the conditional *Xpa* construct and obtained heterozygous *Xpa*$^{c/+}$ ES cells (Fig. 1B, right panel) at a frequency of 17%. After confirming the 5' region excluding chromosomal abnormalities and additional random integrations (data not shown), two independent *Xpa*$^{c/+}$ ES cell clones were used for blastocyst injections and the generation of chimeric mice. Germ line transmission was obtained for both clones and subsequent experiments with heterozygous (*Xpa*$^{c/+}$) and homozygous (*Xpa*$^{c/c}$) offspring yielded identical results, indicating that the findings reported below are not due to uncontrolled events that might have occurred in one targeted ES clone.

In line with observations made previously for *Xpa*$^{-/-}$ animals (de Vries et al., 1995), *Xpa*$^{c/+}$, *Xpa*$^{c/-}$ and *Xpa*$^{c/c}$ animals do not show any overt phenotype, at least up to an age of 20 months (data not shown). To show that CRE recombinase can also excise the floxed *Xpa* sequence *in vivo*, we bred *Xpa*$^{c/+}$ mice with *Xpa*$^{+/-}$ mice carrying a *Cag*-promoter-driven *Cre* transgene that is expressed immediately after conception (Sakai and Miyazaki, 1997)) to obtain E13.5 *Xpa*$^{c/-}$ and *Xpa*$^{c/-}$*/Cag-Cre* embryos and mouse embryonic fibroblasts (MEFs). Using a *LacZ* probe, we confirmed by Southern blot analysis that expression of the Cre-recombinase transgene in *Xpa*$^{c/-}$ embryos resulted in excision of the floxed sequence at near 100% recombination efficiency (Fig. 2A). Staining with X-gal only yielded blue *Xpa*$^{c/-}$ embryos and MEFs when recombination had occurred in the presence of the *Cag-Cre* transgene (Fig. 2B), which proves the usefulness of the LacZ/GFP reporter. However, it should be noted that LacZ staining patterns are relatively weak, and only visible after overnight staining, while GFP signals did not exceed autofluorescent background levels (data not shown), which may be attributed to the relatively low expression efficiency of the endogenous *Xpa* promoter (Layher and Cleaver, 1997). As expected, inactivation of the conditional allele in *Xpa*$^{c/-}$ MEFs triggered UV-sensitivity (Fig. 2C), as evident from our observation that the UV survival of *Xpa*$^{c/-}$ and *Xpa*$^{c/-}$/*Cag-Cre* MEFs was in the same range as reported for wild type (wt) and *Xpa*$^{-/-}$ MEFs respectively (de Vries et al., 1995).

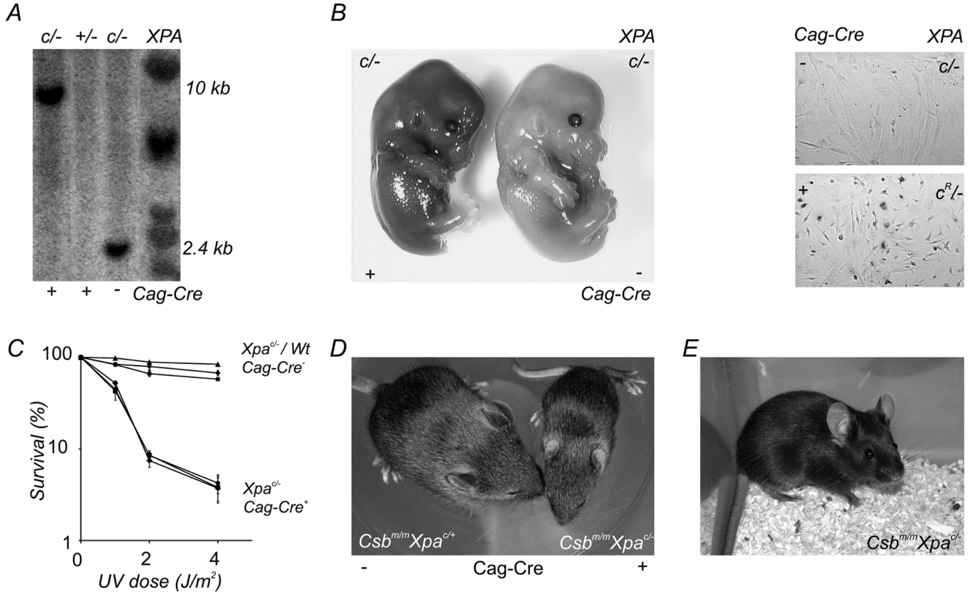

Figure 2. Characterization of conditional Xpa$^{c/-}$ and Csb$^{m/m}$Xpa$^{c/-}$ mice. *A) Southern blot analysis of DNA from E13.5 Xpa$^{c/-}$ and Xpa$^{c/-}$/Cag-Cre embryos, the latter ubiquitously expressing the Cre-recombinase immediately after conception. DNA was digested with EcoRV and hybridized with a LacZ probe. Conditional and recombined (inactivated) conditional Xpa alleles gave fragments of 2.4 and 10 kb, respectively. B) LacZ staining of E13.5 Xpa$^{c/-}$ and Xpa$^{c/-}$/Cag-Cre embryos (left panel) and mouse embryonic fibroblasts (right panel), indicating inactivation of the conditional Xpa allele in Xpa$^{c/-}$/Cag-Cre embryos only. C) Survival of wild type, Xpa$^{c/-}$ and Xpa$^{c/-/}$Cag-Cre MEFs (genotypes indicated in figure), exposed to increasing doses of UV-C light. D) Picture of 16-day old Csb$^{m/m}$Xpa$^{c/-}$ and Csb$^{m/m}$/Xpa$^{c/-}$/Cag-Cre littermates, the latter phenocopying the non-conditional Csb$^{m/m}$Xpa$^{-/-}$ mouse. E) Picture of an 8 week old Csb$^{m/m}$ Xpa$^{c/-}$ mouse, showing complete rescue of the Csb$^{m/m}$/Xpa$^{-/-}$ premature aging phenotype by the conditional Xpa allele.*

We next generated *Csb$^{m/m}$/Xpa$^{c/-}$* and *Csb$^{m/m}$/Xpa$^{c/-}$/Cag-Cre* mice. As predicted on the basis of the phenotype of the classical (non-conditional) *Csb$^{m/m}$/Xpa$^{-/-}$* mouse model (van der Pluijm et al, submitted), *Csb$^{m/m}$Xpa$^{c/-}$/Cag-Cre* pups display the severe postnatal growth retardation (as illustrated in Fig. 2D), cachexia, disturbed gait, and die before weaning. In contrast, *Csb$^{m/m}$/Xpa$^{c/-}$* littermates do not show any overt phenotype, and importantly, remain devoid of any overt (aging-associated) pathology or neurological deficits other than that of *Csb$^{m/m}$* single mutants when developing into adulthood (8 weeks, see Fig. 2E), or when reaching high age (over 2 years; data not shown). From these data, we conclude that the conditional *Xpa* mouse represents a valid animal model to study the *Csb$^{m/m}$/Xpa$^{-/-}$* double mutant phenotype, including premature aging, in a time- and tissue-specific manner.

Post-juvenile growth defect and premature death of brain-specific conditional *Csb$^{m/m}$/Xpa$^{c/-}$* mice

Progressive neurological dysfunction is a hallmark feature of CS. *Csb$^{m/m}$/Xpa$^{-/-}$* animals also display a neurological phenotype, as evident from tremors and flexion rather than extension of hind limbs (pointing to motor coordination problems), and disturbed gait (indicative for ataxia).

Moreover, reduced neurogenesis and increased apoptotic cell death in the cerebellar external granular layer have been observed in *Csb*$^{m/m}$*/Xpa*$^{-/-}$ newborns (Murai et al., 2001). Since *Csb*$^{m/m}$*/Xpa*$^{-/-}$ pups die before weaning, and therefore might not develop the full spectrum of CS-associated neuropathology, we first aimed at ubiquitously inactivating the conditional Xpa allele after animals reached adulthood. To this end, we generated *Csb*$^{m/m}$*/Xpa*$^{c/-}$*/Cre-ER*^{T} mice, expressing a Cre-recombinase that remains inactive until the non-steroidal estrogen analog 4-hydroxytamoxifen (OHT) is given to the animal (Vooijs et al., 2001). However, administration of tamoxifen to 2-month old *Csb*$^{m/m}$*/Xpa*$^{c/-}$*/Cre-ER*^{T} animals appeared lethal. Subsequent investigation revealed severe intestinal pathology. On the basis of preliminary findings we attribute this dramatic outcome to enhanced sensitivity of double mutant animals to tamoxifen-induced DNA damage (for details, see Chapter 4 Appendix).

We next generated a brain-specific *Csb*$^{m/m}$*/Xpa*$^{c/-}$ mouse by crossing in the *CamKIIα-Cre* recombinase transgene (courtesy of S. Zeitlin). The transgenic mouse line used, L7ag#13, expresses the Cre-recombinase from postnatal day 5 throughout the adult brain, with high levels in all forebrain structures and low/moderate levels in the cerebellum (Dragatsis and Zeitlin, 2000). Attempts to visualize LacZ or GFP in *Csb*$^{m/m}$*/Xpa*$^{c/-}$*/CamKIIα-Cre* brains (indicative for successful recombination) rendered negative results, except for moderate LacZ staining of the Lateral Septum (connected to the hippocampus). Nevertheless, when L7ag#13 mice were crossed with a LacZ reporter mouse (carrying a floxed LacZ gene, targeted to the highly expressed Rosa26 locus and activated upon Cre recombination), we observed ubiquitous LacZ staining of the cerebrum (Elgersma, unpublished results), which confirmed previously published findings (Dragatsis and Zeitlin, 2000). We therefore envisage that the conditional Xpa allele has been inactivated throughout the forebrain of *Csb*$^{m/m}$*/Xpa*$^{c/-}$*/CamKIIα-Cre* animals, but that apparently only in the hippocampus the Xpa allele is sufficiently highly expressed to visualize the recombination event by LacZ staining. This explanation is supported by a database search of the Allen Brain Atlas (an interactive genome-wide image database of gene expression in the mouse brain; http://www.brain-map.org/welcome.do) (data not shown). In addition, we were able to show by PCR analysis that Cre-dependent recombination of the floxed Neo marker in the mutant *Csb* allele occurred in all brain regions, except for the cerebellum (data not shown).

Csb$^{m/m}$*/Xpa*$^{c/-}$*/CamKIIα-Cre* pups were obtained at Mendelian ratio (data not shown), and grew into young adulthood without noticeable phenotype (Fig. 3A shows a 6 month old *Csb*$^{m/m}$*/Xpa*$^{c/-}$*/CamKIIα-Cre* mouse). Next, we monitored *CamKIIα-Cre* (serving as NER-proficient “wild type” control), *Csb*$^{m/m}$*/CamKIIα-Cre*, *Xpa*$^{c/-}$*/CamKIIα-Cre* and *Csb*$^{m/m}$*/Xpa*$^{c/-}$*/CamKIIα-Cre* mice in time for the appearance of a phenotype. As evident from body weight measurements, *Csb*$^{m/m}$*/Xpa*$^{c/-}$*/CamKIIα-Cre* mice initially show normal bodyweight (Fig. 3B) and size. However, clear differences became apparent after animals passed the age of 8 months. From that moment, in line with a previous *Csb*$^{m/m}$ cohort study (Wijnhoven, van Steeg, unpublished results), *Csb*$^{m/m}$*/CamKIIα-Cre*, animals gain weight at slower pace than *CamKIIα-Cre* and *Xpa*$^{c/-}$*/CamKIIα-Cre* animals. Interestingly, *Csb*$^{m/m}$*/Xpa*$^{c/-}$*/CamKIICre* animals lag further behind in bodyweight, as compared to the *Csb*$^{m/m}$*/CamKIICre* littermates, and from the age of 10 months even start to lose weight.

At an age of about 15 months, *Csb*$^{m/m}$*/Xpa*$^{c/-}$*/CamKIICre* animals (n=6) started to display reduced motility and seizures, the latter being well illustrated by the frequent loss of consciousness during bodyweight measurements. As shown in Fig. 3C, *Csb*$^{m/m}$*/Xpa*$^{c/-}$*/CamKIICre* animals became moribund and had to be sacrificed between 16 and 22 months of age, whereas wt and single mutant littermates (n=18) show a normal life span. Strikingly, between 1 and 2 months before death, all *Csb*$^{m/m}$*/Xpa*$^{c/-}$*/CamKIICre* male mice developed priapism, a persistent penal erection as a consequence of disease, rather than sexual arousal (Fig. 3C). This phenomenon, which was not observed in *Wt/CamKIICre*, *Csb*$^{m/m}$*/CamKIICre* or *Xpa*$^{c/-}$*/CamKIICre* males, most likely is due of neurogenic origin, although other possibilities are currently not excluded.

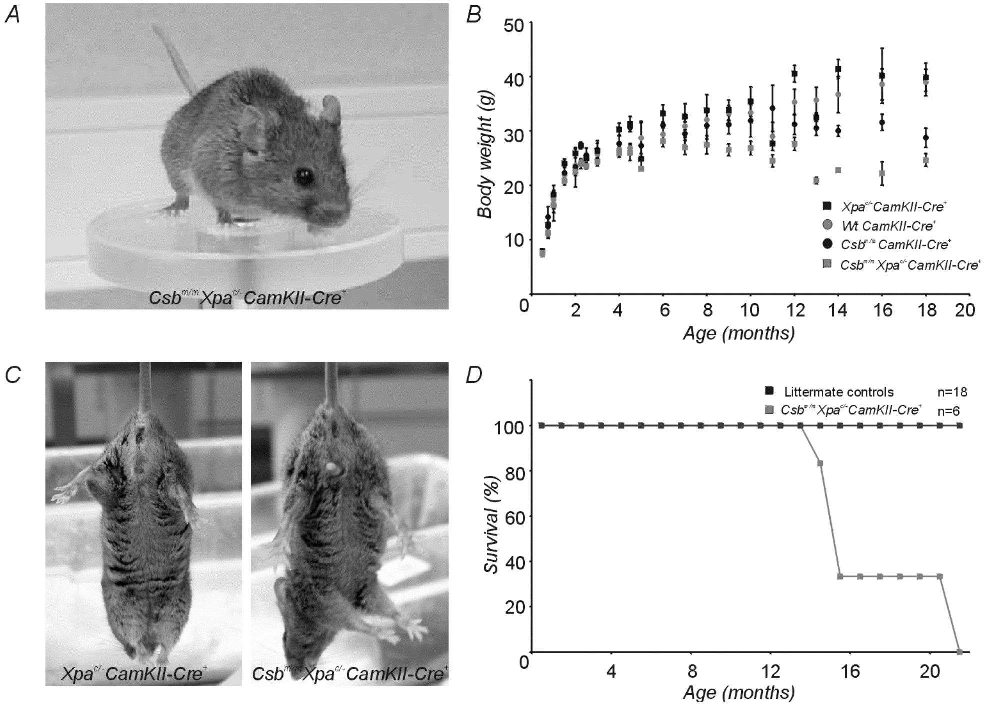

Figure 3. Post-juvenile growth defect and premature death of brain-specific conditional Csb$^{m/m}$/Xpa$^{c/-}$ mice. *A) Photograph of a Csb*$^{m/m}$*/Xpa*$^{c/-}$*/CamKIIα-Cre animal at the age of 6 months. B) Body weight curves of wt/CamKIIα-Cre, Csb*$^{m/m}$*/Xpa*$^{c/-}$*/CamKIIα-Cre, Xpa*$^{c/-}$*/CamKIIα-Cre and Csb*$^{m/m}$*/Xpa*$^{c/-}$*/CamKIIα-Cre. Note that beyond the age of 8 months, the weight of Csb*$^{m/m}$*/Xpa*$^{c/-}$*/CamKIIα-Cre animals starts to differ substantially from their control littermates, including Csb*$^{m/m}$*/Xpa*$^{c/-}$*/CamKIIα-Cre animals. C) Representative photograph of 15 month old Xpa*$^{c/-}$*/CamKIIα-Cre and Csb*$^{m/m}$*/Xpa*$^{c/-}$*/CamKIIα-Cre animals, showing priapism in the latter. D) Survival curve showing premature death of Csb*$^{m/m}$*/Xpa*$^{c/-}$*/CamKIIα-Cre animals (n=6) as compared to littermate controls (n=18).*

Brain-specific conditional *Csb*$^{m/m}$*/Xpa*$^{c/-}$ mice show anxiety-like behavior

During handling of the *Csb*$^{m/m}$*/Xpa*$^{c/-}$*/CamKIICre* animals, we frequently observed freezing behavior, as well as excessive escape behavior when the researcher attempted to lift the animal from the cage, which we subjectively interpreted as anxiety-like behavior. This feature appeared to be progressive with time. We therefore subjected *Csb*$^{m/m}$*/Xpa*$^{c/-}$*/CamKIICre* and littermate controls to an open-field exploratory behavior test at the age of 3, 6, and 12 months. In this assay, ‘anxious’ mice avoid exploration of the central (exposed) part of the open field, and show thigmotactic behavior (taxis in which contact with a solid body is the directive factor) along the walls of the apparatus (Holmes, 2001). Computer-derived movement plots after recording the activity of animals for 30 minutes in the open field (example shown in Fig. 4A), clearly demonstrate that *Csb$^{m/m}$/Xpa$^{c/-}$/CamKIICre* mice are less active in the center than wt *(CamKIICre*) and single mutant animals (n=6 per genotype). Calculation of the anxiety ratio (AR) by dividing the ambulatory activity in the center by the total distance moved, revealed that *Csb$^{m/m}$/Xpa$^{c/-}$/CamKIICre* animals tend to have a lower AR than the control mice at 3 months of age (p=0.056; Mann-Whitney-U test), the difference becoming significant at 6 and 12 months of age (p=0.003 and p=0.02, respectively) (Fig. 4B).

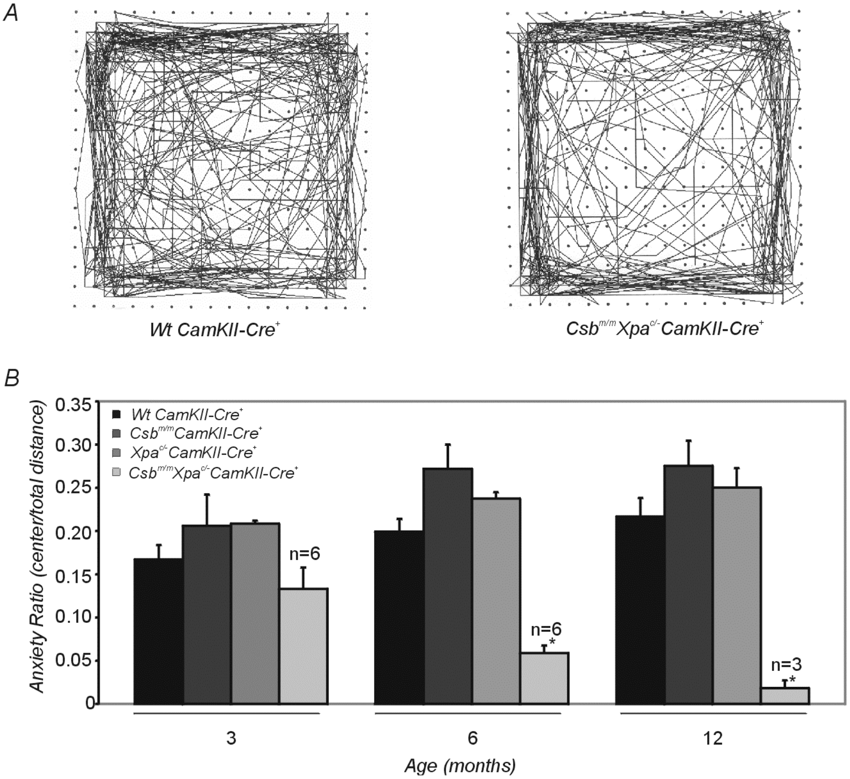

Figure 4. Brain-specific conditional *Csb$^{m/m}$/Xpa$^{c/-}$* mice show anxiety-like behavior. *A) Representative examples of open field plots of a wt and a Csb$^{m/m}$/Xpa$^{c/-}$/CamKIIα-Cre animal. Note the relative avoidance of the center by the mutant mouse when compared to the wt control. B) Bar graphs depicting the anxiety ratio (AR), calculated as center distance divided by total distance, of CamKIIα-Cre (wt), Csb$^{m/m}$/CamKIIα-Cre, Xpa$^{c/-}$/CamKIIα-Cre and Csb$^{m/m}$/Xpa$^{c/-}$/CamKIIα-Cre animals at the age of 3 and 6 and 12 months (n=6 at all timepoints, except for Csb$^{m/m}$/Xpa$^{c/-}$/CamKIIα-Cre animals at the age of 12 months: n=3). A low AR is indicative of anxiety-like behavior. At 3 months the AR of and Csb$^{m/m}$Xpa$^{c/-}$CamKIIα-Cre animals is lower than that of the control groups (p<0.056), which becomes significantly at the age of 6 months (p=0.003) and 12 months of age (p=0.02) as compared to CamKIIα-Cre (wt) animals.*

Noteworthy is that at 12 months of age, we had to exclude 3 animals from the assay because they repeatedly displayed seizures during the assay. Ambulatory activity in an open field is likely to be the result of both anxiety-related approach/avoid conflict and levels of basal locomotor activity (Holmes, 2001). However, locomotory activity differences could be excluded since at a given age (irrespective of the genotype) total movement time and distance was approximately the same. Interestingly, whereas the AR of wild type and single mutant animals is constant over time (and even shows a tendency to increase), the AR of *Csb*$^{m/m}$/*Xpa*$^{c/-}$/*CamKIICre* animals steadily drops with age, indicating that the anxiety-like behavior of *Csb*$^{m/m}$/*Xpa*$^{c/-}$/*CamKIICre* animals worsens progressively (Fig. 4B). In addition, we noticed that *Csb*$^{m/m}$/*Xpa*$^{c/-}$/*CamKIICre* animals do not display normal nest building behavior, which was apparent from their disinterest in, and urine disposal on tissues, provided as nest bedding and cage enrichment material.

Brain-specific conditional *Csb*$^{m/m}$/*Xpa*$^{c/-}$ mice mimic the brain deficits of Cockayne Syndrome

To investigate whether the neurological features, as encountered in the conditional brain *Csb*$^{m/m}$/*Xpa*$^{c/-}$ mouse model, were accompanied by anatomical anomalies, we next performed a neuropathological examination of *Csb*$^{m/m}$/*Xpa*$^{c/-}$/*CamKIICre* and age-matched *Xpa*$^{c/-}$/*CamKIICre* control mice at various ages. To this end, we perfused 6 and 16 month old *Csb*$^{m/m}$/*Xpa*$^{c/-}$/*CamKIICre* and *Xpa*$^{c/-}$/*CamKIICre* mice and isolated the brains. The brain of 16 month old *Csb*$^{m/m}$/*Xpa*$^{c/-}$/*CamKIICre* mice weighed considerably less than that of *Xpa*$^{c/-}$/*CamKIICre* animals (0.372 vs. 0.436 gram). From the macroscopic pictures shown in Fig. 5B it is obvious that the brain of 16 month old *Csb*$^{m/m}$/*Xpa*$^{c/-}$/*CamKIICre* mice is strikingly small, particularly the cerebrum. This finding fits well with the observed enlarged subarachnoidal space between the brain and the skull, observed during the autopsy procedure. Slight differences in outer appearance, along with a reduced brain weight are already visible at the age of 6 months. In general, *Csb*$^{m/m}$/*Xpa*$^{c/-}$/*CamKIICre* brains have an atrophic appearance, which is most pronounced at old age and thus points to a progressive deterioration of the brain. Coronal sections of the brain revealed dilated ventricles and a thin cerebral cortex (Figure 5B), features described as hydrocephalus ex vacuo. Microcephaly was not apparent at the ages examined. In addition, the inner lining of the skull did not show signs of increased intracranial pressure, as evident from the smooth appearance and absence of erosion of the skull. The cerebrum had a general atrophic appearance, including the hippocampal area, which was due to the loss of both white and grey matter. Furthermore, the hippocampus showed disorganization of the neural tissue (Fig. 5B), loss of neuronal cells, and was dramatically reduced in size. There were no obvious signs of infarction and no neurofibrillary tangles were found, whereas signs of gliosis and demyelination were evident. The ependymal cells, both in the lining of the ventricles and the choroid plexuses, were swollen and vacuolated. It remains to be examined whether the pathology observed in the cerebrum of *Csb*$^{m/m}$/*Xpa*$^{c/-}$/*CamKIICre* animals is also present at an earlier age. Preliminary macroscopical data on the brain of 1 month old *Csb*$^{m/m}$/*Xpa*$^{c/-}$/*CamKIICre* animals did not reveal signs of cerebral atrophy and dilated ventricles, which suggests that the observed severe brain pathology is not of developmental origin and develops between 1-6 months of age.

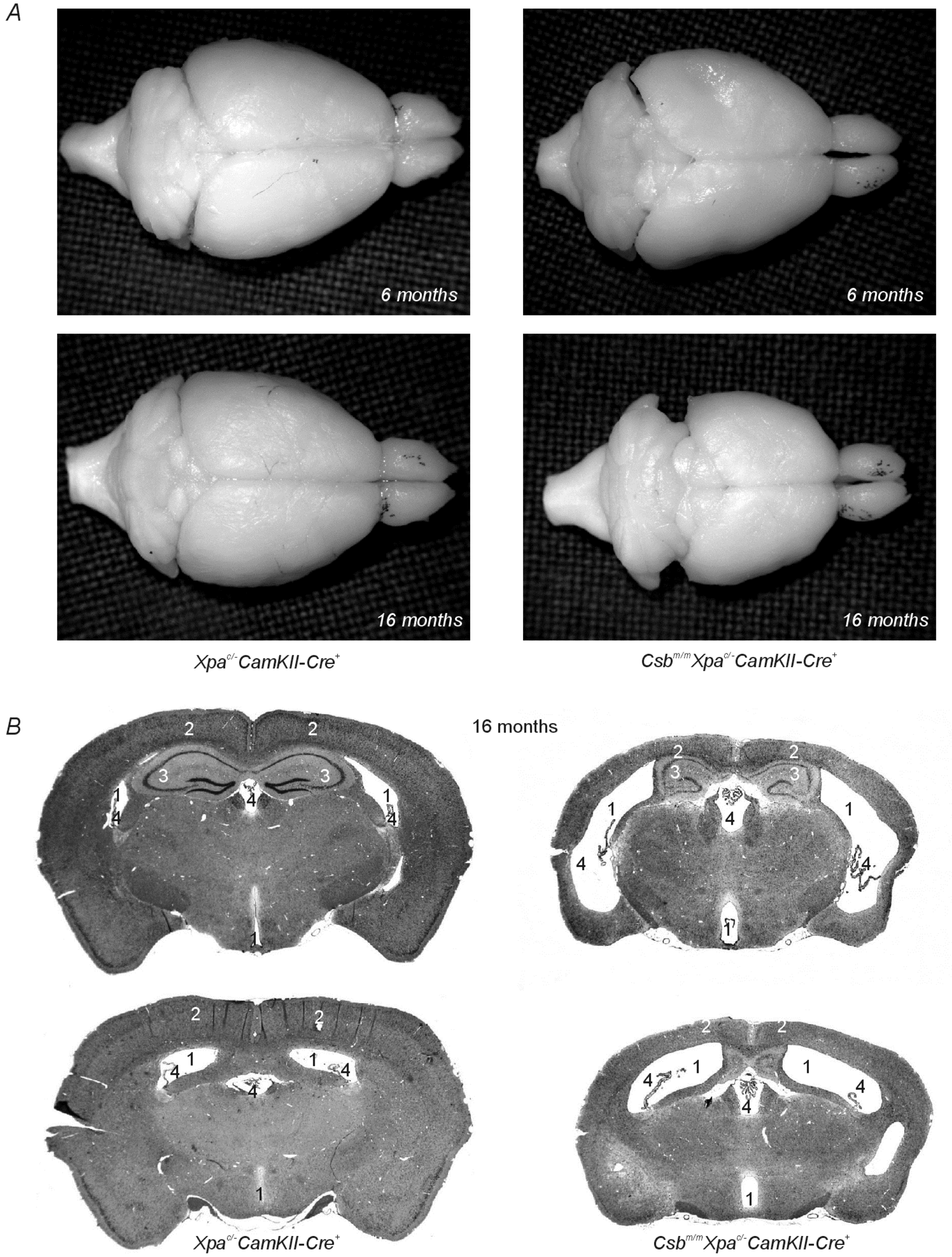
A
6 months
6 months
16 months
16 months
$Xpa^{c/-}$ CamKII-Cre^{+}
$Csb^{m/m}Xpa^{c/-}$ CamKII-Cre^{+}
B
16 months
2
2
3
3
1
4
4
1
4
1
2
2
3
3
1
4
1
4
4
1
2
2
1
4
1
4
4
1
2
2
4
1
1
4
4
1
$Xpa^{c/-}$ CamKII-Cre^{+}
$Csb^{m/m}Xpa^{c/-}$ CamKII-Cre^{+}

Figure 5. Brain-specific conditional *Csb*$^{m/m}$/*Xpa*$^{c/-}$ mice mimic the brain deficits of Cockayne Syndrome. *A) Macroscopic picture of the brain of 6 and 16 month old Xpa*$^{c/-}$*CamKIIα-Cre and Csb*$^{m/m}$*Xpa*$^{c/-}$*CamKIIα-Cre brains showing cerebral atrophy in the latter. Pictures were taken at the same magnification. B) Histological micrographs of 16 month old Xpa*$^{c/-}$*CamKIIα-Cre (left) and Csb*$^{m/m}$*Xpa*$^{c/-}$*CamKIIα-Cre (right) brains, showing dilated ventricles (1), thin cortex (2), small hippocampus (3) and vacuolated ependymal cells (4) in the cerebrum of Csb*$^{m/m}$*Xpa*$^{c/-}$*CamKIIα-Cre animals (right panel). Similar numbers are used to point out the corresponding structures in the cerebrum of Xpa*$^{c/-}$*CamKIIα-Cre animals (left panel), where these abnormalities are not found.*

Discussion

The conditional *Xpa* mouse model and its applications

Recently, have shown that the *Csb*$^{m/m}$/*Xpa*$^{-/-}$ mice provide a better model for human CS than *Csb*$^{m/m}$ single mutant mice (Chapter 2). Apparently, further impairment of repair capacity in *Csb*$^{m/m}$ mice is prerequisite to obtain sufficiently elevated levels of endogenous DNA damage to drive early onset of CS features (including aging-associated pathology) in the absence of a functional CSB protein. To overcome the perinatal lethality associated with *Csb*$^{m/m}$/*Xpa*$^{-/-}$ mouse model, and thus to facilitate analysis of the etiology of (progeroid) CS features in a time- and tissue-specific manner, we now have generated a loxP/Cre recombinase-based conditional *Xpa* mouse model. *Xpa*$^{c/-}$ ES cells and fibroblasts do not display UV sensitivity, unless the conditional *Xpa* allele is recombined out by (transient) expression of a Cre recombinase, showing that the conditional allele is functionally NER-proficient. Moreover, *Xpa*$^{c/-}$ mice, and particularly *Csb*$^{m/m}$/*Xpa*$^{c/-}$ animals, remain devoid of any prominent phenotype for at least 2 years, while *Csb*$^{m/m}$/*Xpa*$^{c/-}$/*Cag-Cre* newborns (expressing the Cre-recombinase immediately after conception), again show the runted growth, cachexia, and premature death, characteristic of non-conditional *Csb*$^{m/m}$/*Xpa*$^{-/-}$ pups. The complete rescue of the severe *Csb*$^{m/m}$*Xpa*$^{-/-}$ phenotype by one *Xpa* allele, as well as the absence of hypo- or hypermorphic effects, best illustrates the proper expression of the genomic/cDNA fusion allele. Visualization of CRE-mediated inactivation of the conditional *Xpa* allele through expression of the LacZ/GFP reporter gene in recombined alleles appeared difficult. Despite CRE-mediated recombination events in virtually all cells, *Csb*$^{m/m}$/*Xpa*$^{c/-}$/*Cag-Cre* embryos and MEFs displayed weak LacZ staining (and in the case of MEFs, only in a limited number of cells) while GFP fluorescence remained below detection limits, which we attribute to low expression levels of the reporter gene. Indeed, human and mouse cells have been reported to contain on average 5 to 8 *Xpa* transcripts (Layher and Cleaver, 1997). Taken together, these data convincingly demonstrate the validity of the conditional *Xpa* model.

A conditional *Xpa* mouse model that allows induction of a complete NER deficiency in a time- and tissue-dependent manner constitutes a powerful tool mouse in cancer and aging research. By only inducing the *Xpa* knockout status in defined tissues, one could refine carcinogenesis studies by for instance (i) zooming in on specific tumors types in NER-deficient tissues in an otherwise ‘healthy’ body, or (ii) by using low doses of genotoxic agents for which the repair-defective organ or tissue is highly sensitive without the chance that animals die due to secondary toxic effects in tissues of non-interest. Moreover, tumors in the above animals can be induced by natural endogenous or exogenous carcinogenic agents, instead of using transgenic animals in which all cells carry already an oncogenic step in the cancer process. In this respect, it is interesting to note that *Csb*$^{m/m}$/*Xpa*$^{-/-}$ cells display increased UV-sensitivity, as compared to single mutant cells (Chapter 2). A keratinocyte-specific conditional *Csb*$^{m/m}$/*Xpa*$^{c/-}$ mouse model would provide an ideal platform to investigate in vivo the effect of UV-induced lesions on apoptosis and on the kinetics of tumor induction and progression in skin carcinogenesis. Additional evidence for enhanced sensitivity of *Csb*$^{m/m}$/*Xpa*$^{-/-}$ cells to genotoxic agents was obtained from our unsuccessful attempt to induce the *Csb*$^{m/m}$/*Xpa*$^{-/-}$ phenotype at an older stage by using a ubiquitously expressed tamoxifen-activated CRE recombinase. Exposed

Csb$^{m/m}$/*Xpa*$^{c/-}$ animals showed severe intestinal pathology, most probably due to genotoxic effects of tamoxifen (see appendix).

In the present study, using a brain-specific conditional *Csb*$^{m/m}$/*Xpa*$^{c/-}$ model, we have made a start with the analysis of the etiology of neurological features in the *Csb*$^{m/m}$ mouse model. To specifically knock out the *Xpa* gene in the brain, we have crossed *Csb*$^{m/m}$/*Xpa*$^{c/-}$ animals with the *CamKIIα-Cre* (L7ag#13) transgenic mouse, which expresses the Cre-recombinase in the cerebrum, and to a lesser extent, the cerebellum (Dragatsis and Zeitlin, 2000). Likely due to the low *Xpa* expression levels (Layher and Cleaver, 1997), we could not detect LacZ expression (indicative of *Xpa* recombination in the brain) except for very moderate staining of the lateral septum, where *Xpa* is expressed at relatively higher levels (Allen Brain Atlas http://www.brain-map.org/welcome.do). Nevertheless, when *CamKIICre* (L7ag#13) mice were crossed with a high-expressor Cre-inducible LacZ reporter mouse, we observed ubiquitous LacZ staining of the brain, except for the cerebellum (Elgersma, unpublished results) (Dragatsis and Zeitlin, 2000). In addition, we were able to show Cre-dependent recombination of the Neo marker in the targeted *Csb* (null) mutant allele in each brain region, except for the cerebellum. Taken together, these data suggest that the conditional *Xpa* allele has been inactivated in the *Csb*$^{m/m}$/*Xpa*$^{c/-}$/*CamKIIα-Cre* brain. We are currently quantifying the recombination efficiency in various brain regions by other means (e.g. quantitative genomic PCR).

Retarded growth, premature death and neurological dysfunction in the brain-specific conditional *Csb*$^{m/m}$/*Xpa*$^{c/-}$ mouse model

Csb$^{m/m}$/*Xpa*$^{c/-}$/*CamKIIα-Cre* animals develop into adulthood without any overt phenotype. However, from the age of 8 months on the animals failed to further gain weight. Late onset growth retardation has also been observed for *Csb*$^{m/m}$ mice (Wijnhoven et al, unpublished results), but is more pronounced in *Csb*$^{m/m}$/*Xpa*$^{c/-}$/*CamKIIα-Cre* mice than in *Csb*$^{m/m}$/*CamKIICre* animals. Furthermore, also in contrast to *Csb* single mutant animals, *Csb*$^{m/m}$/*Xpa*$^{c/-}$/*CamKIIα-Cre* mice display premature death before the age of 2 years. The precise cause of death remains to be resolved. These data imply that long term induction of the *Xpa* knock-out status in the *Csb*$^{-/-}$ brain has an adverse effect on both growth and life span. Recent liver transcriptome analysis of the non-conditional *Csb*$^{m/m}$/*Xpa*$^{-/-}$ mouse model, together with physiological studies, pointed to a scenario where these DNA repair deficient animals mount a systemic response, comprising downregulation of the somatotrophic axis and oxidative (oxidative) metabolism, and upregulation of the anti-oxidant defense system (Chapter 2). This response is hypothesized to be initiated by oxidative stress and/or DNA lesions and is an adaptive event aiming at reducing the DNA damage load and prolonging lifespan. It is still unclear whether this response is initiated tissue-autonomously, or whether enhanced DNA damage levels in defined tissues and organs signal to the remainder of the body. With respect to the latter scenario, it is of prime importance to investigate (e.g. by liver transcriptome analysis) whether a brain-specific *Csb*$^{m/m}$/*Xpa*$^{c/-}$ defect can trigger a systemic response of the somatotrophic axis, metabolism and anti-oxidant defense system.

Interestingly, *Csb*$^{m/m}$/*Xpa*$^{c/-}$/*CamKIIα-Cre* mice show a clear neurological phenotype. Animals displayed seizures, aberrant nest building behavior, and in case of male mice, priapism. Moreover, during handling of the animals, we noticed anxiety-like behavior, which was further investigated using the open field assay. We noticed a progressive decrease in the anxiety ratio (AR) in *Csb*$^{m/m}$/*Xpa*$^{c/-}$/*CamKIIα-Cre* mice, which was not observed in *Csb*$^{m/m}$/*CamKIICre*, *Xpa*$^{c/-}$/*CamKIICre* or (wildtype control) *CamKIICre* animals. Although a low AR is indicative of anxiety-like behavior (Holmes, 2001), the open field activity test (along with the tail suspension test) is used as a primary screen (Tucci, 2006). Secondary screens, such as the Elevated-plus Maze test, should be performed to find out whether *Csb*$^{m/m}$/*Xpa*$^{c/-}$/*CamKIIα-Cre* animals indeed display signs of increased anxiety.

To examine whether other neurological abnormalities occur in *Csb*$^{m/m}$ mice following brain-specific inactivation of the conditional *Xpa* allele, we are currently expanding the behavioral analysis of *Csb*$^{m/m}$/*Xpa*$^{c/-}$/*CamKIICre* and littermate controls with other assays. For instance, in a pilot study with a limited number of animals, hind paw footprint ink tests (as previously performed with the non-conditional *Csb*$^{m/m}$*Xpa*$^{-/-}$ mouse; Chapter 2) did not reveal obvious abnormalities at adult age, which may point to the absence of disturbed gait and ataxia in *Csb*$^{m/m}$/*Xpa*$^{c/-}$/*CamKIICre* mice, and which could be explained by low CamKII-induced recombination levels in the cerebellum. Similarly, initial rotarod studies did not disclose any signs of motor coordination or balance problems up to an age of 6 months. Yet, we noticed that older (12-16 months) *Csb*$^{m/m}$/*Xpa*$^{c/-}$/*CamKIICre* animals failed to increase time spent on the bar in consecutive days of the test, whereas in the initial training session the retention time on the rotarod bar was similar to that of littermate controls, which could point to slightly impaired motor learning skills.

Brain pathology in the brain-specific conditional *Csb*$^{m/m}$/*Xpa*$^{c/-}$ mouse model

Interestingly, macroscopic analysis of the brain at 16 months revealed an atrophic cerebral cortex, the latter resulting from a loss of neurons and glial cells. Furthermore, the ventricular system was dilated. These observations together can be described as hydrocephalus ex vacuo. There were no obvious signs of infarction, whereas signs of gliosis and demyelination were evident. The hippocampal area was reduced in size due to loss of neuronal cells and showed disorganization of the various layers. The very thin and disorganized cortex might explain the seizures, observed in *Csb*$^{m/m}$/*Xpa*$^{c/-}$/*CamKIICre* animals. Notably, the cerebral atrophy was less pronounced in animals at 6 months and most probably absent in animals of 1 month old underlining the progressive nature of the neurodegenerative process. Sofar, we do not know what causes the observed priapism. It could be due to a) loss of vasomotor neurons; b) degeneration of peripheral and/or autonomous nerves; c) disorganization or loss of cerebral nuclei in the brain stem or hypothalamus that control sexual activity or blood pressure. Oxytocinergic neurons, originating in the paraventricular nucleus, that project to extra-hypothalamic brain areas (e.g., hippocampus, medulla oblongata and spinal cord) are known to control penile erection in male rats (Argiolas and Melis, 2005). Priapism may therefore point to neurological malfunction, or in other words continuous neurologic erectogenic stimulation due to loss of the medullary reticular formation neurons which normally inhibit male spinal sexual reflexes (Adams et al., 2001).

As anxiety-like behavior has been associated with defects in the hippocampal area, (Gray, 1982), it is tempting to speculate that the progressive deterioration of the hippocampus underlies the anxiety-like behavior of *Csb*$^{m/m}$/*Xpa*$^{c/-}$/*CamKIIα-Cre* mice. However, as mentioned previously, we need to do more behavioral tests and study the brain pathology at an earlier age to see if we can make such a connection.

The conditional *Csb*$^{m/m}$/*Xpa*$^{c/-}$ mouse model and human CS neuropathology

How do the neuropathological findings in the *Csb*$^{m/m}$/*Xpa*$^{c/-}$/*CamKIIα-Cre* mouse model relate to human CS? Importantly, dilated ventricles and cerebral atrophy are prominent neuropathological features of Cockayne Syndrome, observed in almost each CS patient analyzed (Nance and Berry, 1992; Ozdirim et al., 1996; Pasquier et al., 2006). In early case reports of CS, these observations were referred to as hydrocephalus ex vacuo (Brumback et al., 1978), but as the primary changes observed in the CS brain suggest that hydrocephalus is not likely to play a major pathogenetic role (Soffer et al., 1979), this term is no longer used.

Due to the very limited availability of histopathological reports on brains of CS patients (reviewed by (Soffer et al., 1979)), it is difficult to compare the microscopic pathology and draw conclusions on possible similarities between mouse an human CS. However, in the few detailed reports that are available on brain pathology in CS patients, gliosis, reduction in gray and white matter, demyelination, and disorganization as well as reduced amounts of neuronal cells in the hippocampus, were observed (Leech et al., 1985; Levinson et al., 1982; Soffer et al., 1979; Woody et al., 1991). As these features were also present in the cerebrum of the *Csb*$^{m/m}$/*Xpa*$^{c/-}$/*CamKIIα-Cre* mouse, this suggests that this mouse recapitulates the CS brain pathology to a large extent, and is therefore a good model to study the etiology of CS neurodegeneration. This also holds for abnormal neurological behavior such as seizures, observed in the *Csb*$^{m/m}$/*Xpa*$^{c/-}$/*CamKIIα-Cre* mouse, as well as in 10% of the CS patients (Nance and Berry, 1992). Obviously, more detailed analysis is required to elucidate the full spectrum of neurological deficits and the timeframe of onset.

It is also not yet clear whether in CS aforementioned neuropathological features (e.g. dilated ventricles and cerebral atrophy) are already present at birth, since most CS patients are usually not diagnosed before the age 1,5-2 years (for review see (Nance and Berry, 1992)). Analogously, we observed similar features in some (but not all) *Csb*$^{m/m}$/*Xpa*$^{c/-}$/*CamKIICre* animals at the age of 6 months; the cerebral atrophy, however, appeared pronounced. Although detailed pathology needs to be awaited, preliminary data suggests that at 1 month of age, no overt abnormalities are present.

The absence of microcephaly in *Csb*$^{m/m}$/*Xpa*$^{c/-}$/*CamKIICre* animals (a feature observed in many CS patients (Nance and Berry, 1992)) might be explained by the fact that the *CamKII* promoter driven Cre recombinase transgene becomes active at postnatal day 1 (P1), with highest levels at P5. Thus, the skull is able to develop normally until birth. Similarly, the fact that the *Xpa* gene is inactivated after birth may well explain the “delayed” general brain atrophy in these animals. To investigate the time scale of onset of the neurological phenotype, we are currently setting up a large cohort study.

It is tempting to speculate on the etiology of the observed neurological phenotype in both human CS and the *Csb*$^{m/m}$/*Xpa*$^{c/-}$/*CamKIICre* mouse model. In CS, pathology occurs simultaneously in a number of organs and tissues and it is not excluded that the neurological features are an indirect consequence of dysfunction of other parts of the body. In our conditional mouse model the repair defect is limited to the brain only. Thus, our findings using the conditional mutant support the idea that the neurodegeneration in CS is an organ-autonomous consequence of the repair defect. In view of the DNA repair function of the defective genes, unrepaired DNA damage must play an important role (Chapter 2), (Hasty et al., 2003; Mitchell et al., 2003). The brain is one of the most oxygen-demanding tissues and is therefore very sensitive to oxygen radical generation (Halliwell, 1985). Thus, it is likely that the brain is especially vulnerable to genotoxic insults, since the available repair pathways for a post-mitotic tissue are limited to mechanisms that do not depend on replication. Also, the repair of actively transcribed genes becomes most important, since these are the genes necessary for the brain to function properly. Interestingly, in *in vitro* differentiated neuronal cells both the transcribed as well as non-transcribed strands of active genes have been found to be repaired in contrast to the remainder of the genome. This unusual form of repair has been designated differentiation associated repair (DAR) (Nouspikel and Hanawalt, 2002). Genes involved in NER, or more specifically TC-NER, which can repair damage in the transcribed strands of active genes, might contribute substantially to repair in the brain. Thus, deficiency of these genes might result in the neurodegenerative phenotype observed in CS patients as well as in the *Csb*$^{m/m}$/*Xpa*$^{c/-}$/*CamKIICre* mouse.

In further support, neurodegeneration is observed in many syndromes with a defect in genome maintenance, e.g. Trichothiodystrophy, Xeroderma Pigmentosum (XP-DSC), Ataxia Telangiectasia (AT), spinocerebellar ataxia with axonal neuropathy (SCAN1) and ataxia-oculomotor apraxia (AOA1) (Boder and Sedgwick, 1958; Caldecott, 2004; El-Khamisy et al., 2005; Itoh et al., 1999; Kraemer et al., 1987; Shiloh, 1997). Additionally, oxidative stress has been implicated to play a role in other neurodegenerative disorders (Betarbet et al., 2002). Also, mouse models with defects in genome maintenance show neurological phenotypes. For example, mice deficient in Ku-70 and Ku-80 gene (involved in Non homologous end joining (NHEJ)) show aberrant neuronal apoptosis (Gu et al., 2000). Moreover, the complete inactivation of Ligase IV or XRCC4 (also involved in NHEJ) resulted in embryonic lethality most probably due to aberrant neuronal apoptosis (Barnes et al., 1998; Gao et al., 1998). Finally, multiple mouse models with genes that are defective in NER, show a neurological phenotype from mild to severe, like the *Csb*$^{m/m}$ (van der Horst et al., 1997), *Ercc1*$^{\Delta7/\Delta7}$, *Ercc1*$^{-/-}$ (Weeda et al., 1997), (Niedernhofer et al., unpublished results), *Csb*$^{m/m}$/*Xpa*$^{-/-}$ (Murai et al., 2001), (Chapter 2) mouse models. These findings *in toto* underscore the importance of DNA repair for normal functioning of the neurological system and highlight the significance of spontaneous DNA damage.

In conclusion, we have shown that induction of the *Xpa* knock-out status (and therefore complete inactivation of NER) in the brain of *Csb*$^{m/m}$ animals provides a mouse model that recapitulates most of the neuropathological features of CS. Furthermore, the conditional *Csb*$^{m/m}$/*Xpa*$^{-/-}$ mutant now allows in depth behavioral, physiological, and transcriptome profiling studies, needed to further unravel the etiology of CS.

Materials and Methods

Generation of a mouse conditional *Xpa* targeting construct

A genomic clone containing 10 kb of the 129ola mouse *Xpa* locus (pMMXP3-6#13; (de Vries et al., 1995)), was used to re-clone an approximately 10 kb size BamHI fragment, containing exons 3 to 6, into the psp72 vector. Following XbaI digestion, part of exon 4 and intron 4 was replaced by a cassette containing the mouse *Xpa* cDNA (ensuing in frame fusion of genomic and cDNA sequences), including the natural 3' UTR and polyadenylation signal, followed by a *PGK* promoter-driven Hygromycin selectable marker and a LoxP site respectively. Next, the SmaI site downstream the LoxP site was used to introduce a cassette containing a splice acceptor sequence (SA), an ochre stopcodon multiple reading frame insertion (Murfi) linker, a ribosomal entry site (IRES), and a LacZ/GFP fusion reporter gene (as a blunted SalI fragment). The SmaI site in intron 3 was used to insert a blunted XhoI-SalI loxP fragment from pGEM30 (kindly provided by Dr. W. Gu, University of Cologne). This targeting construct, which was designated pIP-Xpa-con, contains homologous arms of 4kb (5' end) and 5kb (3' end), respectively.

ES cell culture and transfection

The 129ola-derived ES cell line IB10 was electroporated with NotI linearized pIP-Xpa-con DNA and cultured in gelatin-coated dishes as described before (van der Horst et al., 1997). Hygromycin (Roche, 843555) was added 24 hr after electroporation to a final concentration of 100 µg/ml. Cells were maintained under selection for 7-8 days, after which clones were isolated and expanded in 24-well plates. Genomic DNA from individual Hygromycin-resistant clones was digested with EcoRI and analyzed by Southern blotting using a 500 bp DraI fragment (“intron 5/exon 6” probe; obtained from a 7.5 kb PCR fragment spanning exon 5 and 6). EcoRI digested DNA from targeted ES clones was subsequently screened with the hygro (cDNA) probe to confirm proper homologous recombination at the 5' end of the targeting construct.

For the generation of $Xpa^{c/-}$ ES cells, we followed the same procedure as described above, except that $Xpa^{-/-}$ ES cells (de Waard et al., 2003) were used.

To test the functionality of the loxP sites, $Xpa^{c/+}$ ES cells were electroporated with a purCre plasmid (kindly provided by Dr. M. Jaegle, Erasmus MC) and cultured on gelatin dishes as described. Puromycin (Sigma, P7255) was added 24 hr after electroporation to a final concentration of 100 µg/ml. Cells were maintained under selection for 3 days. Genomic DNA from individual puromycin-resistant clones was digested with EcoRV and analyzed by Southern blotting using a 500 bp PCR fragment of the LacZ gene.

Generation of mutant mice

Properly targeted IB10 ES clones were karyotyped and cells from two independent clones (selected for the presence of 40 chromosomes) were injected into 3.5-day-old C57BL/6J blastocysts. Male chimeric mice were mated with C57BL/6J females to obtain heterozygote offspring. Heterozygous males and females were bred to $Xpa^{+/-}$ as well as $Csb^{m/+}$ animals to ultimately obtain $Xpa^{c/-}$, $Xpa^{c/+}$ and $Csb^{m/m}/Xpa^{c/-}$ animals. Genotyping was initially performed by

Southern blot analysis of genomic DNA obtained from tail biopsies of 8-10-day-old born pups. A description of PCR-based genotyping methods is given below.

Xpa$^{c/-}$ and *Csb*$^{m/m}$/*Xpa*$^{c/-}$ animals were also interbred with *Cag-Cre* (Sakai and Miyazaki, 1997) and *CamKII-Cre* (L7ag#13) (Dragatsis and Zeitlin, 2000) Cre-recombinase transgenic mice, which were kindly provided by A. de Wit (ErasmusMC) and S. Zeitlin (Columbia University), respectively.

Primary mouse embryonic fibroblasts from the various mouse single and double mutant mouse models (three independent lines per genotype) were isolated from day 13.5 embryos and cultured as described before (Ng et al., 2002).

Mice and cells were genotyped by PCR for the wild type and (conditional) mutant *Xpa* or *Csb* alleles using a primer mix that (per genotype) amplifies both the wild type and targeted alleles in a single reaction (Berg et al., 2000; de Vries et al., 1995). The presence or absence of the conditional *Xpa* allele was detected by PCR using primers XPAFex3 (5'-TTT GAT CTG CCA ACG TGT G-3') and XPARex4 (5'-GCT TCG CTT CTG TCT TGG T-3'). The presence or absence of the *Cre* transgene was detected by PCR using primers 5'-GCA CGT TCA CCG GCA TCA AC-3' and 5'-CGA TGC AAC GAG TGA TGA GGT TC-3' Both products were amplified with the same PCR program: 5 min. 93°C, 1 min. 93°C, 1 min. 58°C , 2.5 min. 72°C (35 cycles of the latter three steps), 5 min. 72°C.

As required by Dutch law, the generation of genetically modified mice was approved by the Dutch Ministry of Agriculture, Nature and Food Quality.

LacZ staining of embryos and cells

Cells or embryos were fixed for 30 minutes at 4 °C in a buffer containing 1% paraformaldehyde, and subsequently washed 3 x 15 minutes with PBS/0.01% NP40. Cells or embryos were stained overnight at 37°C in dark in a staining solution containing 3.1 mM $K_3Fe(CN)_6$, 3.1 mM $K_4Fe(CN)_6$, 0.15 M NaCl, 1 mM $MgCl_2$ and 1 mg/ml X-gal (Roche Applied Sciences, USA, IN). For tissues, the same procedure was used, except that the fixation time was extended to 3 hours.

For LacZ staining of the brain, animals were perfused with a 1% paraformaldehyde/ 0.5% glutaraldehyde solution. The isolated brains were fixed for another hour at 4 °C and washed overnight in a 10% sucrose/0.1 M phosphate buffer solution at 4 °C. Then, brains were embedded in 11% gelatin/10% sucrose. Sections (40 µm) were stained for lacZ as described above, and counterstained in 1% neutral red.

DNA repair assays

Sparsely seeded cultures at a density of 1000 spontaneously immortalized MEFs on a 6 cm dish were exposed to different doses of UV-C (254 nm, Philips TUV lamp). The cells were allowed to grow for another 7 days after which the resulting clones were fixed, stained and counted. For each independent cell line, the amount of surviving clones at each dose of UV, 3 dishes per dose, was calculated as the percentage of clones on the plate without UV.

Behavioral assays

For the open field test, animals were placed for 30 min in a square (26cm x 26cm x 26cm) open field box, equipped with photobeam sensors (TruScan E63 10-12, Coulbourn Instruments), and attached to a computer to record the following ambulatory parameters: total distance, center distance, total move time, center time and corner time. Each test session was 30 minutes long, and data were collected in 5 minute intervals. The anxiety ratio was calculated by dividing center distance by total distance. Significance was determined by Mann-Whitney-U test for two independent samples. All animal studies were approved by an independent Animal Ethical Committee (Dutch equivalent of the IACUC).

Pathology

Animals were sacrificed by O_2/CO 30 minutes after injection with BrdU (40 mg/kg body weight) and perfused with 20 ml of Phosphate Buffered Saline (PBS), followed by 20 ml of 4% phosphate buffered formalin at room temperature. Internal organs were isolated and weighed, paraffin-embedded, sectioned at 4 μm and stained with haematoxylin/eosin solution for histopathological analysis. For the isolation of the brain, skin was removed from the head and the skull was incubated overnight in 4% phosphate buffered formalin. After this post-fixation step, brains were removed form the skull, weighed, paraffin-embedded, sectioned at 4 μm and stained with haematoxylin/eosin solution for histopathological analysis. Serial sections of the brains were made with a 100 μm interval.

Acknowledgements

This research was supported by the Netherlands Organization for Scientific Research (NWO) through the foundation of the Research Institute Diseases of the Elderly as well as grants from SenterNovem IOP-Genomics (IGE03009), European Community (LSHC-CT-2005-512113), NIH (1PO1 AG17242-02) and NIEHS (1UO1 ES011044).

Chapter 4

Appendix

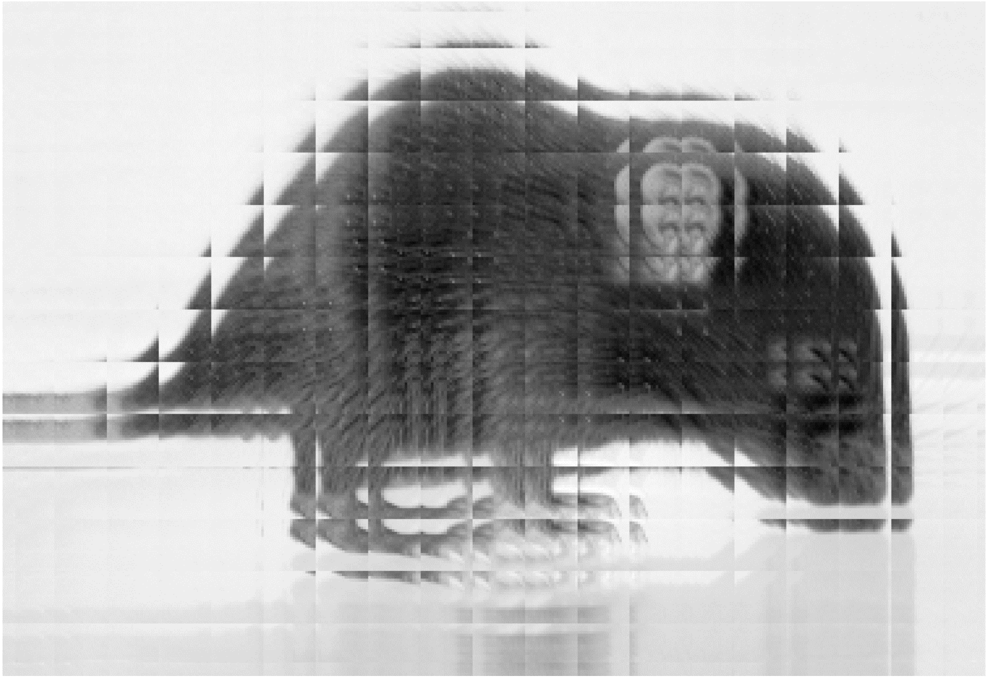

APPENDIX CHAPTER 4

Tamoxifen administration causes lethality in $Csb^{m/m}Xpa^{c/-}$ mice

Ingrid van der Pluijm, Renata Brandt, Marcel Vermeij, Carel Meijers, Jan H.J. Hoeijmakers and Gijsbertus T.J. van der Horst.

As discussed in Chapter 4, we attempted to induce the *Xpa* knock-out status in *Csb*$^{m/m}$ mice over time by crossing in an ubiquitously expressed *Cre-ER*^{T} transgene that can be activated by tamoxifen (Vooijs et al., 2001). This appendix describes the results in more detail.

Results

We first tested whether tamoxifen resulted in inactivation of the conditional *Xpa* allele in *Xpa*$^{c/-}$*/Cre-ER*^{T} animals. On the basis of the available literature (Kuhbandner et al., 2000), we first injected animals intraperitoneally (i.p.) with 1 or 2 mg tamoxifen (per 25 g). Although this dose has been reported to work efficiently, we did not observe significant recombination of the *Xpa* allele in liver, kidney, spleen, heart and lung (data not shown). As higher doses of tamoxifen administration via i.p. injection can have deleterious effects (LD50 dose 200 mg/kg = 5 mg for a mouse of 25 g), we next tried oral administration of tamoxifen by gavage (p.o.) (Seibler et al., 2003). We compared 2 mg i.p. versus 5 mg p.o. for two times 5 days, with a rest period of two days in between. Since the LD50 dose for oral administration of tamoxifen in mice is 5 g/kg (125 mg for a mouse of 25g) (Furr and Jordan, 1984), this method should avoid toxic side-effects. We checked for recombination of the conditional allele in liver, kidney, spleen, heart and lung. Oral administration did give better recombination of the conditional *Xpa* allele, although the efficiency (estimated 15-30%) was not very high (Fig. 1A).

To investigate whether inactivation of the *Xpa* allele in approximately one third of the cells of *Csb*$^{m/m}$*/Xpa*$^{c/-}$ mice would provoke additional pathology, we next crossed *Csb*$^{m/m}$*/Xpa*$^{c/-}$ mice with *Cre-ER*^{T} transgenic animals and orally administered tamoxifen (2 x 5 days, 5 mg/injection, as indicated above) to 18-week old *Csb*$^{m/m}$*/Xpa*$^{c/-}$*/Cre-ER*^{T} mice (n=14) and *Csb*$^{m/m}$*/Xpa*$^{c/-}$ animals (n=6), the latter serving as a control for the effect of tamoxifen. As negative controls, we took along age-matched *Csb*$^{m/m}$*/Xpa*$^{c/-}$ animals (n=12) that were not given tamoxifen. While untreated *Csb*$^{m/m}$*/Xpa*$^{c/-}$ animals were still gaining body weight, we noticed that tamoxifen-treated *Csb*$^{m/m}$*/Xpa*$^{c/-}$ and *Csb*$^{m/m}$*/Xpa*$^{c/-}$*/Cre-ER*^{T} mice lost weight, the effect being most severe in *Csb*$^{m/m}$*/Xpa*$^{c/-}$*/Cre-ER*^{T} animals (Fig. 1B). Moreover, 13 out of 14 tamoxifen-treated *Csb*$^{m/m}$*/Xpa*$^{c/-}$*/Cre-ER*^{T} animals died two weeks after the first tamoxifen treatment (Fig. 1C**)**, while tamoxifen treated *Csb*$^{m/m}$*/Xpa*$^{c/-}$ animals remained alive. Histopathological examination of the tamoxifen-treated *Csb*$^{m/m}$*/Xpa*$^{c/-}$*/Cre-ER*^{T} animals revealed increased apoptosis in the gastro-intestinal tract, along with atypical hyperproliferative crypts reminiscent of carcinoma in situ (Fig. 1D), liver toxicity (mild hepatitis), bone marrow depression and an atrophic skin (data not shown). BrdU and TUNEL staining of these tissues showed that proliferation was reduced to a large extent, whereas the amount of apoptotic cells was increased dramatically (data not shown). Although in the tamoxifen-treated *Csb*$^{m/m}$*/Xpa*$^{c/-}$ animals the same tissues were affected, the pathological findings were by far not as severe as in the tamoxifen-treated *Csb*$^{m/m}$*/Xpa*$^{c/-}$*/Cre-ER*^{T} animals, while proliferation was only slightly reduced. From these data we conclude that *Csb*$^{m/m}$ animals are sensitive to the toxic effects of tamoxifen, and that inactivation of *Xpa* by Cre recombinase further boosts this sensitivity.

In parallel, we already had initiated breedings to obtain *Csb*$^{m/m}$*/Xpa*$^{c/-}$ mice for time specific inactivation of *Xpa* in the liver. To this end, we used *αAT-Cre-ER*^{T} transgenic mice that express the Cre-recombinase from the human hepatocyte specific α1-antitrypsin promoter, and allow

excision of floxed genes at an average yield of 40-50% (Imai et al., 2000). $Csb^{m/m}/Xpa^{c/-}/\alpha AT\text{-}Cre\text{-}ER^{T}$ (conditional liver-specific $Csb^{m/m}/Xpa^{-/-}$), $Csb^{+/m}/Xpa^{c/+}/\alpha AT\text{-}Cre\text{-}ER^{T}$ (wild type), $Csb^{m/m}/Xpa^{c/+}/\alpha AT\text{-}Cre\text{-}ER^{T}$ ($Csb^{m/m}$), $Csb^{+/m}/Xpa^{c/-}/\alpha AT\text{-}Cre\text{-}ER^{T}$ (conditional liver-specific $Xpa^{-/-}$) and $Csb^{+/m}/Xpa^{-/-}/\alpha AT\text{-}Cre\text{-}ER^{T}$ ($Xpa^{-/-}$) animals (n=4 per group, age 36 weeks) were treated with tamoxifen (2 x 5 days, 5 mg p.o., as indicated above) and body weight was recorded at 7 and 14 days after the first tamoxifen treatment. Whereas tamoxifen treatment had little effect on the body weight of wt ($Csb^{+/m}/Xpa^{c/+}/\alpha AT\text{-}Cre\text{-}ER^{T}$) animals, all repair deficient mice substantially lost weight after the first series of administrations, which further increased when the treatment was repeated (Fig. 1E). Classical (e.g. non-conditional) $Xpa^{-/-}$ mice are clearly more sensitive than $Csb^{m/m}$ animals, which suggests that both global NER and transcription-coupled repair defects must contribute to the weight loss. Moreover, liver-specific $Xpa^{-/-}$ mice lose less weight than non-conditonal $Xpa^{-/-}$ animals, which suggests that in addition to the liver, other tissues (e.g. the intestine) could be involved. Weight loss in $Csb^{m/m}$ animals in which *Xpa* was inactivated in the liver ($Csb^{m/m}/Xpa^{c/-}/\alpha AT\text{-}Cre\text{-}ER^{T}$) was almost two-fold stronger than in the single mutant $Csb^{m/m}$ ($Csb^{m/m}/Xpa^{+/c}/\alpha AT\text{-}Cre\text{-}ER^{T}$) and conditional $Xpa^{-/-}$ ($Csb^{+/m}/Xpa^{c/-}/\alpha AT\text{-}Cre\text{-}ER^{T}$) animals, which further points to additive effects of the GG-NER and TCR defects in tamoxifen induced weight loss. We are currently performing histopathological analysis of the liver and intestine.

Taken together, these data demonstrate that GG-NER and TCR defects render the liver and other tissues sensitive to tamoxifen. Given the repair defect, these cytotoxic effects are likely to originate from unrepaired DNA damage.

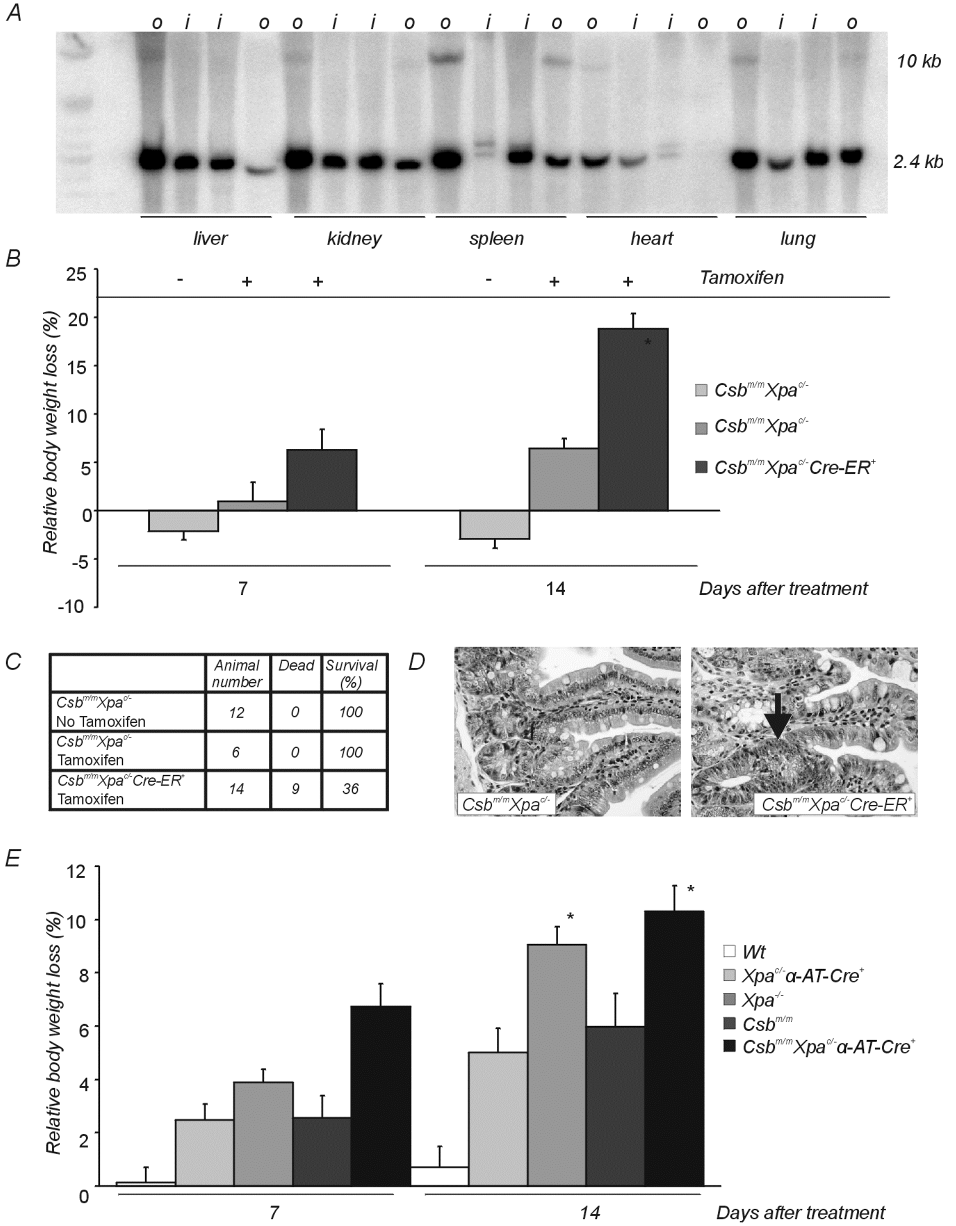

	Animal number	Dead	Survival (%)
$Csb^{m/m}Xpa^{c/-}$ No Tamoxifen	12	0	100
$Csb^{m/m}Xpa^{c/-}$ Tamoxifen	6	0	100
$Csb^{m/m}Xpa^{c/-}Cre\text{-}ER^{+}$ Tamoxifen	14	9	36

Figure 1. Tamoxifen-induced Cre recombination of the conditional Xpa conditional allele in the mouse. *A) Southern blot analysis of DNA from different tissues of $Xpa^{c/+}/Cre\text{-}ER^{T}$ animals that were given tamoxifen via i.p. injection (i) or oral gavage (o) to compare recombination efficiency. Size-separated EcoRV digests were hybridized with a LacZ probe. Recombination of the Xpa allele causes a conversion of a 2.4 kb EcoRV fragment into a 10 kb EcoRI fragment. B) Relative body weight of $Csb^{m/m}/Xpa^{c/-}$ and $Csb^{m/m}/Xpa^{c/-}/Cre\text{-}ER^{T}$ (n=14 at 7 days, n=9 at 14 days) animals after one and two weeks in presence (+) or absence (-) of tamoxifen treatment (*: $p<0.01$). C) Survival of tamoxifen treated $Csb^{m/m}/Xpa^{c/-}$ and $Csb^{m/m}/Xpa^{c/-}/Cre\text{-}ER^{T}$ animals. D) Representative pictures of HE stained duodenum of tamoxifen treated $Csb^{m/m}/Xpa^{c/-}$ and $Csb^{m/m}/Xpa^{c/-}/Cre\text{-}ER^{T}$ animals. The arrow indicates atypical hyperplasia reminiscent of carcinoma in situ. E) Relative body weight loss of $Csb^{+/m}/Xpa^{c/+}/\alpha AT\text{-}Cre\text{-}ER^{T}$ (wild type), $Csb^{+/m}/Xpa^{c/-}/\alpha AT\text{-}Cre\text{-}ER^{T}$ (conditional liver-specific Xpa-/-), $Csb^{+/m}/Xpa^{-/-}/\alpha AT\text{-}Cre\text{-}ER^{T}$ ($Xpa^{-/-}$), $Csb^{m/m}/Xpa^{c/+}/\alpha AT\text{-}Cre\text{-}ER^{T}$ ($Csb^{m/m}$), and $Csb^{m/m}/Xpa^{c/-}/\alpha AT\text{-}Cre\text{-}ER^{T}$ (conditional liver-specific $Csb^{m/m}/Xpa^{-/-}$) animals (n=4 per group) after one and two weeks of tamoxifen administration (*: $p<0.05$).*

Discussion

Timed recombination of floxed genes using a tamoxifen-activated Cre-recombinase has been frequently used as a method to generate mutant mice in a time dependent manner and deleterious side-effects have not been reported in literature (Seibler et al., 2003). Nevertheless, attempts to generate *Csb*$^{m/m}$/*Xpa*$^{-/-}$ mice with this approach remained unsuccessful. Tamoxifen treated *Csb*$^{m/m}$/*Xpa*$^{c/-}$/*Cre-ER*^{T} mice displayed severe weight loss and ultimately died from severe intestinal pathology, consisting of massive apoptosis and reduced proliferation. Surprisingly we also observed atypical hyperplasia, reminiscent of intestinal carcinoma in situ in these animals, which is a rare finding in mice, especially when one considers that it must have developed within two weeks. Tamoxifen-treated *Csb*$^{m/m}$*Xpa*$^{c/-}$ mice also displayed weight loss and reduced proliferation of the intestinal epithelium, but apparently the effect was not severe enough to cause lethality. The latter also applies to tamoxifen treated non-conditional *Xpa*$^{-/-}$ mice and liver specific *Xpa*$^{c/-}$ animals. Taken together, these data indicate that a combined GG-NER/TC-NER defect (as in *Xpa*$^{-/-}$ mice), as well as a TCR defect (as in *Csb*$^{m/m}$ animals) causes tamoxifen sensitivity in an additive manner (as shown by NER/TCR-deficient *Csb*$^{m/m}$/*Xpa*$^{c/-}$/*Cre-ER*^{T} and *Csb*$^{m/m}$/*Xpa*$^{c/-}$/*αAT-Cre-ER*^{T} mice). Although we can not yet exclude that the observed toxic effects are originating from sunflower seed oil (used to dissolve tamoxifen, and containing polyunsaturated fatty acids that after lipid peroxidation may cause oxidative DNA damage), our data point to tamoxifen induced DNA lesions as the underlying cause.

Tamoxifen and its derivative metabolites can damage DNA, which has been shown both in vitro and in vivo (McLuckie et al., 2005; McLuckie et al., 2002; Mizutani et al., 2004; Shibutani et al., 2000a). Also, NER has been shown to be involved in the removal of such tamoxifen-induced DNA adducts (McLuckie et al., 2005; Shibutani et al., 2000b). Moreover, tamoxifen is a known carcinogen, as shown by (i) the increased occurrence of endometrium cancer in estrogen receptor positive breast cancer patients treated with this drug, and (ii) the induction of liver carcinomas in rats that are chronically exposed to high doses tamoxifen (reviewed in (White, 1999)). However, since tamoxifen is not carcinogenic in adult mice, even after 1-2 years administration at a dose of 40 mg/kg, or when given together with tumor promoting agents (White, 1999), and since our pilot study with *Xpa*$^{c/-}$ did not point to severe side-effects, this approach could have worked. On the other hand, the *Csb*$^{m/m}$/*Xpa*$^{c/-}$/*Cre-ER*^{T} and *Csb*$^{m/m}$/*Xpa*$^{c/-}$/*αAT-Cre-ER*^{T} mouse models may well serve to further delineate the mechanism of cytotoxic and genotoxic effects of tamoxifen and its derivatives.

Evidently, other approaches should be taken to establish spatiotemporal inactivation of the conditional *Xpa* allele in the *Csb*$^{m/m}$/*Xpa*$^{c/-}$ mouse model. For example, one could use transgenic Cre-recombinase mice that express the enzyme from a tetracyclin-inducible (Tet-On system) promoter, or in which the Cre-recombinase transgene is kept silent in the presence of the antibiotic (Tet-Off system), although one might have a toxicity problem there too. For a comprehensive review on methods of conditional gene silencing, see (Porter, 1998). Alternatively, to obtain a *Csb*$^{m/m}$/*Xpa*$^{c/-}$ mouse model that survives weaning, one could use the Balancer Cre-recombinase mouse (Betz et al., 1996), which would lead to chimaeric double mutant animal in which the faith of *Csb*$^{m/m}$/*Xpa*$^{-/-}$ cells (and thus the onset and progress of pathology) in a *Csb*$^{m/m}$ tissue can be monitored.

Materials and Methods

Tamoxifen treatment

Tamoxifen (Sigma) was dissolved in 100% ethanol and dispersed in sunflower seed oil (Sigma) to a final concentration of 1, 2 or 5 mg/100 µl. Mice were administered tamoxifen through i.p. injection (1 or 2 mg tamoxifen per day for 5 days), or gavage (2 or 5 mg per day for 5 days) (Kuhbandner et al., 2000; Seibler et al., 2003). This treatment was repeated after two days.

Cre mice

Cre-ER^T and *αAT-Cre-ER*^{T} mice were kindly provided by J. Jonkers and P. Chambon, respectively (Imai et al., 2000) (Vooijs et al., 2001).

Pathology

Animals were sacrificed 45 min. after injection with BrdU at an amount of 50 µg per gram bodyweight. Internal organs were isolated and weighed, then fixed in 10% phosphate-buffered formalin, paraffin-embedded, sectioned at 5 µm and stained with haematoxylin/eosin solution for histopathological analysis. Paraffin sections (5 µm) were dewaxed and rehydrated. Antigen retrieval used a 0.01M sodium citrate buffer with treatment for 1 x 7 and 2 x 3 minutes in a 700-W microwave. Sections were washed in PBS for 2 minutes. Endogenous peroxidase activity was blocked in PBS: 30%H_2O_2: 12.5%sodiumazide (100:2:1) for 30 minutes. Sections were washed in PBS for 2 minutes, then washed in a 1xPBS, 0.5% protifar, 0.15% glycine (PBS+) buffer 2 x 2 minutes. For detection of BrdU, prior to the first antibody, sections were covered with 0.1M HCl for 60 minutes at 37 ^oC with humidity and rinsed with PBS. Sections were then incubated with the primary antibody against BrdU (Bu20a, mouse, DAKO, dilution 1:100) in PBS+ overnight at 4 ^oC. Sections were washed in PBS+ 3x 5 minutes before incubation for 1 hour at room temperature in rat-anti-mouse Immunoglobulin antibody (1:1000) coupled to horseradish peroxidase (DAKO). Sections were washed 3 X 5 minutes in PBS+ and 2 minutes in PBS. Color was developed for 8 minutes in 3,3'-diaminobenzidine solution (DAKO Liquid Dab substrate-chromogen system), all according to manufacturers' instructions. Sections were counterstained in hematoxylin before dehydratation and mounting. All histology images were acquired on an Olympus (London, United Kingdom) BX40 with a ccd camera at x40 objective magnification. Apoptotic cells were detected using a TdT-mediated dUTP Nick-End Labeling (TUNEL) assay as described by the manufacturer (Apoptag Plus Peroxidase *In Situ* Apoptosis Detection Kit, Chemicon).

Chapter 5

CHAPTER 5

Mouse models for Cockayne Syndrome: towards an intervention strategy

Ingrid van der Pluijm, Renata M.C. Brandt, Sander Barnhoorn, Shanoe Mahabir, Mark Jochims, Norbert Looije, Alia, Claude Backendorf, Harry van Steeg, Jan H.J. Hoeijmakers, and Gijsbertus T.J. van der Horst

Abstract

Cockayne Syndrome is a human progeroid disorder, caused by mutations in the CSB or CSA gene, leading to a defect in transcription-coupled DNA excision repair. In addition to a sun-sensitive skin, patients display early cessation of growth and progressive neurodegeneration, followed by death at young age. No therapy is available. Mouse models for CS display mild CS-like pathology if the Csb gene is mutated ($Csb^{m/m}$*), which is dramatically aggravated by additional inactivation of the Xpa repair gene (*$Csb^{m/m}/Xpa^{-/-}$*). Both models have pointed to oxidative DNA damage (originating from reactive oxygen byproducts of metabolism) as important underlying cause of the observed progeria. In the present study, the frequency of *$Csb^{m/m}/Xpa^{-/-}$* pups surviving birth stress and their life span was utilized to explore the use of radical scavengers as potential preventive agents that alleviate CS pathology. Intervention studies, in which pregnant/lactating females were given high concentrations of D-mannitol or L-proline, revealed a significant increase in the percentage of surviving *$Csb^{m/m}/Xpa^{-/-}$* offspring, while D-mannitol also significantly extended their lifespan. Moreover, we provide evidence that differences in food composition can influence the frequency and life span of *$Csb^{m/m}/Xpa^{-/-}$* pups, as well as accelerated photoreceptor-loss observed in *$Csb^{m/m}$* mice. Taken together, these data provide a basis for antioxidant-based interventions in CS and further strengthen the idea that oxidative DNA damage is the underlying cause of CS, including its aging-associated pathology. The *$Csb^{m/m}/Xpa^{-/-}$* model may prove suited for assessing the protective effect of food components for aging-associated pathology in general.*

Introduction

Many theories exist concerning the cause of aging, a complex and multifactorial process. One prevailing hypothesis is the "Free radical Theory of Aging" (Harman, 1956), which proposes that free radicals continuously damage biomolecules, thereby setting off aging, as well as aging-associated degenerative diseases (reviewed by (Balaban et al., 2005)). Well-known free radicals are reactive oxygen species (ROS; e.g. singlet oxygen, hydroxyl radicals, superoxide anions, nitric oxide, hydrogen peroxide) that are byproducts of cellular metabolism. ROS can damage biomolecules like lipids, proteins and DNA, which all may contribute to aging. Also, increased resistance to oxidative stress can extend the life-span of *C. elegans*, *Drosophila*, and rodent mutants (Melov et al., 2000; Orr and Sohal, 1994; Schriner et al., 2005), while hypersensitivity to oxygen, significantly reduces the life-span, as shown for nematodes (Ishii et al., 1998). There are many clues pointing to the involvement of DNA damage in the aging process. For example, DNA damage levels (i.e. 8-OH-G) have been found to increase with age (Hamilton et al., 2001), reviewed in (Lombard et al., 2005) and DNA damage triggers cellular senescence (Campisi, 2001). Moreover, cancer increases with age and is found to be due to acquired mutations in the genome, highlighting genome maintenance and the importance of DNA damage.

The relation between DNA damage and aging is further underscored by the fact that many human inherited syndromes with defective DNA repair display progeroid symptoms (Kipling et al., 2004; Martin, 2005; Puzianowska-Kuznicka and Kuznicki, 2005). One such condition is Cockayne Syndrome (CS), a rare autosomal recessive disorder in which mutations in the *CSA* or *CSB* gene eliminate the transcription-coupled repair (TC-) sub-pathway of nucleotide excision repair (NER). NER is a complex mechanism that removes helix-distorting DNA damages that are induced by UV and numerous chemicals. This repair machinery consists of two sub-pathways: global genome NER (GG-NER) and TC-NER. GG-NER removes DNA lesions from the entire genome, whereas TC-NER removes lesions from the transcribed strand of active genes that are actually arresting transcription (Hanawalt, 2002) and is believed to also apply to transcription-blocking oxidative DNA lesions (de Waard et al., 2003; Spivak and Hanawalt, 2006). As a consequence of the repair defect, CS patients have a sun-sensitive skin resulting from enhanced apoptosis, triggered by stalled transcription due to unrepaired UV-induced DNA damage. In addition, CS patients experience growth retardation, notably in the first or second year of life, cachexia, dwarfism, and develop skeletal abnormalities (e.g. a bird-like face, kyphosis, and in older patients, osteoporosis), retarded psychomotor development, microcephaly, and progressive neurological features (e.g. disturbed gait, ataxia, sensorineuronal hearing loss, pigmentary retinopathy). Patients die at an average age of 12 years (Lehmann, 2003; Nance and Berry, 1992; Rapin et al., 2000). As CS patients display some, but not all features of accelerated aging, this disorder is considered a "segmental progeroid syndrome" (Martin, 2005). Whereas the UV-sensitive skin is readily explained by the TC-NER defect of UV-induced lesions, the progeroid symptoms are difficult to explain with this scenario. Therefore unrepaired endogenous DNA damage could be the underlying cause of these symptoms.

Aiming at understanding the etiology of CS, we have previously generated transgenic mice with a premature stopcodon in the *Csb* gene, as also found in a patient (CS1AN), belonging to CS complementation group B (van der Horst et al., 1997). Although the *Csb*$^{m/m}$ mouse model reliably mimics the repair defect and UV-sensitive phenotype of the patient, animals show only mild growth retardation and neurological abnormalities, which is accompanied by age-related retinal degeneration due to photoreceptor loss by enhanced apoptosis (van der Horst et al., 1997) (Chapter 3). Interestingly, a mouse genetic approach in which TCR-defective *Csb*$^{m/m}$ mice were crossed with completely NER-deficient *Xpa*$^{-/-}$ animals (de Vries et al., 1995), yielded a double mutant model that surprisingly well phenocopies human CS, including its age-related pathology (Chapter 2). Although devoid of any aberrant embryonic developmental phenotype, *Csb*$^{m/m}$/*Xpa*$^{-/-}$ pups display severe postnatal growth retardation, impaired psychomotor development, ataxia, progressive cachexia, and kyphosis. Loss of retinal photoreceptors is also further accelerated, as compared to *Csb*$^{m/m}$ animals (Chapter 2). Moreover, most *Csb*$^{m/m}$/*Xpa*$^{-/-}$ newborns die during or shortly after birth, whereas animals that survive birth stress do not get older than three weeks.

The premature aging phenotype of *Csb*$^{m/m}$/*Xpa*$^{-/-}$ pups is further underlined by the marked resemblance of their liver transcriptome to that of old, rather than young wild type mice (Chapter 2). Importantly, this genomic approach uncovered a systemic response, comprising attenuation of the GH/IGF-1 somatotroph axis, down-regulation of oxidative metabolism, and up-regulation of antioxidant defense (the latter was not observed in aging mice), together with hypoglycemia and hepatic glycogen and fat accumulation. A comparable response is, to a large extent, also seen in pro-oxidant treated wild type animals (Chapter 2), in NER/crosslink repair-deficient *Ercc1*$^{-/-}$ mice (Niedernhofer et al., pending revision), and – paradoxically – also in long-lived Ames and Snell dwarf mice, characterized by an attenuated GH/IGF-1 axis (Andersen et al., 1995; Brown-Borg et al., 1999; Brown-Borg and Rakoczy, 2000; Li et al., 1990). Taken together, these observations prompted us to hypothesize that an enhanced damage load in the genome, including in the transcribed strand of active genes, triggers an adaptive response. This response encompasses reduction of metabolic activity through down-regulation of the somatotrophic axis, and improvement of antioxidant defense and aims at slowing down aging-related pathology and postponing death by reducing ROS, and accordingly DNA damage levels (Chapter 2). Although *Csb*$^{m/m}$/*Xpa*$^{-/-}$ animals (and likely CS patients) initiate this response constitutively at very early age, with early cessation of growth (dwarfism) as a consequence, loss of tissue homeostasis via enhanced apoptosis or cellular senescence eventually can not be prevented, as illustrated by the enhanced photoreceptor loss. In this scenario and in agreement with the segmental character of aging in CS, the spectrum and time of onset of pathological events will largely depend on how individual tissues and organs cope with the unrepaired DNA damage and on their individual regeneration potential.

Currently, the prognosis for CS patients is poor and there is no treatment for the disease, other than avoidance of sun exposure (to prevent sunburn) and, if possible, treatment of the individual symptoms as they present themselves. The *Csb*$^{m/m}$/*Xpa*$^{-/-}$ mouse data (Chapter 2), together with the observation that exposure to low doses of ionizing radiation enhances photoreceptor loss in the *Csb*$^{m/m}$ mouse retina (Chapter 3), point to the involvement of endogenous (ROS-induced) DNA damage in the etiology of CS. To test the hypothesis that the

Csb$^{m/m}$/*Xpa*$^{-/-}$ phenotype is caused by the accumulation of unrepaired endogenous damage, and to investigate whether lowering the intracellular level of ROS and other harmful reactive byproducts of metabolism can attenuate the premature onset of age-related features in this mouse model, we set out to explore the possibilities of antioxidant-based intervention. Ultimately, this approach is expected to result in the identification of components that may help to alleviate the symptoms in CS patients. The current manuscript describes the effects of two compounds with radical scavenger properties, as well as the effect of different brands of mouse chow on the phenotype of *Csb*$^{m/m}$/*Xpa*$^{-/-}$ mice. In addition, we investigated whether photoreceptor-loss in the *Csb*$^{m/m}$ or *Csb*$^{m/m}$/*Xpa*$^{-/-}$ retina could serve as a parameter for intervention studies.

Results

Principle of the intervention study

As a basis for radical-scavenger intervention studies with the *Csb*$^{m/m}$/*Xpa*$^{-/-}$ mouse model, we used a breeding protocol, comprising matings between *Csb*$^{m/-}$/*Xpa*$^{-/-}$ and *Csb*$^{m/m}$/*Xpa*$^{+/-}$ animals to always obtain *Csb*$^{m/m}$/*Xpa*$^{-/-}$ pups at a maximum (Mendelian) frequency of 25%. In this protocol, *Csb*$^{+/m}$/*Xpa*$^{+/-}$ mice served as “wild type” littermate controls, as animals were devoid of any overt phenotype. As biological readouts for the effect of antioxidants we used “frequency” and “survival” (see also Experimental Procedures section). Frequency was chosen because *Csb*$^{m/m}$/*Xpa*$^{-/-}$ newborns (in contrast to wild type or single mutant littermates) show considerable lethality during or shortly after birth (60-80% loss of pups) (Chapter 2). Survival was measured because *Csb*$^{m/m}$/*Xpa*$^{-/-}$ pups that survive birth usually die in their 3rd week of life (Chapter 2). Any positive effect of radical scavengers is expected to result in a higher frequency of viable *Csb*$^{m/m}$/*Xpa*$^{-/-}$ pups and/or increased survival in or beyond week 2 after birth.

D-mannitol administered via an osmotic pump postpones premature death of *Csb*$^{m/m}$/*Xpa*$^{-/-}$ pups

Antioxidants are often administered via an osmotic pump by dissolving them in D-mannitol (Liu et al., 2003). Since D-mannitol itself can function as a hydroxyl radical scavenger, we also tested the effect of this often used dissolvent via an osmotic pump. On the basis of a literature study on application methods for D-mannitol, we decided to provide pregnant females from *Csb*$^{m/-}$/*Xpa*$^{-/-}$ x *Csb*$^{m/m}$/*Xpa*$^{+/-}$ matings with osmotic pumps with 270 mM (5%) D-mannitol or PBS (control) (Liu et al., 2003). Pumps were implanted four days after detection of the copulatory plug and released the injected substance at a constant rate of (68 nmol/hour) for 4 weeks, meaning release of the injected compound till 11 days after birth.

We first determined the frequency of *Csb*$^{m/m}$/*Xpa*$^{-/-}$ pups in the control and treated groups. In the control group (PBS only), we noticed a frequency of 3% (n=3/87) (Fig. 1A), which is slightly lower than what we normally observed. As it has recently been shown that exposure of rats to isoflurane increases malondialdehyde (MDA) and DNA damage levels in a variety of tissues, this difference might be due to the anesthesia required for the insertion of the pump (Kim et al., 2006). Nevertheless, in the group treated with 270 mM D-mannitol, the frequency of

Csb$^{m/m}$/*Xpa*$^{-/-}$ pups showed a significant 6-fold increase ($p < 0.05$) to 18% (n=11/61) (Fig. 1A). Litter sizes were not significantly different (4.7+/-1.8 for the PBS group and 5.0+/-1.6 for the D-mannitol group), excluding effects of D-mannitol on litter size. This finding shows that D-mannitol can rescue the low frequency of *Csb*$^{m/m}$/*Xpa*$^{-/-}$ pups.

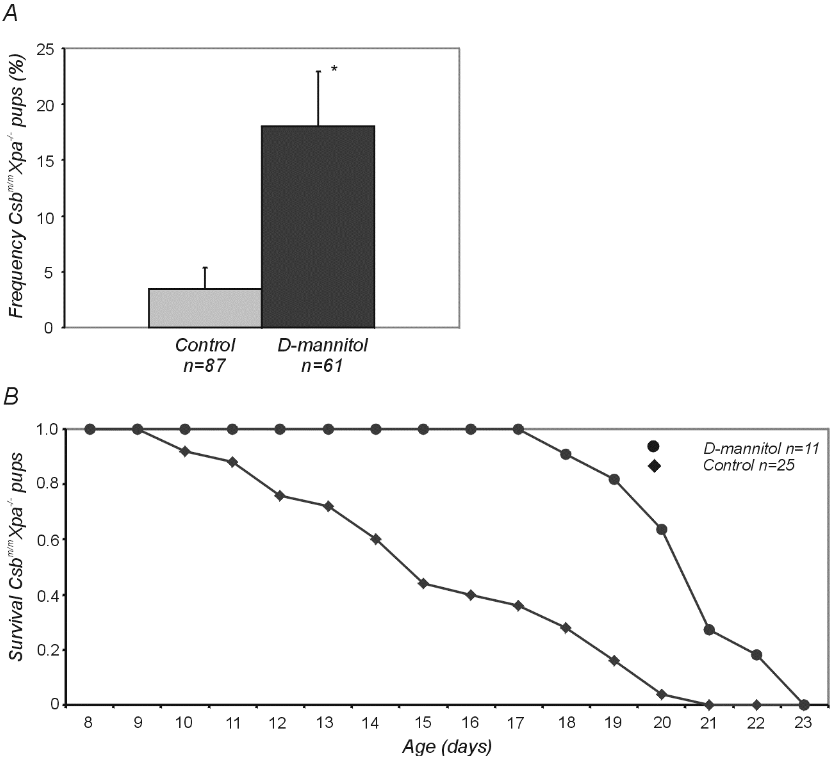

Figure 1: Effect of D-mannitol on frequency and survival of *Csb*$^{m/m}$/*Xpa*$^{-/-}$ pups. *Csb*$^{m/-}$/*Xpa*$^{-/-}$ *x Csb*$^{m/m}$/*Xpa*$^{+/-}$ *breeding couples were set up. Pregnant females (identified by the presence of a copulatory plug) were given osmotic pumps with either PBS, or 270 mM D-mannitol in PBS, implanted under the skin at post-coital day 3.5. A) Frequency of Csb*$^{m/m}$/*Xpa*$^{-/-}$ *pups. For explanation of error bars, see experimental procedures (*; p<0.05). B) Kaplan-Meier plot of the survival of Csb*$^{m/m}$/*Xpa*$^{-/-}$ *animals that reached postnatal day 8 from untreated mothers (diamonds) and mothers treated with D-mannitol (circles). Note: due to the low frequency of double knockout pups in the untreated groups, we have included survival data from other breeding programs, performed in the same period and with the same batch of food.*

We next determined the survival of *Csb*$^{m/m}$/*Xpa*$^{-/-}$ pups and noticed that all double mutant animals survived for minimally 18 days (Fig. 1B). Mean, median and maximal lifespan were 20.8 +/- 1.5, 21 and 23 days respectively. Due to the low frequency of *Csb*$^{m/m}$/*Xpa*$^{-/-}$ pups in the untreated group, we did not have enough animals to reliably determine the survival. We therefore included data from other *Csb*$^{m/m}$/*Xpa*$^{-/-}$ breeding programs and untreated experimental groups, performed in the same period and in which animals were given the same batch of food. Mean, median and maximal lifespan in this control group were 15.6 +/- 3.4, 15 and 21 days, respectively. The ages of *Csb*$^{m/m}$/*Xpa*$^{-/-}$ pups from the treated mothers differed significantly (p<

0.05) from that of *Csb*$^{m/m}$/*Xpa*$^{-/-}$ pups from untreated mothers. Although it is not yet clear whether this effect can be attributed to its radical scavenger function, D-mannitol does not only rescue birth frequency, but also increases lifespan of *Csb*$^{m/m}$/*Xpa*$^{-/-}$ pups.

D-mannitol and L-proline administered via water rescue the perinatal lethality of *Csb*$^{m/m}$/*Xpa*$^{-/-}$ pups

As the previous experiment shows that D-mannitol, when given to pregnant and lactating females via an osmotic pump, increases the survival and lifespan of *Csb*$^{m/m}$/*Xpa*$^{-/-}$ pups, we next investigated whether other simpler application methods could also have this same positive effect.

D-mannitol can be supplied via food and drinking water and is not toxic up to a concentration of 5% (Abdo et al., 1983). After having excluded potential addictive or aversive effects of water containing D-mannitol (data not shown), we chose 110 mM (2%) D-mannitol for this intervention experiment as this was the highest possible concentration without aversive effects. Thus, matings between *Csb*$^{m/-}$/*Xpa*$^{-/-}$ and *Csb*$^{m/m}$/*Xpa*$^{+/-}$ animals were started, and after detection of a copulatory plug, breeding couples were given normal water or water containing 110 mM (2%) D-mannitol. We observed a 5% frequency of *Csb*$^{m/m}$/*Xpa*$^{-/-}$ pups (n=6/118) in the group that was given normal water (i.e. in the same range as found in matings before), whereas in the D-mannitol treated group, we registered a frequency of 14% (n=12/85) (Fig. 2A). Again, litter sizes were not significantly different between groups (4.7+/-1.7 for the control group and 4.9+/-1.6 for the D-mannitol group). Although D-mannitol has a significant effect on the number of *Csb*$^{m/m}$/*Xpa*$^{-/-}$ pups (2.8-fold increase; $p< 0.05$), the effect seems not as profound as when D-mannitol was administered via an osmotic pump, which suggests that for D-mannitol the osmotic pump is the best way of administration.

We next wished to investigate whether a different type of molecule with radical scavenger properties could have a similar effect on the frequency of *Csb*$^{m/m}$/*Xpa*$^{-/-}$ pups. The amino acid L-Proline has been shown to act as a singlet oxygen radical scavenger (Alia et al., 2001), but, as with D-mannitol, has many other functions. L-proline is a non-toxic natural compound, and can be easily administered via the drinking water. Therefore, we first chose to test L-Proline via water administration, as this is less laborious and less stressful for the animals. To investigate whether the results of an L-proline intervention study could be influenced by aberrant drinking behavior of treated animals, we first provided wild type mice with either normal water or water containing 200 mM L-proline (n=8 per group). As we could not detect any difference in water consumption (data not shown), potential addictive or aversive effects of L-proline are not likely to interfere.

Matings between *Csb*$^{m/-}$/*Xpa*$^{-/-}$ and *Csb*$^{m/m}$/*Xpa*$^{+/-}$ animals were started, and after detection of a copulatory plug, breeding couples were given normal water or water containing 200 mM L-proline. In the untreated group, we observed a 4.2% frequency of *Csb*$^{m/m}$/*Xpa*$^{-/-}$ pups (n=2/47), consistent with earlier findings. Interestingly, the frequency of double mutant pups in the L-proline group was 3.2-fold increased ($p < 0.01$) to 20% (n=17/84) (Fig. 2A). Litter sizes were not significantly different between groups (5.0+/-1.6 for the control group and 5.6+/-1.6 for the L-Proline group), which excluded a positive effect of L-Proline on litter size.

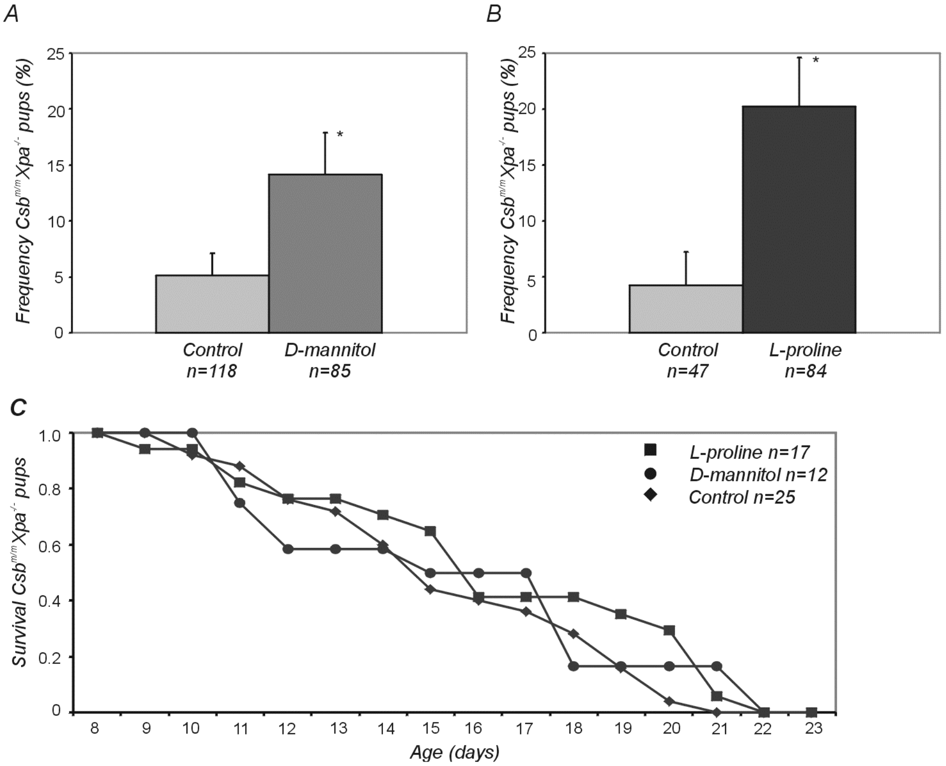

Figure 2: Effect of L-proline and D-mannitol on frequency and survival of *Csb*$^{m/m}$*/Xpa*$^{-/-}$ pups. *Csb*$^{m/-}$*/Xpa*$^{-/-}$ *x Csb*$^{m/m}$*/Xpa*$^{+/-}$ *breeding couples were given ad libitum access to either normal water, or water with 200 mM L-proline or 110 mM D-mannitol. A) Frequency of Csb*$^{m/m}$*/Xpa*$^{-/-}$ *pups in litters given D-mannitol (*; p<0.05). B) Frequency of Csb*$^{m/m}$*/Xpa*$^{-/-}$ *pups in litters given L-proline (*; p<0.01). For explanation of error bars, see experimental procedures. C) Kaplan-Meier plot of the survival of Csb*$^{m/m}$*/Xpa*$^{-/-}$ *animals that reached postnatal day 8 from untreated mothers (diamonds) and mothers treated with D-mannitol (circles) or L-proline (squares). Note: due to the low frequency of double knockout pups in the untreated groups, we have included survival data from other breeding programs, performed in the same period and with the same batch of food (as in Fig1B).*

As we also recorded the age at death of *Csb*$^{m/m}$*/Xpa*$^{-/-}$ that survived beyond 8 days in the D-mannitol and L-proline intervention experiments, we next asked whether these compounds also affect the life span of the double knockout pups. Due to the low frequency of *Csb*$^{m/m}$*/Xpa*$^{-/-}$ pups in the untreated groups, we again did not have enough animals to reliably determine the survival. We therefore included the same data for the control group as in the previous experiment. We did not detect any significant difference in the mean, median or maximal age of death of *Csb*$^{m/m}$*/Xpa*$^{-/-}$ pups in the control (15.6 +/- 3.4 15 and 21 days, respectively), L-proline (16.5 +/- 4.2, 16 and 22 days, respectively) or D-mannitol group (15.7 +/- 4.2, 15 and 22 days, respectively) (Fig. 2C).

Taken together, the L-proline and D-mannitol data demonstrate that administration of these compounds to pregnant/lactating females significantly rescues the perinatal loss of *Csb*$^{m/m}$*/Xpa*$^{-/-}$ pups. Moreover, since both compounds have radical scavenging properties, this finding might point to the fact that reduction of endogenous (oxidative) DNA damage can attenuate the severe $Csb^{m/m}/Xpa^{-/-}$ phenotype.

Frequency and survival of $Csb^{m/m}/Xpa^{-/-}$ animals is affected by food

During subsequent experiments we noted that there was variation in the frequency of $Csb^{m/m}/Xpa^{-/-}$ pups surviving birth stress in our normal breeding programs. After careful investigation of what could be the cause of the variation it became clear that the fluctuations correlated with changes in the food composition. Similar effects had been observed for $Csb^{m/m}/Xpa^{-/-}$ breeding programs at another facility (i.e. National Institute of Public Health and the Environment, Bilthoven, the Netherlands). Standard laboratory mouse chow diets (i) contain many antioxidants and vitamins, the latter (depending on the concentration) acting as anti- or as pro-oxidants, and (ii) are formulated from natural ingredients (e.g. grains, fruits, and vegetables), resulting in inter-brand as well as inter-batch (e.g. seasonal effects) variation (e.g. vitamin A; see Table 1).

contents CRM (P)			jan-03/mar-03	apr-03/jun-03	jul-03/sep-03	okt-03/dec-03	jan-04/mar-04	apr-04/jun-04		okt-04/dec-04	jan-05/mar-05		jul-sept 2005	okt-dec 2005
moisture		%	10,80	11,50	10,30	11,30	12,20	12,50	-	12,30	12,30	-	11,00	13,20
crude fat		%	2,80	4,80	-	-	-	-	-	-	-	-	-	-
crude fibre	3,70	%	-	-	3,37	3,90	4,10	3,60	-	3,20	3,20	-	3,70	3,60
ash	3,80	%	-	-	5,14	5,10	5,30	5,00	-	5,10	5,10	-	5,60	4,80
oil	3,40	%	-	-	3,20	3,80	4,00	3,90	-	3,80	3,80	-	3,40	3,00
crude protein	18,80	%	19,10	18,70	18,70	19,00	18,00	19,20	-	18,70	18,70	-	18,50	18,20
calcium	0,80	%	0,85	0,77	0,78	0,76	0,96	0,86	-	-	-	-	1,00	-
phosphorus	0,64	%	0,62	0,64	0,58	0,61	0,65	0,66	-	-	-	-	0,65	-
vitamin A	16,80	iu/g	16,00	8,60	12,00	15,00	13,00	17,00	-	20,00	20,00	-	23,00	9,40
vitamin E	103,20	mg/kg	116,00	62,00	111,00	101,00	-	-	-	-	-	-	-	92,00

Table 1. Fluctuation in food composition of CRM with time. Mixtures of batches form a period of two months were analyzed after use.

We therefore set out to test the effect of mouse chow in a controlled study, using CRM(P) batch 4873 (Special Diets Services) and Diet: SRM(A) (Hope Farms), hereafter referred to as CRM and SRM. We set up two subsequent rounds of matings with $Csb^{m/-}/Xpa^{-/-}$ x $Csb^{m/m}/Xpa^{+/-}$ breeding couples that were fed either CRM or SRM. We obtained double knockout pups at a frequency of 17% (n= 13/75) for breeding couples that were given CRM batch 4873 (Fig. 3A). In marked contrast, breeding couples that were given SRM yielded $Csb^{m/m}/Xpa^{-/-}$ pups at a low frequency of 2.7% (1/37) (Fig. 3A), which was a statistically significant difference ($p<0.05$). Litter sizes were not significantly different between groups (4.5+/-1.2 for the SRM and 4.4+/-1.6 for the CRM group), which excluded effects of these two types of food on litter size.

To see whether the animals yielding a low frequency of $Csb^{m/m}/Xpa^{-/-}$ pups were actually able to produce a higher number of double mutant offspring we switched the group that received the SRM chow to CRM food and allowed them to deliver two more litters. The CRM fed breeding couples were kept on CRM to assess reproducibility. As shown in Fig 3A, breeding couples that were maintained on CRM gave $Csb^{m/m}/Xpa^{-/-}$ pups at a frequency of 9.1% (n=8/88) which is lower but not significantly different as compared to the first part of this experiment. Animals that were previously kept on SRM chow now yielded $Csb^{m/m}/Xpa^{-/-}$ offspring at a frequency of 9.2% (n=6/65) (Fig 3A) i.e. very similar to the other group, indicating reproducibility under identical conditions. These data show that different types of food and perhaps other unknown factors can influence the frequency of $Csb^{m/m}/Xpa^{-/-}$ pups, underscoring that intervention experiments should be done in parallel at the same time with the same batch of food, as done for the D-mannitol and L-proline experiments.

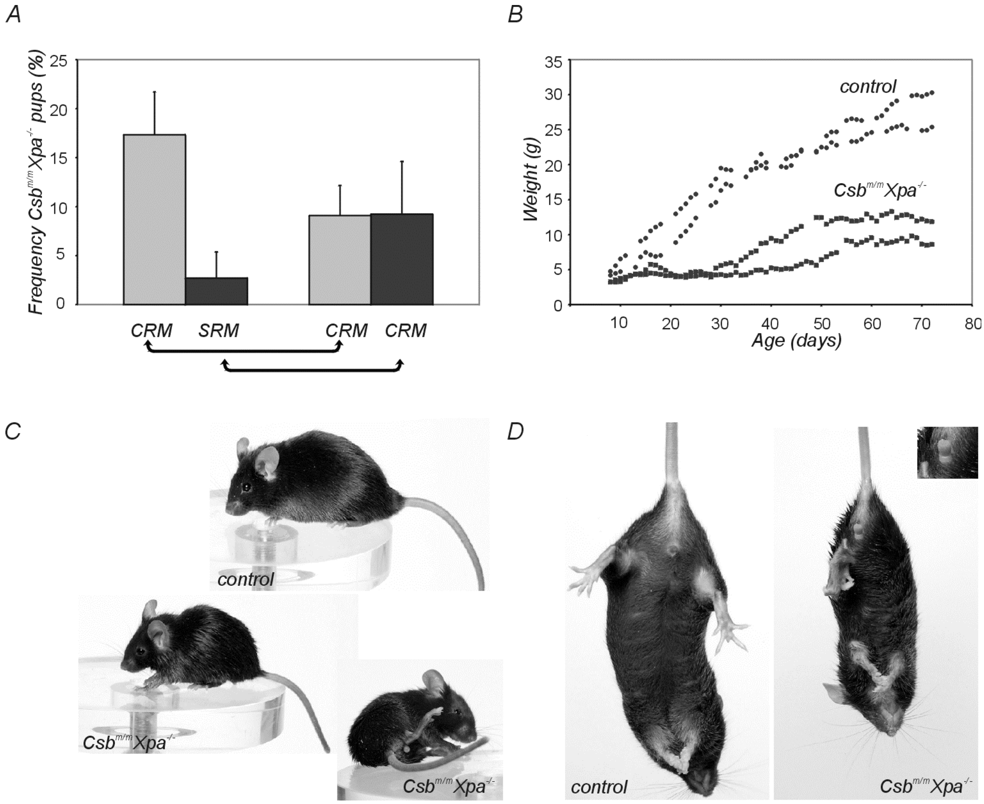

Figure 3: Effect of food on frequency and survival of $Csb^{m/m}/Xpa^{-/-}$ pups. *$Csb^{m/-}/Xpa^{-/-}$ x $Csb^{m/m}/Xpa^{+/-}$ breeding couples were maintained on regular CRM or SRM chow and were allowed to mate. Note that throughout the experiment food was obtained from the same batches. A) Frequency of $Csb^{m/m}/Xpa^{-/-}$ pups on CRM or SRM chow and after transfer to CRM chow (transfer indicated by lines underneath the figure). For explanation of error bars, see experimental procedures. B) Body weight of a male and female $Csb^{m/m}/Xpa^{-/-}$ mouse (and littermate controls) that survived beyond weaning when animals were given moisturized, crunched AIN93-G pellets. C) Photographs of a $Csb^{m/m}/Xpa^{-/-}$ male mouse that survived on moisturized, crunched AIN93-G pellets, and a control mouse, age 72 days, displaying kyphosis in the first, together with a photograph of the $Csb^{m/m}/Xpa^{-/-}$ male mouse, displaying imbalance D) Photographs of the same 72 day old $Csb^{m/m}/Xpa^{-/-}$ male and control mouse. Note the abnormal posture during the tail suspension assay (crossing rather than spreading of hind limbs) and priapism as compared to the littermate control.*

Since the above used mouse chow is subject to batch-to-batch variation (Table 1), we next investigated whether a synthetic food, which is expected to experience less variation between batches, would be a better alternative for intervention based on frequency of $Csb^{m/m}/Xpa^{-/-}$ pups. AIN93-G was chosen, as it is a fixed formula synthetic diet that contains all necessary constituents and, in contrast to regular laboratory mouse chow, is of constant quality. Litters from breeding couples that were given AIN-93G resulted in a frequency of double knockout pups of 11.1% (n=4/36). This is a relatively high number when one would like to study the effect of compounds and such a frequency in the control group would demand a high number of pups to reach statistical significance. However, other formulas may be more suitable for this purpose.

A synthetic diet dramatically extends the lifespan of some $Csb^{m/m}/Xpa^{-/-}$ animals

Previously, we have made several attempts to postpone the premature death of $Csb^{m/m}/Xpa^{-/-}$ pups to beyond the weaning period. For example, newborn mice switch from milk to solid food in their third week of life. Reasoning that the fragile condition and short stature of $Csb^{m/m}/Xpa^{-/-}$ animals might prevent them from properly doing so, we have provided litters with double knockout pups with a mixture of crunched CRM or SRM chow pellets and water from day 15 onwards, to exclude malnutrition or dehydration as a cause of death. Also we provided $Csb^{m/m}/Xpa^{-/-}$ pups new lactating mothers. However, we were never able to obtain animals that lived longer than 23 days (Chapter 2 and data not shown). Surprisingly, when we performed a similar pilot experiment with the synthetic AIN-93G diet, 2 out of 4 $Csb^{m/m}/Xpa^{-/-}$ pups (one male and one female) survived for over 2 months, which is a near 3 to 4-fold increase in life span. Similar to their short-lived double mutant littermates, the surviving $Csb^{m/m}/Xpa^{-/-}$ animals displayed severe post-natal growth retardation (Fig. 3B) and from weaning on maintained a constant (low) body weight for 10 to 20 days, after which animals started to gain weight again (i.e. 2-3-fold increase as compared to body weight at weaning). In addition, animals developed kyphosis (Fig 3C) and displayed pronounced ataxia or inability to keep in balance (Fig 3C). We also observed dystonia, (i.e. abnormal posture in the tail suspension assay, with hindlimbs crossed together rather than wide compared to the normal posture exhibited by the littermate control, Fig 3D) and waltzing type behavior. Both $Csb^{m/m}/Xpa^{-/-}$ animals showed paralysis of one of their hind limbs, which in case of the female progressed into muscular atrophy. Furthermore, the $Csb^{m/m}/Xpa^{-/-}$ male developed priapism (a persistent erection of the penis as a consequence of disease, rather than sexual arousal), the latter first noticed at day 58 (Fig 3D). Eventually, after some loss of body weight, both $Csb^{m/m}/Xpa^{-/-}$ mice became moribund and were sacrificed at day 72 and 100, respectively. For both cases, autopsy revealed food in the stomach of the animal, excluding malnutrition as the cause of weight loss and physical deterioration. A detailed histopathological examination of the $Csb^{m/m}/Xpa^{-/-}$ mice is in progress.

Apoptosis of photoreceptor cells as a possible read-out of intervention

Given the observed variation in birth frequency of $Csb^{m/m}/Xpa^{-/-}$ pups, we searched for independent additional parameters to monitor potential effects of intervention. Retinal degeneration is a hallmark of CS, reported in 55% of the patients (Nance and Berry, 1992) (Dollfus et al., 2003; Levin et al., 1983), and is also observed in $Csb^{m/m}$ animals, which display spontaneous photoreceptor-loss that can be can be amplified by the effects of low-dose ionizing radiation induced (oxidative) DNA damage (van der Horst et al., 1997), (Chapter 3). Moreover, the retina appears particularly susceptible to oxidative stress because of its high consumption of oxygen, high concentration of polyunsaturated fatty acids, and exposure to light (Beatty et al., 2000). Taken together, photoreceptor loss in CS mouse models may constitute a relevant additional assay for intervention screens in the intact animal.

We thus performed a pilot study in which newborn wild type (wt) and *Csb*$^{m/m}$ animals were placed on CRM, SRM or AIN93-G food. At the age of 10 weeks, animals were sacrificed and the retina was subjected to TUNEL staining, followed by quantification of the number of apoptotic cells in the outer nuclear layer (ONL, containing the photoreceptor cells) and inner nuclear layer (INL, containing the cell bodies of bipolar, horizontal, amacrine and Müller cells).

A

		CRM(P)	*SRM(A)*	*AIN93G*
ONL	*Wt*	*0.6 ± 0.5*	*0.6 ± 0.3*	*ND*
	Csb$^{m/m}$	*2.7 ± 1.0*	*9.5 ± 2.5*	*3.2 ± 0.9*
INL	*Wt*	*0*	*0.11 ± 0.12*	*ND*
	Csb$^{m/m}$	*0.1 ± 0.2*	*0.4 ± 0.3*	*0.6 ± 0.5*

B

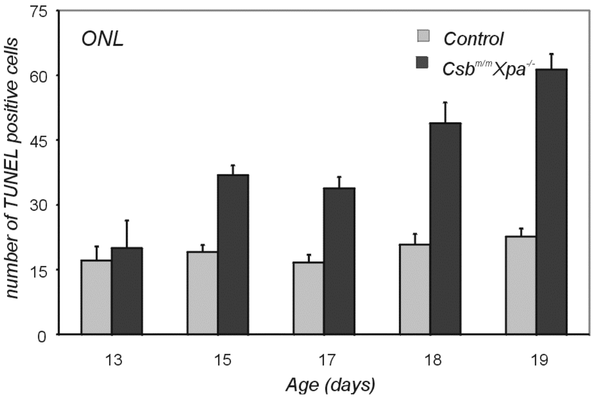

Figure 4. Photoreceptor cell loss in mouse models for CS. *A) Quantification of apoptotic (TUNEL-positive) cells in the outer (ONL) and inner nuclear layer (INL) of Csb*$^{m/m}$ *mice, maintained on CRM or SRM chow, or on a synthetic AIN93-G diet. The observed differences in the number of apoptotic cells were tested for significance using a Student t-test and one-way analysis of variance (ANOVA). In case of statistical significance the ANOVA was followed by the post hoc test of Student-Newman-Keuls (S-N-K). Significance was accepted at p < 0.05. B) Number of TUNEL positive photoreceptor cells in the ONL of Csb*$^{m/m}$*/Xpa*$^{-/-}$ *pups and control littermates at various ages. Animals were fed with CRM chow. Error bars indicate standard errors of the mean.*

In *Csb*$^{m/m}$ animals that were given CRM chow, we observed on average 2.7 ± 1.0 TUNEL positive cells in ONL and 0.1 ± 0.2 in the INL (Fig. 4A, n=4). Strikingly, and in line with the lower performance of *Csb*$^{m/m}$*/Xpa*$^{-/-}$ pups on this food, SRM fed *Csb*$^{m/m}$ animals showed on average 9.5 ± 2.5 and 0.4 ± 0.3 TUNEL-positive cells in ONL and INL, respectively (Fig. 4A, n=6), which, at least for the ONL, is significantly increased (p<0.05) compared to *Csb*$^{m/m}$ animals maintained on CRM chow. Interestingly, wt animals did not show any food-related differences in apoptosis in the ONL and INL (Fig. 4A). *Csb*$^{m/m}$ animals fed with AIN93-G on average had 3.2 ± 0.9 TUNEL positive cells in ONL and 0.6 ± 0.5 in the INL (Fig. 4A, n=6), which was similar to the data obtained with the CRM food. In conclusion, the diet offered to the animal appears to have an influence on the amount of apoptotic photoreceptor cells in the *Csb*$^{m/m}$ retina.

Recently, we have demonstrated that 15-day old *Csb*$^{m/m}$/*Xpa*$^{-/-}$ mice show enhanced photoreceptor loss, as compared to *Csb*$^{m/m}$ single mutant littermates (Chapter 2). Therefore, we now determined the amount of TUNEL-positive photoreceptor cells in the ONL retina of wt and *Csb*$^{m/m}$/*Xpa*$^{-/-}$ animals at day 13, 15, 17, 18 and 19 to investigate whether photoreceptor-loss progressively worsens in time. As shown in Fig. 4B, starting at day 15, the number of apoptotic photoreceptor cells in the *Csb*$^{m/m}$/*Xpa*$^{-/-}$ retina rapidly increases in time, while apoptosis in the wild type retina remains constant. This result was confirmed by staining for Active Caspase 3 (data not shown), which is a specific marker for apoptosis. From this finding we conclude that the kinetics of onset of photoreceptor loss in the *Csb*$^{m/m}$/*Xpa*$^{-/-}$ retina could be a valuable endpoint in intervention studies.

Discussion

Cockayne Syndrome is a rare, autosomal inherited DNA repair deficient disorder, characterized by (early onset) disturbed growth, progressive neurodegeneration and premature death, along with many progeroid features (Martin, 2005; Nance and Berry, 1992). Up to now there is no therapy for this disease other than treatment of individual symptoms when possible. *Csb*$^{m/m}$/*Xpa*$^{-/-}$ animals share many similarities with CS, including postnatal growth retardation, skeletal abnormalities, retinal degeneration, Purkinje cell loss, ataxia and premature death, and therefore seem a good animal model to test possible therapeutical intervention strategies to alleviate CS symptoms. Since our previous (transcriptome) analysis of *Csb*$^{m/m}$/*Xpa*$^{-/-}$ mice points to unrepaired endogenous DNA damage (inflicted by reactive oxygen species), as a likely trigger for CS pathology (Chapter 2), we now have explored the effect of compounds with radical scavenger properties on the *Csb*$^{m/m}$/*Xpa*$^{-/-}$ phenotype.

D-mannitol and L-proline alleviate early perinatal death and postpone premature death in *Csb*$^{m/m}$/*Xpa*$^{-/-}$ mice

We have shown that D-mannitol and L-proline significantly increase the yield of *Csb*$^{m/m}$/*Xpa*$^{-/-}$ offspring when pregnant/lactating females are given these compounds via drinking water. Moreover, when D-mannitol was delivered to the mother subcutaneously (through an osmotic pump), we observed additionally a significant increase in the lifespan of *Csb*$^{m/m}$/*Xpa*$^{-/-}$ animals. It remains to be seen whether L-proline will have a similar effect, when provided via an osmotic pump. Importantly, as previously hypothesized (Chapter 2), these intervention studies provide evidence that compounds with radical scavenger properties can have a positive effect on the phenotype of *Csb*$^{m/m}$/*Xpa*$^{-/-}$ animals.

However, besides the scavenging properties it is possible that the positive effects of L-proline and D-mannitol originate from or are strengthened by other properties of these molecules. For instance, D-mannitol has been shown to increase glucose transport and open the blood-brain barrier (Cosolo et al., 1989; Hwang and Ismail-Beigi, 2001), whereas L-proline was found to inhibit ROS-mediated apoptosis and to act as an activator of transcription (Chen and Dickman, 2005; Sellick and Reece, 2003). For this it would be helpful to test compounds with a similar structure, but lacking scavenging activity.

Still, the common property of both compounds is radical scavenging. Therefore, it is tempting to speculate that this is the property that contributes to the observed effects. The most plausible scenario would then be that radical scavenging lowers the intracellular ROS level, and as an immediate consequence, the harmful side effects of these metabolic byproducts on cellular macromolecules. In view of the repair defect of the CS mouse models, it is reasonable to assume that the positive effect of such radical scavenging is exerted through reducing the amount of DNA damage, which would strengthen the idea that the accumulation of unrepaired DNA damage is at the basis of the etiology of CS pathology.

Besides the mechanism of action of both compounds, we would also like to know if the observed effects display dose-dependency, by repeating the experiment with varying doses of L-proline and D-mannitol. In parallel, such studies will reveal the optimal dose that should be given to pregnant/lactating mothers, which subsequently will also allow us to investigate whether combined administration of L-proline and D-mannitol has additive/synergistic effects. In addition, we want to obtain insight in the actual concentration of L-proline and D-mannitol in blood and tissues of *Csb*$^{m/m}$/*Xpa*$^{-/-}$ pups. To address this question, we have performed a study in which pregnant/lactating wild type females were given three different doses of L-proline or D-mannitol via drinking water, and in which serum levels of these compounds in mother and offspring were measured. These experiments point to a rapid clearance of these compounds by the kidney (as we found detected both in urine) and/or a fast metabolic conversion or uptake in organs and tissues. Therefore constitutive serum levels appeared low. Since we observed a clear biological effect, these compounds apparently already exert an effect at a low serum dose. We are now using radiolabeled D-mannitol and L-proline, to determine relevant pharmacokinetic and -dynamic parameters of these compounds. This will provide insight in the clearance rates and transmission efficiency via placenta and mother milk.

Food influences the severe pathology of *Csb*$^{m/m}$/*Xpa*$^{-/-}$ mice

We uncovered inter-brand (i.e. CRM vs. SRM) effects of chow diets on the yield of double knockout offspring. Moreover, we obtained indications for time-dependent changes in frequencies of *Csb*$^{m/m}$/*Xpa*$^{-/-}$ pups, while using one and the same batch of food. These data not only point to sensitivity of the *Csb*$^{m/m}$/*Xpa*$^{-/-}$ mouse model to food components, but more generally, may also explain discrepancies between observed phenotypes when a particular mouse model is studied in different labs. Thus, particularly when studying animal models in which the phenotype may depend on, or may be influenced by pro- and anti-oxidants (e.g. neurodegeneration, carcinogenesis, life span), the effect of food should be considered. More importantly, when testing intervention in the above described endpoints, this should be done in parallel at the same time with the same batch of food, as was done for the D-mannitol and L-proline studies, to exclude these variable factors.

Since the *Csb*$^{m/m}$/*Xpa*$^{-/-}$ pups might be expected to encounter difficulties in reaching the food compartment and/or chewing the solid food pellets due to their severe phenotype, we also attempted to extend the life span of these animals by giving moisturized, crunched food pellets.

When performed with CRM or SRM chow, this approach did not have any effect. However, in a first experiment in which a litter was given moisturized crunched AIN-93G pellets, two out of four $Csb^{m/m}/Xpa^{-/-}$ animals lived way beyond the age of 21 to 23 days. Apart from the known $Csb^{m/m}/Xpa^{-/-}$ features (i.e. postnatal growth retardation, ataxia, progressive cachexia, and kyphosis, see Chapter 2), the long-lived animals also showed new phenotypical features such as hind limb paralysis, waltzing behavior, and aberrant tail suspension behavior. In addition, the male mouse developed priapism, which is also observed in the brain conditional $Csb^{m/m}/Xpa^{c/-}$ mouse model (Chapter 4), and thus further points to neurological dysfunction. Animals became moribund at the age of 72 and 100 days, and are currently subjected to detailed histopathological analysis. A possible explanation for the prolonged survival of $Csb^{m/m}/Xpa^{-/-}$ mice on the moisturized crunched AIN-93G diet (in contrast to regular chow) could be that food components might dissolve more easily. These findings once more show what impact food can have on the phenotype of the $Csb^{m/m}/Xpa^{-/-}$ mouse. In addition, we conclude that apparently $Csb^{m/m}/Xpa^{-/-}$ animals encounter at least two critical stages early in life, the first being birth, the second being weaning when animals change from milk to solid diets. Apparently both (stressful) events can be modulated.

Food modulates mild pathology of the $Csb^{m/m}$ mouse

Although the $Csb^{m/m}/Xpa^{-/-}$ mouse model represents a suitable tool for intervention studies that aim at alleviating the pathology of CS, we wished to find additional CS-related endpoints to study the effects of intervention compounds. Preferably, candidate phenotypes should develop in a relatively short time to avoid unnecessarily long experiments. Furthermore, statistical significance of interventions should be reached with relatively low numbers of animals. Detection of retinal photoreceptor loss in the $Csb^{m/m}$ mouse model (Chapter 3) well fits these criteria. Since the number of TUNEL-positive photoreceptor cells was found to differ when $Csb^{m/m}$ animals are placed on different types of mouse chow, this suggests that apoptotic cells in the retina may serve as a good endpoint. Thus, we are currently testing the effect of D-mannitol and L-proline on retinal degeneration in the $Csb^{m/m}$ mouse model. Moreover, as we have shown that photoreceptor loss in $Csb^{m/m}$ animals is dramatically enhanced by inactivation of *Xpa* (Chapter 2 and this study), and as we have generated a conditional *Xpa* mouse model (Chapter 4), the assay could be further sensitized by using a photoreceptor-specific conditional $Csb^{m/m}/Xpa^{c/-}$ mouse model. Such a mouse model will make it possible to study the effects of compounds on enhanced photoreceptor cell loss in an adult $Csb^{m/m}$ mouse.

Towards clinical application

Our finding that mouse CS features can be modulated by scavengers and possibly also food composition provides a clear hint that human CS pathology might be alleviated by nutraceutical or pharmaceutical intervention strategies that attempt to lower the accumulation of unrepaired DNA damage. Although this strategy will probably not cure the disease, it hopefully may help to improve quality of life of CS patients. Extensive follow-up research in animal models is needed to find the most favorable compound and to define the optimal concentration and delivery method, along with detailed studies that exclude negative side effects of chronic administration of the compound of choice. Furthermore, as the limited number of CS patients precludes double-blind placebo-controlled treatment studies, a start should be made to determine parameters that report on successful intervention in clinical trials with human CS patients. On the basis of our previous work, circulating IGF1 levels (detected in serum) and brain atrophy (detected by MRI) may well serve that purpose (see also Chapters 2 and 3). Finally, once intervention in CS patients will turn out to be successful, we anticipate that the identified compounds will not only be beneficial to other ROS/DNA damage based (progeroid) disorders, but (when provided as food supplements) will also promote healthy aging in general.

Materials and Methods

Mice

The generation and characterization of NER-deficient $Csb^{m/m}$ and $Xpa^{-/-}$ mice has been described previously (de Vries et al., 1995; van der Horst et al., 1997). All mice were kept in a homogeneous C57BL/6J genetic background. Mice were genotyped by PCR using a primer mix that amplifies both the wild type and targeted alleles in a single reaction (de Vries et al., 1995; van der Horst et al., 1997). Animals are maintained in a controlled environment (19-24 ^{o}C, 12h light: 12 hr dark cycle), received CRM(P) standard rodent maintenance chow (Special Diets Services, Witham, UK) and water *ad libitum*, and were housed at the Animal Resource Center (Erasmus University Medical Center), which operates in compliance with the “Animal Welfare Act” of the Dutch government, using the “Guide for the Care and Use of Laboratory Animals” as its standard.

Intervention studies

For intervention studies, we used a breeding protocol involving matings between $Csb^{m/-}/Xpa^{-/-}$ and $Csb^{m/m}/Xpa^{+/-}$ animals, which yields $Csb^{m/m}/Xpa^{-/-}$ pups at a maximum (Mendelian) frequency of 25%. Animals were daily screened for discomfort and weighed once a week, except for $Csb^{m/m}/Xpa^{-/-}$, which after identification (see below) were weighed every day. The number of $Csb^{m/m}/Xpa^{-/-}$ pups was recorded, as well as their age at death. Food and water consumption by the pregnant/lactating female were registered by weighing the food pellets and drinking bottle.

Experimental animals were fed ad libitum with CRM(P) standard rodent maintenance chow batch 4873 (Special Diets Services, Witham, UK) or Diet: SRM(A) (Hope Farms/Arie Blok, Woerden, the Netherlands). Alternatively, animals were given the (fixed formula) synthetic pelleted diet AIN-93G, lacking antioxidant tertiary-butylhydroquinone (TBHQ) (Harlan Teklad, Horst, the Netherlands). As transfer of pups from milk to solid food occurs around day 18, in some experiments pups were given a mixture of crunched food pellets and water from day 15 onwards to exclude malnutrition as a cause of death.

L-proline (Sigma, P5607) and D-mannitol (Sigma, M4125) were provided via drinking water at concentrations of 200 and 110 mM, respectively, using normal water as a control. Bottles were refreshed twice a week. Alternatively, pregnant females (as determined by the presence of a vaginal copulatory plug) received an ALZET 2004 osmotic pump (DURECT Corporation, Cupertino CA, USA) with 270 mM D-mannitol in phosphate-buffered saline (PBS) or PBS only, that was implanted under the skin under anesthesia with isoflurane. Release rates were 0.25 µl/hr, as indicated by the manufacturer.

Biological parameters tested

As biological readouts for the effect of antioxidants and food, we used “frequency”, “survival”, and “retinal cell loss”.

The frequency represents the number of $Csb^{m/m}/Xpa^{-/-}$ pups that reach post-partum day 8 (the age at which genotyping is performed), and expressed as percentage of the total number of newborns at that age. Observed differences in frequency were tested for significance using a simple z-test and validated with the Chi-square test. Significance was accepted at $p < 0.05$. Standard errors are calculated with the formula $\sqrt{[(f)*(1-f)/n]}$ based on number of animals (n) and frequency (f). To exclude that the observed $Csb^{m/m}/Xpa^{-/-}$ frequencies between treated and untreated groups were influenced by litter size, average litter size per group was calculated for the non-$Csb^{m/m}/Xpa^{-/-}$ pups, by correcting for the amount of $Csb^{m/m}/Xpa^{-/-}$ pups with the formula (‘total number of pups’ – ‘number of $Csb^{m/m}/Xpa^{-/-}$ pups’)/’number of litters’. This number should be constant between treated and untreated groups if the treatment does not influence litter size. Differences in litter size were tested for significance using a Student t-test. Significance was accepted at $p < 0.05$.

Survival was determined by the Kaplan–Meier method, using the SSPS statistics program version 11.01 (SPSS Inc., Chicago, IL USA). Animals that became moribund were killed and therefore were counted as dead in the survival analysis. Mean and median age were calculated with the formulas ‘mean=sum of ages/sample size’ and ‘median= 0.5*(n+1)st observation’.

Retinal cell loss was determined by TUNEL staining of horizontal sections of the eye, as described in more detail below. Observed differences in the number of apoptotic cells were tested for significance using a Student t-test and one-way analysis of variance (ANOVA). In case of statistical significance the ANOVA was followed by the post hoc test of Student-Newman-Keuls (S-N-K).

As required by Dutch law, all animal studies were approved by an independent Animal Ethical Committee (Dutch equivalent of the IACUC).

Immunohistological procedures

The isolation of the eye and visualization of apoptosis in the retina have been described in detail elsewhere (Chapter 3). In short, animals were anaesthetized by CO_2 inhalation, followed by cervical dislocation. Eyes were marked on the nasal side with Alcian blue, enucleated, fixed in 4 % paraformaldehyde (in 0.1 M phosphate buffer), washed in PBS, and embedded in paraffin. Horizontal sections (5 µm thick) of the retina were cut and sections in the middle of the retina were selected by Alcian blue marking and proximity of the optic nerve. Sections were stained for degenerating cells by TdT-mediated dUTP Nick-End Labeling (TUNEL), according to the manufacturer’s instructions (Apoptag Plus Peroxidase *In Situ* Apoptosis Detection Kit, Chemicon). For quantification, the number of TUNEL-positive cells in the inner nuclear layer (INL) and outer nuclear layer (ONL) were counted in 6 whole sections per mouse.

Acknowledgements

This research was supported by the Netherlands Organization for Scientific Research (NWO) through the foundation of the Research Institute Diseases of the Elderly, as well as grants from SenterNovem IOP-Genomics (IGE03009), European Community (LSHC-CT-2005-512113) NIH (1PO1 AG17242-02), NIEHS (1UO1 ES011044) and DNage.

Chapter 6

CHAPTER 6

Concluding remarks and perspectives

Samenvatting

References

Dankwoord

Curriculum Vitae

Concluding remarks and perspectives

DNA damage can be deleterious to both cells as well as the entire organism. Thus, it is of vital importance that the genome is protected from genotoxic insults. Unrepaired DNA damage can interfere with cellular key processes like transcription and replication, resulting in cell death by apoptosis, and growth arrest or they induce mutations that ultimately may result in the onset of cancer (see (Hoeijmakers, 2001)). Accumulation of DNA damage has also proposed to be a major contributor to age-related diseases (e.g. (Hasty et al., 2003; Mitchell et al., 2003)). This is demonstrated by Cockayne Syndrome (CS), an inherited progeroid disorder, which is caused by a defect in the transcription coupled repair subpathway of nucleotide excision repair (TC-NER) CS is characterized by UV-sensitivity of the skin, progressive growth failure, together with many neurological symptoms. CS is recognized as a “segmental” progeroid syndrome, as evident from the observation that patients show early onset of a subset, but not all features of normal aging. No cure is available for this disease other than treatment of the symptoms that present themselves. In this thesis we set out to investigate the underlying mechanism that results in the very severe progeroid phenotype observed in CS by use of existing and new mouse models.

Repair deficiency

In line with the transcription-coupled NER defect, patients with CS have a UV-sensitive skin. However, these patients do not develop skin cancer (reviewed by (Nance and Berry, 1992)). Similarly, the skin of *Csb*$^{m/m}$ mice (and cells derived thereof) is hypersensitive to UV and easily gets sunburned. In contrast to CS patients, *Csb*$^{m/m}$ animals do get skin cancer after chronic UV-irradiation (van der Horst et al., 1997). In Chapter 3, we show that carcinogenic events in *Csb*$^{m/m}$ mice are not limited to the skin, but also occur in the eye. Chronically UV-exposed *Csb*$^{m/m}$ animals develop corneal hyperplasia and squamous cell carcinomas. These data show that TC-NER acts as a tumor suppressor mechanism. The difference in cancer susceptibility in human and rodent CS is well explained by the fact that UV-induced cyclobutane pyrimidine dimers are the major causative lesion for UV-skin cancer (Jans et al., 2005) and that rodents lack efficient GG-NER for removal of this lesion from the DNA and thus primarily rely on TC-NER (Bohr et al., 1985).

Using a panel of *Csb*$^{m/m}$/*Xpa*$^{-/-}$, *Csb*$^{m/m}$/*Xpc*$^{-/-}$, and *Xpa*$^{-/-}$/*Xpc*$^{-/-}$ mouse embryonic fibroblasts, obtained from intercrosses between *Csb*$^{m/m}$ (TC-NER defect), *Xpa*$^{-/-}$, *Csb*$^{m/m}$/*Xpc*$^{-/-}$, (complete NER defect) and *Xpc*$^{-/-}$ (GG-NER defect) animals, we have shown that inactivation of GG-NER in a *Csb*$^{m/m}$ background renders cells even more UV-sensitive than *Xpa*$^{-/-}$ cells (Chapter 2). This hypersensitivity may be attributed to other DNA damage than photolesions (e.g. oxidative DNA damage). Although CS patient fibroblasts as well as *Csb*$^{m/m}$ MEFs have been shown sensitive to γ-irradiation (de Waard et al., 2003; Deschavanne et al., 1984), reservations exist with respect to the oxidative DNA damage sensitivity of CS cells. In Chapter 3, we provide clear evidence for increased apoptosis in the retina of *Csb*$^{m/m}$ animals after exposure to low doses of ionizing radiation. Interestingly, exposure of 18 day old *Csb*$^{m/m}$/*Xpa*$^{-/-}$ mice to ionizing radiation (Chapter 2), resulted in a higher frequency of apoptotic cells as compared to wild type or *Csb*$^{m/m}$

and *Xpa*$^{-/-}$ single mutant mice. These data suggest that at the organismal level *Csb*$^{m/m}$/*Xpa*$^{-/-}$ mice are even more sensitive to oxidative DNA damage than *Csb*$^{m/m}$ mice.

Progeroid symptoms

CS pathology includes retarded growth and cachexia (cachectic dwarfism), along with kyphosis and variety of neurological abnormalities such as deafness. In contrast to human CS, Csbm/m mice only display a very mild CS phenotype, which includes body weight retardation and retinal degeneration. In Chapter 3, we have investigated in detail the spontaneous photoreceptor loss in Csbm/m mice. The increased apoptosis in the retina of ionizing radiation exposed eyes suggests that the retinal cells loss implies that endogenous (oxidative) DNA damage is the underlying trigger. Importantly, as shown in Chapter 2, inactivation of (global genome) NER dramatically aggravates the mild *Csb*$^{m/m}$ phenotype. *Csb*$^{m/m}$/*Xpa*$^{-/-}$ animals display an extremely short lifespan of about 3 weeks and display many (progeroid) features of CS: normal embryonic development followed by progressive postnatal growth failure, cachexia, ataxia, kyphosis, relatively large limbs compared to a small body, and retinal degeneration.

To provide insight in the etiology of CS, we have examined the liver transcriptome of *Csb*$^{m/m}$/*Xpa*$^{-/-}$ and single mutant and wild type littermates, as well as that of wild type animals at various ages (Chapter 2). Interestingly, the liver transcriptome of *Csb*$^{m/m}$/*Xpa*$^{-/-}$ animals resembles that of old wild type animals, which further points to premature aging in the double mutant mice. Surprisingly, we found systemic suppression of the GH/IGF1 somatotroph axis and oxidative metabolism, along with an increased antioxidant response. Moreover, serum glucose and IGF1 levels were reduced, whereas glycogen and fat accumulated in the liver. This response is reminiscent of a lifespan-prolonging effect as observed in Snell and Ames dwarf animals (Carter et al., 2002; Longo and Finch, 2003). Taken together, our data suggest that unrepaired endogenous DNA damage can induce a systemic response, which we hypothesize to serve as an adaptive response attempting to reduce the level of reactive oxygen species (and as a consequence lower DNA damage levels) to prolong lifespan. This scenario was further supported by the finding that a similar response can be induced in wild type animals that were treated with the pro-oxidant DEHP (Chapter 2). Similar data were obtained with *Ercc1*$^{-/-}$ and *Xpd*$^{TTD/XPCS}$/*Xpa*$^{-/-}$ animals, pointing to a shared general response induced by DNA damage.

Moreover, as *Csb*$^{m/m}$/*Xpa*$^{-/-}$ tune down the somatotrophic axis while still growing into adulthood, this model could explain the dwarfism associated with CS. In this regard, it will be very interesting to investigate whether in CS patients a similar response underlies the observed phenotype.

Neurodegeneration

Neurological abnormalities represent a prominent feature of CS. From the work presented in Chapters 2 and 3 it became clear that whereas proliferative tissues like liver and kidney did not display increased apoptotic death, a post-mitotic tissue like the retina does show an increase in apoptotic cells. Moreover, *Csb*$^{m/m}$/*Xpa*$^{-/-}$ animals are ataxic and were shown to have increased apoptosis in the cerebellum (Murai et al., 2001).

These observations together led us to speculate that the brain would be an important tissue to study the CS phenotype in more detail. However, the *Csb*$^{m/m}$ mouse has only a mild neurological phenotype (assayed by behavioral studies) and so far no aberrant brain pathology was found in these animals. Whereas the *Csb*$^{m/m}$/*Xpa*$^{-/-}$ mouse model forms a better phenocopy of CS than the *Csb*$^{m/m}$ model, the short life span of *Csb*$^{m/m}$/*Xpa*$^{-/-}$ animals precludes detailed research on the etiology of brain (and other) pathology. We therefore generated a conditional *Xpa* mouse for time and tissue specific induction of the *Csb*$^{m/m}$/*Xpa*$^{-/-}$ status (Chapter 4). Interestingly, *Csb*$^{m/m}$/*Xpa*$^{c/-}$/*CamKIIα-Cre* mice (in which *Xpa* is specifically inactivated in the cerebrum), display many CS-like neurological symptoms at older age, including cerebral atrophy and dilated ventricles, the two major neurological deficits reported in the CS brain (Nance and Berry, 1992; Ozdirim et al., 1996; Pasquier et al., 2006). In addition, animals display seizures and anxiety-like behavior, while male mutant mice develop priapism. Although we still need to determine the responsible brain area, as well as time window in which these abnormalities arise, preliminary data suggests that it starts as early as 1 month after birth. As *Xpa* was not knocked out in the cerebellum, it is not surprising that *Csb*$^{m/m}$/*Xpa*$^{c/-}$/*CamKIIα-Cre* animals do not show ataxia. However, it will be interesting to see whether the ataxic phenotype will arise when we only knock out *Xpa* in the cerebellum. Along these lines, we could specifically inactivate *Xpa* in the retina, hippocampus, and so on. These animal models would provide essential tools in further understanding of the different CS neurological aspects.

Neurodegenerative disorders represent a remarkably heterogeneous group of neurological deficits with diverse, but often overlapping clinical features that render their classification challenging (Przedborski et al., 2003). Yet, a large group of neurodegenerative diseases appears to follow a recurrent theme. For instance, neurological deficits often develop in numerous human pathological conditions associated with genetic defects in genome maintenance. Trichothiodystrophy (TTD) patients, as well as patients with some forms of Xeroderma Pigmentosum (XP), also characterized by defects in NER, demonstrate neurological symptoms as a prominent feature of their phenotypes (Bootsma et al., 2002; Bootsma, 1998; Cleaver, 2005), supporting a link between defective NER and neurodegeneration. Furthermore, defects in genes involved in DSB or SSB repair, like ataxia telangiectasia (AT) (Boder and Sedgwick, 1958; Shiloh, 1997), oculomotor apraxia (AOA1) and spinocerebellar ataxia with axonal neuropathy (SCAN1) (Caldecott, 2004), results in neurodegeneration. This insinuates a selective vulnerability of neurons to DNA damage and draws attention to the importance of DNA damage processing for long-lasting neuronal function.

TCR, part of which is TC-NER, appears not restricted to NER and can remove transcription-blocking lesions from the transcribed strand of active genes (Hanawalt, 2002; Hanawalt et al., 1994). For instance, limited evidence suggests that the function of the CSB protein might not only be restricted to TC-NER but that it also acts in other repair pathways (e.g. BER) aimed at repairing (non-NER) lesions that could still interfere with ongoing transcription (Stevnsner et al., 2002; Thorslund et al., 2005; Tuo et al., 2002). In addition, it has been previously suggested that TCR might also apply to oxidative DNA lesions, a likely scenario that has not been, however, formally proven so far (de Waard et al., 2003; Dianov et al., 1999; Spivak and Hanawalt, 2006). We have similarly shown that the *Csb*$^{m/m}$ and *Csb*$^{m/m}$/*Xpa*$^{-/-}$ animals is sensitive to oxidative DNA damage (Chapter 2 and 3).

The most obvious endogenous source of DNA damage appears to be reactive oxygen species (ROS) and other natural by products of (redox) metabolism. Owing to their extraordinary high metabolic rate, neurons are thought to be particularly susceptible to the damaging effects of ROS, the natural by products of oxidative metabolism (Limoli et al., 2004). These observations together with our data (Chapters 2, 3 and 4) suggest that the observed neurological phenotype of CS patients and the corresponding $Csb^{m/m}/Xpa^{-/-}$ and $Csb^{m/m}/Xpa^{c/-}$*/CamKIIα-Cre* mouse models is caused by unrepaired endogenous DNA damage.

CS and intervention

Since ROS represent a major source of endogenous damage, we hypothesized that lowering ROS levels would result in reduced DNA damage levels, and as a consequence, would alleviate the phenotype of the $Csb^{m/m}/Xpa^{-/-}$ mouse. Indeed, when we tested two small compounds with radical scavenging properties, we were able to increase the yield and survival of $Csb^{m/m}/Xpa^{-/-}$ pups significantly (Chapter 5). In addition, we observed that food composition has a huge effect on the $Csb^{m/m}/Xpa^{-/-}$ phenotype, and as a consequence, the intervention assay. Moreover, we were even able to increase the lifespan of $Csb^{m/m}/Xpa^{-/-}$ animals from a maximum of 23 days to at least 72 days by changing food composition. Interestingly, a male $Csb^{m/m}/Xpa^{-/-}$ mouse that survived beyond weaning, displayed priapism later in life, a feature also observed in the brain-specific $Csb^{m/m}/Xpa^{c/-}$*/CamKIIα-Cre* mouse and which points to neurological dysfunction (Chapter 5).

These findings pave the path for the development of cellular and animal screening assays for compounds that have a beneficial effect on the CS phenotype. Considering that the $Csb^{m/m}/Xpa^{-/-}$ survival/lifespan assay is very sensitive, we need to develop more specific and more robust assays. We suggested that the increase in apoptotic cell death (either naturally with age or induced by DNA damage) could be a possible better read-out system. Importantly, since animal experiments cannot be performed at high throughput scale, one would like to employ a cell-based pre-screening system to find potential candidate compounds for intervention studies in the live animal. To this end, we may use $Csb^{m/m}$ and $Csb^{m/m}/Xpa^{-/-}$ MEFs, but also CS patient fibroblast cell lines in a semi-high throughput system. We could then challenge these cells with chronic doses of genotoxic agents and see which compounds have a positive counter-acting effect on cellular endpoints like cell viability and cell death. Since the brain seems to play a key role in the observed phenotypes, one could ideally implement such an assay on retinal cell layers or brain slices kept in culture. To study more suitable endpoints in the described CS mouse models, and to find compounds that have a positive effect, it will be crucial to uncover as many parallels with CS as possible. Preferably, one would want to study non-invasive parameters to monitor the alleviating effect of administered nutraceuticals and pharmaceuticals on the progression of the disease. In this regard, IGF-1 and glucose serum levels (without fasting; see also Chapter 2) could be measured in CS patients. Also, we should aim at finding CS-associated biomarkers in urine of patients. Last but not least, by using conditional $Csb^{m/m}/Xpa^{c/-}$ mouse models, we will be able to focus intervention strategies on specific CS features, such as neurodegeneration (as in $Csb^{m/m}/Xpa^{c/-}$*/CamKIIα-Cre* animals), photoreceptor-loss, and other tissues and symptoms.

In conclusion, the findings described in this thesis have elucidated several important questions as to the how and why of the CS phenotype and could together open perspectives towards an intervention strategy. But, as it often happens in science, we answered some important questions, yet we opened the door to many more that need to be answered in the future.

Samenvatting

Inleiding

Het lichaam van de mens is opgebouwd uit miljoenen cellen die elk een unieke functie vervullen. Er bestaan ongeveer 200 verschillende soorten cellen, waaronder zenuwcellen, huidcellen en levercellen. Al deze cellen samen vormen een organisme. Cellen zijn opgebouwd uit lipiden (vetten), eiwitten en DNA. Deze structuren worden continu beschadigd tijdens het leven van een organisme. In dit proefschrift bespreken we voornamelijk de gevolgen van schade aan het DNA, met nadruk op de erfelijke ziekte Cockayne syndroom. Patienten met deze ziekte kunnen DNA schade niet goed repareren, met als gevolg groeiproblemen, ernstige neurologische achteruitgang, alsmede een groot aantal symptomen die duiden op vroegtijdige veroudering.

DNA is een macromolecuul dat zich bevindt in de kern van iedere cel. Het bevat de erfelijke informatie voor het uitgroeien van een bevruchte eicel tot een volwaardig individu, alsmede voor het specifiek functioneren van cellen (bijv. spier-, bloed-, zenuwcellen) in de verschillende organen waaruit het lichaam is opgebouwd. Er zijn echter heel veel stoffen en stralingsbronnen die het DNA kunnen beschadigen en daardoor een gevaar vormen voor de integriteit van het DNA, en dus voor het functioneren van de cellen. Hierbij moet men niet alleen denken aan toxische stoffen en stralingsbronnen uit het milieu (bijvoorbeeld zonlicht, röntgenstraling, uitlaatgassen, sigarettenrook, chemische oplosmiddelen), maar ook aan stoffen die door het lichaam zelf worden geproduceerd (zuurstofradikalen). Schade aan het DNA kan verstrekkende gevolgen hebben. Zo kunnen bij het kopiëren van beschadigd DNA permanente veranderingen in de genetische code (mutaties) ontstaan waardoor cellen ongeremd kunnen gaan delen en uiteindelijk kanker kunnen veroorzaken. Ook kunnen DNA beschadigingen leiden tot het stoppen van celdeling of zelfs resulteren in celdood, waardoor de weefselsamenstelling wordt verstoord, met als consequentie veroudering.

Gelukkig heeft de cel meerdere methodes ontwikkeld om DNA beschadigingen te verwijderen. Het DNA herstel mechanisme dat uitgebreid wordt besproken in dit proefschrift is ‘Nucleotide Excision Repair’ (Nucleotide Excisie Herstel), ook wel afgekort als NER. Dit mechanisme verwijdert een groot scala aan DNA lesies (zoals beschadigingen veroorzaakt door zonlicht en veel chemische stoffen) en bestaat uit twee onderdelen. Globaal genoom NER (GG-NER) verwijdert schade in al het DNA, maar heeft als nadeel dat het niet altijd even efficient werkt. Transcriptie-gekoppeld NER (TC-NER) zorgt voor het schadevrij houden van actieve genen om te voorkomen dat DNA beschadigingen het overschrijven van het DNA in boodschapper RNA moleculen (transcriptie, nodig voor het aanmaken van eiwitten) belemmeren.

Defecten in NER kunnen ernstige gevolgen hebben voor de gezondheid, wat wordt geïllustreerd door een groep van erfelijke ziekten, bestaande uit Xeroderma Pigmentosum (XP, veroorzaakt door mutaties in de genen *XPA* tot en met *G*), Trichothiodystrofie (TTD, veroorzaakt door mutaties in de genen *XPB*, *XPD* en *TTDA*) en Cockayne Syndrome (CS, veroorzaakt door mutaties in de genen *CSA* en *CSB*). XP patiënten zijn erg gevoelig voor zonlicht en kunnen UV-geïnduceerde DNA lesies niet repareren, waardoor ze een sterk verhoogd risico hebben op het krijgen van huidkanker op zon-geëxposeerde delen van het lichaam. CS patiënten zijn ook gevoelig voor zonlicht, maar krijgen geen huidkanker. Wel hebben deze patiënten een groot aantal andere ernstige symptomen, zoals groeiachterstand, botproblemen, neurologische afwijkingen en een sterk verkorte levensduur (gemiddelde leeftijd van overlijden 12 jaar). TTD patiënten vertonen vergelijkbare symptomen als CS patiënten, maar hebben daarbij ook een geschilferde huid en breekbaar haar. Zowel TTD als CS worden beschouwd als verouderingssyndromen.

Dit proefschrift

In dit proefschrift hebben we gebruik gemaakt van muismodellen voor CS om inzicht te verkrijgen in het ontstaan en verloop van de ziekte. Bovendien zijn de diermodellen gebruikt om te onderzoeken of het mogelijk is om het verloop van de ziekte te vertragen.

Resultaten en conclusies

De $Csb^{m/m}$ muis (een van de twee eerder in ons laboratorium gegenereerde diermodellen voor CS) heeft, net als CS patiënten, alleen een defect in TC-NER en een UV-gevoelige huid. De dieren vertonen echter nauwelijks andere CS symptomen zoals groeiproblemen en neurologische afwijkingen. In hoofdstuk 2 laten we zien dat uitschakeling van GG-NER in de $Csb^{m/m}$ muis (door gelijktijdige inactivatie van het *Xpa* gen) resulteert in een muis die heel veel overeenkomst vertoont met de CS patiënt. $Csb^{m/m}/Xpa^{-/-}$ muizen hebben een sterke groeiachterstand en overlijden binnen 3 weken na geboorte. Verder hebben we door middel van micro-array analyse gekeken naar de boodschapper RNA profielen in de lever van de 2 weken oude $Csb^{m/m}/Xpa^{-/-}$ muis. Deze methode laat zien welke genen actief zijn en of die genen in de $Csb^{m/m}/Xpa^{-/-}$ muis juist meer of minder actief zijn dan in de lever van een even oude normale nestgenoot. Uit deze experimenten bleek allereerst dat het gen expressie patroon van de $Csb^{m/m}/Xpa^{-/-}$ lever sterk overeenkwam met dat van een normale lever van een zeer oude muis. Bovendien bleek in het gehele lichaam van de $Csb^{m/m}/Xpa^{-/-}$ dieren een respons te zijn opgewekt (verlaging GH/IGF1 as en metabolisme, verhoging anti-oxidant respons) die probeert het niveau van reactieve metabolieten (en daardoor DNA schade) te verlagen. Deze response verklaart ook de groeiproblemen in CS. Een zelfde respons is ook aangetoond in muizen die door mutaties van bepaalde genen langer leven en werd door ons ook gevonden in normale muizen die waren behandeld met DNA beschadigende stoffen. Hieruit bleek dat een hoger DNA schade niveau, veroorzaakt door het transcriptie-gekoppeld DNA herstel defect, een respons induceert die het leven zou moeten verlengen. Omdat de $Csb^{m/m}/Xpa^{-/-}$ muizen niet waren blootgesteld aan DNA beschadigende stoffen, moet de oorzaak voor deze schade van binnen af komen (bijvoorbeeld via reactieve zuurstof radikalen). De conclusie van deze bevindingen is dus dat DNA schade, in combinatie met een TC-NER defect bijdraagt aan het proces van veroudering.

In hoofdstuk 3 hebben we ons gericht op een bepaald aspect van het ziektebeeld van CS, namelijk oogafwijkingen. We vonden dat blootstelling van de $Csb^{m/m}$ muis aan UV in het oog resulteerde in ernstige oogtumoren. Bovendien vonden we dat de $Csb^{m/m}$ muis van nature fotoreceptor cellen verliest uit de retina van het oog, naarmate deze ouder wordt. Dit verschijnsel, retinale degeneratie, is een veel voorkomende oogafwijking bij CS. Het verlies van fotoreceptor cellen kon ook worden geïnduceerd door middel van DNA beschadigende stoffen. Dit betekent dat (ongerepareerde) DNA schade de onderliggende oorzaak van de retinale degeneratie zou kunnen zijn.

In hoofdstuk 4 hebben we het ontstaan van neurologische afwijkingen in CS nader onderzocht. Omdat de $Csb^{m/m}$ muis nauwelijks een neurologisch phenotype vertoont, en $Csb^{m/m}/Xpa^{-/-}$ muizen te kort leven om neurologische afwijkingen tot in detail te bestuderen, hebben we een conditionele *Xpa* muis gegenereerd. In dit diermodel kan het *Xpa* gen naar keuze worden uitgeschakeld in bepaalde weefsels. We hebben gevonden dat inactivatie van het *Xpa* gen in de grote hersenen van de $Csb^{m/m}$ muis tot gevolg heeft dat in oudere dieren de hersenen kleiner worden (atrofie) en dat de ventrikels sterk vergroot waren. Deze pathologische afwijkingen worden ook gevonden in de CS patiënt. Deze resultaten tonen wederom aan dat aspecten van het CS ziektebeeld kunnen worden veroorzaakt door ongerepareerde endogene DNA schade. Dit nieuwe muismodel zal in vervolgonderzoek worden gebruikt om het neurologische aspect van CS verder te onderzoeken.

CS een zeer ernstige ziekte, waarvoor geen behandeling bestaat, maar waarbij wel wordt geprobeerd de afzonderlijke symptomen te verlichten (bijvoorbeeld het geven van een rolstoel wanneer de patiënt niet meer kan lopen). Derhalve bestaat er behoefte aan een interventie methode, waarbij het ontstaan van de symptomen zo lang mogelijk wordt uitgesteld en de ernst van de symptomen wordt afgezwakt. Een dergelijke methode zou kunnen bestaan uit het verlagen van de kans op het ontstaan van DNA schade door reactieve metabolieten. Radicalen kunnen worden weggevangen door radicaal scavengers. In hoofdstuk 5 hebben we aangetoond dat behandeling van $Csb^{m/m}/Xpa^{-/-}$ muizen met twee stoffen met een scavenger functie een positief effect had op de overleving. Verder bleek ook dat de samenstelling van het muisvoer van invloed is op de levensverwachting van de $Csb^{m/m}/Xpa^{-/-}$ muis. Deze bevindingen openen mogelijk nieuwe deuren voor het ontwikkelen van een interventiestrategie voor CS.

References

Abdo, K. M., Haseman, J. K., Boorman, G., Farnell, D. R., Prejean, J. D., and Kovatch, R. (1983). Absence of carcinogenic response in F344 rats and B6C3F1 mice given D-mannitol in the diet for two years. Food Chem Toxicol *21*, 259-262.

Aboussekhra, A., Biggerstaff, M., Shivji, M. K., Vilpo, J. A., Moncollin, V., Podust, V. N., Protic, M., Hubscher, U., Egly, J. M., and Wood, R. D. (1995). Mammalian DNA nucleotide excision repair reconstituted with purified protein components. Cell *80*, 859-868.

Adams, D. D., Lucas, W. O., Williams, B. G., Berkeley, B. B., Turner, K. W., and Schofield, J. C. (2001). A mouse genetic locus with death clock and life clock features. Mech Ageing Dev *122*, 173-189.

Ahima, R., and Osei, S. Y. (2004). Leptin and appetite control in lipodystrophy. J Clin Endocrinol Metab *89*, 4254-4257.

Alia, Mohanty, P., and Matysik, J. (2001). Effect of proline on the production of singlet oxygen. Amino Acids *21*, 195-200.

Ames, B. N. (1989). Endogenous oxidative DNA damage, aging, and cancer. Free Radic Res Commun *7*, 121-128.

Ames, B. N., Gold, L. S., and Willett, W. C. (1995). The causes and prevention of cancer. Proc Natl Acad Sci U S A *92*, 5258-5265.

Amoaku, W. M., Frew, L., Mahon, G. J., Gardiner, T. A., and Archer, D. B. (1989). Early ultrastructural changes after low-dose X-irradiation in the retina of the rat. Eye *3 (Pt 5)*, 638-646.

Andersen, B., Pearse, R. V., 2nd, Jenne, K., Sornson, M., Lin, S. C., Bartke, A., and Rosenfeld, M. G. (1995). The Ames dwarf gene is required for Pit-1 gene activation. Dev Biol *172*, 495-503.

Andressoo, J. O., Mitchell, J. R., de Wit, J., Hoogstraten, D., Volker, M., Toussaint, W., Speksnijder, E., Beems, R. B., van Steeg, H., Jans, J*., et al.* (2006). An Xpd mouse model for the combined xeroderma pigmentosum/Cockayne syndrome exhibiting both cancer predisposition and segmental progeria. Cancer Cell *10*, 121-132.

Araujo, S. J., Tirode, F., Coin, F., Pospiech, H., Syvaoja, J. E., Stucki, M., Hubscher, U., Egly, J. M., and Wood, R. D. (2000). Nucleotide excision repair of DNA with recombinant human proteins: definition of the minimal set of factors, active forms of TFIIH, and modulation by CAK. Genes Dev *14*, 349-359.

Argiolas, A., and Melis, M. R. (2005). Central control of penile erection: role of the paraventricular nucleus of the hypothalamus. Prog Neurobiol *76*, 1-21.

Arking, R. (1998). Biology of aging; observations and principles, 2 edn (Sunderland, Sinauer Associates).

Baker, P. B., Baba, N., and Boesel, C. P. (1981). Cardiovascular abnormalities in progeria. Case report and review of the literature. Arch Pathol Lab Med *105*, 384-386.

Balaban, R. S., Nemoto, S., and Finkel, T. (2005). Mitochondria, oxidants, and aging. Cell *120*, 483-495.

Balajee, A. S., May, A., Dianov, G. L., Friedberg, E. C., and Bohr, V. A. (1997). Reduced RNA polymerase II transcription in intact and permeabilized Cockayne syndrome group B cells. Proc Natl Acad Sci U S A *94*, 4306-4311.

Barnes, D. E., Stamp, G., Rosewell, I., Denzel, A., and Lindahl, T. (1998). Targeted disruption of the gene encoding DNA ligase IV leads to lethality in embryonic mice. Curr Biol *8*, 1395-1398.

Bartke, A. (2003). Is growth hormone deficiency a beneficial adaptation to aging? Evidence from experimental animals. Trends Endocrinol Metab *14*, 340-344.

Bartke, A., Chandrashekar, V., Bailey, B., Zaczek, D., and Turyn, D. (2002). Consequences of growth hormone (GH) overexpression and GH resistance. Neuropeptides *36*, 201-208.

Bartke, A., Wright, J. C., Mattison, J. A., Ingram, D. K., Miller, R. A., and Roth, G. S. (2001). Extending the lifespan of long-lived mice. Nature *414*, 412.

Batty, D., Rapic'-Otrin, V., Levine, A. S., and Wood, R. D. (2000). Stable binding of human XPC complex to irradiated DNA confers strong discrimination for damaged sites. J Mol Biol *300*, 275-290.

Beatty, S., Koh, H., Phil, M., Henson, D., and Boulton, M. (2000). The role of oxidative stress in the pathogenesis of age-related macular degeneration. Surv Ophthalmol *45*, 115-134.

Beckman, K. B., and Ames, B. N. (1997). Oxidative decay of DNA. J Biol Chem *272*, 19633-19636.

Beckman, K. B., and Ames, B. N. (1998). The free radical theory of aging matures. Physiol Rev *78*, 547-581.

Berg, R. J., Rebel, H., van der Horst, G. T., van Kranen, H. J., Mullenders, L. H., van Vloten, W. A., and de Gruijl, F. R. (2000). Impact of global genome repair versus transcription-coupled repair on ultraviolet carcinogenesis in hairless mice. Cancer Res *60*, 2858-2863.

Berg, R. J., Ruven, H. J., Sands, A. T., de Gruijl, F. R., and Mullenders, L. H. (1998). Defective global genome repair in XPC mice is associated with skin cancer susceptibility but not with sensitivity to UVB induced erythema and edema. J Invest Dermatol *110*, 405-409.

Bernstein, C., Bernstein, H., Payne, C. M., and Garewal, H. (2002). DNA repair/pro-apoptotic dual-role proteins in five major DNA repair pathways: fail-safe protection against carcinogenesis. Mutat Res *511*, 145-178.

Bessho, T. (1999). Nucleotide excision repair 3' endonuclease XPG stimulates the activity of base excision repairenzyme thymine glycol DNA glycosylase. Nucleic Acids Res *27*, 979-983.

Betarbet, R., Sherer, T. B., and Greenamyre, J. T. (2002). Animal models of Parkinson's disease. Bioessays *24*, 308-318.

Betz, U. A., Vosshenrich, C. A., Rajewsky, K., and Muller, W. (1996). Bypass of lethality with mosaic mice generated by Cre-loxP-mediated recombination. Curr Biol *6*, 1307-1316.

Blasco, M. A., Lee, H. W., Hande, M. P., Samper, E., Lansdorp, P. M., DePinho, R. A., and Greider, C. W. (1997). Telomere shortening and tumor formation by mouse cells lacking telomerase RNA. Cell *91*, 25-34.

Boder, E., and Sedgwick, R. P. (1958). Ataxia-telangiectasia; a familial syndrome of progressive cerebellar ataxia, oculocutaneous telangiectasia and frequent pulmonary infection. Pediatrics *21*, 526-554.

Bohr, V. A., Smith, C. A., Okumoto, D. S., and Hanawalt, P. C. (1985). DNA repair in an active gene: removal of pyrimidine dimers from the DHFR gene of CHO cells is much more efficient than in the genome overall. Cell *40*, 359-369.

Bootsma, D., and Hoeijmakers, J. H. (1993). DNA repair. Engagement with transcription. Nature *363*, 114-115.

Bootsma, D., Kraemer, K. H., J.E., C., and Hoeijmakers, J. (2002). Nucleotide excision repair syndromes: Xeroderma Pigmentosum, Cockayne Syndrome and trichthiodystrophy (New York, McGraw-Hill Medical Publishing Division).

Bootsma, D., Kraemer,K.H., Cleaver,J.E., Hoeijmakers,J.H.J. (1998). Nucleotide excision repair syndromes: xeroderma pigmentosum, Cockayne syndrome and trichothiodystrophy. In The genetic basis of human cancer, B. Vogelstein, Kinzler, K.W., ed. (McGraw-Hill New-York), pp. 245-274.

Bootsma, D., Kraemer,K.H., Cleaver,J.E., Hoeijmakers,J.H.J. (2001). Nucleotide excision repair syndromes: xeroderma pigmentosum, Cockayne syndrome and trichothiodystrophy. In The metabolic and molecular basis of inherited disease, C. R. Scriver, Beaudet, A. L., Sly, W. S. & Valle, D., ed. (New York, McGraw-Hill, New York, 2001), pp. 677-703.

Bootsma, D., Weeda, G., Vermeulen, W., van Vuuren, H., Troelstra, C., van der Spek, P., and Hoeijmakers, J. (1995). Nucleotide excision repair syndromes: molecular basis and clinical symptoms. Philos Trans R Soc Lond B Biol Sci *347*, 75-81.

Bradsher, J., Coin, F., and Egly, J. M. (2000). Distinct roles for the helicases of TFIIH in transcript initiation and promoter escape. J Biol Chem *275*, 2532-2538.

Brooks, P. J., Wise, D. S., Berry, D. A., Kosmoski, J. V., Smerdon, M. J., Somers, R. L., Mackie, H., Spoonde, A. Y., Ackerman, E. J., Coleman, K*., et al.* (2000). The oxidative DNA lesion 8,5'-(S)-cyclo-2'-deoxyadenosine is repaired by the nucleotide excision repair pathway and blocks gene expression in mammalian cells. J Biol Chem *275*, 22355-22362.

Brown-Borg, H. M., Bode, A. M., and Bartke, A. (1999). Antioxidative mechanisms and plasma growth hormone levels: potential relationship in the aging process. Endocrine *11*, 41-48.

Brown-Borg, H. M., Johnson, W.T., Rakoczy, S., Romanick, M (2001). Mitochondrial oxidant generation and oxidative damage in Ames dwarf and GH transgenic mice. J Am Aging Assoc *85*, 85-100.

Brown-Borg, H. M., and Rakoczy, S. G. (2000). Catalase expression in delayed and premature aging mouse models. Exp Gerontol *35*, 199-212.

Brumback, R. A., Yoder, F. W., Andrews, A. D., Peck, G. L., and Robbins, J. H. (1978). Normal pressure hydrocephalus. Recognition and relationship to neurological abnormalities in Cockayne's syndrome. Arch Neurol *35*, 337-345.

Burton, G. W., Foster, D. O., Perly, B., Slater, T. F., Smith, I. C., and Ingold, K. U. (1985). Biological antioxidants. Philos Trans R Soc Lond B Biol Sci *311*, 565-578.

Buschta-Hedayat, N., Buterin, T., Hess, M. T., Missura, M., and Naegeli, H. (1999). Recognition of nonhybridizing base pairs during nucleotide excision repair of DNA. Proc Natl Acad Sci U S A *96*, 6090-6095.

Cadet, J., Berger, M., Douki, T., and Ravanat, J. L. (1997). Oxidative damage to DNA: formation, measurement, and biological significance. Rev Physiol Biochem Pharmacol *131*, 1-87.

Cadet, J., Douki, T., Gasparutto, D., and Ravanat, J. L. (2003). Oxidative damage to DNA: formation, measurement and biochemical features. Mutat Res *531*, 5-23.

Caldecott, K. W. (2004). DNA single-strand breaks and neurodegeneration. DNA Repair (Amst) *3*, 875-882.

Camougrand, N., and Rigoulet, M. (2001). Aging and oxidative stress: studies of some genes involved both in aging and in response to oxidative stress. Respir Physiol *128*, 393-401.

Campisi, J. (2001). Cellular senescence as a tumor-suppressor mechanism. Trends Cell Biol *11*, S27-31.

Cao, H., and Hegele, R. A. (2003). LMNA is mutated in Hutchinson-Gilford progeria (MIM 176670) but not in Wiedemann-Rautenstrauch progeroid syndrome (MIM 264090). J Hum Genet *48*, 271-274.

Carter, C. S., Ramsey, M. M., Ingram, R. L., Cashion, A. B., Cefalu, W. T., Wang, Z. Q., and Sonntag, W. E. (2002a). Models of growth hormone and IGF-1 deficiency: applications to studies of aging processes and life-span determination. J Gerontol A Biol Sci Med Sci *57*, B177-188.

Carter, C. S., Ramsey, M. M., and Sonntag, W. E. (2002b). A critical analysis of the role of growth hormone and IGF-1 in aging and lifespan. Trends Genet *18*, 295-301.

Carter, R. J., Lione, L. A., Humby, T., Mangiarini, L., Mahal, A., Bates, G. P., Dunnett, S. B., and Morton, A. J. (1999). Characterization of progressive motor deficits in mice transgenic for the human Huntington's disease mutation. J Neurosci *19*, 3248-3257.

Carter-Dawson, L. D., and LaVail, M. M. (1979). Rods and cones in the mouse retina. II. Autoradiographic analysis of cell generation using tritiated thymidine. J Comp Neurol *188*, 263-272.

Chandrashekar, V., Zaczek, D., and Bartke, A. (2004). The consequences of altered somatotropic system on reproduction. Biol Reprod *71*, 17-27.

Chen, C., and Dickman, M. B. (2005). Proline suppresses apoptosis in the fungal pathogen Colletotrichum trifolii. Proc Natl Acad Sci U S A *102*, 3459-3464.

Chen, X., Zhang, Y., Douglas, L., and Zhou, P. (2001). UV-damaged DNA-binding proteins are targets of CUL-4A-mediated ubiquitination and degradation. J Biol Chem *276*, 48175-48182.

Cheo, D. L., Burns, D. K., Meira, L. B., Houle, J. F., and Friedberg, E. C. (1999). Mutational inactivation of the xeroderma pigmentosum group C gene confers predisposition to 2-acetylaminofluorene-induced liver and lung cancer and to spontaneous testicular cancer in Trp53-/- mice. Cancer Res *59*, 771-775.

Cheo, D. L., Meira, L. B., Burns, D. K., Reis, A. M., Issac, T., and Friedberg, E. C. (2000). Ultraviolet B radiation-induced skin cancer in mice defective in the Xpc, Trp53, and Apex (HAP1) genes: genotype-specific effects on cancer predisposition and pathology of tumors. Cancer Res *60*, 1580-1584.

Cheo, D. L., Meira, L. B., Hammer, R. E., Burns, D. K., Doughty, A. T., and Friedberg, E. C. (1996). Synergistic interactions between XPC and p53 mutations in double-mutant mice: neural tube abnormalities and accelerated UV radiation-induced skin cancer. Curr Biol *6*, 1691-1694.

Cheo, D. L., Ruven, H. J., Meira, L. B., Hammer, R. E., Burns, D. K., Tappe, N. J., van Zeeland, A. A., Mullenders, L. H., and Friedberg, E. C. (1997). Characterization of defective nucleotide excision repair in XPC mutant mice. Mutat Res *374*, 1-9.

Chipchase, M. D., O'Neill, M., and Melton, D. W. (2003). Characterization of premature liver polyploidy in DNA repair (Ercc1)-deficient mice. Hepatology *38*, 958-966.

Citterio, E., Van Den Boom, V., Schnitzler, G., Kanaar, R., Bonte, E., Kingston, R. E., Hoeijmakers, J. H., and Vermeulen, W. (2000). ATP-dependent chromatin remodeling by the Cockayne syndrome B DNA repair-transcription-coupling factor. Mol Cell Biol *20*, 7643-7653.

Clarke, G., Collins, R. A., Leavitt, B. R., Andrews, D. F., Hayden, M. R., Lumsden, C. J., and McInnes, R. R. (2000). A one-hit model of cell death in inherited neuronal degenerations. Nature *406*, 195-199.

Cleaver, J. E. (2005). Cancer in xeroderma pigmentosum and related disorders of DNA repair. Nat Rev Cancer *5*, 564-573.

Cockayne, E. A. (1936). Dwarfism with retinal atrophy and deafness. Arch Dis Child *11*, 1-8.

Cooke, M. S., Evans, M. D., Dizdaroglu, M., and Lunec, J. (2003). Oxidative DNA damage: mechanisms, mutation, and disease. Faseb J *17*, 1195-1214.

Cooper, P. K., Nouspikel, T., Clarkson, S. G., and Leadon, S. A. (1997). Defective transcription-coupled repair of oxidative base damage in Cockayne syndrome patients from XP group G. Science *275*, 990-993.

Cosolo, W. C., Martinello, P., Louis, W. J., and Christophidis, N. (1989). Blood-brain barrier disruption using mannitol: time course and electron microscopy studies. Am J Physiol *256*, R443-447.

Curcio, C. A., Millican, C. L., Allen, K. A., and Kalina, R. E. (1993). Aging of the human photoreceptor mosaic: evidence for selective vulnerability of rods in central retina. Invest Ophthalmol Vis Sci *34*, 3278-3296.

Davies, K. J. (1995). Oxidative stress: the paradox of aerobic life. Biochem Soc Symp *61*, 1-31.

de Boer, J., Andressoo, J. O., de Wit, J., Huijmans, J., Beems, R. B., van Steeg, H., Weeda, G., van der Horst, G. T., van Leeuwen, W., Themmen, A. P.*, et al.* (2002). Premature aging in mice deficient in DNA repair and transcription. Science *296*, 1276-1279.

de Boer, J., de Wit, J., van Steeg, H., Berg, R. J., Morreau, H., Visser, P., Lehmann, A. R., Duran, M., Hoeijmakers, J. H., and Weeda, G. (1998a). A mouse model for the basal transcription/DNA repair syndrome trichothiodystrophy. Mol Cell *1*, 981-990.

de Boer, J., Donker, I., de Wit, J., Hoeijmakers, J. H., and Weeda, G. (1998b). Disruption of the mouse xeroderma pigmentosum group D DNA repair/basal transcription gene results in preimplantation lethality. Cancer Res *58*, 89-94.

de Boer, J., and Hoeijmakers, J. H. (2000). Nucleotide excision repair and human syndromes. Carcinogenesis *21*, 453-460.

de Laat, W. L., Appeldoorn, E., Sugasawa, K., Weterings, E., Jaspers, N. G., and Hoeijmakers, J. H. (1998). DNA-binding polarity of human replication protein A positions nucleases in nucleotide excision repair. Genes Dev *12*, 2598-2609.

de Laat, W. L., Jaspers, N. G., and Hoeijmakers, J. H. (1999). Molecular mechanism of nucleotide excision repair. Genes Dev *13*, 768-785.

De Sandre-Giovannoli, A., Bernard, R., Cau, P., Navarro, C., Amiel, J., Boccaccio, I., Lyonnet, S., Stewart, C. L., Munnich, A., Le Merrer, M., and Levy, N. (2003). Lamin a truncation in Hutchinson-Gilford progeria. Science *300*, 2055.

de Vries, A., Dolle, M. E., Broekhof, J. L., Muller, J. J., Kroese, E. D., van Kreijl, C. F., Capel, P. J., Vijg, J., and van Steeg, H. (1997). Induction of DNA adducts and mutations in spleen, liver and lung of XPA-deficient/lacZ transgenic mice after oral treatment with benzo[a]pyrene: correlation with tumour development. Carcinogenesis *18*, 2327-2332.

de Vries, A., van Oostrom, C. T., Hofhuis, F. M., Dortant, P. M., Berg, R. J., de Gruijl, F. R., Wester, P. W., van Kreijl, C. F., Capel, P. J., van Steeg, H., and et al. (1995). Increased susceptibility to ultraviolet-B and carcinogens of mice lacking the DNA excision repair gene XPA. Nature *377*, 169-173.

de Waard, H., de Wit, J., Andressoo, J. O., van Oostrom, C. T., Riis, B., Weimann, A., Poulsen, H. E., van Steeg, H., Hoeijmakers, J. H., and van der Horst, G. T. (2004). Different effects of CSA and CSB deficiency on sensitivity to oxidative DNA damage. Mol Cell Biol *24*, 7941-7948.

de Waard, H., de Wit, J., Gorgels, T. G., van den Aardweg, G., Andressoo, J. O., Vermeij, M., van Steeg, H., Hoeijmakers, J. H., and van der Horst, G. T. (2003). Cell type-specific hypersensitivity to oxidative damage in CSB and XPA mice. DNA Repair (Amst) *2*, 13-25.

Demple, B., Herman, T., and Chen, D. S. (1991). Cloning and expression of APE, the cDNA encoding the major human apurinic endonuclease: definition of a family of DNA repair enzymes. Proc Natl Acad Sci U S A *88*, 11450-11454.

DeSanctis, C. C., A. (1932). L'ídiozia xerodermica. Riv Sper Frentiatr Med Leg Alienazioni Ment *56*, 269-292.

Deschavanne, P. J., Chavaudra, N., Fertil, B., and Malaise, E. P. (1984). Abnormal sensitivity of some Cockayne's syndrome cell strains to UV- and gamma-rays. Association with a reduced ability to repair potentially lethal damage. Mutat Res *131*, 61-70.

Dianov, G., Bischoff, C., Sunesen, M., and Bohr, V. A. (1999). Repair of 8-oxoguanine in DNA is deficient in Cockayne syndrome group B cells. Nucleic Acids Res *27*, 1365-1368.

Dianov, G. L., Houle, J. F., Iyer, N., Bohr, V. A., and Friedberg, E. C. (1997). Reduced RNA polymerase II transcription in extracts of cockayne syndrome and xeroderma pigmentosum/Cockayne syndrome cells. Nucleic Acids Res *25*, 3636-3642.

Dodson, M. L., and Lloyd, R. S. (2002). Mechanistic comparisons among base excision repair glycosylases. Free Radic Biol Med *32*, 678-682.

Dollfus, H., Porto, F., Caussade, P., Speeg-Schatz, C., Sahel, J., Grosshans, E., Flament, J., and Sarasin, A. (2003). Ocular manifestations in the inherited DNA repair disorders. Surv Ophthalmol *48*, 107-122.

Dragatsis, I., and Zeitlin, S. (2000). CaMKIIalpha-Cre transgene expression and recombination patterns in the mouse brain. Genesis *26*, 133-135.

Drapkin, R., Reardon, J. T., Ansari, A., Huang, J. C., Zawel, L., Ahn, K., Sancar, A., and Reinberg, D. (1994). Dual role of TFIIH in DNA excision repair and in transcription by RNA polymerase II. Nature *368*, 769-772.

Du, X., Shen, J., Kugan, N., Furth, E. E., Lombard, D. B., Cheung, C., Pak, S., Luo, G., Pignolo, R. J., DePinho, R. A*., et al.* (2004). Telomere shortening exposes functions for the mouse Werner and Bloom syndrome genes. Mol Cell Biol *24*, 8437-8446.

Dupuy, J. M., Lafforet, D., and Rachman, F. (1974). Xeroderma pigmentosum with liver involvement. Helv Paediatr Acta *29*, 213-219.

El-Khamisy, S. F., Saifi, G. M., Weinfeld, M., Johansson, F., Helleday, T., Lupski, J. R., and Caldecott, K. W. (2005). Defective DNA single-strand break repair in spinocerebellar ataxia with axonal neuropathy-1. Nature *434*, 108-113.

Ellaway, C. J., Duggins, A., Fung, V. S., Earl, J. W., Kamath, R., Parsons, P. G., Anthony, J. A., and North, K. N. (2000). Cockayne syndrome associated with low CSF 5-hydroxyindole acetic acid levels. J Med Genet *37*, 553-557.

Enzlin, J. H., and Scharer, O. D. (2002). The active site of the DNA repair endonuclease XPF-ERCC1 forms a highly conserved nuclease motif. Embo J *21*, 2045-2053.

Eriksson, M., Brown, W. T., Gordon, L. B., Glynn, M. W., Singer, J., Scott, L., Erdos, M. R., Robbins, C. M., Moses, T. Y., Berglund, P.*, et al.* (2003). Recurrent de novo point mutations in lamin A cause Hutchinson-Gilford progeria syndrome. Nature *423*, 293-298.

Evans, E., Moggs, J. G., Hwang, J. R., Egly, J. M., and Wood, R. D. (1997). Mechanism of open complex and dual incision formation by human nucleotide excision repair factors. Embo J *16*, 6559-6573.

Finkel, T. (2001). Reactive oxygen species and signal transduction. IUBMB Life *52*, 3-6.

Finkel, T., and Holbrook, N. J. (2000). Oxidants, oxidative stress and the biology of ageing. Nature *408*, 239-247.

Florini, J. R., Harned, J. A., Richman, R. A., and Weiss, J. P. (1981). Effect of rat age on serum levels of growth hormone and somatomedins. Mech Ageing Dev *15*, 165-176.

Fortini, P., Pascucci, B., Parlanti, E., D'Errico, M., Simonelli, V., and Dogliotti, E. (2003). The base excision repair: mechanisms and its relevance for cancer susceptibility. Biochimie *85*, 1053-1071.

Fraser, H. B., Khaitovich, P., Plotkin, J. B., Paabo, S., and Eisen, M. B. (2005). Aging and gene expression in the primate brain. PLoS Biol *3*, e274.

Fridovich, I. (1995). Superoxide radical and superoxide dismutases. Annu Rev Biochem *64*, 97-112.

Friedberg, E. C. (2003). DNA damage and repair. Nature *421*, 436-440.

Friedberg, E. C., Walker, G.C., and Siede, W. (2006). DNA repair and mutagenesis (Washington, D.C., ASM Press).

Frosina, G. (2004). Commentary: DNA base excision repair defects in human pathologies. Free Radic Res *38*, 1037-1054.

Frystyk, J. (2004). Free insulin-like growth factors -- measurements and relationships to growth hormone secretion and glucose homeostasis. Growth Horm IGF Res *14*, 337-375.

Fujimoto, W. Y., Green, M. L., and Seegmiller, J. E. (1969). Cockayne's syndrome: report of a case with hyperlipoproteinemia, hyperinsulinemia, renal disease, and normal growth hormone. J Pediatr *75*, 881-884.

Furr, B. J., and Jordan, V. C. (1984). The pharmacology and clinical uses of tamoxifen. Pharmacol Ther *25*, 127-205.

Gao, Y., Sun, Y., Frank, K. M., Dikkes, P., Fujiwara, Y., Seidl, K. J., Sekiguchi, J. M., Rathbun, G. A., Swat, W., Wang, J.*, et al.* (1998). A critical role for DNA end-joining proteins in both lymphogenesis and neurogenesis. Cell *95*, 891-902.

Giese, H., Dolle, M. E., Hezel, A., van Steeg, H., and Vijg, J. (1999). Accelerated accumulation of somatic mutations in mice deficient in the nucleotide excision repair gene XPA. Oncogene *18*, 1257-1260.

Giglia-Mari, G., Coin, F., Ranish, J. A., Hoogstraten, D., Theil, A., Wijgers, N., Jaspers, N. G., Raams, A., Argentini, M., van der Spek, P. J.*, et al.* (2004). A new, tenth subunit of TFIIH is responsible for the DNA repair syndrome trichothiodystrophy group A. Nat Genet *36*, 714-719.

Gillet, L. C., and Scharer, O. D. (2006). Molecular mechanisms of mammalian global genome nucleotide excision repair. Chem Rev *106*, 253-276.

Graham, J. M., Jr., Anyane-Yeboa, K., Raams, A., Appeldoorn, E., Kleijer, W. J., Garritsen, V. H., Busch, D., Edersheim, T. G., and Jaspers, N. G. (2001). Cerebro-oculo-facio-skeletal syndrome with a nucleotide excision-repair defect and a mutated XPD gene, with prenatal diagnosis in a triplet pregnancy. Am J Hum Genet *69*, 291-300.

Gray, J. A. M., N. (1982). The neuropsychology of anxiety: an enquiry into the functions of the septo-hippocampal system. In (Oxford, Oxford University Press).

Gray, M. D., Shen, J. C., Kamath-Loeb, A. S., Blank, A., Sopher, B. L., Martin, G. M., Oshima, J., and Loeb, L. A. (1997). The Werner syndrome protein is a DNA helicase. Nat Genet *17*, 100-103.

Gregory, S. M., and Sweder, K. S. (2001). Deletion of the CSB homolog, RAD26, yields Spt(-) strains with proficient transcription-coupled repair. Nucleic Acids Res *29*, 3080-3086.

Groisman, R., Kuraoka, I., Chevallier, O., Gaye, N., Magnaldo, T., Tanaka, K., Kisselev, A. F., Harel-Bellan, A., and Nakatani, Y. (2006). CSA-dependent degradation of CSB by the ubiquitin-proteasome pathway establishes a link between complementation factors of the Cockayne syndrome. Genes Dev *20*, 1429-1434.

Groisman, R., Polanowska, J., Kuraoka, I., Sawada, J., Saijo, M., Drapkin, R., Kisselev, A. F., Tanaka, K., and Nakatani, Y. (2003). The ubiquitin ligase activity in the DDB2 and CSA complexes is differentially regulated by the COP9 signalosome in response to DNA damage. Cell *113*, 357-367.

Gu, Y., Sekiguchi, J., Gao, Y., Dikkes, P., Frank, K., Ferguson, D., Hasty, P., Chun, J., and Alt, F. W. (2000). Defective embryonic neurogenesis in Ku-deficient but not DNA-dependent protein kinase catalytic subunit-deficient mice. Proc Natl Acad Sci U S A *97*, 2668-2673.

Halliwell, B. G., JM. (1985). Oxygen radicals and the nervous system. Trends in Neurosciences *8*, 22-26.

Halliwell, B. G., JM. (1989). Free Radicals in Biology and Medicine.

Hamdi, M., Kool, J., Cornelissen-Steijger, P., Carlotti, F., Popeijus, H. E., van der Burgt, C., Janssen, J. M., Yasui, A., Hoeben, R. C., Terleth, C*., et al.* (2005). DNA damage in transcribed genes induces apoptosis via the JNK pathway and the JNK-phosphatase MKP-1. Oncogene *24*, 7135-7144.

Hamilton, M. L., Van Remmen, H., Drake, J. A., Yang, H., Guo, Z. M., Kewitt, K., Walter, C. A., and Richardson, A. (2001). Does oxidative damage to DNA increase with age? Proc Natl Acad Sci U S A *98*, 10469-10474.

Hanawalt, P. C. (2002). Subpathways of nucleotide excision repair and their regulation. Oncogene *21*, 8949-8956.

Hanawalt, P. C., Donahue, B. A., and Sweder, K. S. (1994). Repair and transcription. Collision or collusion? Curr Biol *4*, 518-521.

Harada, Y. N., Shiomi, N., Koike, M., Ikawa, M., Okabe, M., Hirota, S., Kitamura, Y., Kitagawa, M., Matsunaga, T., Nikaido, O., and Shiomi, T. (1999). Postnatal growth failure, short life span, and early onset of cellular senescence and subsequent immortalization in mice lacking the xeroderma pigmentosum group G gene. Mol Cell Biol *19*, 2366-2372.

Harman, D. (1956). Aging: a theory based on free radical and radiation chemistry. J Gerontol *11*, 298-300.

Hasty, P., Campisi, J., Hoeijmakers, J., van Steeg, H., and Vijg, J. (2003). Aging and genome maintenance: lessons from the mouse? Science *299*, 1355-1359.

Hatahet, Z., Purmal, A. A., and Wallace, S. S. (1994). Oxidative DNA lesions as blocks to in vitro transcription by phage T7 RNA polymerase. Ann N Y Acad Sci *726*, 346-348.

Hauck, S. B., A (2001). Effects of growth hormone on hypothalamic catalase and Cu/Zn superoxide dismutase. Free Radic Biol Med *28*, 970-978.

Helfand, S. L., and Rogina, B. (2003). Molecular genetics of aging in the fly: is this the end of the beginning? Bioessays *25*, 134-141.

Henning, K. A., Li, L., Iyer, N., McDaniel, L. D., Reagan, M. S., Legerski, R., Schultz, R. A., Stefanini, M., Lehmann, A. R., Mayne, L. V., and et al. (1995). The Cockayne syndrome group A gene encodes a WD repeat protein that interacts with CSB protein and a subunit of RNA polymerase II TFIIH. Cell *82*, 555-564.

Herrera, E., Samper, E., Martin-Caballero, J., Flores, J. M., Lee, H. W., and Blasco, M. A. (1999). Disease states associated with telomerase deficiency appear earlier in mice with short telomeres. Embo J *18*, 2950-2960.

Hess, M. T., Schwitter, U., Petretta, M., Giese, B., and Naegeli, H. (1997). Bipartite substrate discrimination by human nucleotide excision repair. Proc Natl Acad Sci U S A *94*, 6664-6669.

Hirano, T., Yamaguchi, Y., Hirano, H., and Kasai, H. (1995). Age-associated change of 8-hydroxyguanine repair activity in cultured human fibroblasts. Biochem Biophys Res Commun *214*, 1157-1162.

Hirosawa, N., Yano, K., Suzuki, Y., and Sakamoto, Y. (2006). Endocrine disrupting effect of di-(2-ethylhexyl)phthalate on female rats and proteome analyses of their pituitaries. Proteomics *6*, 958-971.

Hoeijmakers, J. H. (2001). Genome maintenance mechanisms for preventing cancer. Nature *411*, 366-374.

Hollander, M. C., Philburn, R. T., Patterson, A. D., Velasco-Miguel, S., Friedberg, E. C., Linnoila, R. I., and Fornace, A. J., Jr. (2005). Deletion of XPC leads to lung tumors in mice and is associated with early events in human lung carcinogenesis. Proc Natl Acad Sci U S A *102*, 13200-13205.

Holmes, A. (2001). Targeted gene mutation approaches to the study of anxiety-like behavior in mice. Neurosci Biobehav Rev *25*, 261-273.

Horibata, K., Iwamoto, Y., Kuraoka, I., Jaspers, N. G., Kurimasa, A., Oshimura, M., Ichihashi, M., and Tanaka, K. (2004). Complete absence of Cockayne syndrome group B gene product gives rise to UV-sensitive syndrome but not Cockayne syndrome. Proc Natl Acad Sci U S A *101*, 15410-15415.

Hosack, D. A., Dennis, G., Jr., Sherman, B. T., Lane, H. C., and Lempicki, R. A. (2003). Identifying biological themes within lists of genes with EASE. Genome Biol *4*, R70.

Htun, H., and Johnston, B. H. (1992). Mapping adducts of DNA structural probes using transcription and primer extension approaches. Methods Enzymol *212*, 272-294.

Hwang, B. J., Ford, J. M., Hanawalt, P. C., and Chu, G. (1999). Expression of the p48 xeroderma pigmentosum gene is p53-dependent and is involved in global genomic repair. Proc Natl Acad Sci U S A *96*, 424-428.

Hwang, B. J., Toering, S., Francke, U., and Chu, G. (1998). p48 Activates a UV-damaged-DNA binding factor and is defective in xeroderma pigmentosum group E cells that lack binding activity. Mol Cell Biol *18*, 4391-4399.

Hwang, D. Y., and Ismail-Beigi, F. (2001). Stimulation of GLUT-1 glucose transporter expression in response to hyperosmolarity. Am J Physiol Cell Physiol *281*, C1365-1372.

Imai, T., Chambon, P., and Metzger, D. (2000). Inducible site-specific somatic mutagenesis in mouse hepatocytes. Genesis *26*, 147-148.

Ishii, N., Fujii, M., Hartman, P. S., Tsuda, M., Yasuda, K., Senoo-Matsuda, N., Yanase, S., Ayusawa, D., and Suzuki, K. (1998). A mutation in succinate dehydrogenase cytochrome b causes oxidative stress and ageing in nematodes. Nature *394*, 694-697.

Itin, P. H., and Pittelkow, M. R. (1990). Trichothiodystrophy: review of sulfur-deficient brittle hair syndromes and association with the ectodermal dysplasias. J Am Acad Dermatol *22*, 705-717.

Itin, P. H., Sarasin, A., and Pittelkow, M. R. (2001). Trichothiodystrophy: update on the sulfur-deficient brittle hair syndromes. J Am Acad Dermatol *44*, 891-920; quiz 921-894.

Itoh, M., Hayashi, M., Shioda, K., Minagawa, M., Isa, F., Tamagawa, K., Morimatsu, Y., and Oda, M. (1999). Neurodegeneration in hereditary nucleotide repair disorders. Brain Dev *21*, 326-333.

Jacks, T., Remington, L., Williams, B. O., Schmitt, E. M., Halachmi, S., Bronson, R. T., and Weinberg, R. A. (1994). Tumor spectrum analysis in p53-mutant mice. Curr Biol *4*, 1-7.

Jackson, G. R., Owsley, C., and Curcio, C. A. (2002). Photoreceptor degeneration and dysfunction in aging and age-related maculopathy. Ageing Res Rev *1*, 381-396.

Jans, J., Schul, W., Sert, Y. G., Rijksen, Y., Rebel, H., Eker, A. P., Nakajima, S., van Steeg, H., de Gruijl, F. R., Yasui, A.*, et al.* (2005). Powerful Skin Cancer Protection by a CPD-Photolyase Transgene. Curr Biol *15*, 105-115.

Ji, L. L., Leeuwenburgh, C., Leichtweis, S., Gore, M., Fiebig, R., Hollander, J., and Bejma, J. (1998). Oxidative stress and aging. Role of exercise and its influences on antioxidant systems. Ann N Y Acad Sci *854*, 102-117.

Johanson, A. J., and Blizzard, R. M. (1981). Low somatomedin-C levels in older men rise in response to growth hormone administration. Johns Hopkins Med J *149*, 115-117.

Kalu, D. N. (1995). Bone. In Handbook of Physiology of Aging, Masoro, ed. (New York, Oxford University Press), pp. 395-411.

Kamiuchi, S., Saijo, M., Citterio, E., de Jager, M., Hoeijmakers, J. H., and Tanaka, K. (2002). Translocation of Cockayne syndrome group A protein to the nuclear matrix: possible relevance to transcription-coupled DNA repair. Proc Natl Acad Sci U S A *99*, 201-206.

Kaneko, H., and Kondo, N. (2004). Clinical features of Bloom syndrome and function of the causative gene, BLM helicase. Expert Rev Mol Diagn *4*, 393-401.

Kaneko, T., Tahara, S., and Matsuo, M. (1996). Non-linear accumulation of 8-hydroxy-2'-deoxyguanosine, a marker of oxidized DNA damage, during aging. Mutat Res *316*, 277-285.

Karow, J. K., Chakraverty, R. K., and Hickson, I. D. (1997). The Bloom's syndrome gene product is a 3'-5' DNA helicase. J Biol Chem *272*, 30611-30614.

Karow, J. K., Constantinou, A., Li, J. L., West, S. C., and Hickson, I. D. (2000). The Bloom's syndrome gene product promotes branch migration of holliday junctions. Proc Natl Acad Sci U S A *97*, 6504-6508.

Keeney, S., Chang, G. J., and Linn, S. (1993). Characterization of a human DNA damage binding protein implicated in xeroderma pigmentosum E. J Biol Chem *268*, 21293-21300.

Kenyon, C. (2005). The plasticity of aging: insights from long-lived mutants. Cell *120*, 449-460.

Kim, H., Oh, E., Im, H., Mun, J., Yang, M., Khim, J. Y., Lee, E., Lim, S. H., Kong, M. H., Lee, M., and Sul, D. (2006). Oxidative damages in the DNA, lipids, and proteins of rats exposed to isofluranes and alcohols. Toxicology *220*, 169-178.

Kipling, D., Davis, T., Ostler, E. L., and Faragher, R. G. (2004). What can progeroid syndromes tell us about human aging? Science *305*, 1426-1431.

Kirkwood, T. B., and Austad, S. N. (2000). Why do we age? Nature *408*, 233-238.

Kirkwood, T. B., and Rose, M. R. (1991). Evolution of senescence: late survival sacrificed for reproduction. Philos Trans R Soc Lond B Biol Sci *332*, 15-24.

Klungland, A., Hoss, M., Gunz, D., Constantinou, A., Clarkson, S. G., Doetsch, P. W., Bolton, P. H., Wood, R. D., and Lindahl, T. (1999). Base excision repair of oxidative DNA damage activated by XPG protein. Mol Cell *3*, 33-42.

Koubova, J., and Guarente, L. (2003). How does calorie restriction work? Genes Dev *17*, 313-321.

Kraemer, K. H. (1997). Sunlight and skin cancer: another link revealed. Proc Natl Acad Sci U S A *94*, 11-14.

Kraemer, K. H., Lee, M. M., and Scotto, J. (1984). DNA repair protects against cutaneous and internal neoplasia: evidence from xeroderma pigmentosum. Carcinogenesis *5*, 511-514.

Kraemer, K. H., Lee, M. M., and Scotto, J. (1987). Xeroderma pigmentosum. Cutaneous, ocular, and neurologic abnormalities in 830 published cases. Arch Dermatol *123*, 241-250.

Krokan, H. E., Nilsen, H., Skorpen, F., Otterlei, M., and Slupphaug, G. (2000). Base excision repair of DNA in mammalian cells. FEBS Lett *476*, 73-77.

Krokan, H. E., Standal, R., and Slupphaug, G. (1997). DNA glycosylases in the base excision repair of DNA. Biochem J *325 (Pt 1)*, 1-16.

Kuhbandner, S., Brummer, S., Metzger, D., Chambon, P., Hofmann, F., and Feil, R. (2000). Temporally controlled somatic mutagenesis in smooth muscle. Genesis *28*, 15-22.

Kuraoka, I., Bender, C., Romieu, A., Cadet, J., Wood, R. D., and Lindahl, T. (2000). Removal of oxygen free-radical-induced 5',8-purine cyclodeoxynucleosides from DNA by the nucleotide excision-repair pathway in human cells. Proc Natl Acad Sci U S A *97*, 3832-3837.

Kyng, K. J., May, A., Kolvraa, S., and Bohr, V. A. (2003). Gene expression profiling in Werner syndrome closely resembles that of normal aging. Proc Natl Acad Sci U S A *100*, 12259-12264.

Lakowski, B., and Hekimi, S. (1998). The genetics of caloric restriction in Caenorhabditis elegans. Proc Natl Acad Sci U S A *95*, 13091-13096.

Lambooij, A. C., Kliffen, M., Kuijpers, R. W., Houtsmuller, A. B., Broerse, J. J., and Mooy, C. M. (2000). Apoptosis is present in the primate macula at all ages. Graefes Arch Clin Exp Ophthalmol *238*, 508-514.

Lans, H., and Hoeijmakers, J. H. (2006). Cell biology: ageing nucleus gets out of shape. Nature *440*, 32-34.

Laszlo, A., and Simon, M. (1986). Serum lipid and lipoprotein levels in premature ageing syndromes: total lipodystrophy and Cockayne syndrome. Arch Gerontol Geriatr *5*, 189-196.

Layher, S. K., and Cleaver, J. E. (1997). Quantification of XPA gene expression levels in human and mouse cell lines by competitive RT-PCR. Mutat Res *383*, 9-19.

Lee, S. K., Yu, S. L., Prakash, L., and Prakash, S. (2002). Requirement of yeast RAD2, a homolog of human XPG gene, for efficient RNA polymerase II transcription. implications for Cockayne syndrome. Cell *109*, 823-834.

Leech, R. W., Brumback, R. A., Miller, R. H., Otsuka, F., Tarone, R. E., and Robbins, J. H. (1985). Cockayne syndrome: clinicopathologic and tissue culture studies of affected siblings. J Neuropathol Exp Neurol *44*, 507-519.

Lehmann, A. R. (1982). Three complementation groups in Cockayne syndrome. Mutat Res *106*, 347-356.

Lehmann, A. R. (2001). The xeroderma pigmentosum group D (XPD) gene: one gene, two functions, three diseases. Genes Dev *15*, 15-23.

Lehmann, A. R. (2003). DNA repair-deficient diseases, xeroderma pigmentosum, Cockayne syndrome and trichothiodystrophy. Biochimie *85*, 1101-1111.

Lehmann, A. R., Kirk-Bell, S., and Mayne, L. (1979). Abnormal kinetics of DNA synthesis in ultraviolet light-irradiated cells from patients with Cockayne's syndrome. Cancer Res *39*, 4237-4241.

Leveillard, T., Andera, L., Bissonnette, N., Schaeffer, L., Bracco, L., Egly, J. M., and Wasylyk, B. (1996). Functional interactions between p53 and the TFIIH complex are affected by tumour-associated mutations. Embo J *15*, 1615-1624.

Levin, P. S., Green, W. R., Victor, D. I., and MacLean, A. L. (1983). Histopathology of the eye in Cockayne's syndrome. Arch Ophthalmol *101*, 1093-1097.

Levinson, E. D., Zimmerman, A. W., Grunnet, M. L., Lewis, R. A., and Spackman, T. J. (1982). Cockayne syndrome. J Comput Assist Tomogr *6*, 1172-1174.

Li, L., Lu, X., Peterson, C. A., and Legerski, R. J. (1995). An interaction between the DNA repair factor XPA and replication protein A appears essential for nucleotide excision repair. Mol Cell Biol *15*, 5396-5402.

Li, S., Crenshaw, E. B., 3rd, Rawson, E. J., Simmons, D. M., Swanson, L. W., and Rosenfeld, M. G. (1990). Dwarf locus mutants lacking three pituitary cell types result from mutations in the POU-domain gene pit-1. Nature *347*, 528-533.

Liang, H., Masoro, E. J., Nelson, J. F., Strong, R., McMahan, C. A., and Richardson, A. (2003). Genetic mouse models of extended lifespan. Exp Gerontol *38*, 1353-1364.

Licht, C. L., Stevnsner, T., and Bohr, V. A. (2003). Cockayne syndrome group B cellular and biochemical functions. Am J Hum Genet *73*, 1217-1239.

Limoli, C. L., Rola, R., Giedzinski, E., Mantha, S., Huang, T. T., and Fike, J. R. (2004). Cell-density-dependent regulation of neural precursor cell function. Proc Natl Acad Sci U S A *101*, 16052-16057.

Lindahl, T. (1993). Instability and decay of the primary structure of DNA. Nature *362*, 709-715.

Lindahl, T., and Wood, R. D. (1999). Quality control by DNA repair. Science *286*, 1897-1905.

Lindenbaum, Y., Dickson, D., Rosenbaum, P., Kraemer, K., Robbins, I., and Rapin, I. (2001). Xeroderma pigmentosum/cockayne syndrome complex: first neuropathological study and review of eight other cases. Eur J Paediatr Neurol *5*, 225-242.

Liu, F., Yu, Z. J., Sui, J. L., Bai, B., and Zhou, P. K. (2006). siRNA-mediated silencing of Cockayne Cyndrome group B gene potentiates radiation-induced apoptosis and antiproliferative effect in HeLa cells. Chin Med J (Engl) *119*, 731-739.

Liu, R., Liu, I. Y., Bi, X., Thompson, R. F., Doctrow, S. R., Malfroy, B., and Baudry, M. (2003). Reversal of age-related learning deficits and brain oxidative stress in mice with superoxide dismutase/catalase mimetics. Proc Natl Acad Sci U S A *100*, 8526-8531.

Ljungman, M., and Lane, D. P. (2004). Transcription - guarding the genome by sensing DNA damage. Nat Rev Cancer *4*, 727-737.

Ljungman, M., Zhang, F., Chen, F., Rainbow, A. J., and McKay, B. C. (1999). Inhibition of RNA polymerase II as a trigger for the p53 response. Oncogene *18*, 583-592.

Lombard, D. B., Beard, C., Johnson, B., Marciniak, R. A., Dausman, J., Bronson, R., Buhlmann, J. E., Lipman, R., Curry, R., Sharpe, A., *et al.* (2000). Mutations in the WRN gene in mice accelerate mortality in a p53-null background. Mol Cell Biol *20*, 3286-3291.

Lombard, D. B., Chua, K. F., Mostoslavsky, R., Franco, S., Gostissa, M., and Alt, F. W. (2005). DNA repair, genome stability, and aging. Cell *120*, 497-512.

Longman, C., Sewry, C. A., and Muntoni, F. (2004). Muscle involvement in the cerebro-oculo-facio-skeletal syndrome. Pediatr Neurol *30*, 125-128.

Longo, V. D., and Finch, C. E. (2003). Evolutionary medicine: from dwarf model systems to healthy centenarians? Science *299*, 1342-1346.

Lowe, S. W., Schmitt, E. M., Smith, S. W., Osborne, B. A., and Jacks, T. (1993). p53 is required for radiation-induced apoptosis in mouse thymocytes. Nature *362*, 847-849.

Lowry, R. B. (1982). Early onset of Cockayne syndrome. Am J Med Genet *13*, 209-210.

Lu, T., Pan, Y., Kao, S. Y., Li, C., Kohane, I., Chan, J., and Yankner, B. A. (2004). Gene regulation and DNA damage in the ageing human brain. Nature *429*, 883-891.

Ma, G. T., Roth, M. E., Groskopf, J. C., Tsai, F. Y., Orkin, S. H., Grosveld, F., Engel, J. D., and Linzer, D. I. (1997). GATA-2 and GATA-3 regulate trophoblast-specific gene expression in vivo. Development *124*, 907-914.

Mair, W., Goymer, P., Pletcher, S. D., and Partridge, L. (2003). Demography of dietary restriction and death in Drosophila. Science *301*, 1731-1733.

Martin, G. M. (2005). Genetic modulation of senescent phenotypes in Homo sapiens. Cell *120*, 523-532.

Masutani, C., Kusumoto, R., Yamada, A., Dohmae, N., Yokoi, M., Yuasa, M., Araki, M., Iwai, S., Takio, K., and Hanaoka, F. (1999). The XPV (xeroderma pigmentosum variant) gene encodes human DNA polymerase eta. Nature *399*, 700-704.

Masutani, C., Sugasawa, K., Yanagisawa, J., Sonoyama, T., Ui, M., Enomoto, T., Takio, K., Tanaka, K., van der Spek, P. J., Bootsma, D., and et al. (1994). Purification and cloning of a nucleotide excision repair complex involving the xeroderma pigmentosum group C protein and a human homologue of yeast RAD23. Embo J *13*, 1831-1843.

Matsuda, N., Azuma, K., Saijo, M., Iemura, S., Hioki, Y., Natsume, T., Chiba, T., and Tanaka, K. (2005). DDB2, the xeroderma pigmentosum group E gene product, is directly ubiquitylated by Cullin 4A-based ubiquitin ligase complex. DNA Repair (Amst) *4*, 537-545.

Matsumoto, Y., and Kim, K. (1995). Excision of deoxyribose phosphate residues by DNA polymerase beta during DNA repair. Science *269*, 699-702.

Matsunaga, T., Park, C. H., Bessho, T., Mu, D., and Sancar, A. (1996). Replication protein A confers structure-specific endonuclease activities to the XPF-ERCC1 and XPG subunits of human DNA repair excision nuclease. J Biol Chem *271*, 11047-11050.

Mayne, L. V., and Lehmann, A. R. (1982). Failure of RNA synthesis to recover after UV irradiation: an early defect in cells from individuals with Cockayne's syndrome and xeroderma pigmentosum. Cancer Res *42*, 1473-1478.

McCarroll, S. A., Murphy, C. T., Zou, S., Pletcher, S. D., Chin, C. S., Jan, Y. N., Kenyon, C., Bargmann, C. I., and Li, H. (2004). Comparing genomic expression patterns across species identifies shared transcriptional profile in aging. Nat Genet *36*, 197-204.

McCuaig, C., Marcoux, D., Rasmussen, J. E., Werner, M. M., and Gentner, N. E. (1993). Trichothiodystrophy associated with photosensitivity, gonadal failure, and striking osteosclerosis. J Am Acad Dermatol *28*, 820-826.

McLuckie, K. I., Crookston, R. J., Gaskell, M., Farmer, P. B., Routledge, M. N., Martin, E. A., and Brown, K. (2005). Mutation spectra induced by alpha-acetoxytamoxifen-DNA adducts in human DNA repair proficient and deficient (xeroderma pigmentosum complementation group A) cells. Biochemistry *44*, 8198-8205.

McLuckie, K. I., Routledge, M. N., Brown, K., Gaskell, M., Farmer, P. B., Roberts, G. C., and Martin, E. A. (2002). DNA adducts formed from 4-hydroxytamoxifen are more mutagenic than those formed by alpha-acetoxytamoxifen in a shuttle vector target gene replicated in human Ad293 cells. Biochemistry *41*, 8899-8906.

McWhir, J., Selfridge, J., Harrison, D. J., Squires, S., and Melton, D. W. (1993). Mice with DNA repair gene (ERCC-1) deficiency have elevated levels of p53, liver nuclear abnormalities and die before weaning. Nat Genet *5*, 217-224.

Medawar, P. B. (1952). An unsolved problem of biology.

Meira, L. B., Graham, J. M., Jr., Greenberg, C. R., Busch, D. B., Doughty, A. T., Ziffer, D. W., Coleman, D. M., Savre-Train, I., and Friedberg, E. C. (2000). Manitoba aboriginal kindred with original cerebro-oculo-facio-skeletal syndrome has a mutation in the Cockayne syndrome group B (CSB) gene. Am J Hum Genet *66*, 1221-1228.

Mellon, I., Bohr, V. A., Smith, C. A., and Hanawalt, P. C. (1986). Preferential DNA repair of an active gene in human cells. Proc Natl Acad Sci U S A *83*, 8878-8882.

Mellon, I., Spivak, G., and Hanawalt, P. C. (1987). Selective removal of transcription-blocking DNA damage from the transcribed strand of the mammalian DHFR gene. Cell *51*, 241-249.

Melov, S., Doctrow, S. R., Schneider, J. A., Haberson, J., Patel, M., Coskun, P. E., Huffman, K., Wallace, D. C., and Malfroy, B. (2001). Lifespan extension and rescue of spongiform encephalopathy in superoxide dismutase 2 nullizygous mice treated with superoxide dismutase-catalase mimetics. J Neurosci *21*, 8348-8353.

Melov, S., Ravenscroft, J., Malik, S., Gill, M. S., Walker, D. W., Clayton, P. E., Wallace, D. C., Malfroy, B., Doctrow, S. R., and Lithgow, G. J. (2000). Extension of life-span with superoxide dismutase/catalase mimetics. Science *289*, 1567-1569.

Melov, S., Schneider, J. A., Day, B. J., Hinerfeld, D., Coskun, P., Mirra, S. S., Crapo, J. D., and Wallace, D. C. (1998). A novel neurological phenotype in mice lacking mitochondrial manganese superoxide dismutase. Nat Genet *18*, 159-163.

Melton, D. W., Ketchen, A. M., Nunez, F., Bonatti-Abbondandolo, S., Abbondandolo, A., Squires, S., and Johnson, R. T. (1998). Cells from ERCC1-deficient mice show increased genome instability and a reduced frequency of S-phase-dependent illegitimate chromosome exchange but a normal frequency of homologous recombination. J Cell Sci *111 (Pt 3)*, 395-404.

Mitchell, D. L., and Nairn, R. S. (1989). The biology of the (6-4) photoproduct. Photochem Photobiol *49*, 805-819.

Mitchell, J. R., Hoeijmakers, J. H., and Niedernhofer, L. J. (2003). Divide and conquer: nucleotide excision repair battles cancer and ageing. Curr Opin Cell Biol *15*, 232-240.

Mizutani, A., Okada, T., Shibutani, S., Sonoda, E., Hochegger, H., Nishigori, C., Miyachi, Y., Takeda, S., and Yamazoe, M. (2004). Extensive chromosomal breaks are induced by tamoxifen and estrogen in DNA repair-deficient cells. Cancer Res *64*, 3144-3147.

Mobbs, C. V., Bray, G. A., Atkinson, R. L., Bartke, A., Finch, C. E., Maratos-Flier, E., Crawley, J. N., and Nelson, J. F. (2001). Neuroendocrine and pharmacological manipulations to assess how caloric restriction increases life span. J Gerontol A Biol Sci Med Sci *56 Spec No 1*, 34-44.

Moggs, J. G., Yarema, K. J., Essigmann, J. M., and Wood, R. D. (1996). Analysis of incision sites produced by human cell extracts and purified proteins during nucleotide excision repair of a 1,3-intrastrand d(GpTpG)-cisplatin adduct. J Biol Chem *271*, 7177-7186.

Moshiri, A., Close, J., and Reh, T. A. (2004). Retinal stem cells and regeneration. Int J Dev Biol *48*, 1003-1014.

Mostoslavsky, R., Chua, K. F., Lombard, D. B., Pang, W. W., Fischer, M. R., Gellon, L., Liu, P., Mostoslavsky, G., Franco, S., Murphy, M. M*., et al.* (2006). Genomic instability and aging-like phenotype in the absence of mammalian SIRT6. Cell *124*, 315-329.

Mu, D., Hsu, D. S., and Sancar, A. (1996). Reaction mechanism of human DNA repair excision nuclease. J Biol Chem *271*, 8285-8294.

Murai, M., Enokido, Y., Inamura, N., Yoshino, M., Nakatsu, Y., van der Horst, G. T., Hoeijmakers, J. H., Tanaka, K., and Hatanaka, H. (2001). Early postnatal ataxia and abnormal cerebellar development in mice lacking Xeroderma pigmentosum Group A and Cockayne syndrome Group B DNA repair genes. Proc Natl Acad Sci U S A *98*, 13379-13384.

Nag, A., Bondar, T., Shiv, S., and Raychaudhuri, P. (2001). The xeroderma pigmentosum group E gene product DDB2 is a specific target of cullin 4A in mammalian cells. Mol Cell Biol *21*, 6738-6747.

Nakabayashi, K., Amann, D., Ren, Y., Saarialho-Kere, U., Avidan, N., Gentles, S., MacDonald, J. R., Puffenberger, E. G., Christiano, A. M., Martinez-Mir, A*., et al.* (2005). Identification of C7orf11 (TTDN1) gene mutations and genetic heterogeneity in nonphotosensitive trichothiodystrophy. Am J Hum Genet *76*, 510-516.

Nakane, H., Takeuchi, S., Yuba, S., Saijo, M., Nakatsu, Y., Murai, H., Nakatsuru, Y., Ishikawa, T., Hirota, S., Kitamura, Y., and et al. (1995). High incidence of ultraviolet-B-or chemical-carcinogen-induced skin tumours in mice lacking the xeroderma pigmentosum group A gene. Nature *377*, 165-168.

Nakatsu, Y., Asahina, H., Citterio, E., Rademakers, S., Vermeulen, W., Kamiuchi, S., Yeo, J. P., Khaw, M. C., Saijo, M., Kodo, N*., et al.* (2000). XAB2, a novel tetratricopeptide repeat protein involved in transcription-coupled DNA repair and transcription. J Biol Chem *275*, 34931-34937.

Nance, M. A., and Berry, S. A. (1992). Cockayne syndrome: review of 140 cases. Am J Med Genet *42*, 68-84.

Ng, J. M., Vermeulen, W., van der Horst, G. T., Bergink, S., Sugasawa, K., Vrieling, H., and Hoeijmakers, J. H. (2003). A novel regulation mechanism of DNA repair by damage-induced and RAD23-dependent stabilization of xeroderma pigmentosum group C protein. Genes Dev *17*, 1630-1645.

Ng, J. M., Vrieling, H., Sugasawa, K., Ooms, M. P., Grootegoed, J. A., Vreeburg, J. T., Visser, P., Beems, R. B., Gorgels, T. G., Hanaoka, F., *et al.* (2002). Developmental defects and male sterility in mice lacking the ubiquitin-like DNA repair gene mHR23B. Mol Cell Biol *22*, 1233-1245.

Niedernhofer, L. J., Essers, J., Weeda, G., Beverloo, B., de Wit, J., Muijtjens, M., Odijk, H., Hoeijmakers, J. H., and Kanaar, R. (2001). The structure-specific endonuclease Ercc1-Xpf is required for targeted gene replacement in embryonic stem cells. Embo J *20*, 6540-6549.

Nigg, E. A. (1995). Cyclin-dependent protein kinases: key regulators of the eukaryotic cell cycle. Bioessays *17*, 471-480.

Niki, E. (2000). Oxidative stress and aging. Intern Med *39*, 324-326.

Niki, E., Yamamoto, Y., Takahashi, M., Yamamoto, K., Komuro, E., Miki, M., Yasuda, H., and Mino, M. (1988). Free radical-mediated damage of blood and its inhibition by antioxidants. J Nutr Sci Vitaminol (Tokyo) *34*, 507-512.

Nishi, R., Okuda, Y., Watanabe, E., Mori, T., Iwai, S., Masutani, C., Sugasawa, K., and Hanaoka, F. (2005). Centrin 2 stimulates nucleotide excision repair by interacting with xeroderma pigmentosum group C protein. Mol Cell Biol *25*, 5664-5674.

Norwood, W. (1964). The Marinesco-Sjogren syndrome. J Pediatric *65*, 431-437.

Nouspikel, T., and Hanawalt, P. C. (2002). DNA repair in terminally differentiated cells. DNA Repair (Amst) *1*, 59-75.

Novelli, G., Muchir, A., Sangiuolo, F., Helbling-Leclerc, A., D'Apice, M. R., Massart, C., Capon, F., Sbraccia, P., Federici, M., Lauro, R., *et al.* (2002). Mandibuloacral dysplasia is caused by a mutation in LMNA-encoding lamin A/C. Am J Hum Genet *71*, 426-431.

Nussenzweig, A., Chen, C., da Costa Soares, V., Sanchez, M., Sokol, K., Nussenzweig, M. C., and Li, G. C. (1996). Requirement for Ku80 in growth and immunoglobulin V(D)J recombination. Nature *382*, 551-555.

O'Donovan, A., Davies, A. A., Moggs, J. G., West, S. C., and Wood, R. D. (1994a). XPG endonuclease makes the 3' incision in human DNA nucleotide excision repair. Nature *371*, 432-435.

O'Donovan, A., Scherly, D., Clarkson, S. G., and Wood, R. D. (1994b). Isolation of active recombinant XPG protein, a human DNA repair endonuclease. J Biol Chem *269*, 15965-15968.

Ogi, T., and Lehmann, A. R. (2006). The Y-family DNA polymerase kappa (pol kappa) functions in mammalian nucleotide-excision repair. Nat Cell Biol *8*, 640-642.

Orr, W. C., and Sohal, R. S. (1994). Extension of life-span by overexpression of superoxide dismutase and catalase in Drosophila melanogaster. Science *263*, 1128-1130.

Ortolan, T. G., Tongaonkar, P., Lambertson, D., Chen, L., Schauber, C., and Madura, K. (2000). The DNA repair protein rad23 is a negative regulator of multi-ubiquitin chain assembly. Nat Cell Biol *2*, 601-608.

Osterod, M., Larsen, E., Le Page, F., Hengstler, J. G., Van Der Horst, G. T., Boiteux, S., Klungland, A., and Epe, B. (2002). A global DNA repair mechanism involving the Cockayne syndrome B (CSB) gene product can prevent the in vivo accumulation of endogenous oxidative DNA base damage. Oncogene *21*, 8232-8239.

Ozdirim, E., Topcu, M., Ozon, A., and Cila, A. (1996). Cockayne syndrome: review of 25 cases. Pediatr Neurol *15*, 312-316.

Park, S. K., Chang, S. H., Cho, S. B., Baek, H. S., and Lee, D. Y. (1994). Cockayne syndrome: a case with hyperinsulinemia and growth hormone deficiency. J Korean Med Sci *9*, 74-77.

Parrinello, S., Samper, E., Krtolica, A., Goldstein, J., Melov, S., and Campisi, J. (2003). Oxygen sensitivity severely limits the replicative lifespan of murine fibroblasts. Nat Cell Biol *5*, 741-747.

Partridge, L., Gems, D., and Withers, D. J. (2005). Sex and death: what is the connection? Cell *120*, 461-472.

Pasquier, L., Laugel, V., Lazaro, L., Dollfus, H., Journel, H., Edery, P., Goldenberg, A., Martin, D., Heron, D., Le Merrer, M., *et al.* (2006). Wide clinical variability among 13 new Cockayne syndrome cases confirmed by biochemical assays. Arch Dis Child *91*, 178-182.

Pearl, R. (1928). The rate of living.

Peeters, P. J., Gohlmann, H. W., Van den Wyngaert, I., Swagemakers, S. M., Bijnens, L., Kass, S. U., and Steckler, T. (2004). Transcriptional response to corticotropin-releasing factor in AtT-20 cells. Mol Pharmacol *66*, 1083-1092.

Pollex, R. L., and Hegele, R. A. (2004). Hutchinson-Gilford progeria syndrome. Clin Genet *66*, 375-381.

Porter, A. (1998). Controlling your losses: conditional gene silencing in mammals. Trends Genet *14*, 73-79.

Prasher, J. M., Lalai, A. S., Heijmans-Antonissen, C., Ploemacher, R. E., Hoeijmakers, J. H., Touw, I. P., and Niedernhofer, L. J. (2005). Reduced hematopoietic reserves in DNA interstrand crosslink repair-deficient Ercc1-/- mice. Embo J *24*, 861-871.

Przedborski, S., Vila, M., and Jackson-Lewis, V. (2003). Neurodegeneration: what is it and where are we? J Clin Invest *111*, 3-10.

Puigserver, P., Rhee, J., Donovan, J., Walkey, C. J., Yoon, J. C., Oriente, F., Kitamura, Y., Altomonte, J., Dong, H., Accili, D., and Spiegelman, B. M. (2003). Insulin-regulated hepatic gluconeogenesis through FOXO1-PGC-1alpha interaction. Nature *423*, 550-555.

Puzianowska-Kuznicka, M., and Kuznicki, J. (2005). Genetic alterations in accelerated ageing syndromes. Do they play a role in natural ageing? Int J Biochem Cell Biol *37*, 947-960.

Rapin, I., Lindenbaum, Y., Dickson, D. W., Kraemer, K. H., and Robbins, J. H. (2000). Cockayne syndrome and xeroderma pigmentosum. Neurology *55*, 1442-1449.

Ratner, J. N., Balasubramanian, B., Corden, J., Warren, S. L., and Bregman, D. B. (1998). Ultraviolet radiation-induced ubiquitination and proteasomal degradation of the large subunit of RNA polymerase II. Implications for transcription-coupled DNA repair. J Biol Chem *273*, 5184-5189.

Risinger, M. A., and Groden, J. (2004). Crosslinks and crosstalk: human cancer syndromes and DNA repair defects. Cancer Cell *6*, 539-545.

Rodriguez-Lopez, A. M., Jackson, D. A., Iborra, F., and Cox, L. S. (2002). Asymmetry of DNA replication fork progression in Werner's syndrome. Aging Cell *1*, 30-39.

Rudman, D., Kutner, M. H., Rogers, C. M., Lubin, M. F., Fleming, G. A., and Bain, R. P. (1981). Impaired growth hormone secretion in the adult population: relation to age and adiposity. J Clin Invest *67*, 1361-1369.

Rudolph, K. L., Chang, S., Lee, H. W., Blasco, M., Gottlieb, G. J., Greider, C., and DePinho, R. A. (1999). Longevity, stress response, and cancer in aging telomerase-deficient mice. Cell *96*, 701-712.

Sakai, K., and Miyazaki, J. (1997). A transgenic mouse line that retains Cre recombinase activity in mature oocytes irrespective of the cre transgene transmission. Biochem Biophys Res Commun *237*, 318-324.

Sands, A. T., Abuin, A., Sanchez, A., Conti, C. J., and Bradley, A. (1995). High susceptibility to ultraviolet-induced carcinogenesis in mice lacking XPC. Nature *377*, 162-165.

Sarkar, P. K., and Shinton, R. A. (2001). Hutchinson-Guilford progeria syndrome. Postgrad Med J *77*, 312-317.

Sato, K., Niki, E., and Shimasaki, H. (1990). Free radical-mediated chain oxidation of low density lipoprotein and its synergistic inhibition by vitamin E and vitamin C. Arch Biochem Biophys *279*, 402-405.

Satoh, M. S., Jones, C. J., Wood, R. D., and Lindahl, T. (1993). DNA excision-repair defect of xeroderma pigmentosum prevents removal of a class of oxygen free radical-induced base lesions. Proc Natl Acad Sci U S A *90*, 6335-6339.

Satoh, M. S., and Lindahl, T. (1994). Enzymatic repair of oxidative DNA damage. Cancer Res *54*, 1899s-1901s.

Schaeffer, L., Moncollin, V., Roy, R., Staub, A., Mezzina, M., Sarasin, A., Weeda, G., Hoeijmakers, J. H., and Egly, J. M. (1994). The ERCC2/DNA repair protein is associated with the class II BTF2/TFIIH transcription factor. Embo J *13*, 2388-2392.

Schaeffer, L., Roy, R., Humbert, S., Moncollin, V., Vermeulen, W., Hoeijmakers, J. H., Chambon, P., and Egly, J. M. (1993). DNA repair helicase: a component of BTF2 (TFIIH) basic transcription factor. Science *260*, 58-63.

Schriner, S. E., Linford, N. J., Martin, G. M., Treuting, P., Ogburn, C. E., Emond, M., Coskun, P. E., Ladiges, W., Wolf, N., Van Remmen, H., *et al.* (2005). Extension of murine life span by overexpression of catalase targeted to mitochondria. Science *308*, 1909-1911.

Seibler, J., Zevnik, B., Kuter-Luks, B., Andreas, S., Kern, H., Hennek, T., Rode, A., Heimann, C., Faust, N., Kauselmann, G., *et al.* (2003). Rapid generation of inducible mouse mutants. Nucleic Acids Res *31*, e12.

Selby, C. P., and Sancar, A. (1997). Cockayne syndrome group B protein enhances elongation by RNA polymerase II. Proc Natl Acad Sci U S A *94*, 11205-11209.

Sellick, C. A., and Reece, R. J. (2003). Modulation of transcription factor function by an amino acid: activation of Put3p by proline. Embo J *22*, 5147-5153.

Seth, P. K. (1982). Hepatic effects of phthalate esters. Environ Health Perspect *45*, 27-34.

Shibutani, S., Ravindernath, A., Suzuki, N., Terashima, I., Sugarman, S. M., Grollman, A. P., and Pearl, M. L. (2000a). Identification of tamoxifen-DNA adducts in the endometrium of women treated with tamoxifen. Carcinogenesis *21*, 1461-1467.

Shibutani, S., Reardon, J. T., Suzuki, N., and Sancar, A. (2000b). Excision of tamoxifen-DNA adducts by the human nucleotide excision repair system. Cancer Res *60*, 2607-2610.

Shiloh, Y. (1997). Ataxia-telangiectasia and the Nijmegen breakage syndrome: related disorders but genes apart. Annu Rev Genet *31*, 635-662.

Shimamoto, A., Sugimoto, M., and Furuichi, Y. (2004). Molecular biology of Werner syndrome. Int J Clin Oncol *9*, 288-298.

Shiomi, N., Kito, S., Oyama, M., Matsunaga, T., Harada, Y. N., Ikawa, M., Okabe, M., and Shiomi, T. (2004). Identification of the XPG region that causes the onset of Cockayne syndrome by using Xpg mutant mice generated by the cDNA-mediated knock-in method. Mol Cell Biol *24*, 3712-3719.

Shiomi, N., Mori, M., Kito, S., Harada, Y. N., Tanaka, K., and Shiomi, T. (2005). Severe growth retardation and short life span of double-mutant mice lacking Xpa and exon 15 of Xpg. DNA Repair (Amst) *4*, 351-357.

Shivji, M. K., Eker, A. P., and Wood, R. D. (1994). DNA repair defect in xeroderma pigmentosum group C and complementing factor from HeLa cells. J Biol Chem *269*, 22749-22757.

Shivji, M. K., Podust, V. N., Hubscher, U., and Wood, R. D. (1995). Nucleotide excision repair DNA synthesis by DNA polymerase epsilon in the presence of PCNA, RFC, and RPA. Biochemistry *34*, 5011-5017.

Sijbers, A. M., de Laat, W. L., Ariza, R. R., Biggerstaff, M., Wei, Y. F., Moggs, J. G., Carter, K. C., Shell, B. K., Evans, E., de Jong, M. C*., et al.* (1996). Xeroderma pigmentosum group F caused by a defect in a structure-specific DNA repair endonuclease. Cell *86*, 811-822.

Sobol, R. W., Horton, J. K., Kuhn, R., Gu, H., Singhal, R. K., Prasad, R., Rajewsky, K., and Wilson, S. H. (1996). Requirement of mammalian DNA polymerase-beta in base-excision repair. Nature *379*, 183-186.

Soffer, D., Grotsky, H. W., Rapin, I., and Suzuki, K. (1979). Cockayne syndrome: unusual neuropathological findings and review of the literature. Ann Neurol *6*, 340-348.

Sohal, R. S. (1976). Meatbolic rate and lifespan. Cellular aging: Concepts and Mechanisms, 25-40.

Sohal, R. S., and Weindruch, R. (1996). Oxidative stress, caloric restriction, and aging. Science *273*, 59-63.

Sonntag, W. E., Steger, R. W., Forman, L. J., and Meites, J. (1980). Decreased pulsatile release of growth hormone in old male rats. Endocrinology *107*, 1875-1879.

Spivak, G., and Hanawalt, P. C. (2005). Host cell reactivation of plasmids containing oxidative DNA lesions is defective in Cockayne syndrome but normal in UV-sensitive syndrome fibroblasts. DNA Repair (Amst).

Spivak, G., and Hanawalt, P. C. (2006). Host cell reactivation of plasmids containing oxidative DNA lesions is defective in Cockayne syndrome but normal in UV-sensitive syndrome fibroblasts. DNA Repair (Amst) *5*, 13-22.

Stefanini, M., Vermeulen, W., Weeda, G., Giliani, S., Nardo, T., Mezzina, M., Sarasin, A., Harper, J. I., Arlett, C. F., Hoeijmakers, J. H., and et al. (1993). A new nucleotide-excision-repair gene associated with the disorder trichothiodystrophy. Am J Hum Genet *53*, 817-821.

Stevnsner, T., Nyaga, S., de Souza-Pinto, N. C., van der Horst, G. T., Gorgels, T. G., Hogue, B. A., Thorslund, T., and Bohr, V. A. (2002). Mitochondrial repair of 8-oxoguanine is deficient in Cockayne syndrome group B. Oncogene *21*, 8675-8682.

Sugasawa, K., Masutani, C., Uchida, A., Maekawa, T., van der Spek, P. J., Bootsma, D., Hoeijmakers, J. H., and Hanaoka, F. (1996). HHR23B, a human Rad23 homolog, stimulates XPC protein in nucleotide excision repair in vitro. Mol Cell Biol *16*, 4852-4861.

Sugasawa, K., Ng, J. M., Masutani, C., Iwai, S., van der Spek, P. J., Eker, A. P., Hanaoka, F., Bootsma, D., and Hoeijmakers, J. H. (1998). Xeroderma pigmentosum group C protein complex is the initiator of global genome nucleotide excision repair. Mol Cell *2*, 223-232.

Sugasawa, K., Ng, J. M., Masutani, C., Maekawa, T., Uchida, A., van der Spek, P. J., Eker, A. P., Rademakers, S., Visser, C., Aboussekhra, A*., et al.* (1997). Two human homologs of Rad23 are functionally interchangeable in complex formation and stimulation of XPC repair activity. Mol Cell Biol *17*, 6924-6931.

Sugasawa, K., Okuda, Y., Saijo, M., Nishi, R., Matsuda, N., Chu, G., Mori, T., Iwai, S., Tanaka, K., and Hanaoka, F. (2005). UV-induced ubiquitylation of XPC protein mediated by UV-DDB-ubiquitin ligase complex. Cell *121*, 387-400.

Sun, H., Karow, J. K., Hickson, I. D., and Maizels, N. (1998). The Bloom's syndrome helicase unwinds G4 DNA. J Biol Chem *273*, 27587-27592.

Sunesen, M., Stevnsner, T., Brosh Jr, R. M., Dianov, G. L., and Bohr, V. A. (2002). Global genome repair of 8-oxoG in hamster cells requires a functional CSB gene product. Oncogene *21*, 3571-3578.

Svejstrup, J. Q., Wang, Z., Feaver, W. J., Wu, X., Bushnell, D. A., Donahue, T. F., Friedberg, E. C., and Kornberg, R. D. (1995). Different forms of TFIIH for transcription and DNA repair: holo-TFIIH and a nucleotide excision repairosome. Cell *80*, 21-28.

Takagi, Y., Masuda, C. A., Chang, W. H., Komori, H., Wang, D., Hunter, T., Joazeiro, C. A., and Kornberg, R. D. (2005). Ubiquitin ligase activity of TFIIH and the transcriptional response to DNA damage. Mol Cell *18*, 237-243.

Tan, T., and Chu, G. (2002). p53 Binds and activates the xeroderma pigmentosum DDB2 gene in humans but not mice. Mol Cell Biol *22*, 3247-3254.

Tanaka, K., Kawai, K., Kumahara, Y., Ikenaga, M., and Okada, Y. (1981). Genetic complementation groups in cockayne syndrome. Somatic Cell Genet *7*, 445-455.

Tang, J. Y., Hwang, B. J., Ford, J. M., Hanawalt, P. C., and Chu, G. (2000). Xeroderma pigmentosum p48 gene enhances global genomic repair and suppresses UV-induced mutagenesis. Mol Cell *5*, 737-744.

Thorslund, T., von Kobbe, C., Harrigan, J. A., Indig, F. E., Christiansen, M., Stevnsner, T., and Bohr, V. A. (2005). Cooperation of the Cockayne syndrome group B protein and poly(ADP-ribose) polymerase 1 in the response to oxidative stress. Mol Cell Biol *25*, 7625-7636.

Tian, M., Shinkura, R., Shinkura, N., and Alt, F. W. (2004). Growth retardation, early death, and DNA repair defects in mice deficient for the nucleotide excision repair enzyme XPF. Mol Cell Biol *24*, 1200-1205.

Tirode, F., Busso, D., Coin, F., and Egly, J. M. (1999). Reconstitution of the transcription factor TFIIH: assignment of functions for the three enzymatic subunits, XPB, XPD, and cdk7. Mol Cell *3*, 87-95.

Tornaletti, S., Reines, D., and Hanawalt, P. C. (1999). Structural characterization of RNA polymerase II complexes arrested by a cyclobutane pyrimidine dimer in the transcribed strand of template DNA. J Biol Chem *274*, 24124-24130.

Traboulsi, E. I., De Becker, I., and Maumenee, I. H. (1992). Ocular findings in Cockayne syndrome. Am J Ophthalmol *114*, 579-583.

Troelstra, C., van Gool, A., de Wit, J., Vermeulen, W., Bootsma, D., and Hoeijmakers, J. H. (1992). ERCC6, a member of a subfamily of putative helicases, is involved in Cockayne's syndrome and preferential repair of active genes. Cell *71*, 939-953.

Tucci, V., Blanco, G., Nolan, P.M. (2006). Behavioral and Neurological Phenotyping in the mouse. In Standards of Mouse Model Phenotyping, W. Wiley-VCH Verlag GmbH & Co. KGaA, Germany, ed., pp. 135-175.

Tuo, J., Chen, C., Zeng, X., Christiansen, M., and Bohr, V. A. (2002a). Functional crosstalk between hOgg1 and the helicase domain of Cockayne syndrome group B protein. DNA Repair (Amst) *1*, 913-927.

Tuo, J., Jaruga, P., Rodriguez, H., Bohr, V. A., and Dizdaroglu, M. (2003). Primary fibroblasts of Cockayne syndrome patients are defective in cellular repair of 8-hydroxyguanine and 8-hydroxyadenine resulting from oxidative stress. Faseb J *17*, 668-674.

Tuo, J., Jaruga, P., Rodriguez, H., Dizdaroglu, M., and Bohr, V. A. (2002b). The cockayne syndrome group B gene product is involved in cellular repair of 8-hydroxyadenine in DNA. J Biol Chem *277*, 30832-30837.

Tuo, J., Ning, B., Bojanowski, C. M., Lin, Z. N., Ross, R. J., Reed, G. F., Shen, D., Jiao, X., Zhou, M., Chew, E. Y*., et al.* (2006). Synergic effect of polymorphisms in ERCC6 5' flanking region and complement factor H on age-related macular degeneration predisposition. Proc Natl Acad Sci U S A.

Tyner, S. D., Venkatachalam, S., Choi, J., Jones, S., Ghebranious, N., Igelmann, H., Lu, X., Soron, G., Cooper, B., Brayton, C*., et al.* (2002). p53 mutant mice that display early ageing-associated phenotypes. Nature *415*, 45-53.

van der Horst, G. T., Meira, L., Gorgels, T. G., de Wit, J., Velasco-Miguel, S., Richardson, J. A., Kamp, Y., Vreeswijk, M. P., Smit, B., Bootsma, D*., et al.* (2002). UVB radiation-induced cancer predisposition in Cockayne syndrome group A (Csa) mutant mice. DNA Repair (Amst) *1*, 143-157.

van der Horst, G. T., van Steeg, H., Berg, R. J., van Gool, A. J., de Wit, J., Weeda, G., Morreau, H., Beems, R. B., van Kreijl, C. F., de Gruijl, F. R*., et al.* (1997). Defective transcription-coupled repair in Cockayne syndrome B mice is associated with skin cancer predisposition. Cell *89*, 425-435.

van Gent, D. C., Hoeijmakers, J. H., and Kanaar, R. (2001). Chromosomal stability and the DNA double-stranded break connection. Nat Rev Genet *2*, 196-206.

van Hoffen, A., Natarajan, A. T., Mayne, L. V., van Zeeland, A. A., Mullenders, L. H., and Venema, J. (1993). Deficient repair of the transcribed strand of active genes in Cockayne's syndrome cells. Nucleic Acids Res *21*, 5890-5895.

van Hoffen, A., Venema, J., Meschini, R., van Zeeland, A. A., and Mullenders, L. H. (1995). Transcription-coupled repair removes both cyclobutane pyrimidine dimers and 6-4 photoproducts with equal efficiency and in a sequential way from transcribed DNA in xeroderma pigmentosum group C fibroblasts. Embo J *14*, 360-367.

van Steeg, H., Klein, H., Beems, R. B., and van Kreijl, C. F. (1998). Use of DNA repair-deficient XPA transgenic mice in short-term carcinogenicity testing. Toxicol Pathol *26*, 742-749.

Venema, J., Mullenders, L. H., Natarajan, A. T., van Zeeland, A. A., and Mayne, L. V. (1990a). The genetic defect in Cockayne syndrome is associated with a defect in repair of UV-induced DNA damage in transcriptionally active DNA. Proc Natl Acad Sci U S A *87*, 4707-4711.

Venema, J., van Hoffen, A., Karcagi, V., Natarajan, A. T., van Zeeland, A. A., and Mullenders, L. H. (1991). Xeroderma pigmentosum complementation group C cells remove pyrimidine dimers selectively from the transcribed strand of active genes. Mol Cell Biol *11*, 4128-4134.

Venema, J., van Hoffen, A., Natarajan, A. T., van Zeeland, A. A., and Mullenders, L. H. (1990b). The residual repair capacity of xeroderma pigmentosum complementation group C fibroblasts is highly specific for transcriptionally active DNA. Nucleic Acids Res *18*, 443-448.

Vermeulen, W., Rademakers, S., Jaspers, N. G., Appeldoorn, E., Raams, A., Klein, B., Kleijer, W. J., Hansen, L. K., and Hoeijmakers, J. H. (2001). A temperature-sensitive disorder in basal transcription and DNA repair in humans. Nat Genet *27*, 299-303.

Vermeulen, W., Scott, R. J., Rodgers, S., Muller, H. J., Cole, J., Arlett, C. F., Kleijer, W. J., Bootsma, D., Hoeijmakers, J. H., and Weeda, G. (1994a). Clinical heterogeneity within xeroderma pigmentosum associated with mutations in the DNA repair and transcription gene ERCC3. Am J Hum Genet *54*, 191-200.

Vermeulen, W., van Vuuren, A. J., Chipoulet, M., Schaeffer, L., Appeldoorn, E., Weeda, G., Jaspers, N. G., Priestley, A., Arlett, C. F., Lehmann, A. R., and et al. (1994b). Three unusual repair deficiencies associated with transcription factor BTF2(TFIIH): evidence for the existence of a transcription syndrome. Cold Spring Harb Symp Quant Biol *59*, 317-329.

Vijg, J., and Calder, R. B. (2004). Transcripts of aging. Trends Genet *20*, 221-224.

Volker, M., Mone, M. J., Karmakar, P., van Hoffen, A., Schul, W., Vermeulen, W., Hoeijmakers, J. H., van Driel, R., van Zeeland, A. A., and Mullenders, L. H. (2001). Sequential assembly of the nucleotide excision repair factors in vivo. Mol Cell *8*, 213-224.

Vooijs, M., Jonkers, J., and Berns, A. (2001). A highly efficient ligand-regulated Cre recombinase mouse line shows that LoxP recombination is position dependent. EMBO Rep *2*, 292-297.

Wakasugi, M., Reardon, J. T., and Sancar, A. (1997). The non-catalytic function of XPG protein during dual incision in human nucleotide excision repair. J Biol Chem *272*, 16030-16034.

Wang, F., Saito, Y., Shiomi, T., Yamada, S., Ono, T., and Ikehata, H. (2006). Mutation spectrum in UVB-exposed skin epidermis of a mildly-affected Xpg-deficient mouse. Environ Mol Mutagen *47*, 107-116.

Wang, Q. E., Zhu, Q., Wani, G., El-Mahdy, M. A., Li, J., and Wani, A. A. (2005). DNA repair factor XPC is modified by SUMO-1 and ubiquitin following UV irradiation. Nucleic Acids Res *33*, 4023-4034.

Wang, X. W., Vermeulen, W., Coursen, J. D., Gibson, M., Lupold, S. E., Forrester, K., Xu, G., Elmore, L., Yeh, H., Hoeijmakers, J. H., and Harris, C. C. (1996). The XPB and XPD DNA helicases are components of the p53-mediated apoptosis pathway. Genes Dev *10*, 1219-1232.

Ward, J. (1975). Molecular Mechanisms of radiation-induced damage to nucleic acids. Adv Rad Biol *5*, 181-239.

Weeda, G., Donker, I., de Wit, J., Morreau, H., Janssens, R., Vissers, C. J., Nigg, A., van Steeg, H., Bootsma, D., and Hoeijmakers, J. H. (1997). Disruption of mouse ERCC1 results in a novel repair syndrome with growth failure, nuclear abnormalities and senescence. Curr Biol *7*, 427-439.

Weismann, A. (1889). Essays upon heredity and kindred biological problems. *1*.

Weiss, A., Arbell, I., Steinhagen-Thiessen, E., and Silbermann, M. (1991). Structural changes in aging bone: osteopenia in the proximal femurs of female mice. Bone *12*, 165-172.

Westerveld, A., Hoeijmakers, J. H., van Duin, M., de Wit, J., Odijk, H., Pastink, A., Wood, R. D., and Bootsma, D. (1984). Molecular cloning of a human DNA repair gene. Nature *310*, 425-429.

White, I. N. (1999). The tamoxifen dilemma. Carcinogenesis *20*, 1153-1160.

Wijnhoven, S. W., Beems, R. B., Roodbergen, M., van den Berg, J., Lohman, P. H., Diderich, K., van der Horst, G. T., Vijg, J., Hoeijmakers, J. H., and van Steeg, H. (2005a). Accelerated aging pathology in ad libitum fed Xpd(TTD) mice is accompanied by features suggestive of caloric restriction. DNA Repair (Amst).

Wijnhoven, S. W., Beems, R. B., Roodbergen, M., van den Berg, J., Lohman, P. H., Diderich, K., van der Horst, G. T., Vijg, J., Hoeijmakers, J. H., and van Steeg, H. (2005b). Accelerated aging pathology in ad libitum fed Xpd(TTD) mice is accompanied by features suggestive of caloric restriction. DNA Repair (Amst) *4*, 1314-1324.

Wijnhoven, S. W., Kool, H. J., Mullenders, L. H., Slater, R., van Zeeland, A. A., and Vrieling, H. (2001). DMBA-induced toxic and mutagenic responses vary dramatically between NER-deficient Xpa, Xpc and Csb mice. Carcinogenesis *22*, 1099-1106.

Wijnhoven, S. W., Kool, H. J., Mullenders, L. H., van Zeeland, A. A., Friedberg, E. C., van der Horst, G. T., van Steeg, H., and Vrieling, H. (2000). Age-dependent spontaneous mutagenesis in Xpc mice defective in nucleotide excision repair. Oncogene *19*, 5034-5037.

Wilson, D. M., 3rd, and Thompson, L. H. (1997). Life without DNA repair. Proc Natl Acad Sci U S A *94*, 12754-12757.

Winkler, G. S., Araujo, S. J., Fiedler, U., Vermeulen, W., Coin, F., Egly, J. M., Hoeijmakers, J. H., Wood, R. D., Timmers, H. T., and Weeda, G. (2000). TFIIH with inactive XPD helicase functions in transcription initiation but is defective in DNA repair. J Biol Chem *275*, 4258-4266.

Wood, R. D. (1999). DNA damage recognition during nucleotide excision repair in mammalian cells. Biochimie *81*, 39-44.
Woody, R. C., Harding, B. N., Brumback, R. A., and Leech, R. W. (1991). Absence of beta-amyloid immunoreactivity in mesial temporal lobe in Cockayne's syndrome. J Child Neurol *6*, 32-34.
Wu, L., Chan, K. L., Ralf, C., Bernstein, D. A., Garcia, P. L., Bohr, V. A., Vindigni, A., Janscak, P., Keck, J. L., and Hickson, I. D. (2005). The HRDC domain of BLM is required for the dissolution of double Holliday junctions. Embo J *24*, 2679-2687.
Yu, B. P. (1994). Cellular defenses against damage from reactive oxygen species. Physiol Rev *74*, 139-162.
Zhu, C., Bogue, M. A., Lim, D. S., Hasty, P., and Roth, D. B. (1996). Ku86-deficient mice exhibit severe combined immunodeficiency and defective processing of V(D)J recombination intermediates. Cell *86*, 379-389.

Dankwoord

Eindelijk kan ik dan het belangrijkste gedeelte van dit proefschrift schrijven; het dankwoord. Het heeft lang geduurd voordat dit boekje af was en er zit veel bloed, zweet en tranen in. Zonder de hulp van heel veel mensen had ik het niet gered. Ik moet zeggen dat ik zo langzamerhand geen inspiratie meer over heb om te schrijven (het komt mijn neus en oren uit), maar ik zal mijn best doen om iedereen die hierbij betrokken was te bedanken en niemand te vergeten. Ik heb zes jaar met veel plezier bij de afdeling Genetica (samen)gewerkt met veel verschillende mensen. Allereerst wil ik Renata (paranimf) ontzettend bedanken: jij hebt zo enorm geholpen bij elk aspect van dit proefschrift. Je hebt keihard gewerkt om te zorgen dat elk experiment goed en op tijd plaatsvond en verder ben je een enorme steun en toeverlaat en een hele goede vriendin. Je hebt zelfs onze zwerfkat Dommel overgenomen! Natuurlijk wil ik ook Bert, copromotor en directe begeleider, enorm bedanken voor al je hulp. Het enige waar ik nooit aan zal kunnen wennen is dat je alles op het laatste moment doet (dan ben je op je best), zodat ik daardoor alles net te laat moet doen. Ik heb je dan ook op het laatst in gedachten meerdere malen met een betonnen versie van mijn proefschrift afgeranseld. Desalniettemin ben ik blij dat jij mijn begeleider bent geweest. Je zit vol goede ideeën en je bent niet bang om iets compleet nieuws uit te proberen. Ook heb je me gesteund in alles wat ik deed; ik heb veel van je geleerd. Op deze plek moet ik natuurlijk ook mijn promotor, Jan bedanken: Jan, je was altijd een bron van inspiratie en ik wil je bedanken dat ik zo lang op de afdeling met veel plezier heb mogen werken en dat je me vrij liet om qua onderzoek mij eigen weg in te slaan. Nils, andere paranimf, ik ken je al zo lang als ik werk bij Genetica. In het begin dronken we heel vaak koffie samen, jammer genoeg is dat er het laatste jaar bij ingeschoten. Je stond altijd voor me klaar; als ik weer een teen had gebroken of wilde drinken tijdens een feestje, dan reed jij naar huis. Heel erg bedankt! Then of course I would like to thank George; I learned a lot from you the past two years and not only about science. We've had numerous (endless) scientific discussions and it was a pleasure to work with you; I would even go as far as to say that I consider you a good friend. Toen ik bij Genetica kwam heb ik de eerste beginselen van muizen werk geleerd van Manja en Theo. Manja, bedankt voor je eindeloze geduld en uitleg. Theo, ik heb door de jaren heen veel met je samen gewerkt en dat altijd als prettig ervaren. Ik heb je in al die tijd geen een keer boos gezien; ik hoop dat ik dat ooit nog mee mag maken! Je was altijd rustig en beheerst en als ik weer een beetje doordraafde, wist je dat altijd goed te relativeren. Verder wil ik ook Jessie bedanken; we hebben samen heel veel meegemaakt op het lab en daarbuiten. Je was compleet gek en altijd heel gezellig. Ik vind het jammer dat je nu in Amerika zit en ik hoop dat je snel weer terugkomt. Hennie, Judith, Karin, Inez, Emine en Phebe, we hebben samen heel wat leuke dingen gedaan zowel binnen als buiten het lab; bedankt voor alle gezelligheid. Yvette, Phebe en Yvonne; jullie hebben me in het begin enorm geholpen met experimenten, zeker toen ik dat zelf door omstandigheden even niet kon; ik wil jullie daar heel erg voor bedanken; zonder jullie weet ik niet wat ik had moeten doen. Yvette, ik ken je al sinds dat ik stage liep bij Annelies; jij was een gezellige collega en ook een goede vriendin. Ik vind het jammer dat je niet meer bij Genetica werkt; ik mis je enorm. Laura, I learned a lot from you as well; you taught me how to do research and how to write. You stimulated me to think and work like a scientist. Moreover, you were a good friend. You even took me to your sister and parents and showed me the other side of America that you normally don't see. Thanks for everything! Roald, Roos, Michael, Esther en Henk, jullie waren gezellige labgenoten in 1018; bedankt voor alle lol. Roald, ik mis alle scheldpartijen die we hadden; je kon schelden alsof de wereld verging als je een leeg epje op de grond liet vallen; je hebt me vaak de slappe lach bezorgd. Ik hoop je snel weer eens tegen te komen. Anja, Hannie, Esther, Nicole, Jeroen, Iris, en de rest op de 6e verdieping; het was altijd gezellig koffie drinken en ook op feestjes zorgden jullie altijd voor veel lol. Jeroen, jij hebt me vaak goed advies gegeven en daar wil ik je graag nog eens extra voor bedanken. En natuurlijk Wim; jij zit altijd vol goed advies en dat heeft me vaak geholpen. Je bent goed in het aanhoren van mijn oeverloze gezeur; bedankt; hoe doe je dat toch? Steven; met jou heb ik veel (wetenschappelijke) discussies gehad en daar heb ik altijd veel plezier aan beleefd. Ik wil ook graag alle dierverzorgers en medewerkers van het muishuis bedanken, in het bijzonder Patrick, Vincent, Daniella, Jacqueline, Albertina en Iris (en iedereen die ik toch nog vergeten ben): bedankt voor al jullie goede zorgen en ook voor jullie eindeloze geduld als ik weer eens iets fout deed. Zonder jullie had ik nooit al deze muizen experimenten kunnen uitvoeren. Ruud; bedankt voor de hulp bij de muizenfoto's, en Tom; bedankt voor de hulp bij het mooier maken van de figuren en de voorkant. Marcel, je hebt enorm geholpen met de pathologie van de muizen die ik bestudeerde. Zelfs als ik ergens op het laatste moment mee kwam, deed je altijd je best om te zorgen dat het toch goed kwam; bedankt voor je onuitputtelijke enthousiasme en inzet. Ik heb ook veel samengewerkt met de mensen van het RIVM; Harry, Susan, Conny en Dolf: bedankt voor de goede samenwerking. Susan, ik ben meerdere malen met je op congres geweest en dat was een groot succes; bedankt voor je gezelligheid. Ik wil ook graag Jasperina, Marike, Rita van het secretariaat enorm bedanken: zeker op het laatst moeten jullie wel gek van me zijn geworden; maar jullie blijven altijd volkomen kalm en regelen de meest ingewikkelde dingen in een handomdraai. Ook wil ik de mensen van de inkoop en de keuken bedanken; zonder jullie is geen een experiment mogelijk! Verder natuurlijk al mijn labgenoten op de 7e: bedankt voor de gezelligheid en samenwerking (for those of you that still don't know any Dutch: I would like to thank all my other labmates at the 7th floor for the good cooperation and fun times we had together). Verder wil ik ook graag mijn nieuwe DNage medewerkers bedanken: Sander (Barnie), Sander, Shanoe en Mark (en natuurlijk ook weer Renata). Jullie hebben je allemaal ingezet om te zorgen dat alles goed verliep. Bedankt ook voor jullie eindeloze geduld; dankzij het schrijven van dit proefschrift had ik wel eens heel druk en dat hebben jullie goed opgevangen. Tol, ik wil speciaal ook jou bedanken; jij hebt me al veel geleerd over hoe het er in het bedrijfsleven aan toe gaat altijd en me ook ontzettend gesteund, ondanks dat ik mijn proefschrift nog moest schrijven. Als ik het even niet meer zag zitten wist je me altijd weer op te vrolijken (in de DE bar met koffie en een koekje). Irene; ik ken je nog maar net, maar ik beschouw je nu al als een goede vriendin; je staat altijd voor me klaar en hebt me heel veel geholpen met de lay-out van dit boekje; zonder jou (en je persoonlijke helpdesk) had ik het nooit gered. Je deelt een kamer met me en hebt zoveel gezeur aan moeten horen, dat je er onderhand immuun voor bent geworden. Ik hoop dat ik snel iets terug kan doen. Ook wil ik nog iedereen bedanken die ik vergeten ben te noemen en toch niet boos is geworden! Als laatste wil ik ook graag mijn familie en vrienden bedanken; sommigen van jullie weten waarschijnlijk niet eens meer hoe ik er uit zie; zo lang ben ik niet langs geweest. Daar ga ik in de toekomst verandering in brengen. In het bijzonder wil ik ook mijn ouders, zussen en zwagers bedanken voor hun eindeloze steun en interesse; ook dankzij jullie heb ik volgehouden als ik het niet meer zag zitten (en dat was vaak het geval, zeker op het laatst). En dan natuurlijk als allerlaatst Brian; jij hebt het denk ik heel moeilijk gehad; al die avonden dat ik laat thuis was en al die keren dat je jezelf moest vermaken omdat ik het weer te druk had (al heeft de nieuwe motor de pijn vast wel iets verzacht); ik vind het knap dat je het met me hebt uitgehouden, want vaak was ik niet te genieten. Ik weet niet hoe ik je ooit kan bedanken voor al je steun en geduld; je bent de beste vriend die ik heb.

Het feit dat er meer dan dertig keer bedankt staat in dit kleine stukje laat wel zien hoe belangrijk het is om samen te werken met mensen en interactie te hebben; hierdoor is dit proefschrift geworden zoals het is. Ik vond het een leuke tijd en heb er van genoten, maar het was ook vermoeiend en soms onmogelijk om te doen. Ik ben blij dat het eindelijk voorbij is; het werd wel tijd. Op naar de volgende stap…

I'ma make a new plan
Time for me to just stand up, and travel new land
Time for me to just take matters into my own hands
Once I'm over these tracks man I'ma never look back
And I'm gone, I know right where I'm goin
Sorry momma I'm grown, I must travel alone
ain't gon' follow the footsteps I'm making my own
Only way that I know how to escape from this 8 Mile Road
(Eminem, 8 mile

Curriculum Vitae

Ingrid Kolenbrander-van der Pluijm

26-05-1977, Rotterdam

Education

M.S.	September 1995, Utrecht University Utrecht, Netherlands Major subjects: Molecular Biology and Genetics cum laude

Employment/Research experience

2006-2007	Project Manager Employer: Rein Strijker DNage, spin-off of Department of Cell Biology & Genetics, Erasmus Medical Center, Rotterdam, Netherlands Area of research: Development of new tools to study aging and prevention of age-related disease
2005	Research associate Employer: Prof. Dr. Jan H.J. Hoeijmakers/DNage Department of Cell Biology & Genetics, Erasmus Medical Center, Rotterdam, Netherlands Area of research: Intervention of aging by use of NER deficient premature aging mouse models
2000-2005	Ph.D. student Employer: Prof. Dr. Jan H.J. Hoeijmakers Department of Cell Biology & Genetics, Erasmus Medical Center, Rotterdam, Netherlands Area of research: Study the causes and consequences of aging by use of NER deficient premature aging mouse models, including the generation of a conditional, tissue-specific and time-dependent XPA knockout mouse

Publications

Impaired Genome Maintenance Suppresses the GH/IGF1 Axis in Cockayne Syndrome Mice. Ingrid van der Pluijm, George A. Garinis, Renata M.C. Brandt, Theo G.M.F. Gorgels, Susan W. Wijnhoven, Karin E.M. Diderich, James R. Mitchell, Conny van Oostrom, Rudolf Beems, Laura J. Niedernhofer, Susana Velasco, Errol C. Friedberg, Kiyoji Tanaka, Harry van Steeg, Jan H.J. Hoeijmakers, and Gijsbertus T.J. van der Horst. (pending revision)

Retinal degeneration and ionizing radiation hypersensitivity in a mouse model for Cockayne syndrome Theo G.M.F. Gorgels, Ingrid van der Pluijm, Renata M.C. Brandt, Harry van Steeg, Gerard van den Aardweg, Gerard H. Jansen, Jan M. Ruijter, Arthur A.B. Bergen, Dirk van Norren, Jan H.J. Hoeijmakers, Gijsbertus T.J. van der Horst. (pending revision)

Defective repair of oxidative damage from mitochondrial DNA sensitizes
csb-/- cells to oxidative stress. Pia Madeleine Øistad, Ruth Halsne, Christine Gran, Barbro Elisabeth Sæther, Rune Johansen Forstrøm, Ingrid van der Pluijm, Bert van der Horst, Arne Klungland and Lars Eide. (submitted)

Arrest of transcription stimulated by poly(ADP-ribosyl)ation accelerates the overall repair of oxidative DNA base modifications and inhibits the accumulation of these lesions in ogg1$^{-/-}$ *mice. Claudia Flohr-Beckhaus, Christian Trapp, Ingrid. van der Pluijm, Gijsbertus T.J. van der Horst, Kiyoji Tanaka, Josiane Ménissier de Murcia, Bernd Kaina, Arne Klungland and Bernd Epe (submitted)*

Patent

Prematurely aging mouse models for the role of DNA damage in aging and intervention in aging-related pathology, Patent no. 0478128.8

Compositions for prevention and treatment of DNA damage and aging syndromes. Patent no. 06113951.5.